N74-73049

No. 493
G. L. Evans
NASA Hdqtrs.
Code RA
X67-18927

HYPERSONIC AIRCRAFT TECHNOLOGY CONFERENCE

PROGRAM AND SLIDES

MAY 16-18, 1967

AMES RESEARCH CENTER
NATIONAL AERONAUTICS AND SPACE ADMINISTRATION

CLASSIFICATION CHANGE

TO = UNCLASSIFIED

By authority of [redacted] GDS Gp-4

Changed by Odessa L. Smith Date 11/6/75

GROUP 4
Down[redacted]ear inter-
v[redacted]declassified after
years.

This material contains information affecting the na[redacted]ing of the espionage laws, Title 18, U.S.C., Secs. 793 and 794, the transmission or revelation of which in any manner to an unauthorized person is prohibited by law.

NOTICE
This document should not be returned after it has satisfied your requirements. It may be disposed of in accordance with your local security regulations or the appropriate provisions of the Industrial Security Manual for Safe-Guarding Classified Information.

[redacted]

PROGRAM

MAY 16-18, 1967

WELCOME
H. Julian Allen, Director, Ames Research Center

OPENING REMARKS
Mac C. Adams, Associate Administrator, Office of Advanced Research and Technology, NASA Headquarters

INTRODUCTION TO CONFERENCE
Clarence A. Syvertson, Assistant Director for Astronautics, Ames Research Center

[redacted]

[redacted]

May 18, 1967

V. STRUCTURES AND MATERIALS

Session Chairman - Richard R. Heldenfels

24. Introductory Remarks - Richard R. Heldenfels 24

25. Structural Comparison of All-Body and Wing-Body Liquid Hydrogen Fueled Hypersonic Aircraft - Mark D. Ardema and Thomas J. Gregory 25

26. Structural Materials for Hypersonic Aircraft - Bland A. Stein, Walter Illg, and John D. Buckley 26

27. A Carbon Dioxide Purge and Thermal Protection System for Liquid Hydrogen Tanks - L. Robert Jackson and Ellsworth L. Sharpe 27

28. Fuselage and Tank Structures for Hypersonic Aircraft - John L. Shideler and L. Robert Jackson 28

29. Analysis of Wing Structures for Hypersonic Aircraft - Melvin S. Anderson, James C. Robinson, and George F. Klich 29

30. Regeneratively Cooled Structures for Hypersonic Aircraft - H. Neale Kelly and John L. Shideler 30

31. Dynamic and Aeroelastic Consideration of Hypersonic Aircraft - A. Gerald Rainey and Dennis J. Martin 31

32. Flutter Design of Stiffened Skin Panels for Hypersonic Aircraft - Herman L. Bohon, Melvin S. Anderson, and Walter L. Heard 32

[redacted]

1. Hypersonic Technology Problems Identified in Mission Studies - Hubert M. Drake, Thomas J. Gregory, and Richard H. Petersen 1

TYPICAL CONFIGURATION

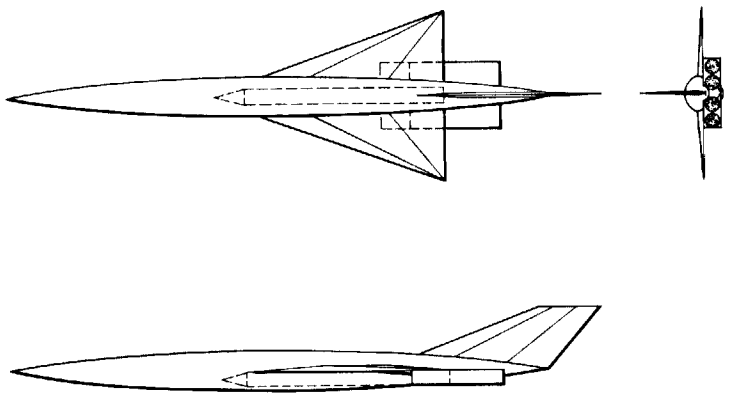

Slide 1.

HYPERSONIC TRANSPORT
RANGE-PAYLOAD CAPABILITY

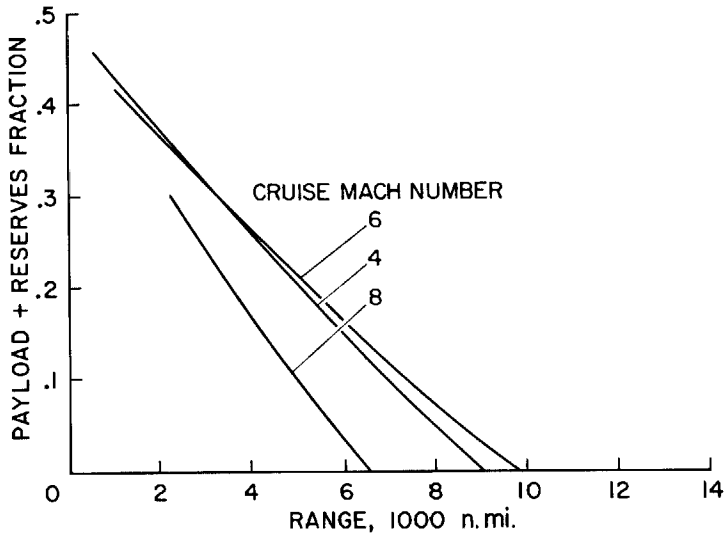

Slide 2.

CONFIDENTIAL

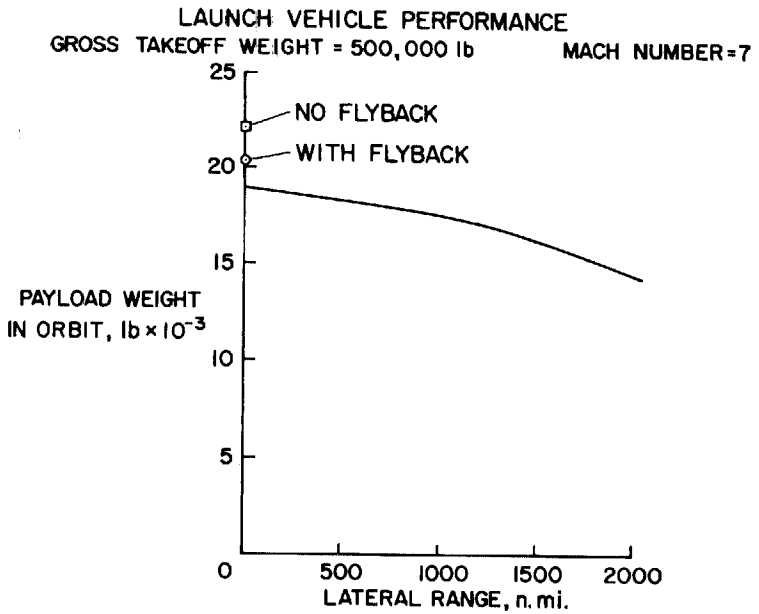

Slide 3.

RECENT STUDIES

MISSION	INVESTIGATOR	REFERENCE
CRUISE	NASA	
	GENERAL DYNAMICS CONVAIR	NAS 2-3180
LAUNCH	NASA	
	DOUGLAS	NAS 2-3191
	MARQUARDT, LOCKHEED, ROCKETDYNE	NAS 7-377
	LOCKHEED	NAS 8-20294
	BOEING	NAS 2-3691
	LOCKHEED	NAS 2-4084

Slide 4.

CONFIDENTIAL

CRUISE AIRCRAFT STUDY
200 PASSENGERS 5000 n. mi. RANGE

CONFIGURATION	GROSS WEIGHT, 10^3 lb		
	SIMPLIFIED PERFORMANCE ESTIMATES	DETAILED PERFORMANCE ESTIMATES	PROJECTED PERFORMANCE ESTIMATES
DELTA-WING BODY	585	750	521
BLENDED WING BODY	555	512	401

Slide 7.

INLET/ENGINE INSTALLATION

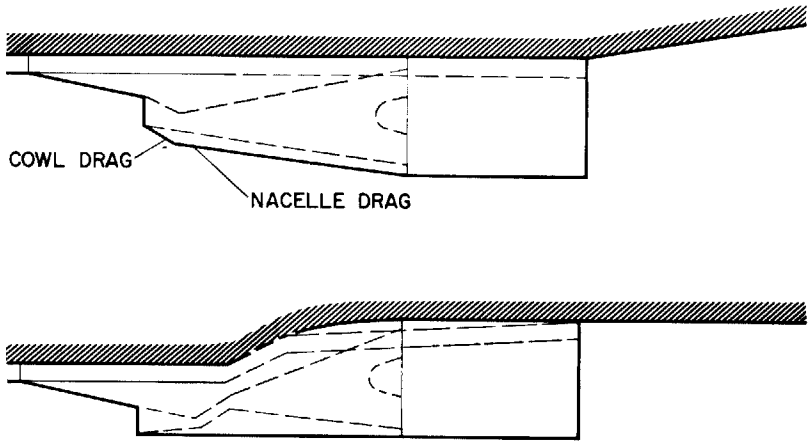

Slide 8.

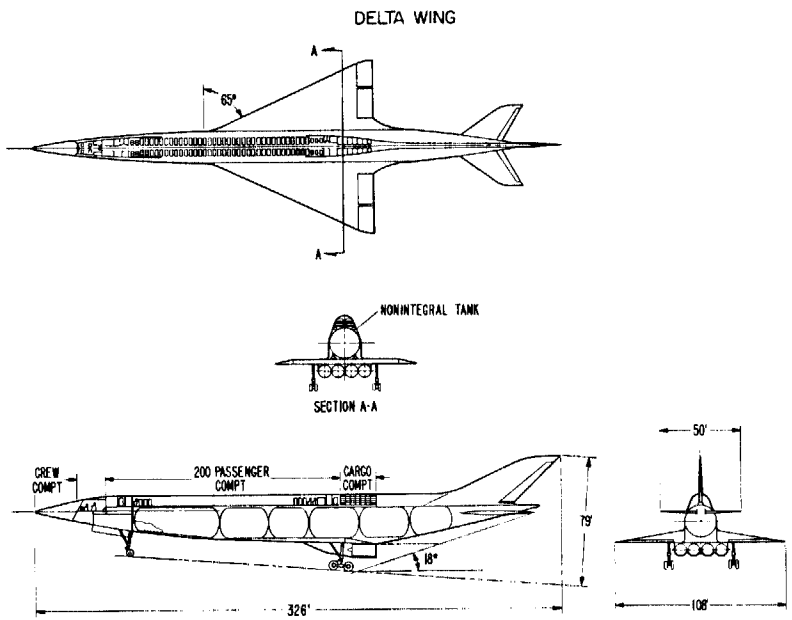

Slide 5.

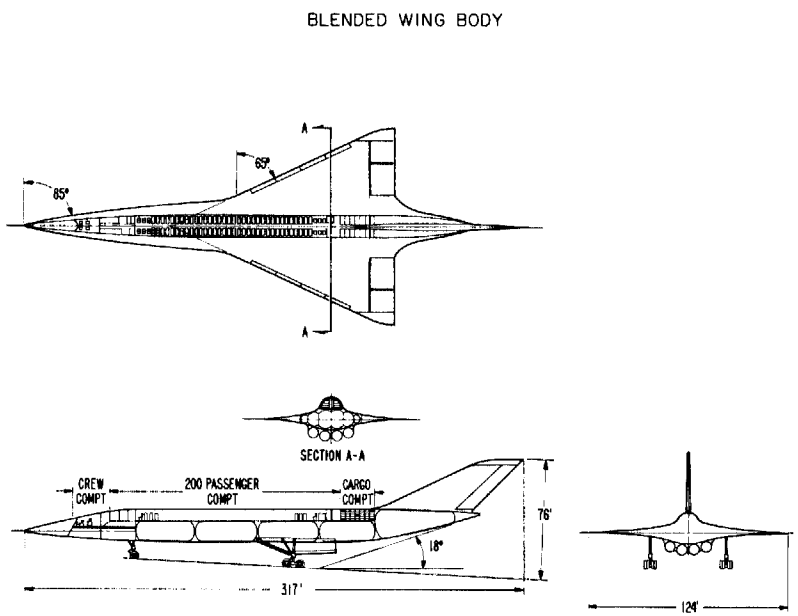

Slide 6.

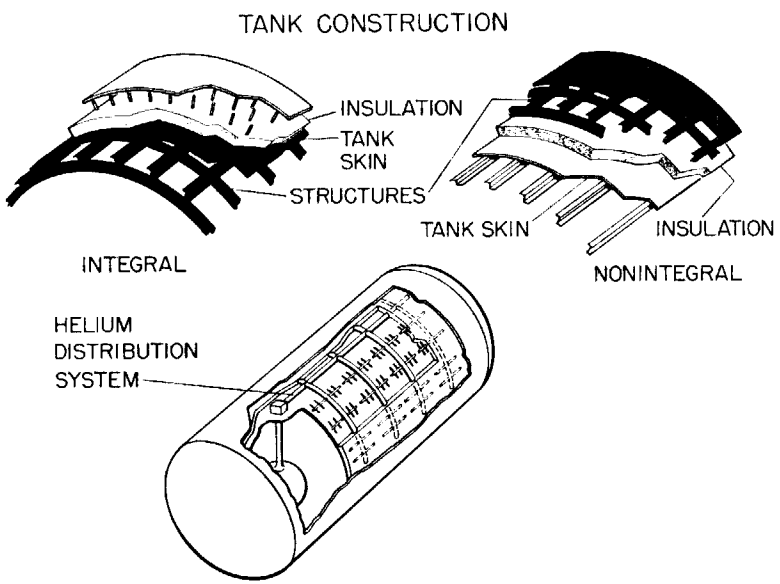

Slide 9.

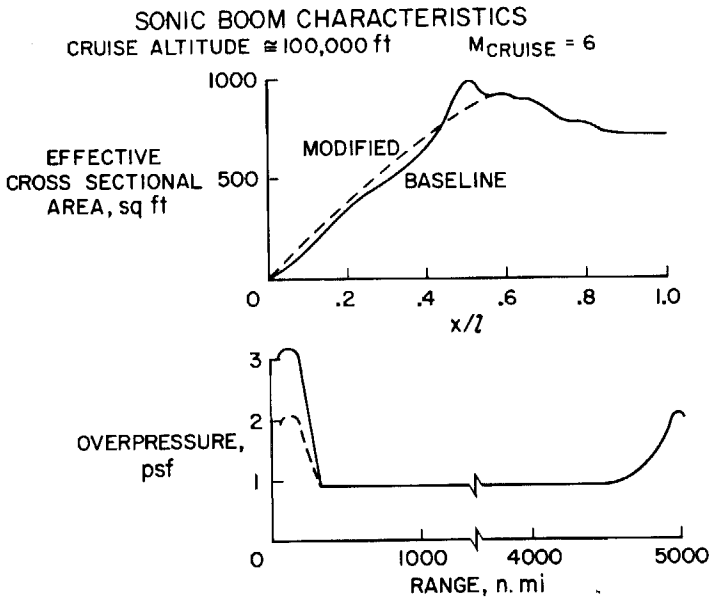

Slide 10.

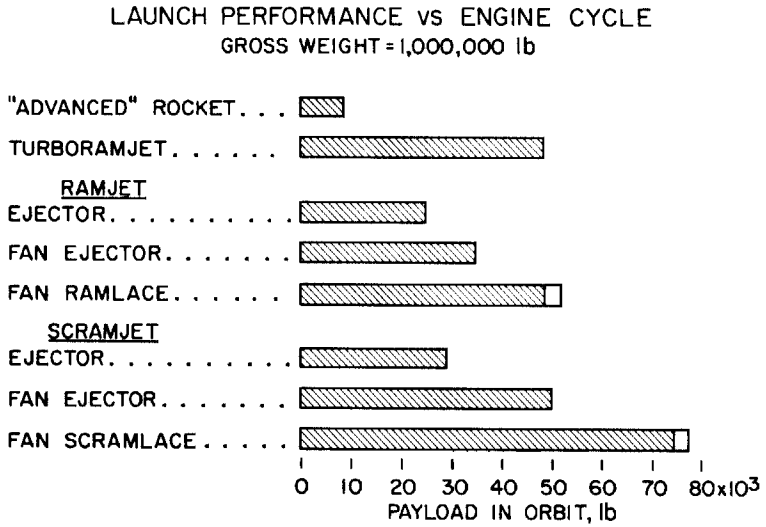
LAUNCH PERFORMANCE vs ENGINE CYCLE
GROSS WEIGHT = 1,000,000 lb
"ADVANCED" ROCKET. . .
TURBORAMJET. . . . . .
RAMJET
EJECTOR. . . . . .
FAN EJECTOR. . . . . .
FAN RAMLACE. . . . . .
SCRAMJET
EJECTOR. . . . . .
FAN EJECTOR. . . . . .
FAN SCRAMLACE. . . . .
0 10 20 30 40 50 60 70 80x10³
PAYLOAD IN ORBIT, lb

Slide 15.

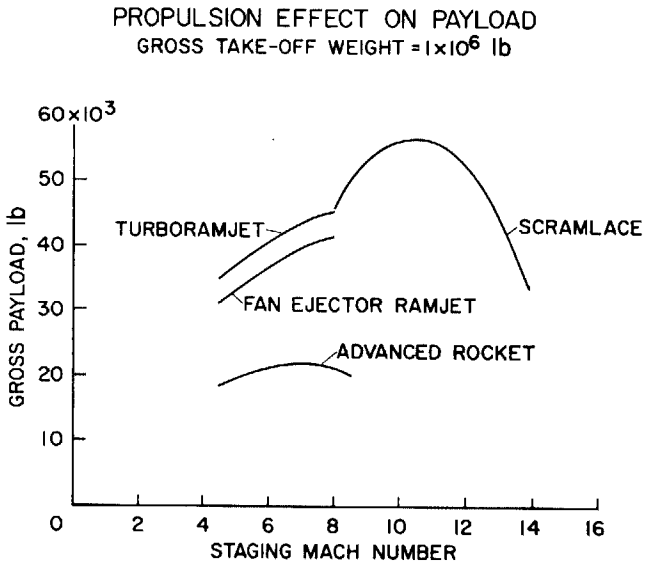

Slide 16.

REUSABLE LAUNCH VEHICLE PAYLOAD RATIO COMPARISON

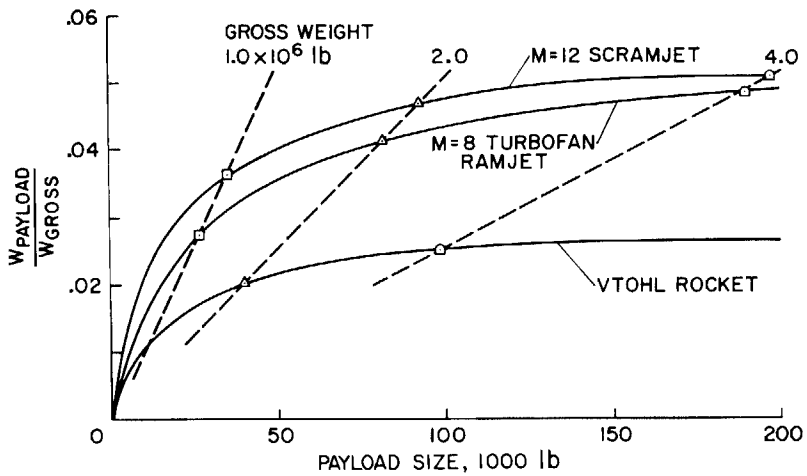

Slide 17.

CONFIGURATION MATRIX

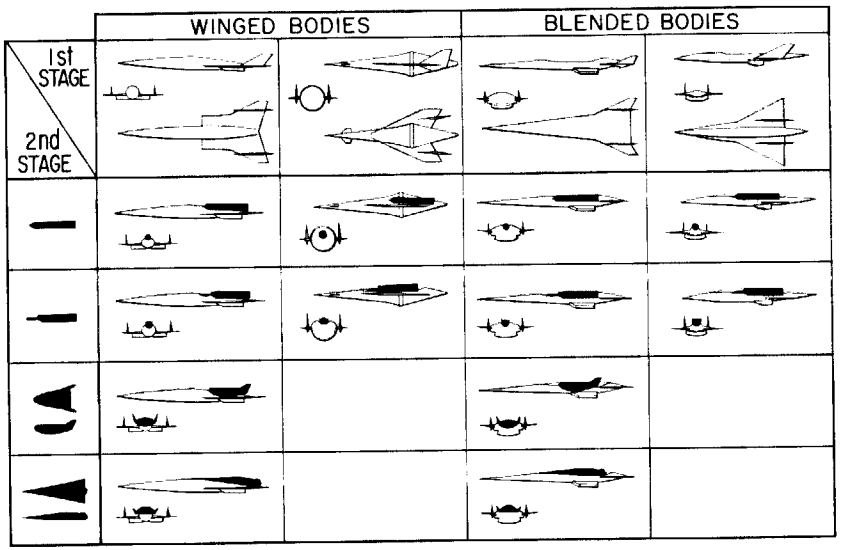

Slide 18.

LAUNCH AIRCRAFT INTEGRATION PROBLEM

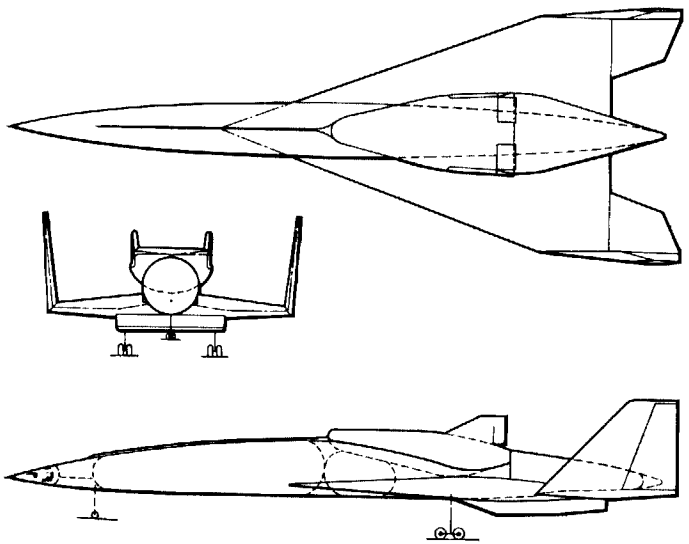

Slide 19.

EFFECT OF UPPER STAGE EXPOSURE ON ORBITAL PAYLOAD

LIFTING BODY UPPER STAGE

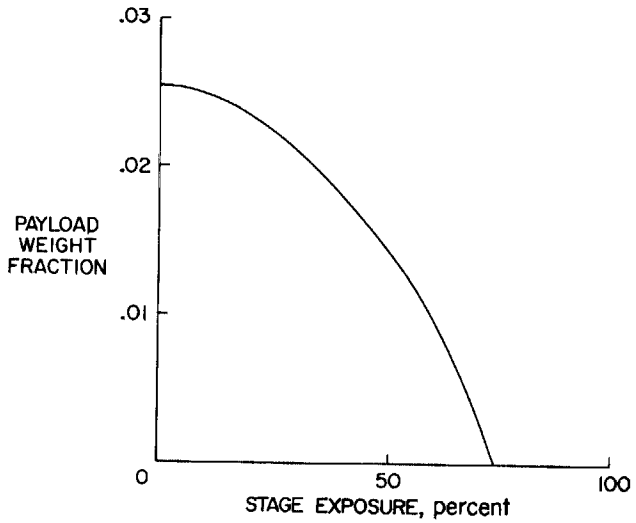

Slide 20.

EFFECT OF SONIC BOOM ON PAYLOAD

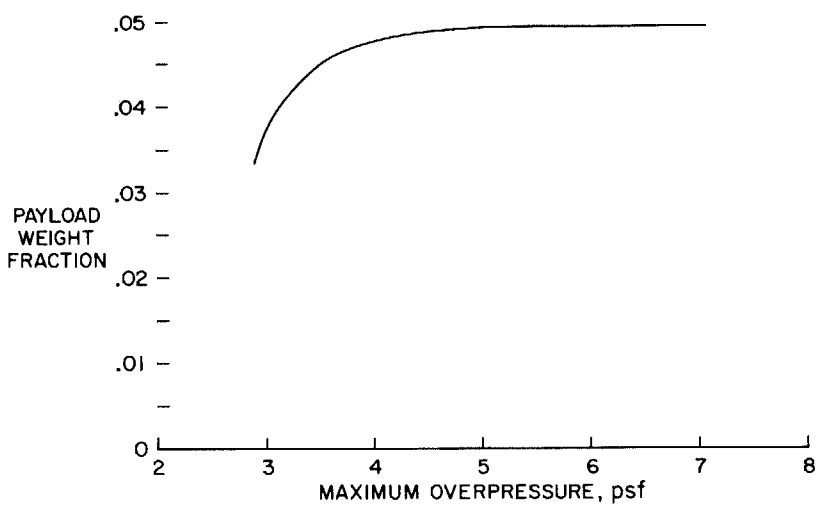

Slide 21.

PROBLEM AREAS

- CONFIGURATION AERODYNAMICS
  - PERFORMANCE
    - HYPERSONIC L/D
    - TRANSONIC DRAG
  - STABILITY AND CONTROL
  - SONIC BOOM
  - TAKE-OFF AND LANDING
  - SECOND STAGE INTEGRATION/SEPARATION
- HYPERSONIC VISCOUS FLOW
  - TRANSITION
  - INTERFERENCE
  - HEATING
- PROPULSION INLET
  - PRESSURE RECOVERY
  - FLOW DISTORTION
  - SIMPLIFICATION
  - COOLING LOAD
- PROPULSION (CONTINUED)
  - ENGINE
    - CYCLE
    - SFC (HYPERSONIC, SUBSONIC)
    - COOLING LOAD
  - NOZZLE
    - EFFICIENCY
    - COOLING LOAD
    - INTEGRATION WITH AIRFRAME
- STRUCTURES CONCEPTS
  - HOT STRUCTURES
  - TANKAGE
  - REGENERATIVE COOLING
  - MATERIALS
  - AEROELASTICITY
- OPERATIONS
  - SAFETY
  - INSPECTION
- COST
  - DEVELOPMENT
  - OPERATING

Slide 22.

CONFIDENTIAL

SESSION II, CHAIRMAN'S REMARKS

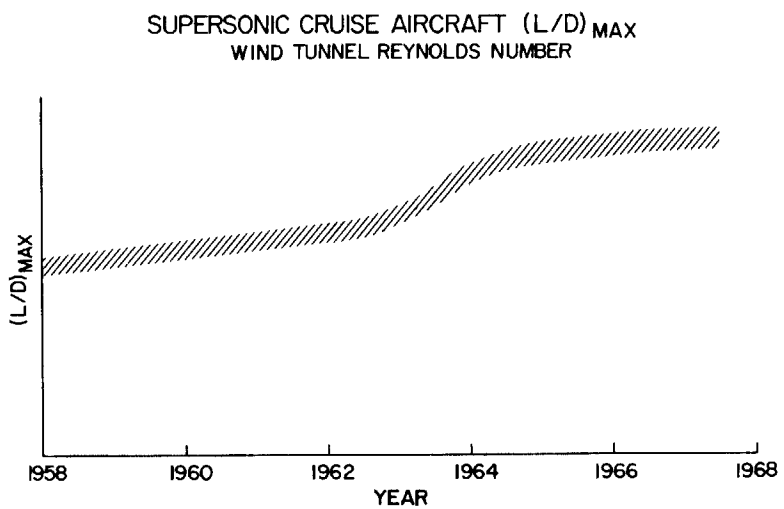

Slide 1.

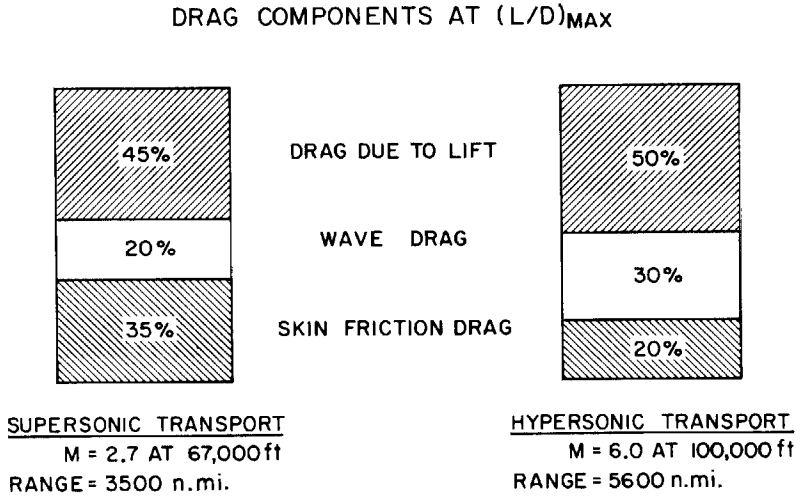

Slide 2.

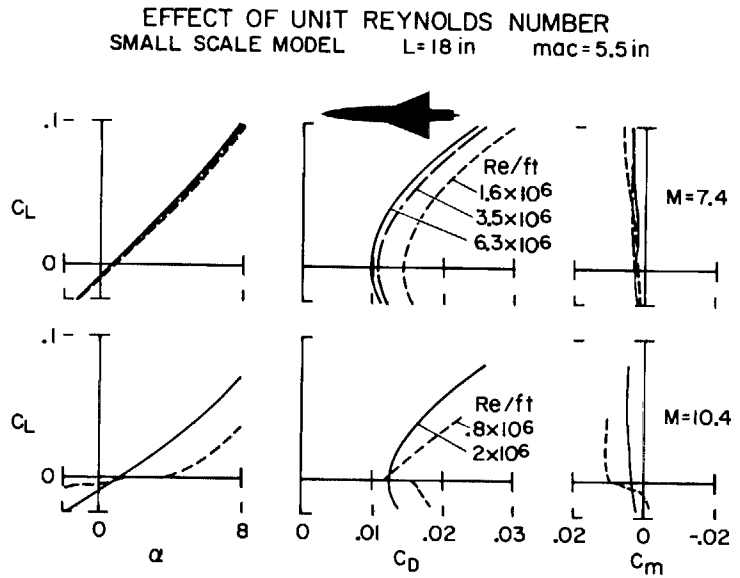

Slide 3.

CONFIGURATION AERODYNAMICS

OPERATIONAL PROBLEMS

- HANDLING QUALITIES
- SONIC BOOM

OPTIMIZATION AND SYNTHESIS

- WINGS
- BODIES
- AIRFRAME-PROPULSION SYSTEM INTEGRATION

EXPERIMENTAL EVALUATION

- CRUISE AIRCRAFT
- LAUNCH VEHICLES

Slide 4.

2. Experimental and Theoretical Aerodynamic Characteristics of Representative Hypersonic Cruise Configurations
Part I - Lift and Drag - Walter P. Nelms
Part II - Stability and Trim - John A. Axelson

W. P. Nelms
J. A. Axelson

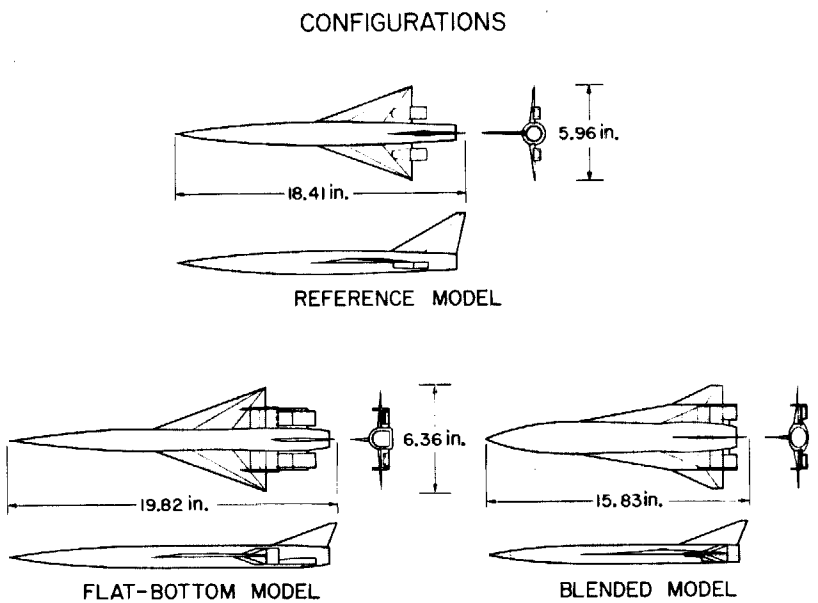

Slide 1.

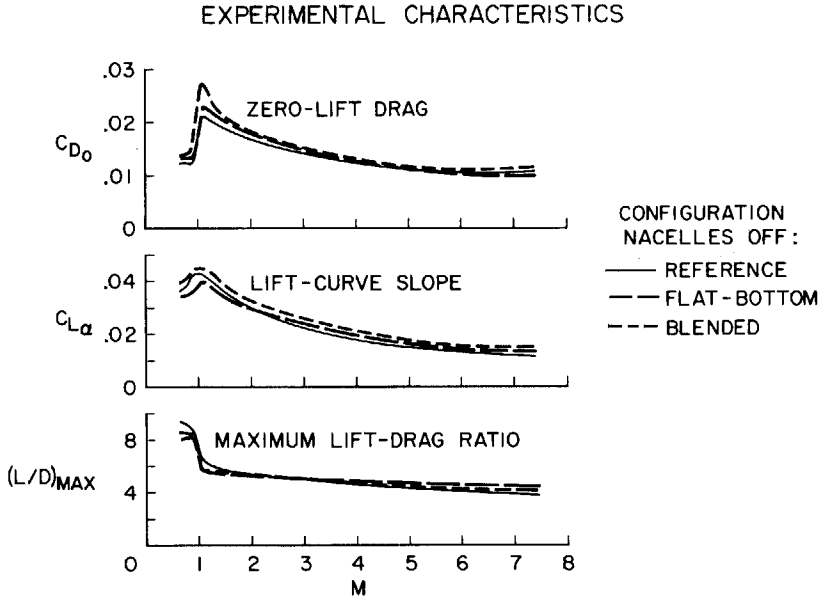

Slide 2.

W. P. Nelms
J. A. Axelson

THEORETICAL PREDICTION TECHNIQUES

PRESSURE FORCES	+	SKIN FRICTION
❶ LINEARIZED METHOD	+	REFERENCE TEMPERATURE
❷ TANGENT CONE AND WEDGE	+	REFERENCE TEMPERATURE
❸ NEWTONIAN	+	REFERENCE TEMPERATURE

Slide 3.

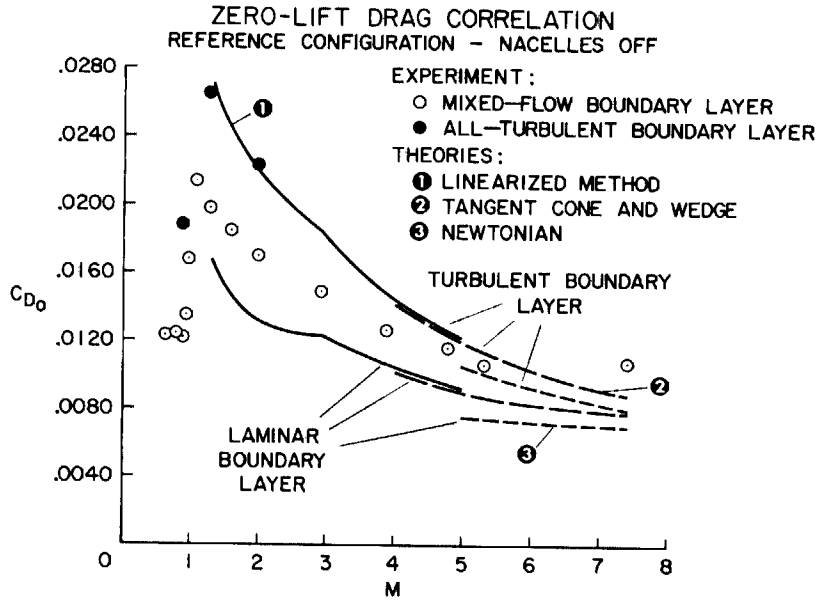

Slide 4.

W. P. Nelms
J. A. Axelson

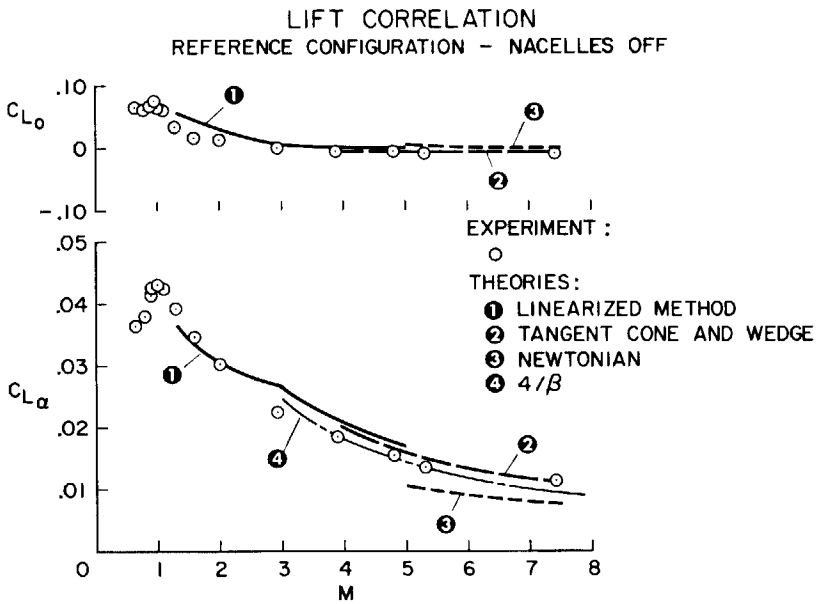

Slide 5.

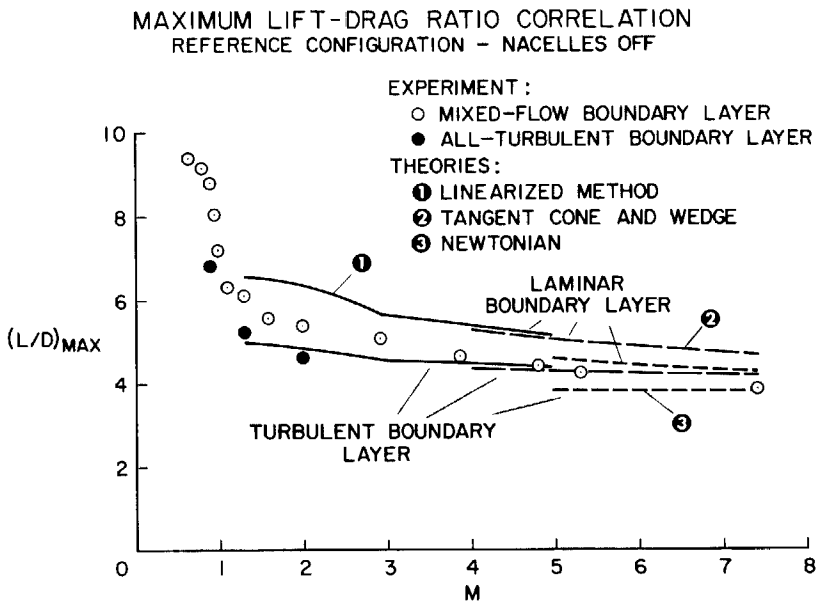

Slide 6.

W. P. Nelms
J. A. Axelson

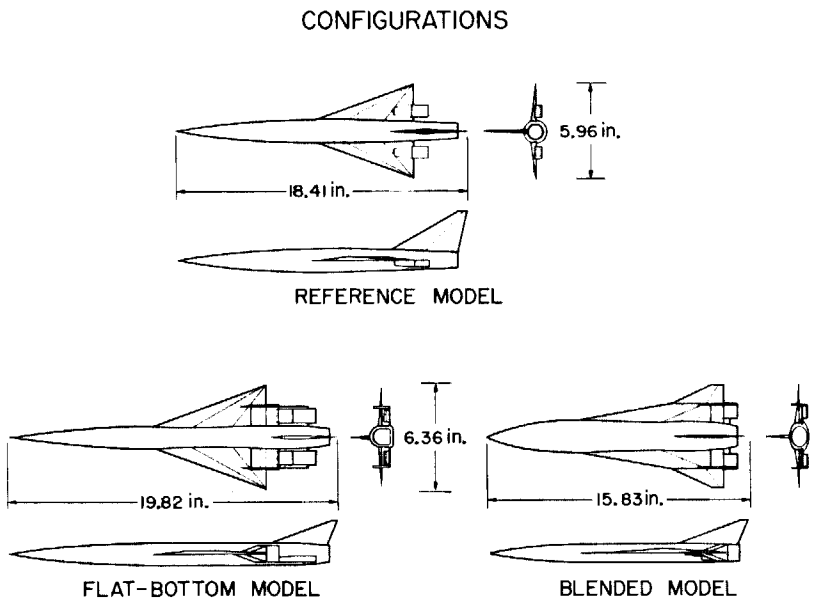

Slide 1.

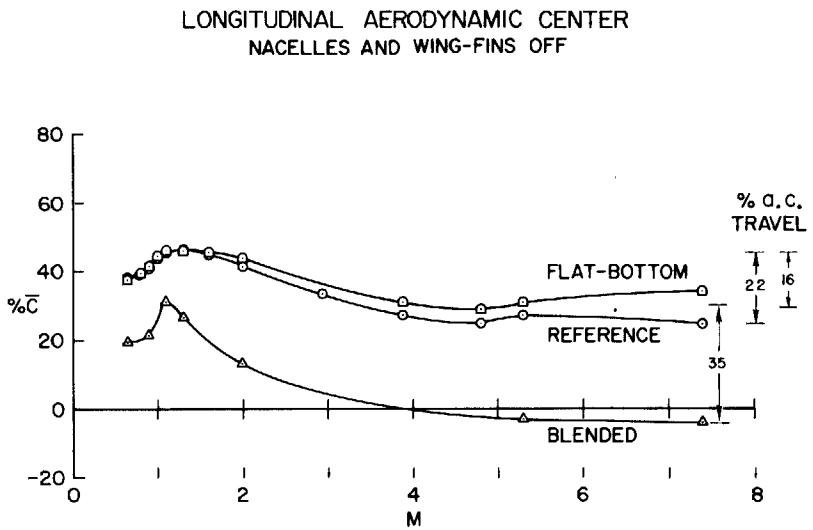

Slide 2.

W. P. Nelms
J. A. Axelson

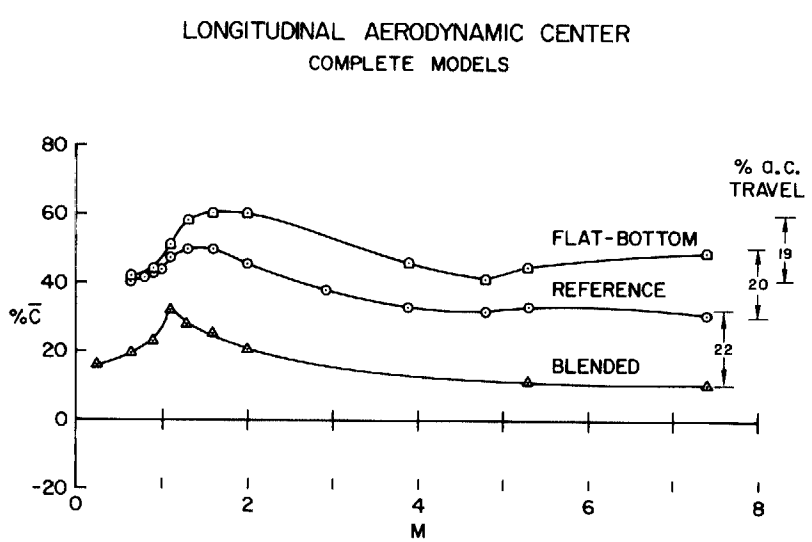

Slide 3.

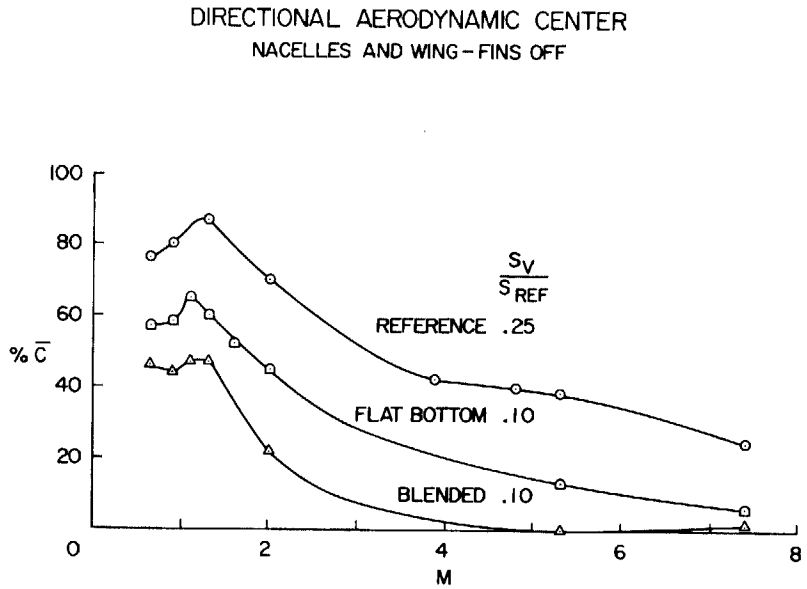

Slide 4.

W. P. Nelms
J. A. Axelson

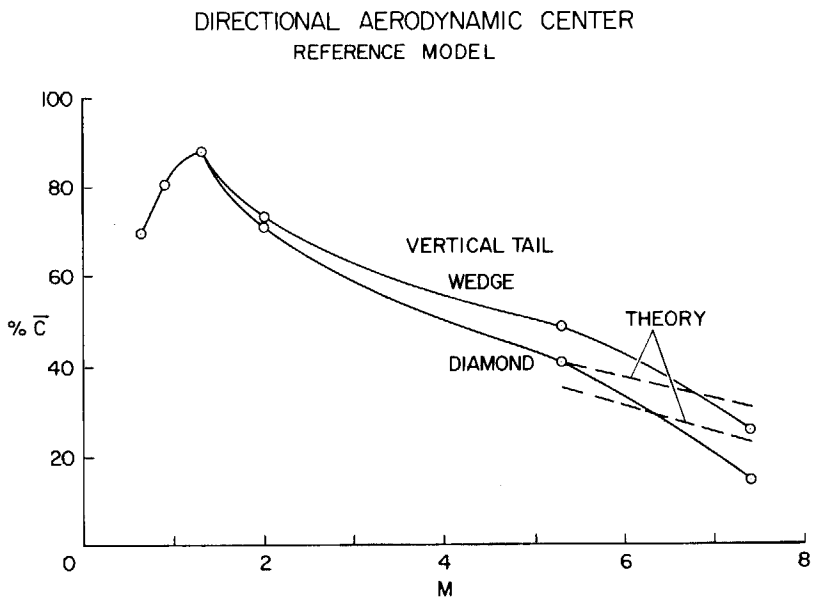

Slide 5.

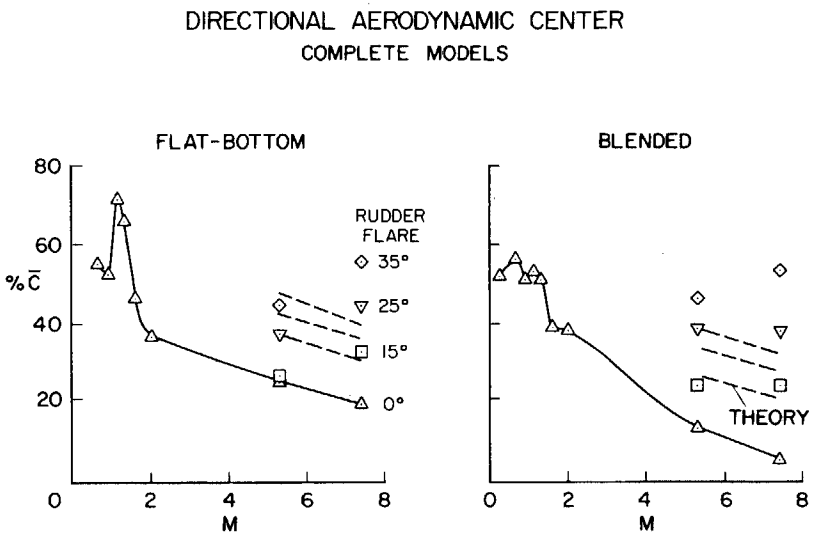

Slide 6.

W. P. Nelms
J. A. Axelson

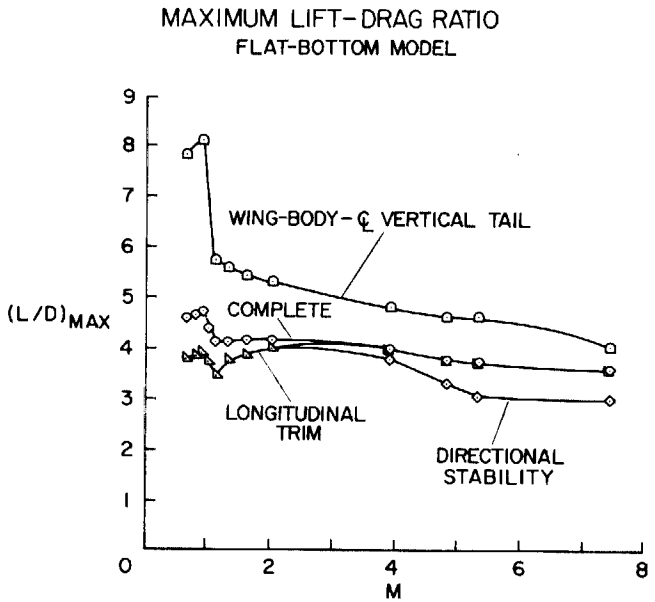

Slide 7.

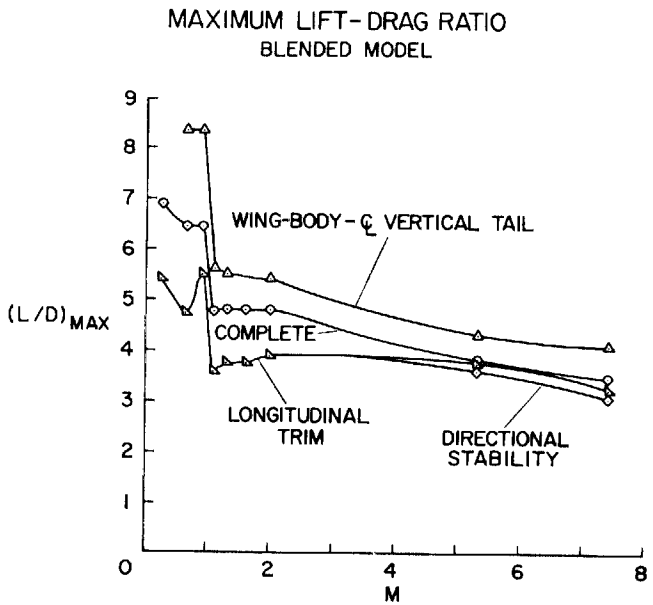

Slide 8.

3. Comparative Aerodynamic Study of Two Hypersonic Cruise Aircraft Configurations Derived From Trade-Off Studies - Jim A. Penland, Clyde L. W. Edwards, Robert D. Witcofski, and Don C. Marcum, Jr. 3

J. A. Penland

GROUND RULES FOR COMPARATIVE CONFIGURATION STUDIES

MISSION	COMMERCIAL TRANSPORT
PAYLOAD	50 000 lb (200 PASSENGERS)
RANGE	5000 n.mi.
CRUISE SPEED	$M_\infty = 6$
PROPULSION	TURBORAMJET
FUEL	LIQUID HYDROGEN
	SPEED, knots
TAKE-OFF	160
LANDING	135

Slide 1.

HYPERSONIC CRUISE AIRCRAFT

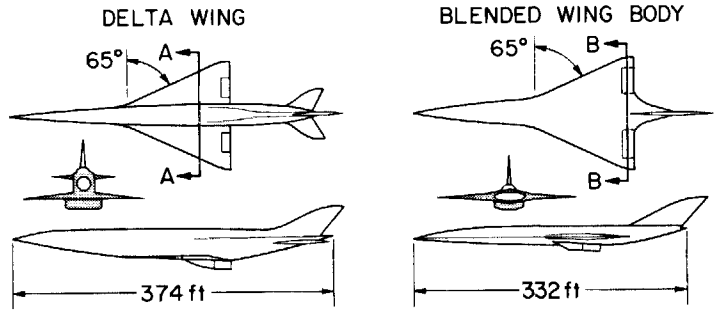

	DELTA WING	BLENDED WING BODY
GROSS WEIGHT, lb	750,000	512,000
$\frac{\text{STRUCTURE WEIGHT}}{\text{GROSS WEIGHT}}$, %	32.5	26.3
$(L/D)_{max}$, CRUISE	4.6	5.1
WING LOADING, psf	76.0	50.0

Slide 2.

CONFIDENTIAL

WIND-TUNNEL TEST CONDITIONS

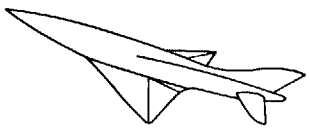

FLIGHT STUDY

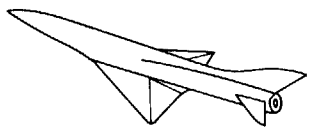

WIND TUNNEL

M_∞	l, in.	R_l
0.1	72	2.2×10^6
.8 TO 1.2	35	11.1
6	18	13.4
6.8	15	5.3

Slide 3.

LONGITUDINAL STABILITY

BLENDED WING BODY

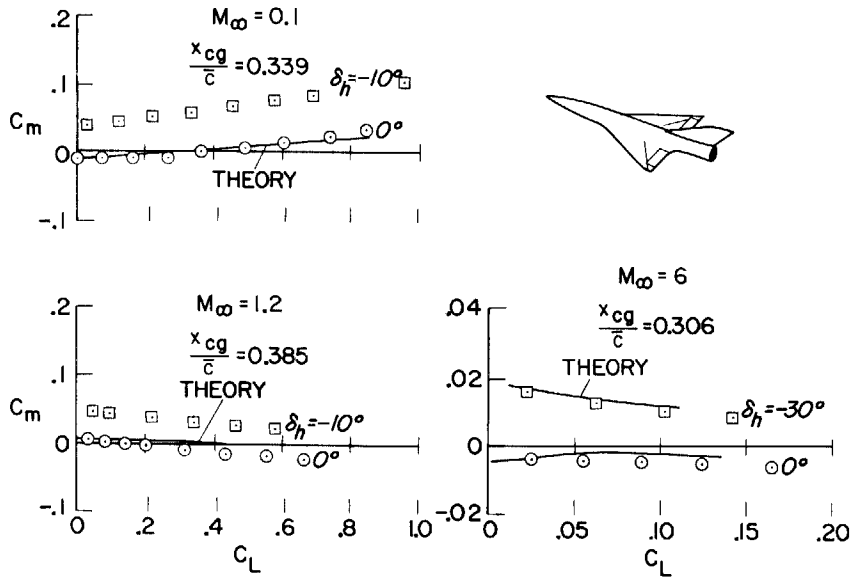

Slide 4.

CONFIDENTIAL

J. A. Penland

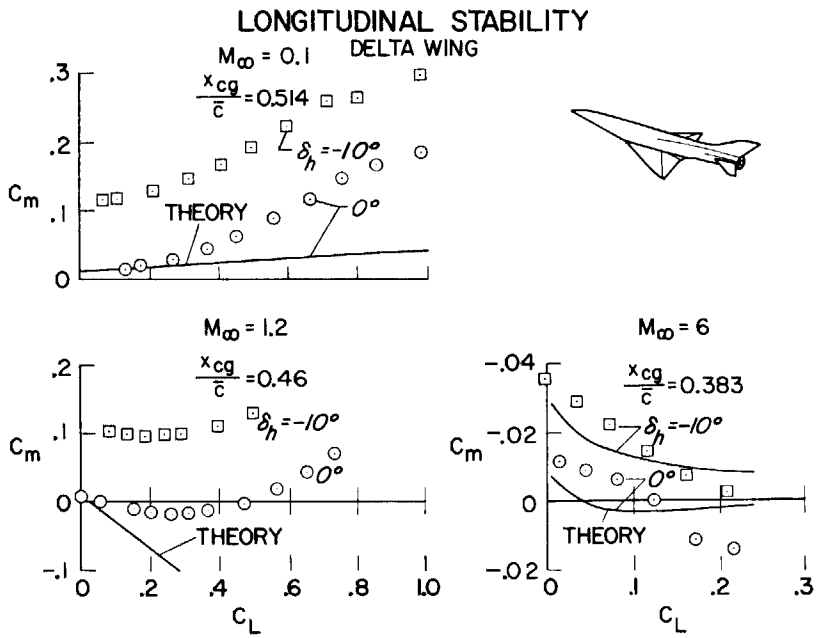

Slide 5.

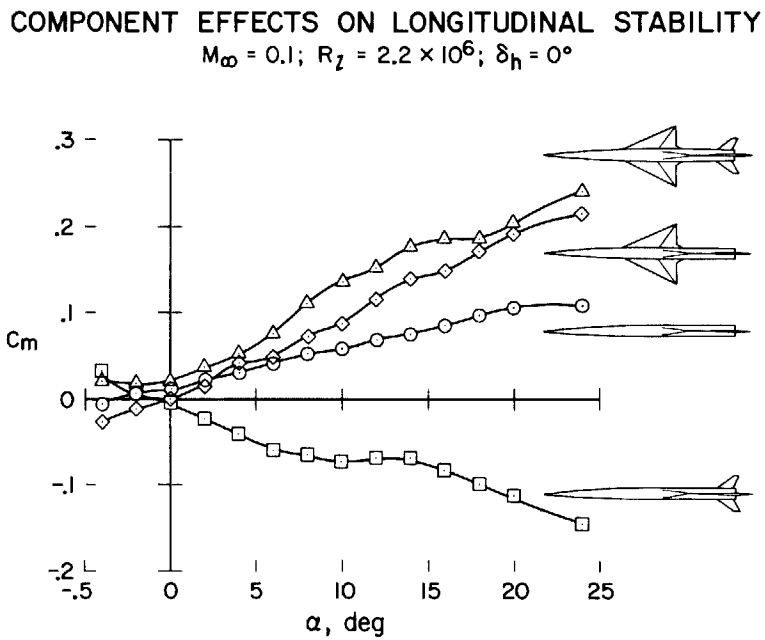

Slide 6.

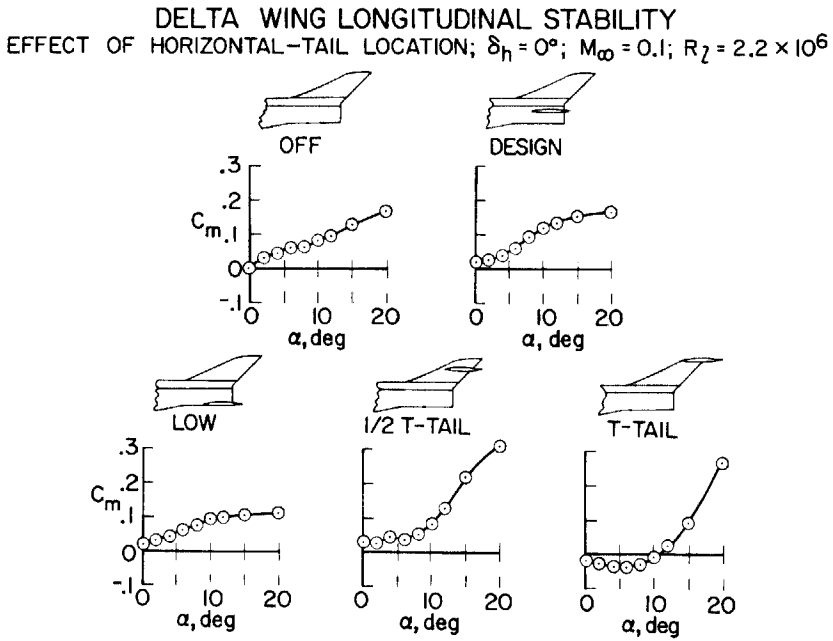

Slide 7.

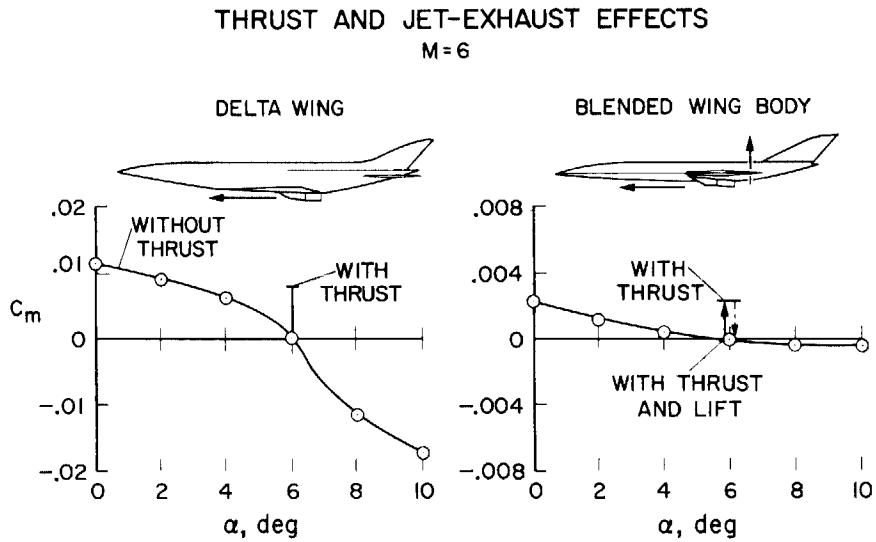

Slide 8.

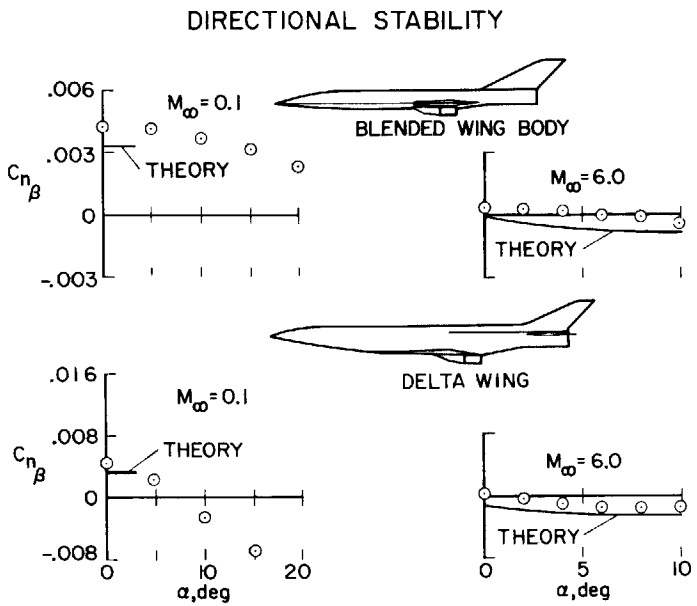

Slide 9.

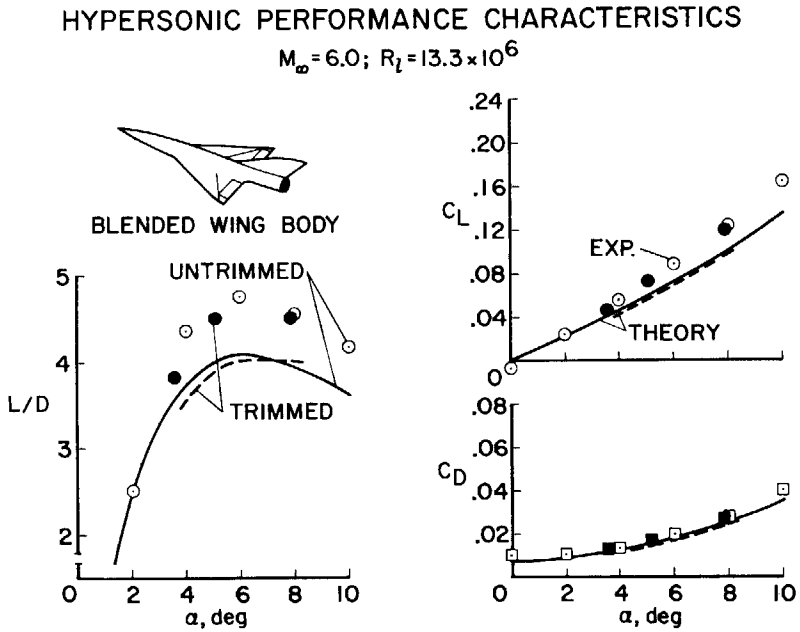

Slide 10.

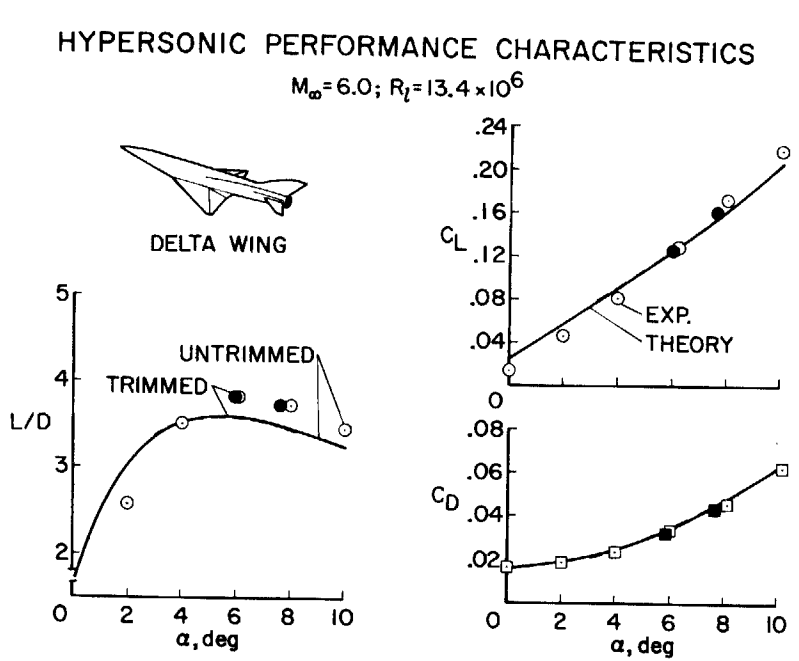

Slide 11.

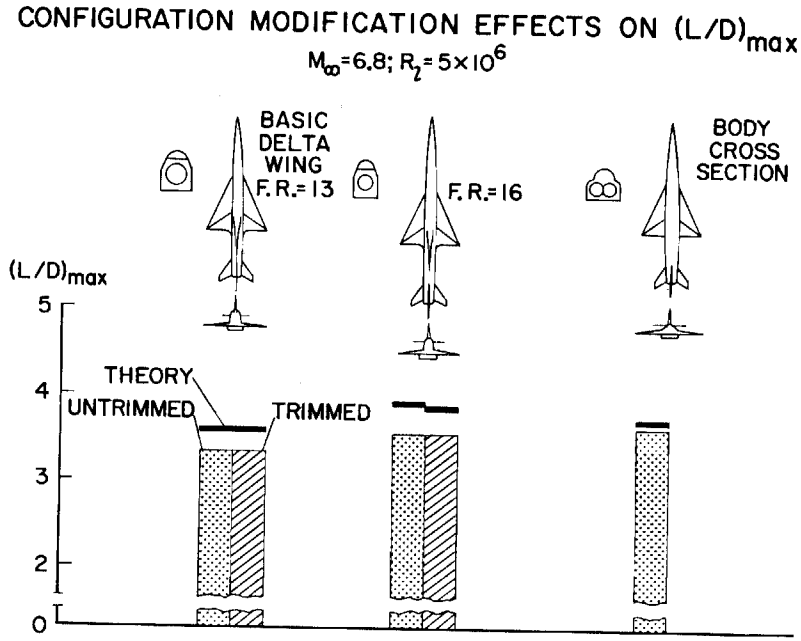

Slide 12.

CONFIGURATION MODIFICATION EFFECTS ON $(L/D)_{max}$

$M_\infty = 6.8; R_l \approx 5 \times 10^6$

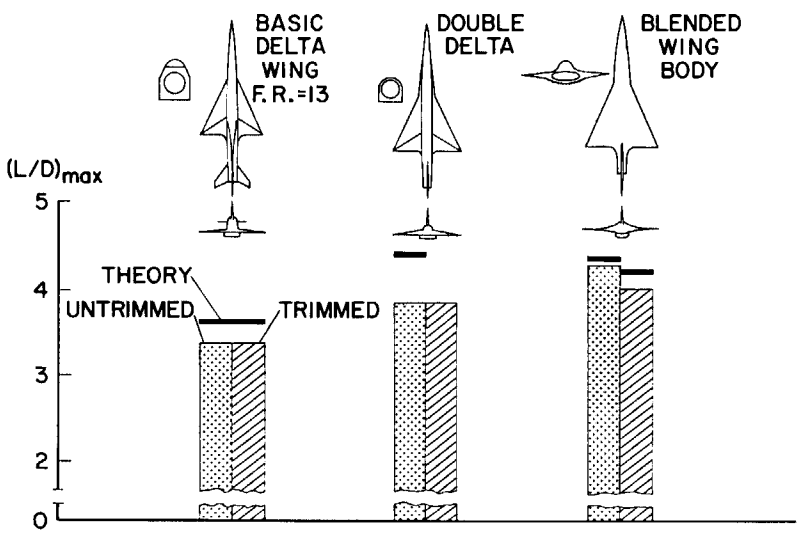

Slide 13.

PARAMETERS AFFECTING FLIGHT EXTRAPOLATIONS OF $(L/D)_{max}$

PRESSURE DRAG, $C_{D,p}$

DRAG DUE TO LIFT, $C_{D,L}$

CONTROL EFFECTIVENESS, ΔC_m, ΔC_L, ΔC_D

FRICTION DRAG, $C_{D,F}$

Slide 14.

4. Experimental Aerodynamics and Analysis of the Stage Separation of Reusable Launch Vehicles - John P. Decker

REUSABLE LAUNCH VEHICLE

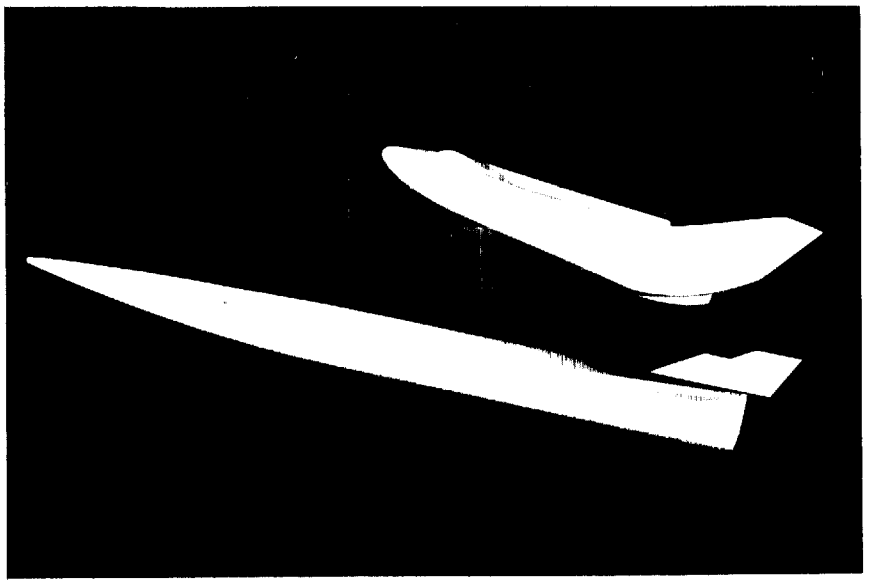

Slide 1.

AERODYNAMIC INTERFERENCE

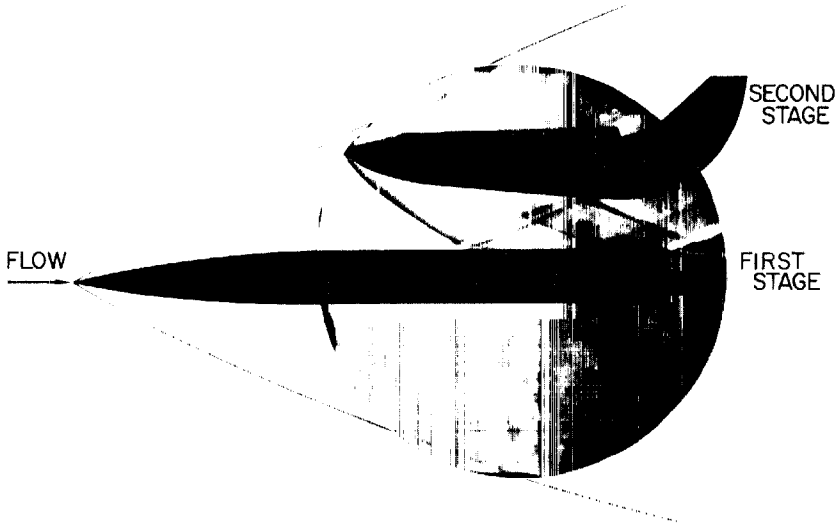

Slide 2.

CONFIDENTIAL

STAGING CONDITIONS

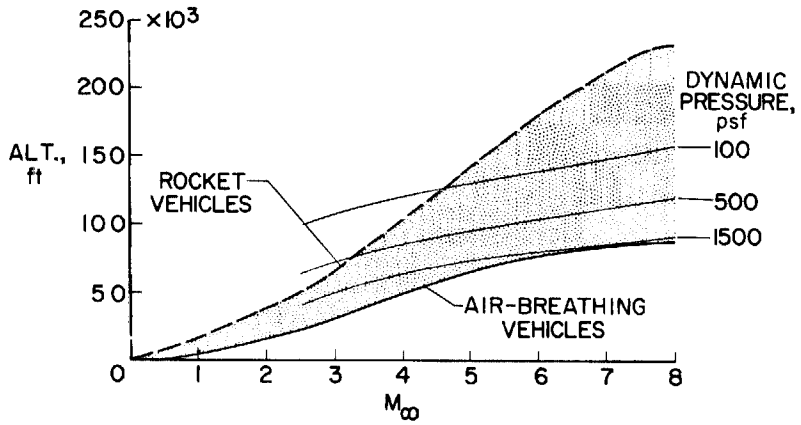

Slide 3.

STAGING SEQUENCE

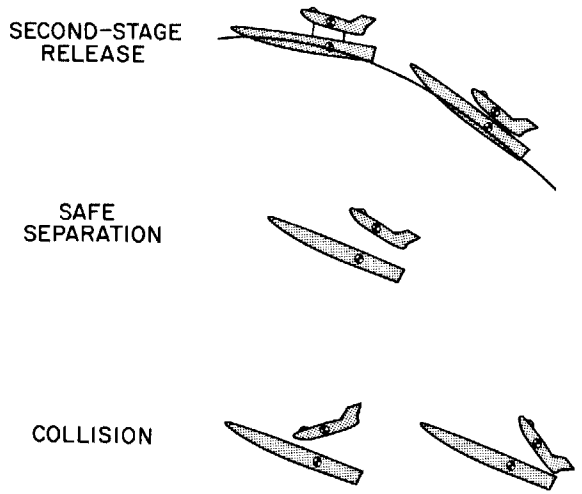

Slide 4.

CONFIDENTIAL

J. P. Decker

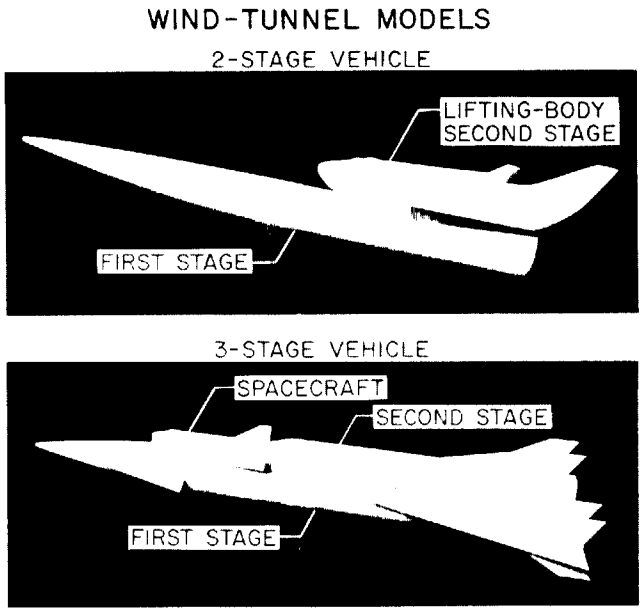

Slide 5.

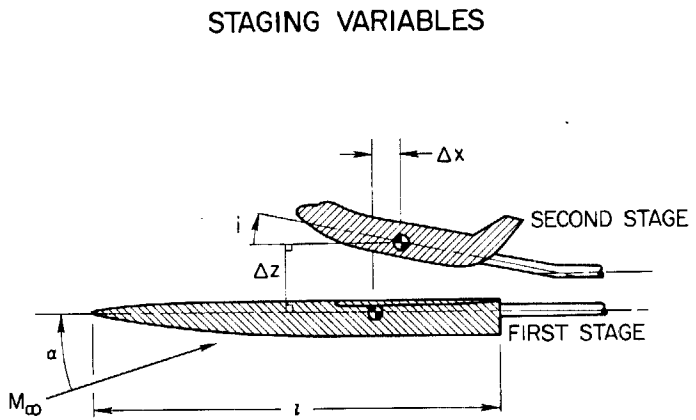

Slide 6.

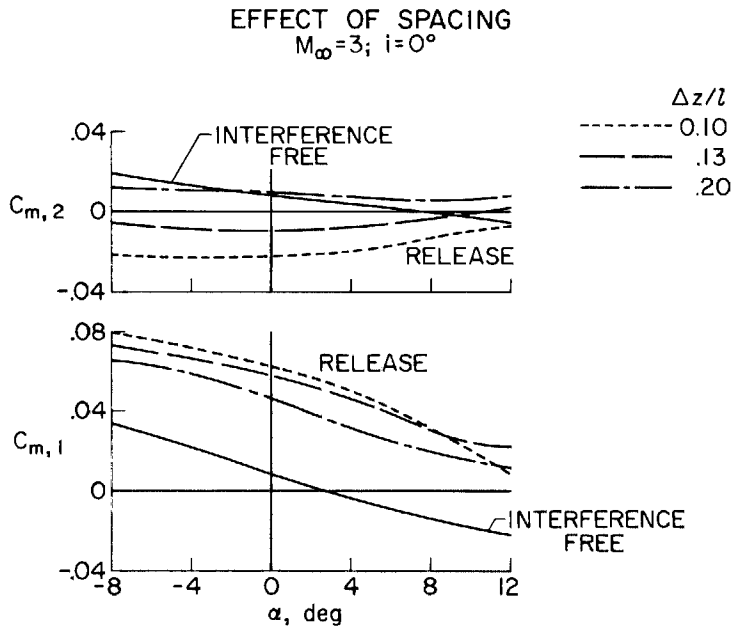

Slide 7.

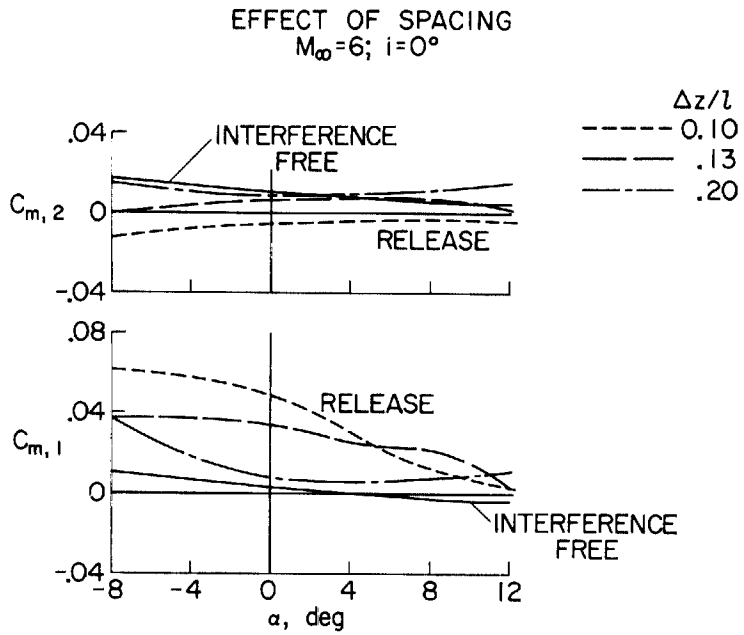

Slide 8.

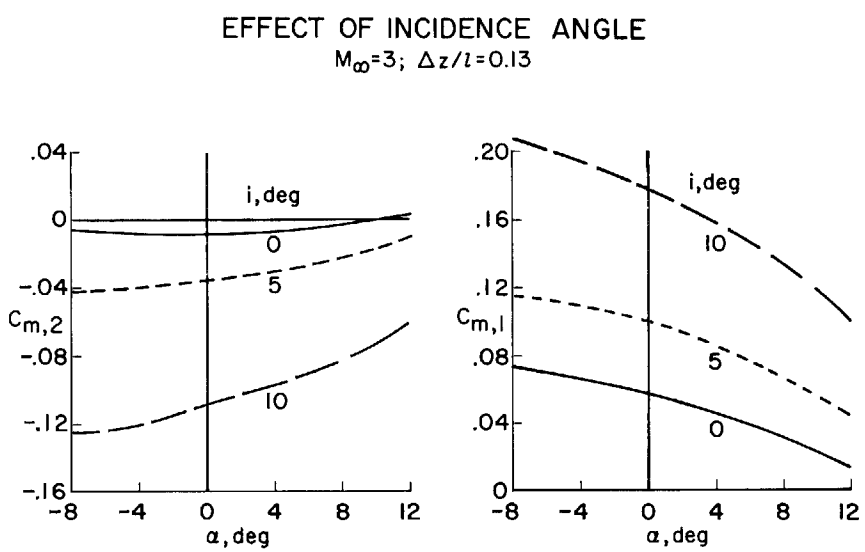

Slide 9.

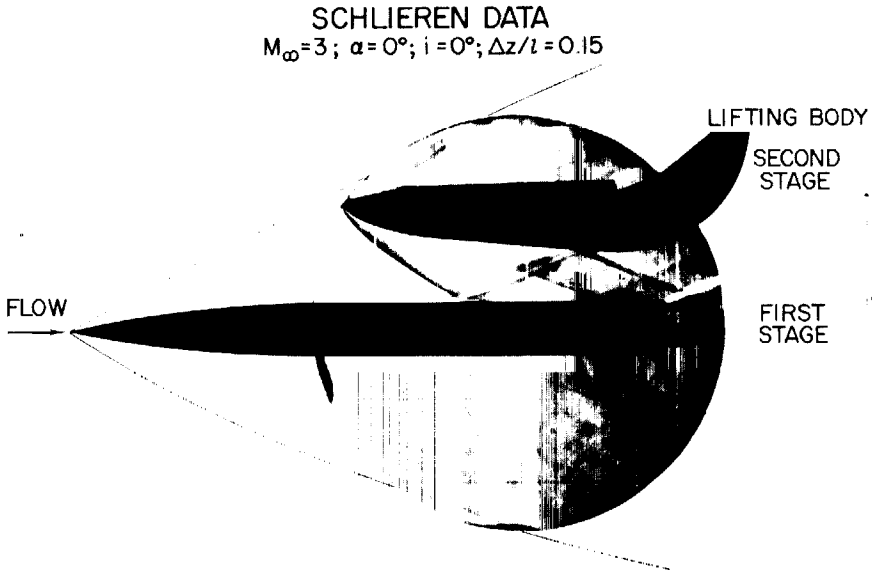

Slide 10.

EFFECT OF SPACING ON LIFTING BODY
$M_\infty = 3$; $i = 0°$

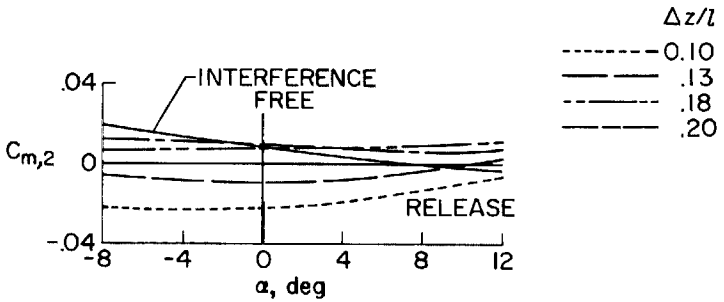

Slide 11.

EFFECT OF SPACING ON 3-STAGE VEHICLE
$M_\infty = 3$; $i = 0°$

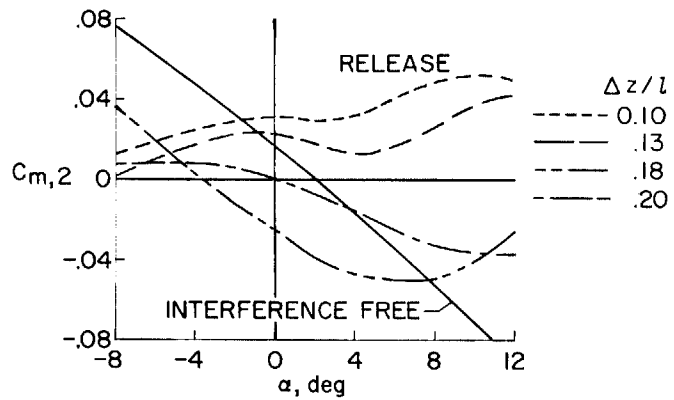

Slide 12.

EFFECT OF SPACING ON 3-STAGE VEHICLE

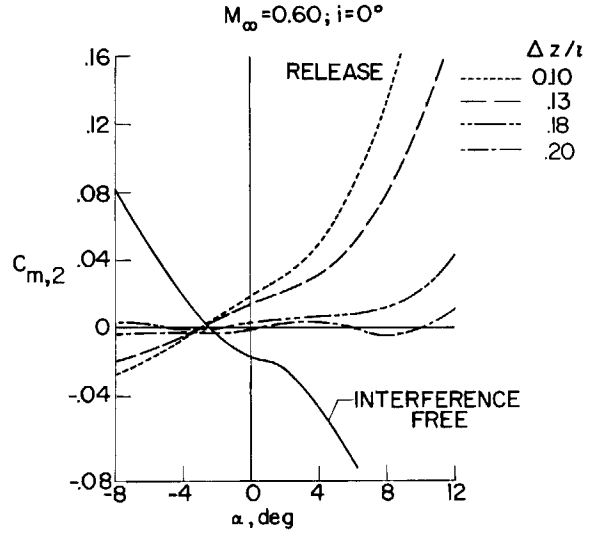

Slide 13.

EFFECT OF DYNAMIC DERIVATIVES

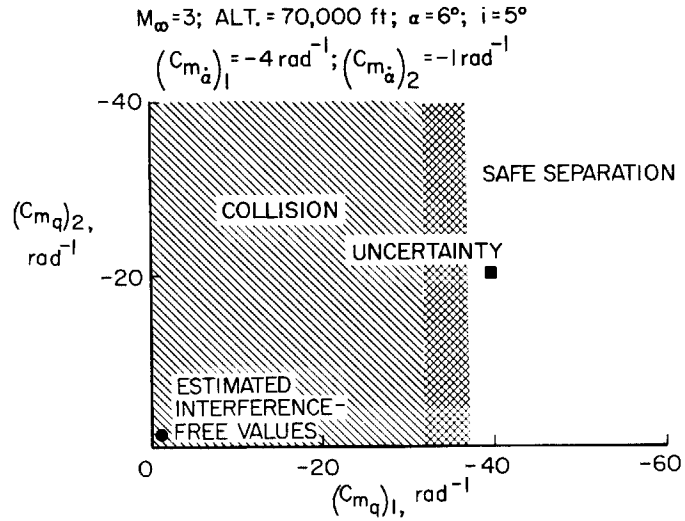

Slide 14.

[redacted]

EFFECT OF INITIAL ATTITUDE

$M_\infty = 3$; ALT. = 70 000 ft; $(C_{m_q})_1 = -40\,\text{rad}^{-1}$;

$(C_{m_q})_2 = -20\,\text{rad}^{-1}$; $(C_{m_{\dot\alpha}})_1 = -4\,\text{rad}^{-1}$; $(C_{m_{\dot\alpha}})_2 = -1\,\text{rad}^{-1}$

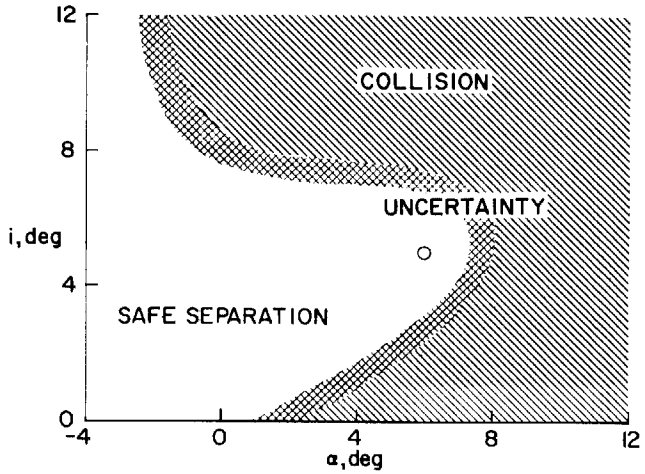

Slide 15.

EFFECT OF DYNAMIC PRESSURE

$M_\infty = 3$; $\alpha = 6°$; $i = 5°$; $(C_{m_q})_1 = -40\,\text{rad}^{-1}$; $(C_{m_q})_2 = -20\,\text{rad}^{-1}$

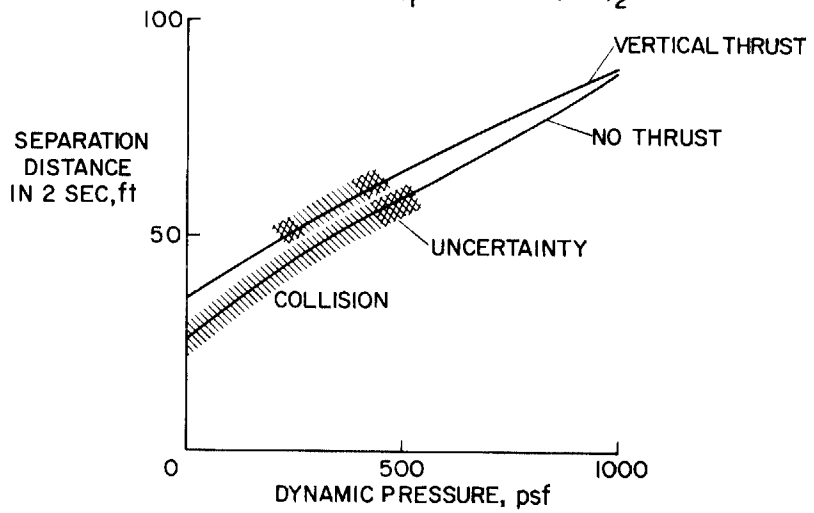

Slide 16.

[redacted]

5. The Prospects of Aerodynamic Performance Gains From Wing Camber and Twist at Low Hypersonic Mach Numbers - Ralph L. Carmichael

DRAG DUE TO LIFT FOR A DELTA WING

$\Lambda = 70°$

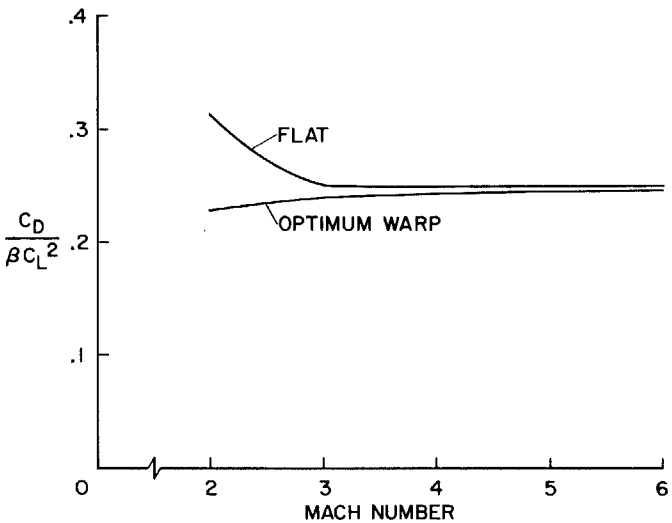

Slide 1.

TYPICAL PANEL LAYOUT FOR WING-BODY COMBINATION

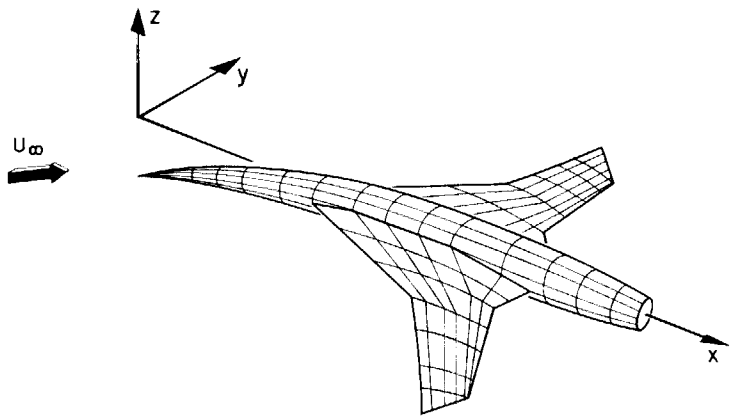

Slide 2.

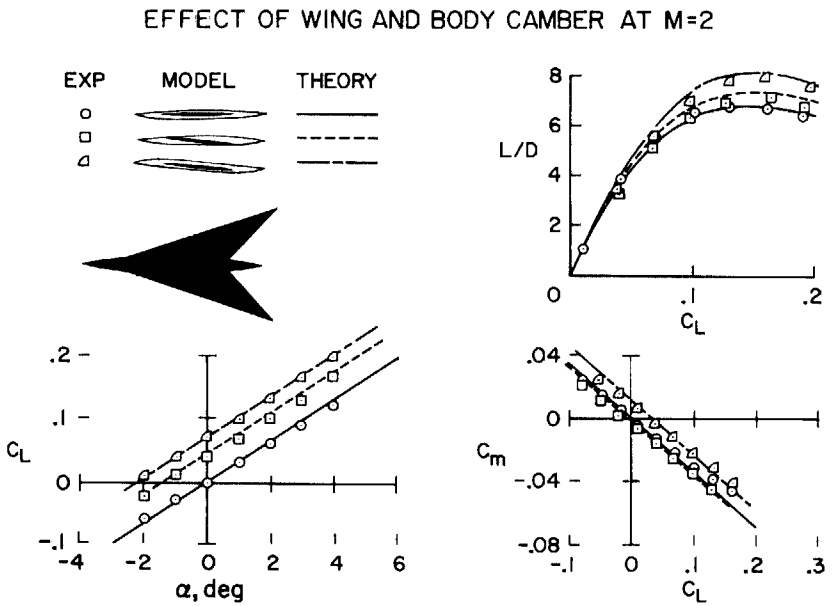

Slide 3.

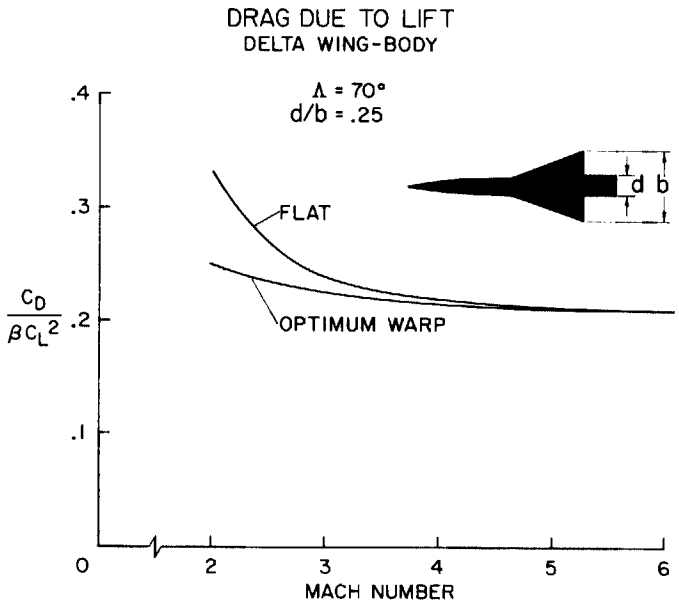

Slide 4.

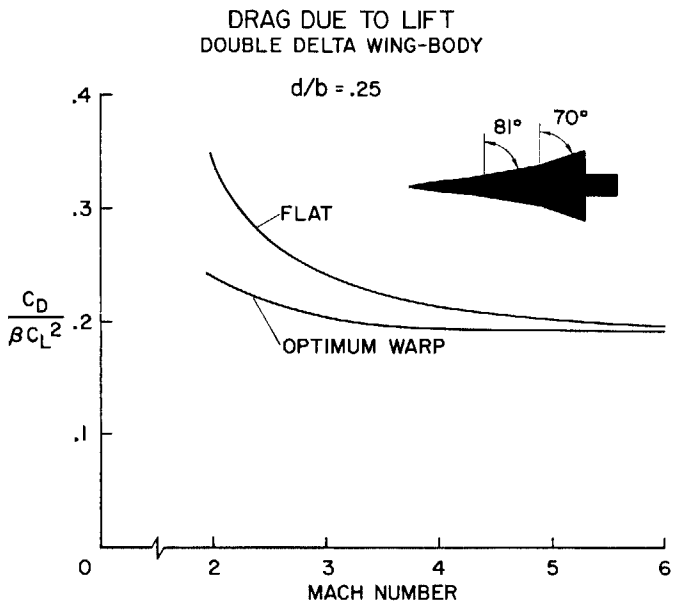

Slide 5.

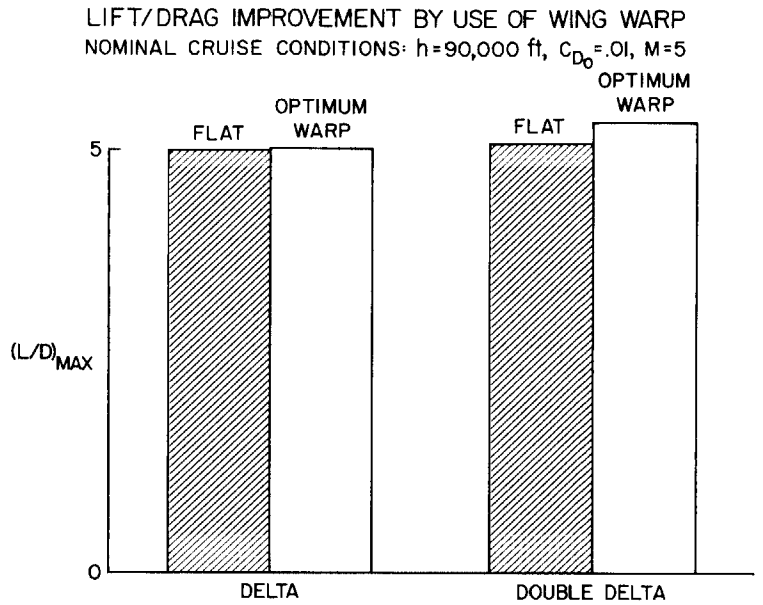

Slide 6.

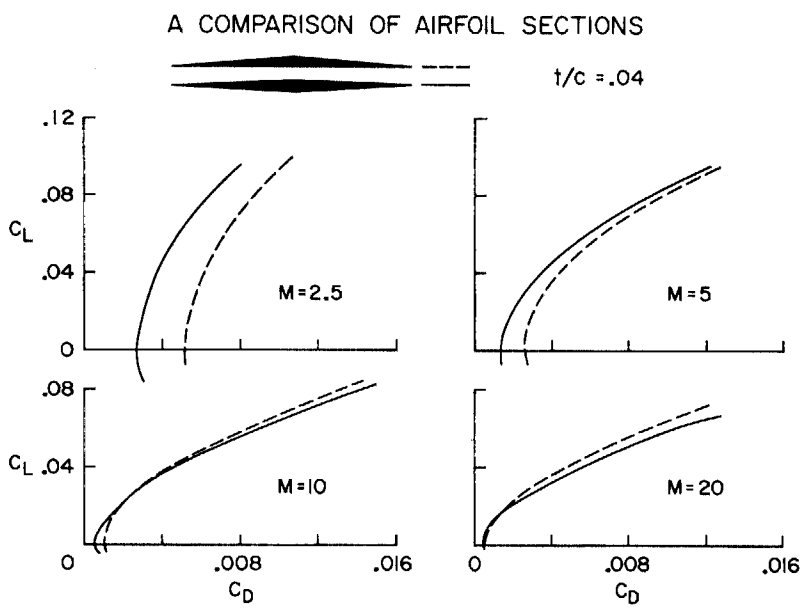
A COMPARISON OF AIRFOIL SECTIONS
t/c =.04
.12
.08
.04
0
C_L
M=2.5
M=5
M=10
M=20
.008
.016
C_D

Slide 7.

[redacted]

6. Studies of Optimum Body Shapes - Louis S. Stivers, Jr., and Bernard Spencer, Jr.

[redacted]

QUESTIONS TO BE CONSIDERED

- WHAT PROFILE SHOULD BE USED?
- WHAT IS THE EFFECT OF BASE AREA?
- WHAT IS THE EFFECT OF CROSS-SECTIONAL SHAPE?

Slide 1.

ILLUSTRATION OF BODY CUT-OFFS

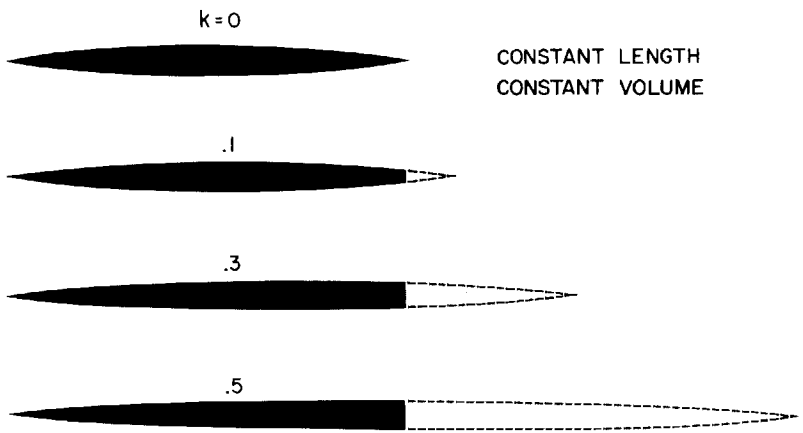

Slide 2.

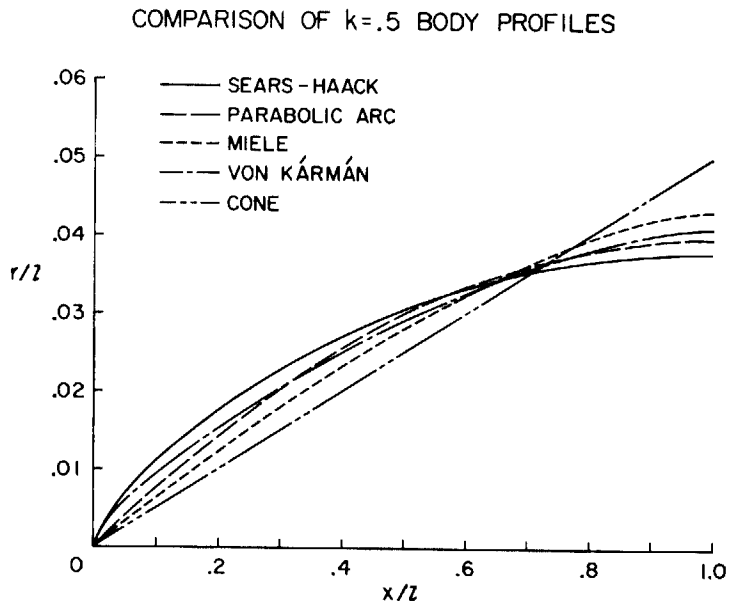

Slide 3.

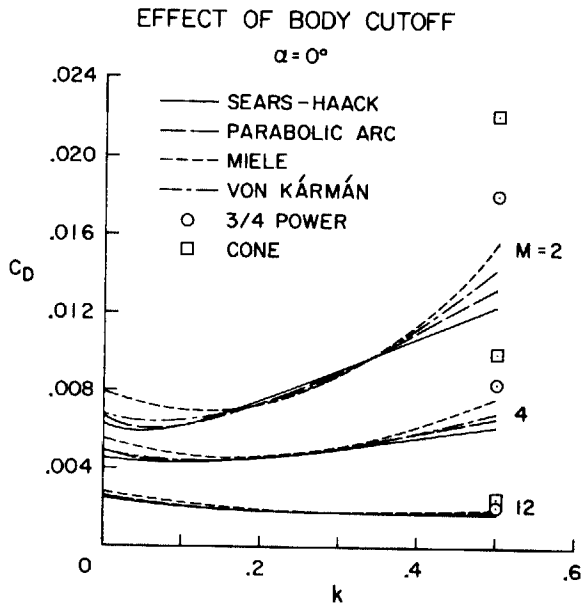

Slide 4.

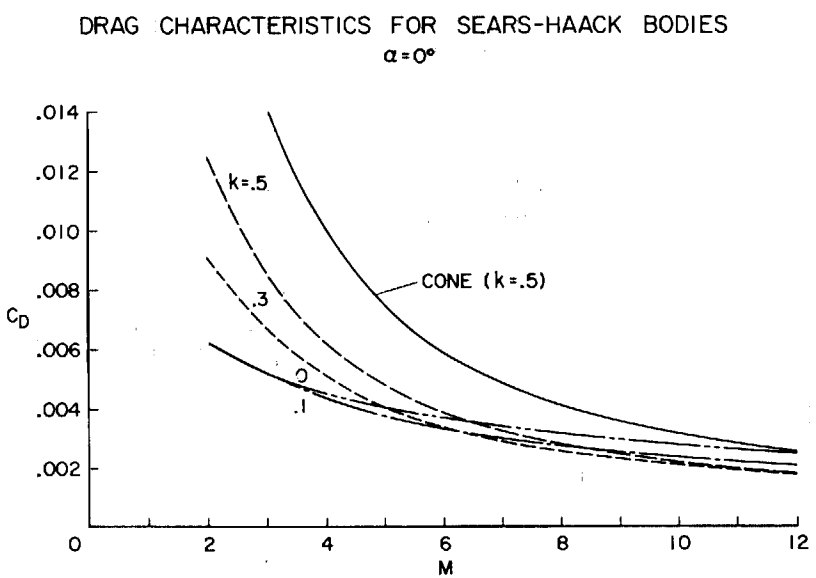

Slide 5.

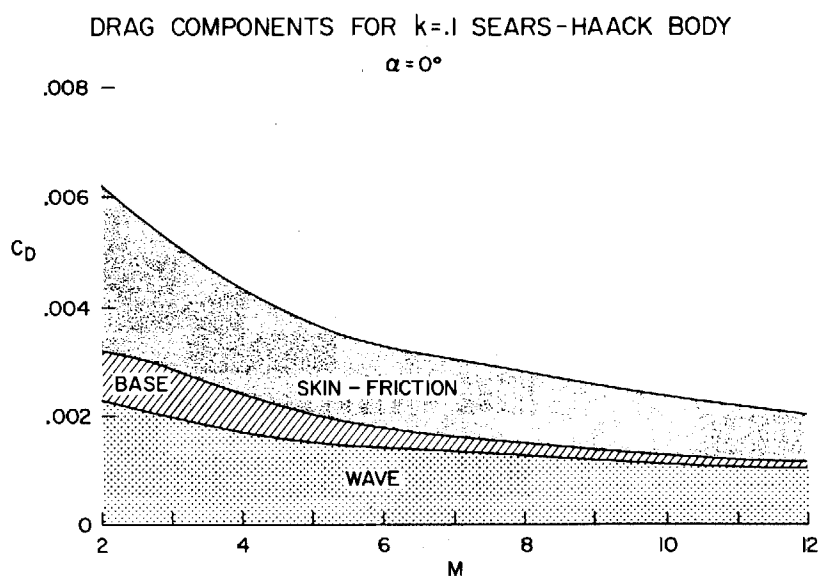

Slide 6.

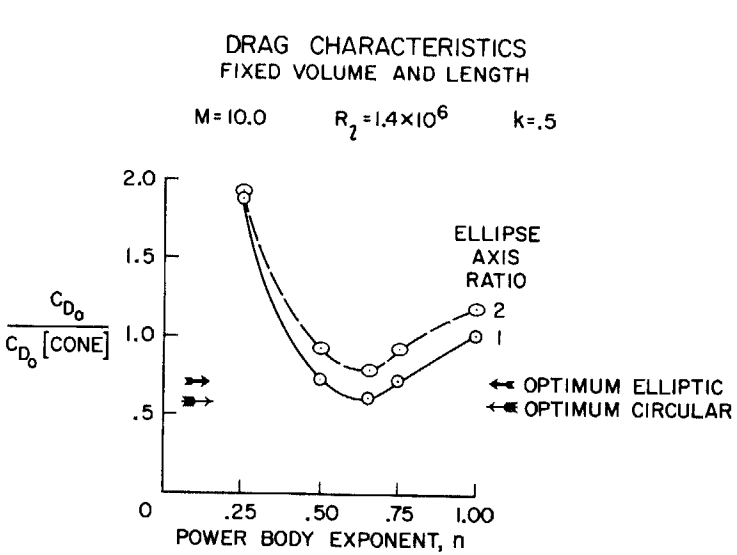

Slide 7.

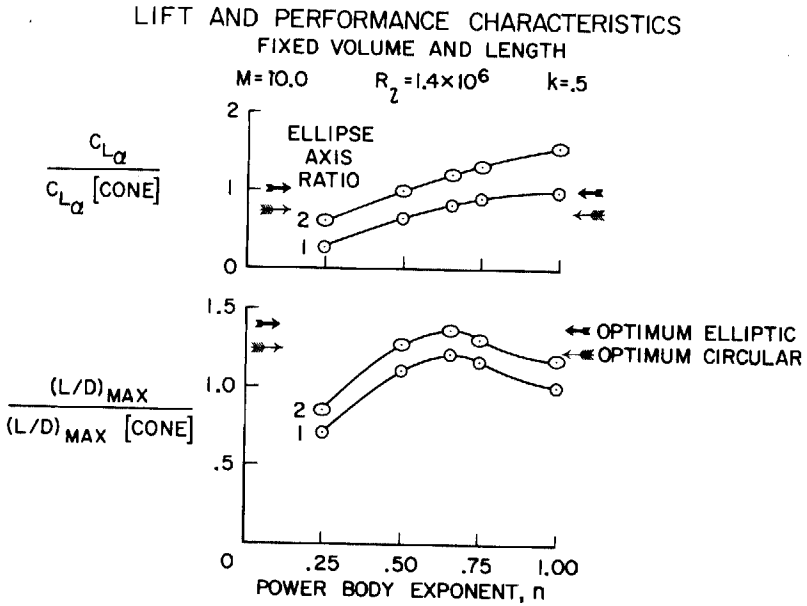

Slide 8.

CONFIDENTIAL

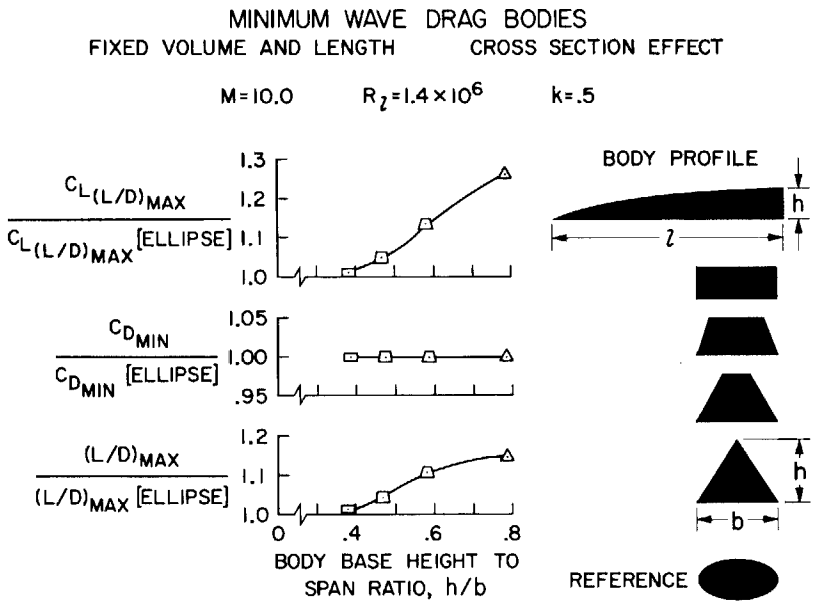

Slide 9.

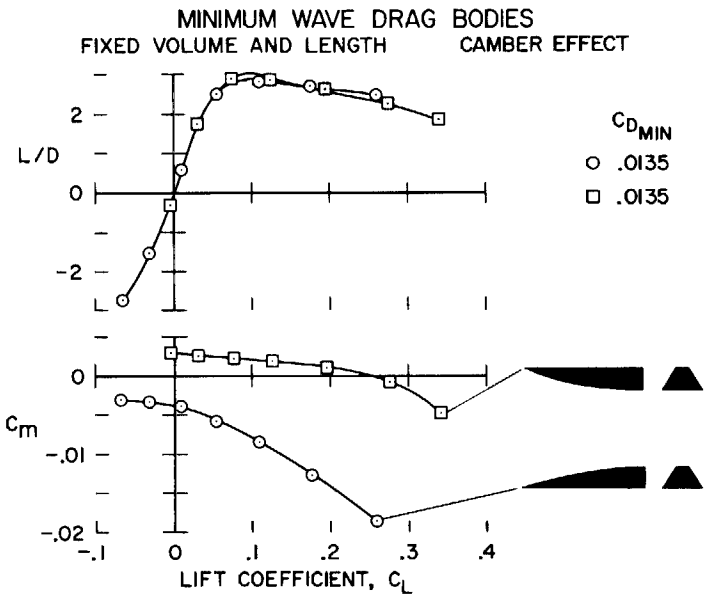

Slide 10.

7. A Study of Numerical Methods for Predicting Flow About Bodies at Angle of Attack - William F. Gallo, John V. Rakich, and Joseph W. Cleary 7

CONFIDENTIAL

THEORETICAL METHODS

1. EXACT THREE-DIMENSIONAL METHOD OF CHARACTERISTICS
2. LINEARIZED METHOD OF CHARACTERISTICS
   $V^2 = (V_0 + \alpha V_1 \cos\phi)^2 + (\alpha w_1 \sin\phi)^2$
3. BABENKO TABULATED CONE SOLUTIONS
4. EQUIVALENT BODY

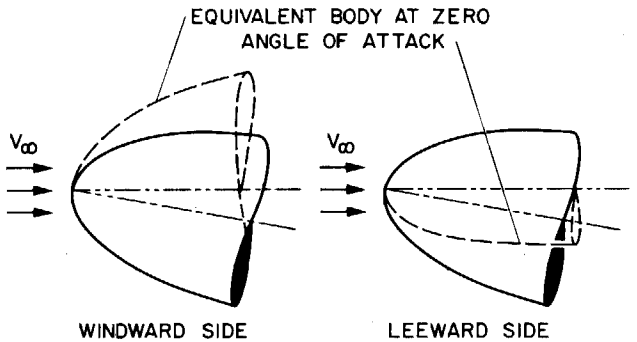

Slide 1.

PITOT PRESSURE PROFILE

15° SHARP CONE $M_\infty = 10.6$ WINDWARD SIDE

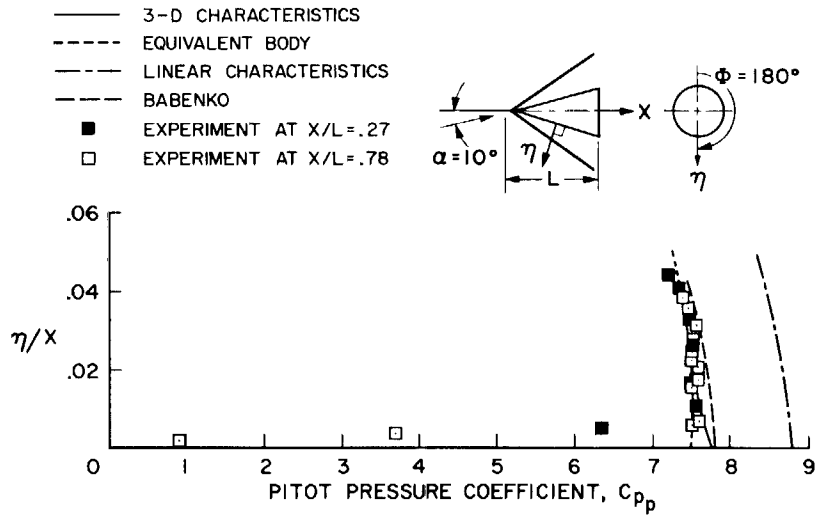

Slide 2.

CONFIDENTIAL

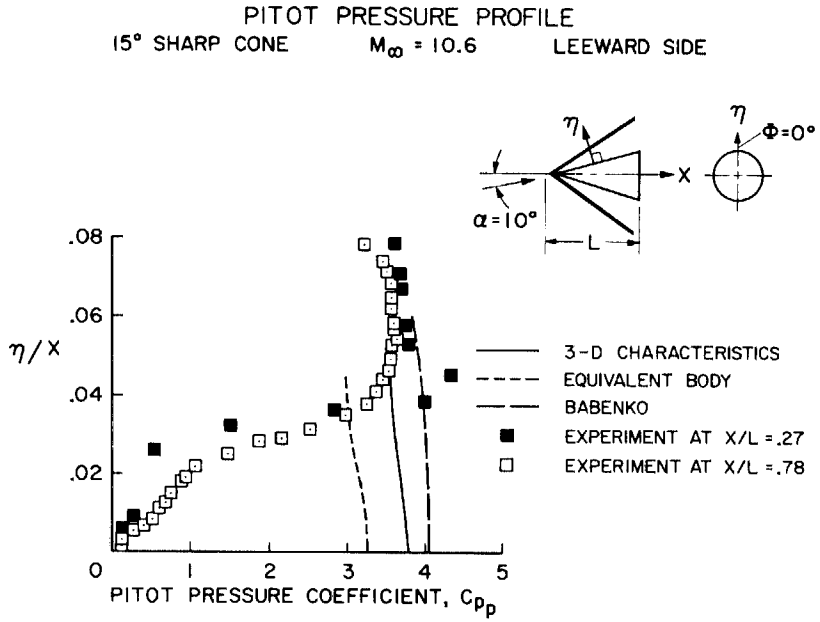

Slide 3.

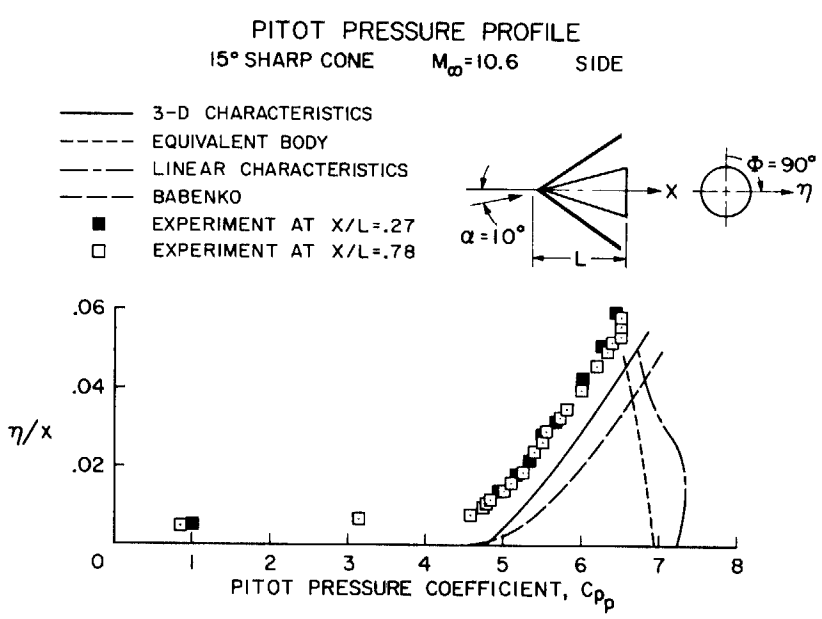

Slide 4.

CONFIDENTIAL

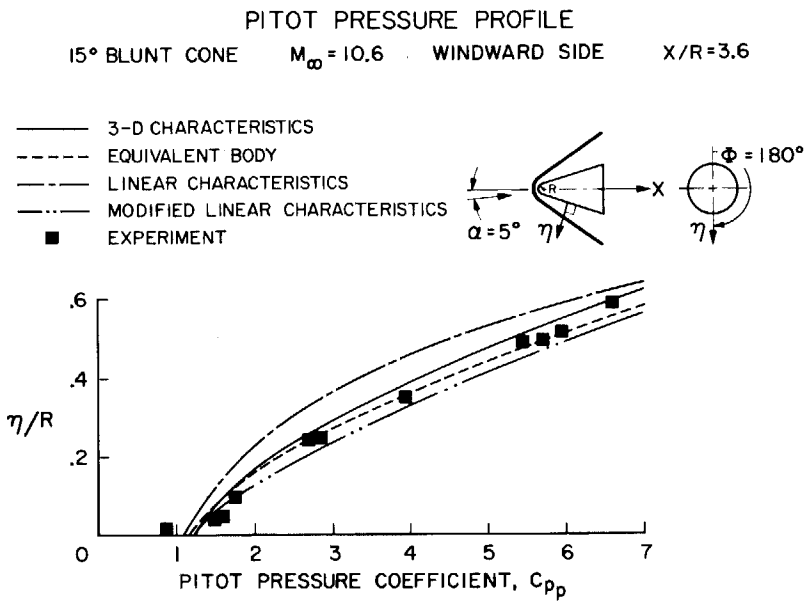

Slide 5.

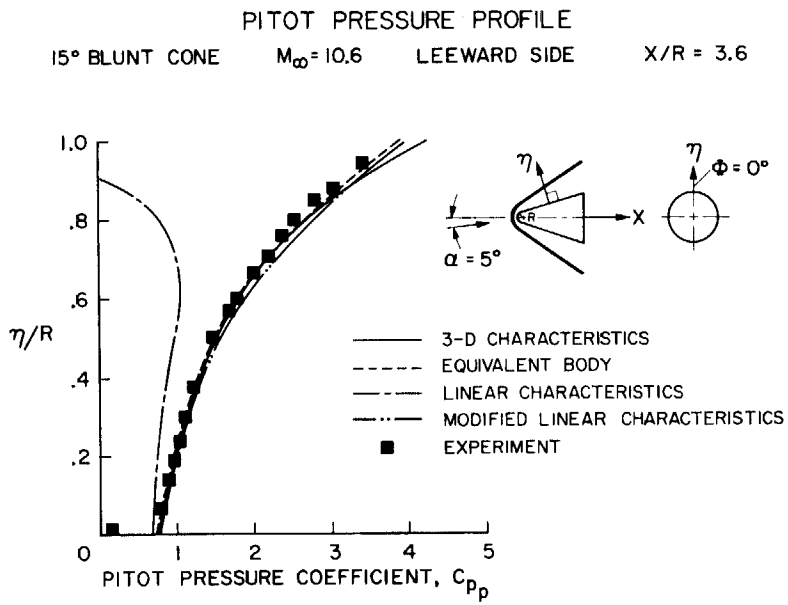

Slide 6.

CONFIDENTIAL

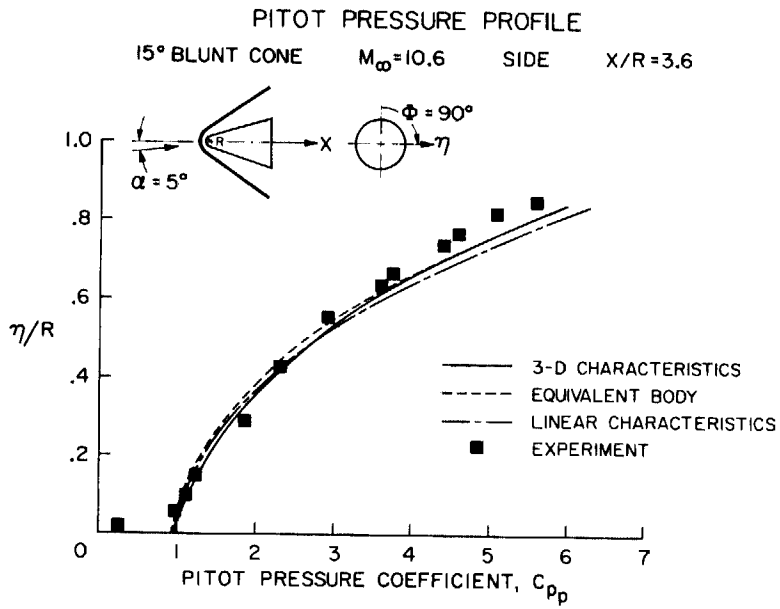

Slide 7.

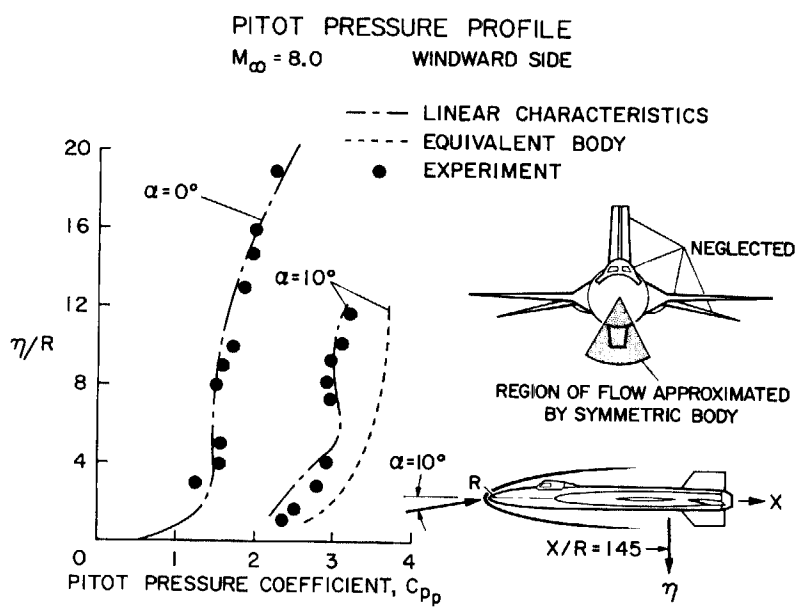

Slide 8.

THEORETICAL MACH NUMBER PROFILE

$M_\infty = 8.0$ WINDWARD SIDE

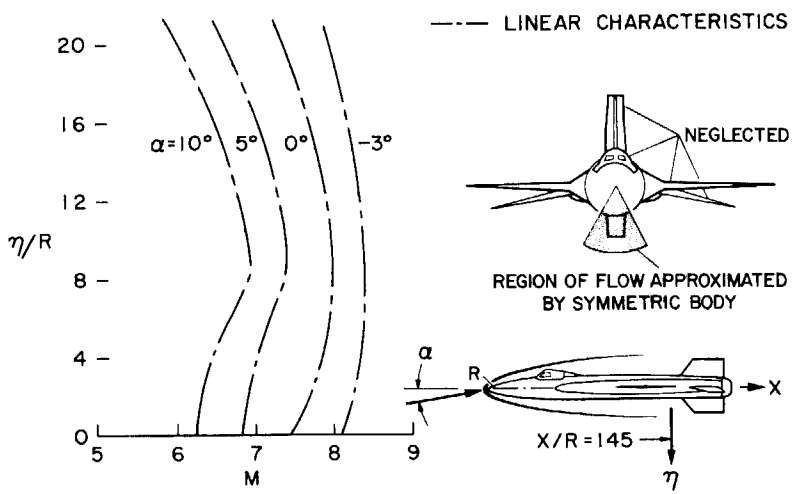

Slide 9.

APPLICABILITY OF THEORIES

	BABENKO CONICAL	3 DIMENSIONAL CHARACTERISTICS	EQUIVALENT BODY	LINEARIZED CHARACTERISTICS	MODIFIED LINEAR
SHARP 15° CONE	GENERALLY GOOD	GENERALLY GOOD	FAIR	FAIR TO POOR	---
BLUNT 15° CONE X/R ≤ 4	---	GOOD	GOOD	POOR	GOOD
SLENDER X-15 FINENESS RATIO ≈ 7	---	---	FAIR	GOOD	---

Slide 10.

8. Studies of Airframe-Propulsion System Integration for Mach 6 Cruise Vehicles - Frank S. Kirkham, James M. Cubbage, Jr., Walter A. Vahl, and William J. Small

MACH 6 CRUISE CONFIGURATION

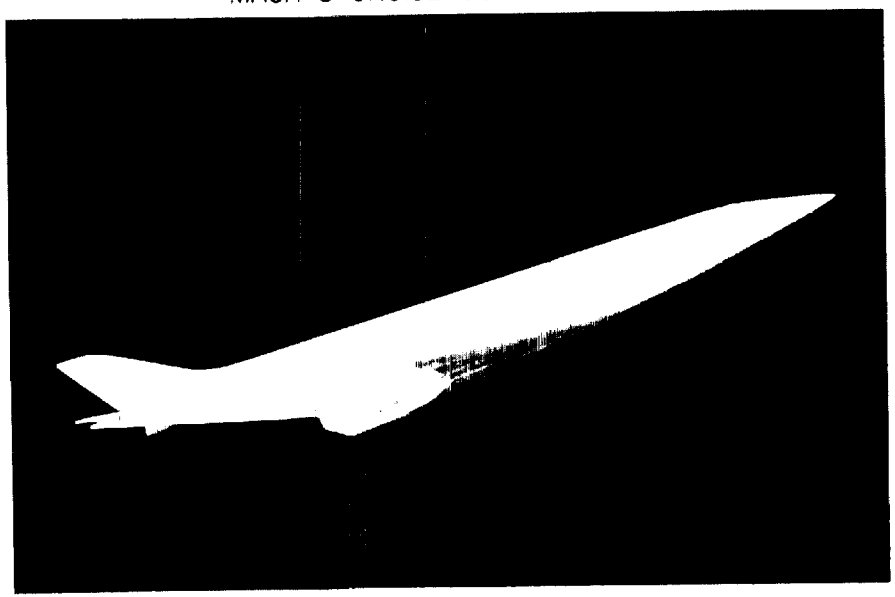

Slide 1.

NOZZLE-EXIT-PRESSURE RATIOS

$M_\infty = 6$

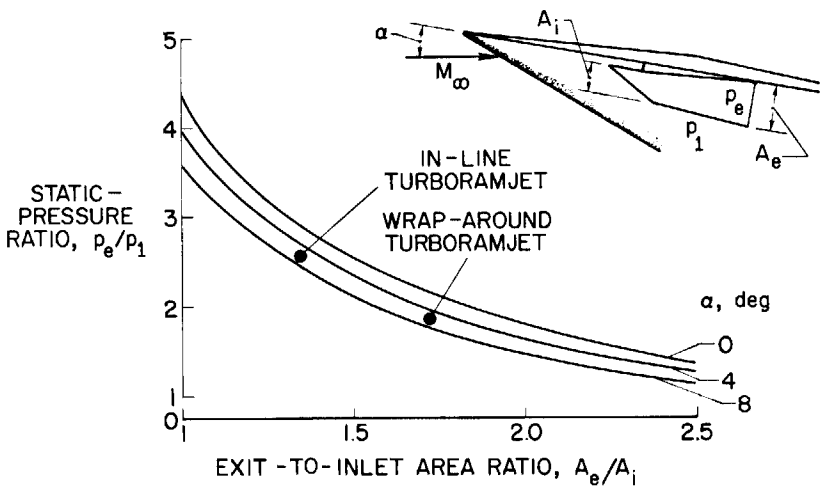

Slide 2.

RAMJET SPECIFIC IMPULSE

$M_\infty = 6$

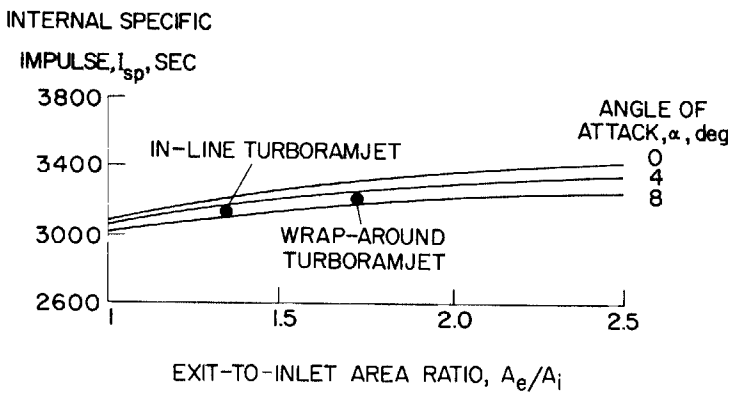

Slide 3.

NACELLE CONFIGURATIONS INVESTIGATED

$M_\infty = 6$; $\frac{A_{i,t}}{S_w} = 0.018$

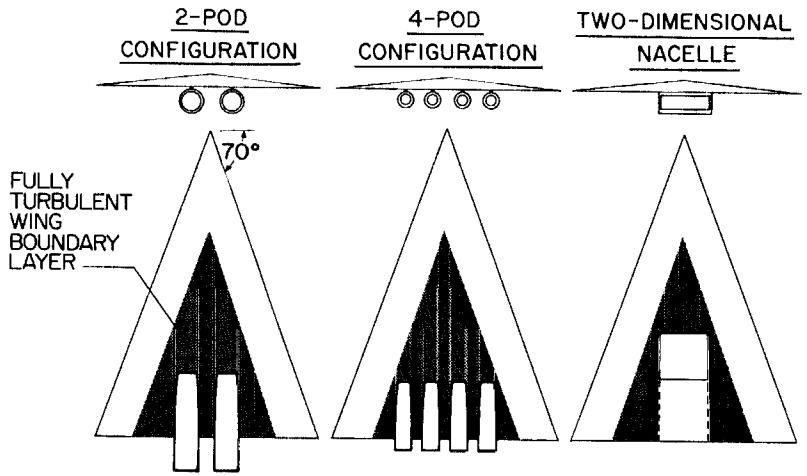

Slide 4.

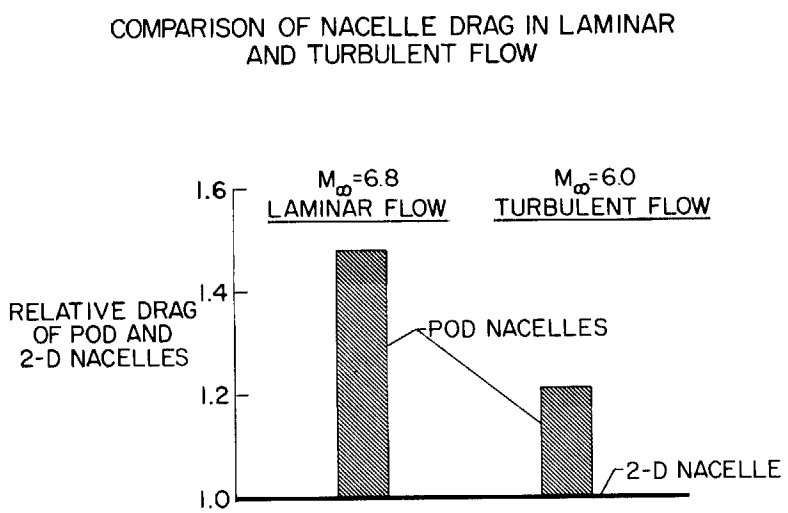

Slide 5.

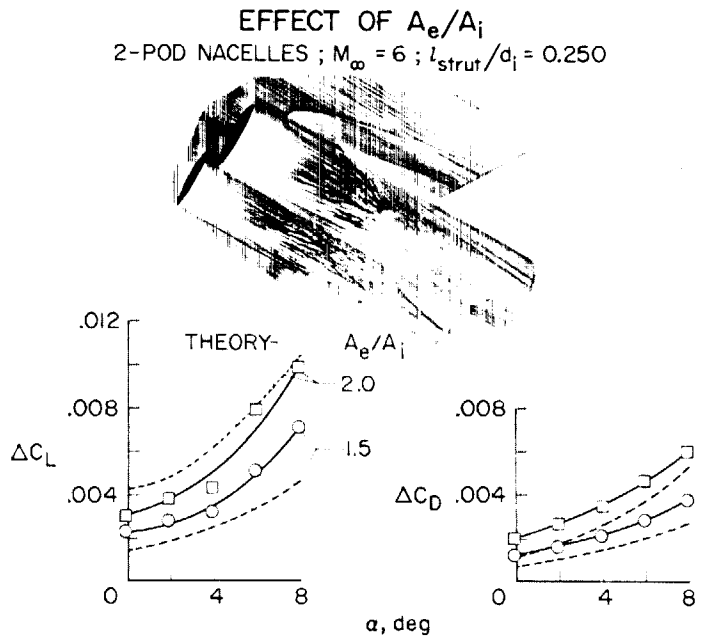

Slide 6.

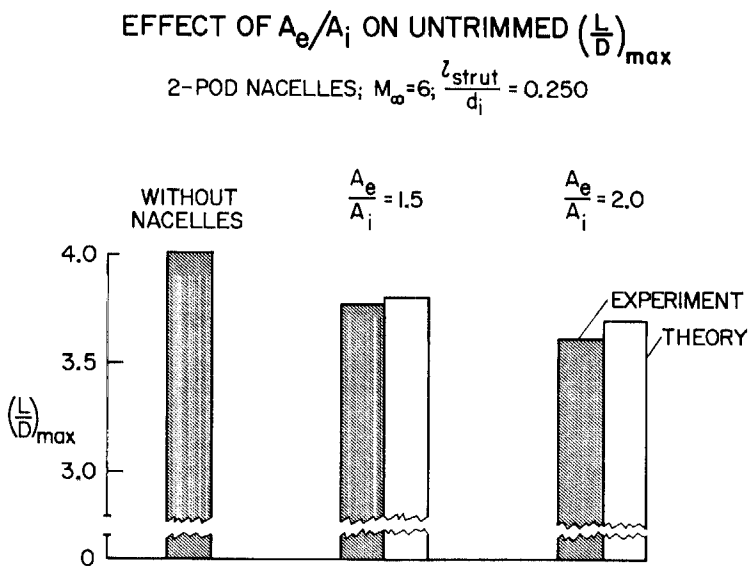

Slide 7.

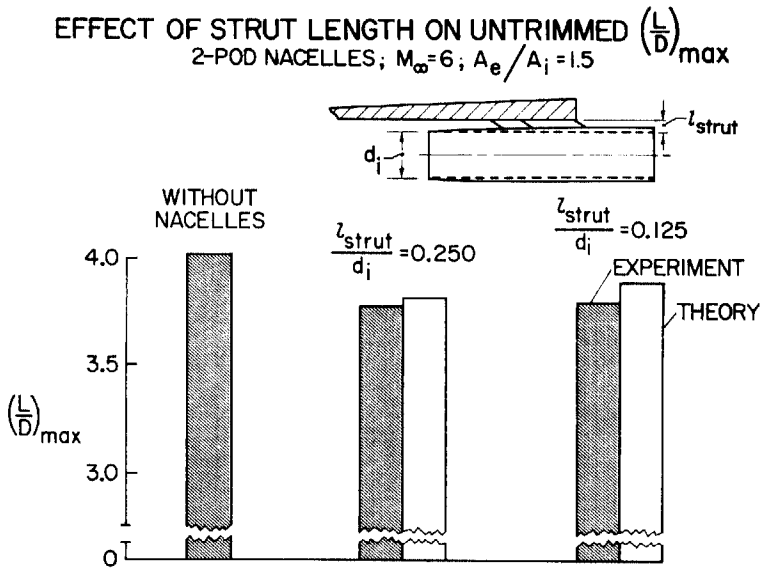

Slide 8.

EFFECT OF NUMBER OF NACELLES ON UNTRIMMED $\left(\frac{L}{D}\right)_{max}$

$M_\infty = 6;\ A_e/A_i = 1.5;\ \frac{l_{strut}}{d_i} = 0.250$

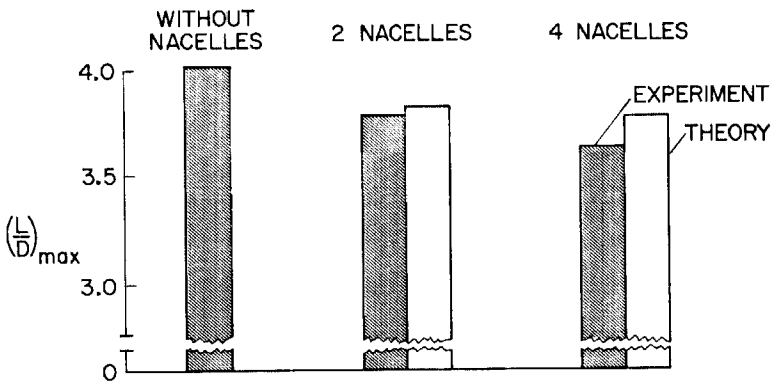

Slide 9.

TWO-DIMENSIONAL NACELLE WITH FLOW-THROUGH DIVERTER

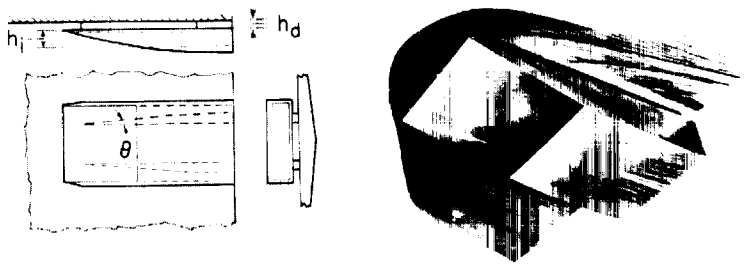

Slide 10.

EFFECT OF 2-DIMENSIONAL NACELLES ON UNTRIMMED $\left(\frac{L}{D}\right)_{max}$

$M_\infty = 6$; $A_e/A_i = 1.5$

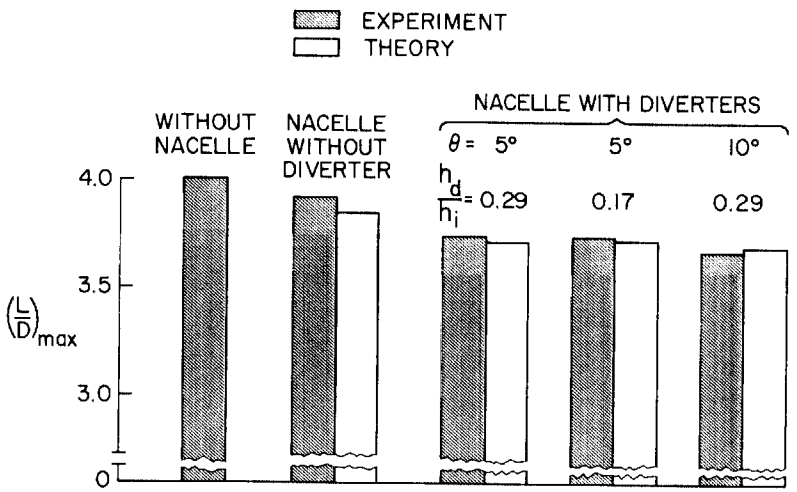

Slide 11.

SUMMARY OF 2-DIMENSIONAL AND POD NACELLE PERFORMANCE

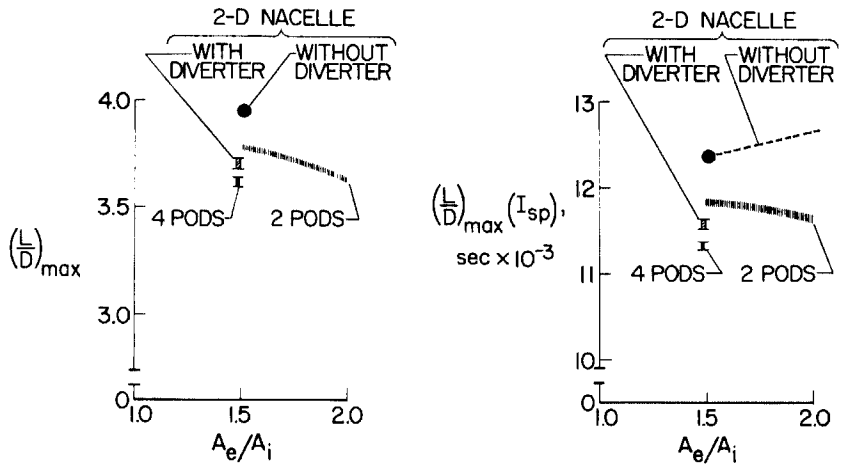

Slide 12.

JET-INTERFERENCE FLOW MODEL

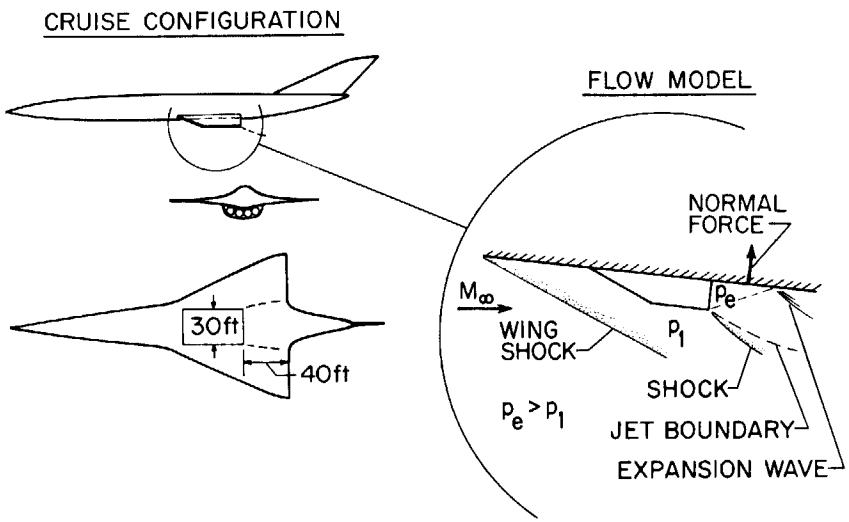

Slide 13.

EFFECT OF JET INTERFERENCE ON $\frac{L}{D}$

$M_\infty = 6$; ALTITUDE = 100000 ft ; $\left(\frac{L}{D}\right)_o = 5$

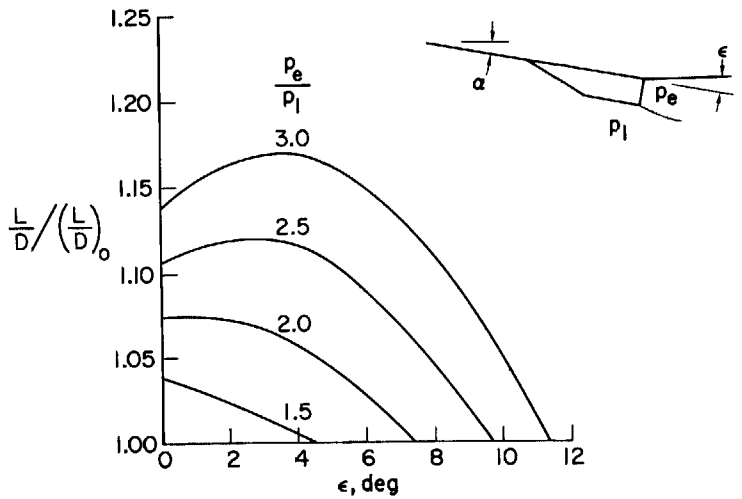

Slide 14.

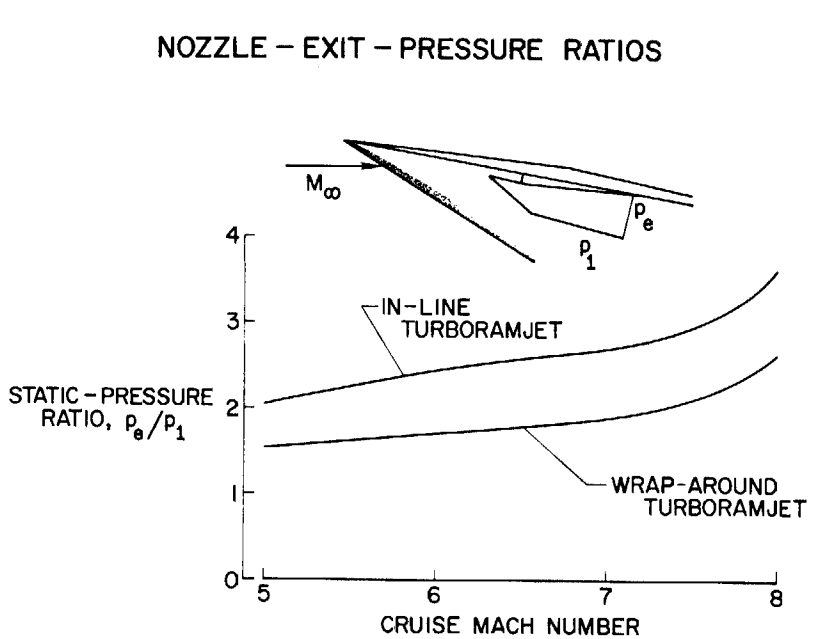

Slide 15.

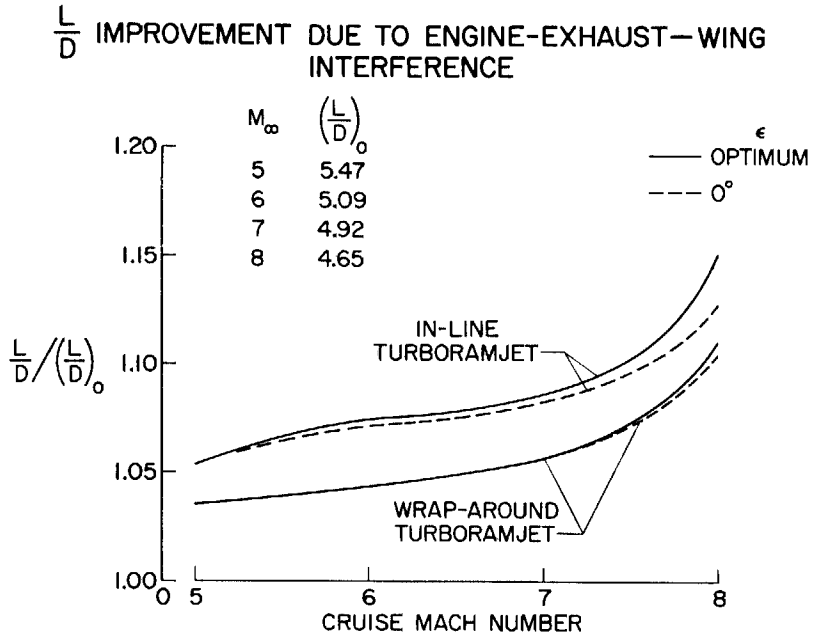

Slide 16.

9. Scramjet Vehicle Engine-Airframe Integration Effects - Louis J. Williams and Darrell E. Wilcox

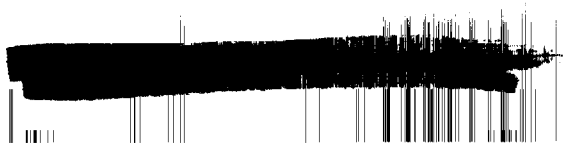

CONFIGURATIONS

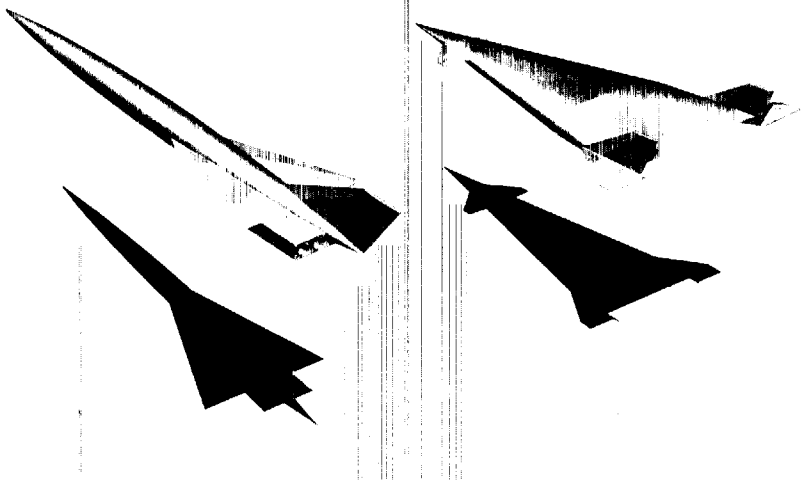

Slide 1.

ENGINE - AIRFRAME INTEGRATION

$$C_I = \frac{(BF)_{ACTUAL}}{(BF)_{IDEAL}}$$

$$(BF)_{IDEAL} = \frac{V(L/D)_{AIRFRAME}\,(I_{SP})_{ENGINE}}{1-(V/V_S)^2}$$

$(L/D)_{AIRFRAME}$ 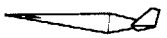

$(I_{SP})_{ENGINE}$ 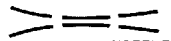

$$(BF)_{ACTUAL} = \frac{WV}{\dot{W}}$$

$$(BF)_{ACTUAL} = C_I\ (BF)_{IDEAL}$$

Slide 2.

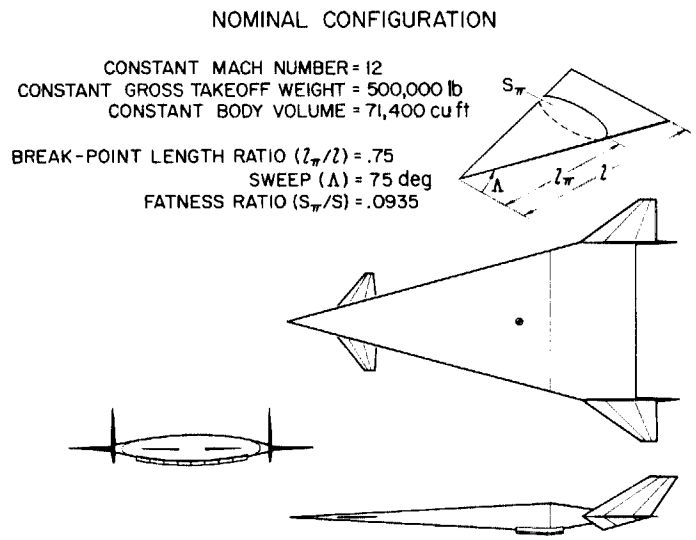

Slide 3.

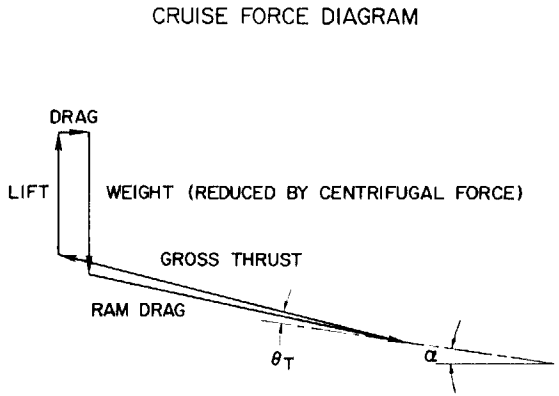

Slide 4.

10. Handling Qualities of Hypersonic Cruise Aircraft - Harold J. Walker and Milton O. Thompson 10

H. J. Walker

HIGH-SPEED CRUISE CONFIGURATIONS

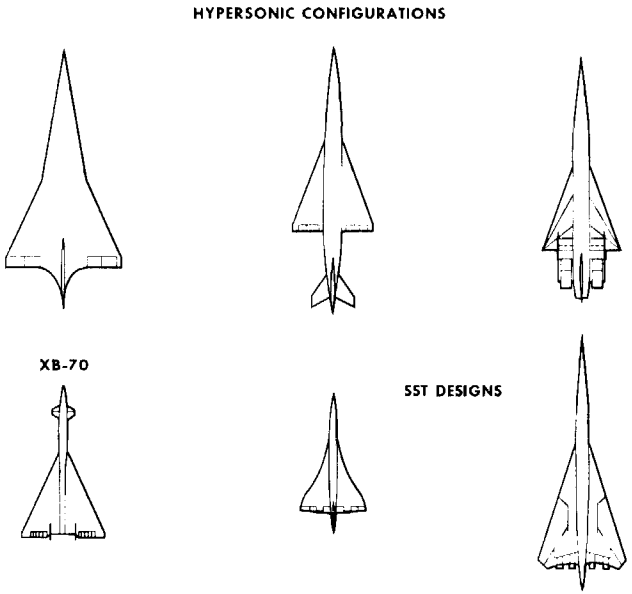

Slide 1.

TREND IN LIFT-TO-MASS RATIO

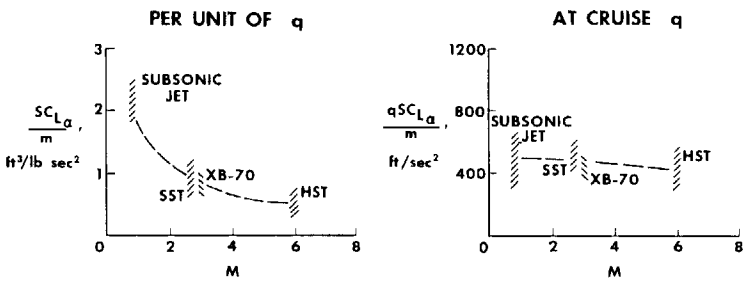

Slide 2.

H. J. Walker

PATH ALTERATION TIME

$$\frac{\Delta t}{\Delta \gamma} \approx \frac{V}{g n_z}; \quad n_z = \frac{1}{10} g$$

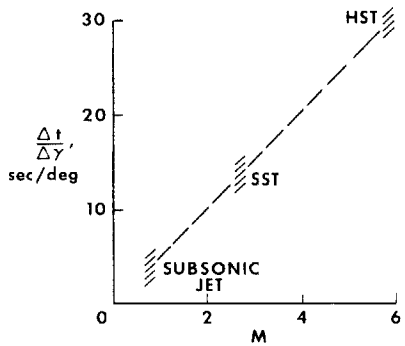

Slide 3.

FLIGHT-PATH ACCURACY

$$\Delta \gamma \approx \frac{1}{V} \Delta \dot{h}$$

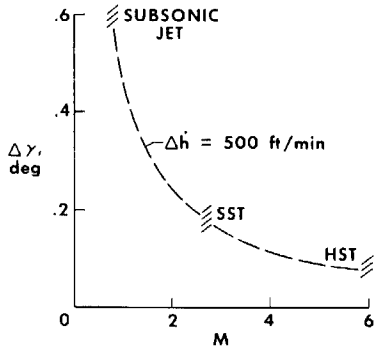

Slide 4.

[redacted]

11. Some Effects of Mach Number and Geometry on Sonic Boom - Raymond M. Hicks, Joel P. Mendoza, and Lynn W. Hunton

[redacted]

DESCRIPTION OF THEORETICAL AND EXPERIMENTAL PROCEDURE

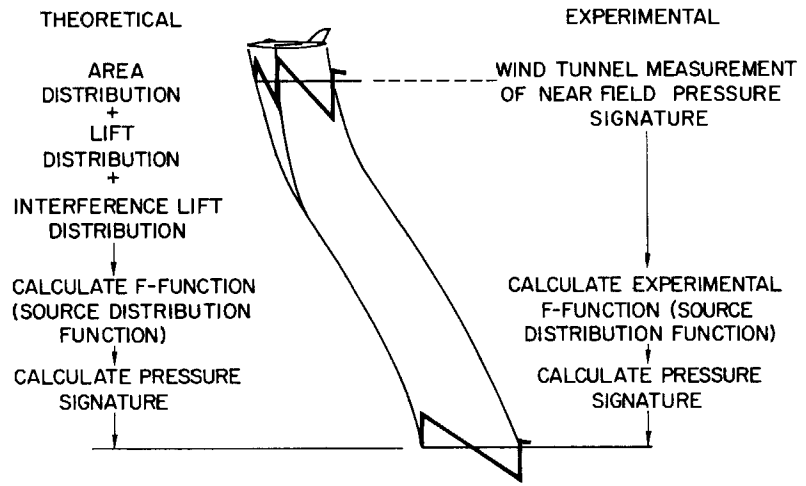
THEORETICAL
AREA DISTRIBUTION + LIFT DISTRIBUTION + INTERFERENCE LIFT DISTRIBUTION
CALCULATE F-FUNCTION (SOURCE DISTRIBUTION FUNCTION)
CALCULATE PRESSURE SIGNATURE
EXPERIMENTAL
WIND TUNNEL MEASUREMENT OF NEAR FIELD PRESSURE SIGNATURE
CALCULATE EXPERIMENTAL F-FUNCTION (SOURCE DISTRIBUTION FUNCTION)
CALCULATE PRESSURE SIGNATURE

Slide 1.

EVALUATION OF EXPERIMENTAL PROCEDURE

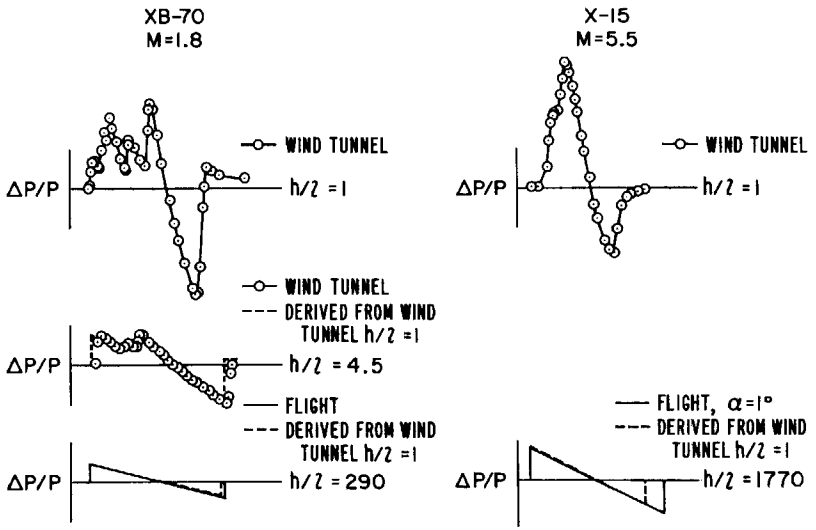

Slide 2.

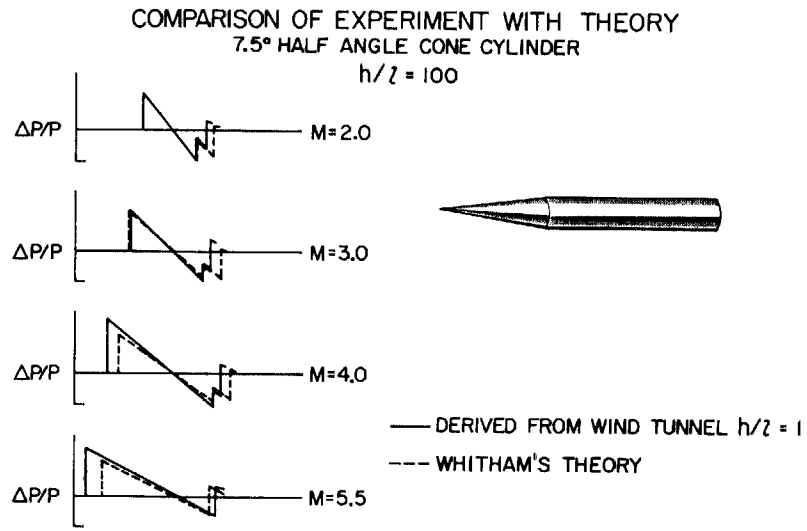

Slide 3.

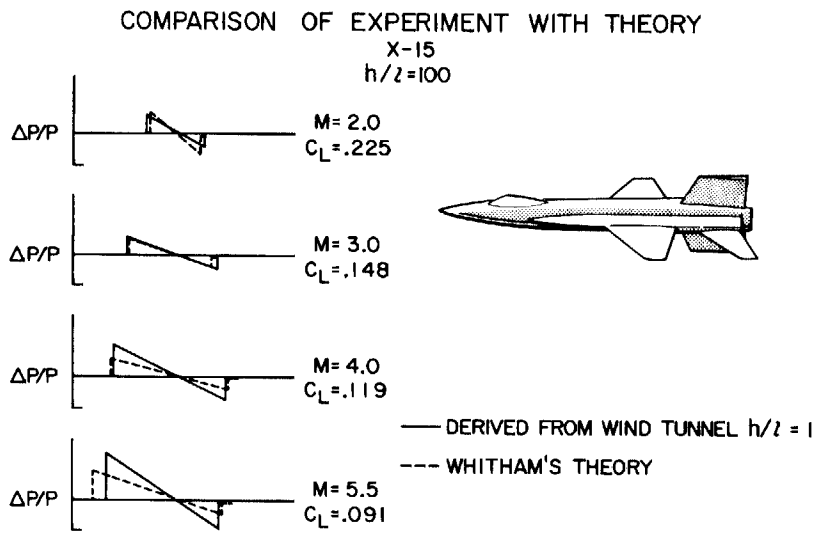

Slide 4.

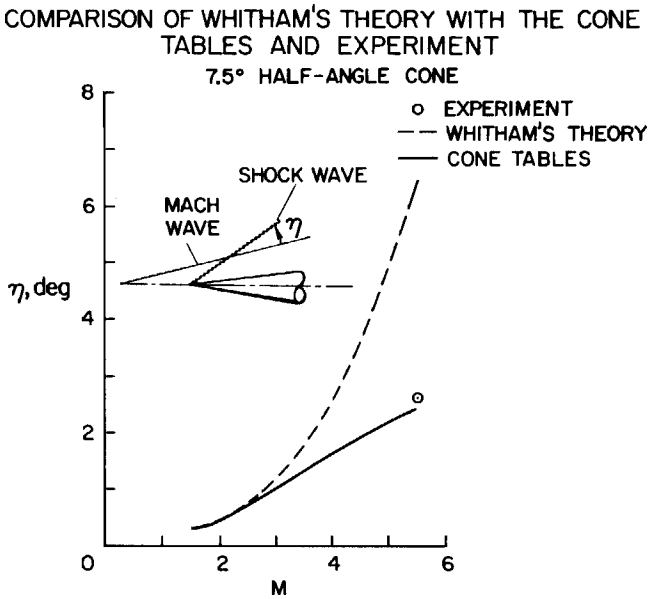

Slide 5.

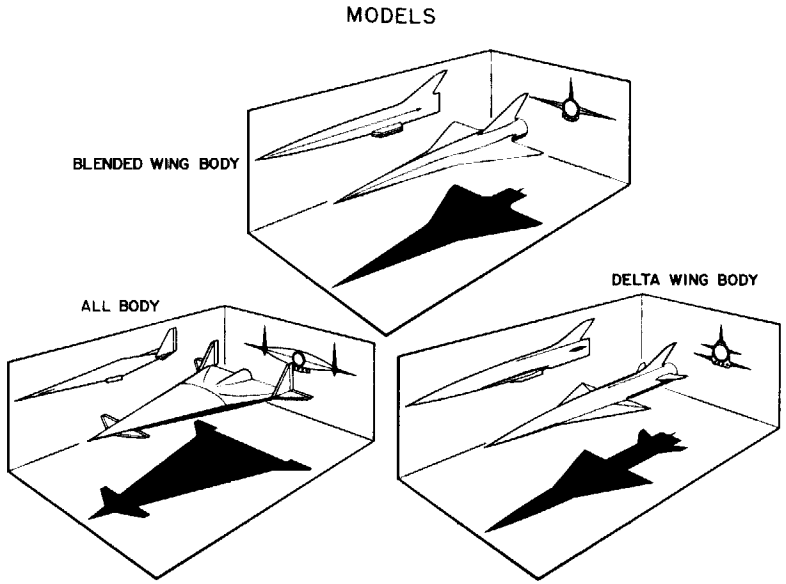

Slide 6.

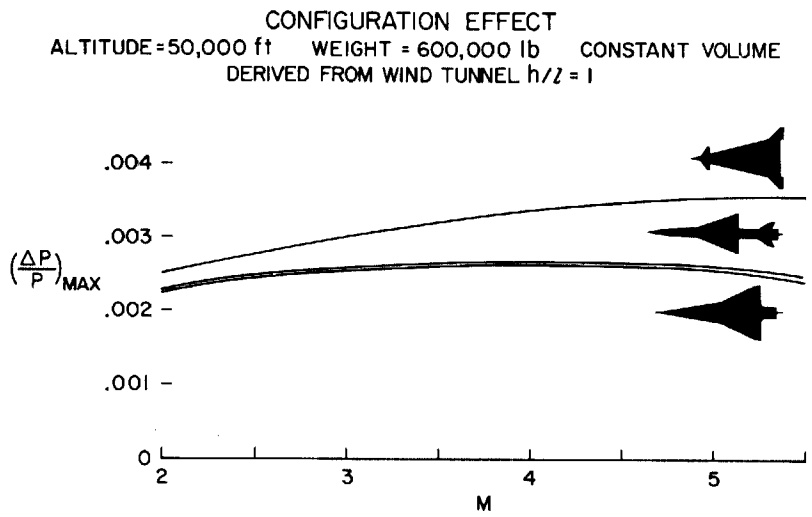

Slide 7.

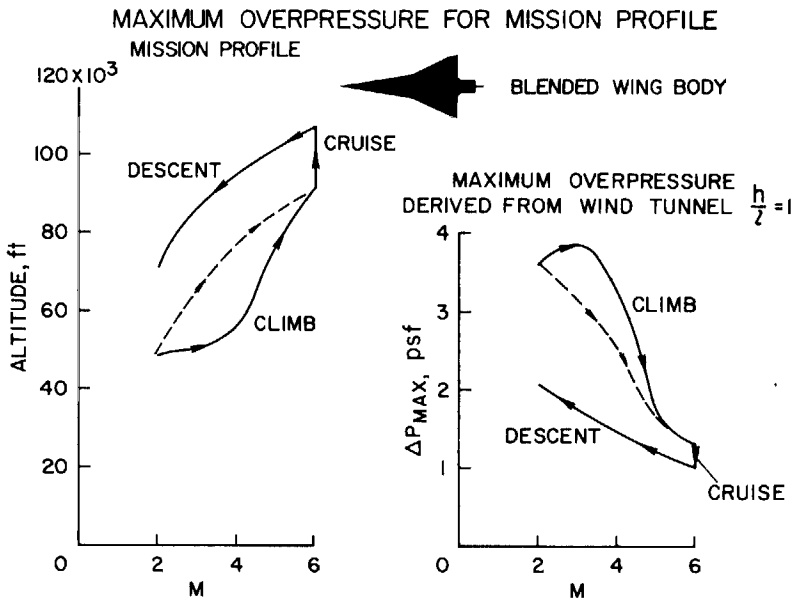

Slide 8.

12. Boundary Layer Transition on Hypersonic Cruise Aircraft - Kazimierz R. Czarnecki, Jerry M. Allen, and Mary W. Jackson

AIRPLANE COMPONENTS AFFECTED BY TRANSITION

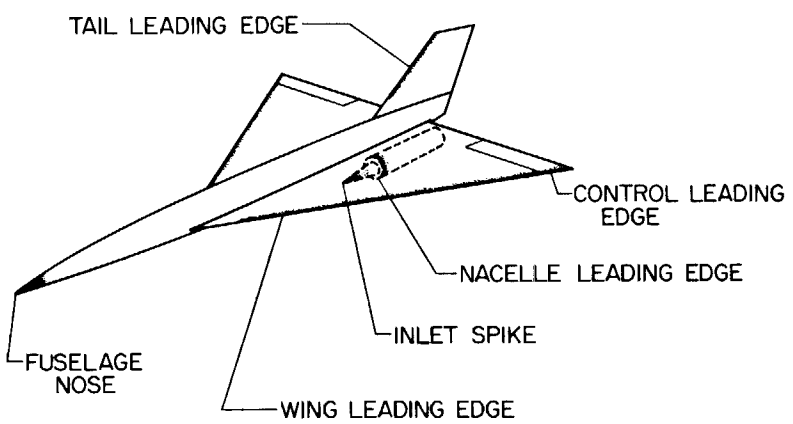

Slide 1.

TYPICAL TRANSITION DATA

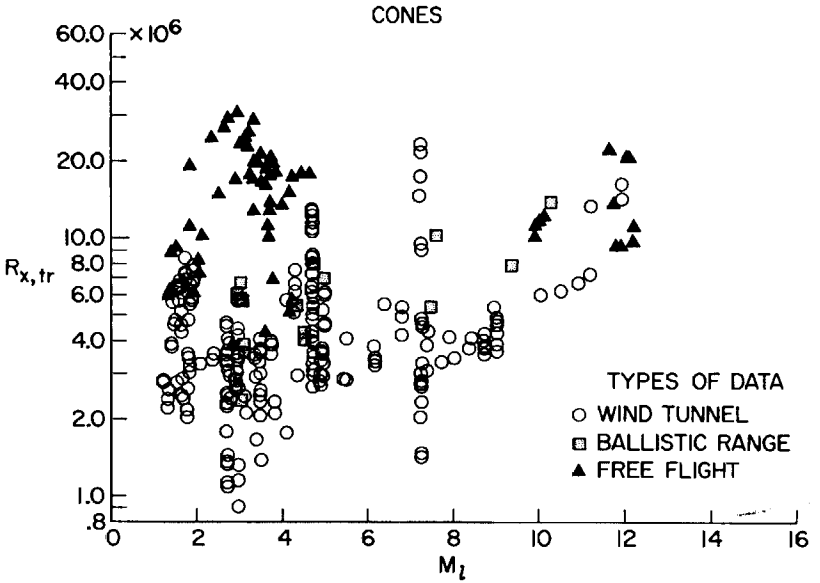

Slide 2.

K. R. Czarnecki

TRANSITION PARAMETERS

MACH NUMBER	STAGNATION TEMPERATURE
UNIT REYNOLDS NUMBER	TWO- OR THREE-DIMENSIONAL FLOW
HEAT TRANSFER	PRESSURE GRADIENTS
NOSE BLUNTING	SURFACE WAVINESS
WING SWEEP	SURFACE ROUGHNESS
ANGLE OF ATTACK	FREE-STREAM TURBULENCE
	NOISE AND VIBRATION

Slide 3.

EFFECT OF M_l AND R/ft ON TRANSITION

EXPERIMENTAL SHARP-CONE DATA

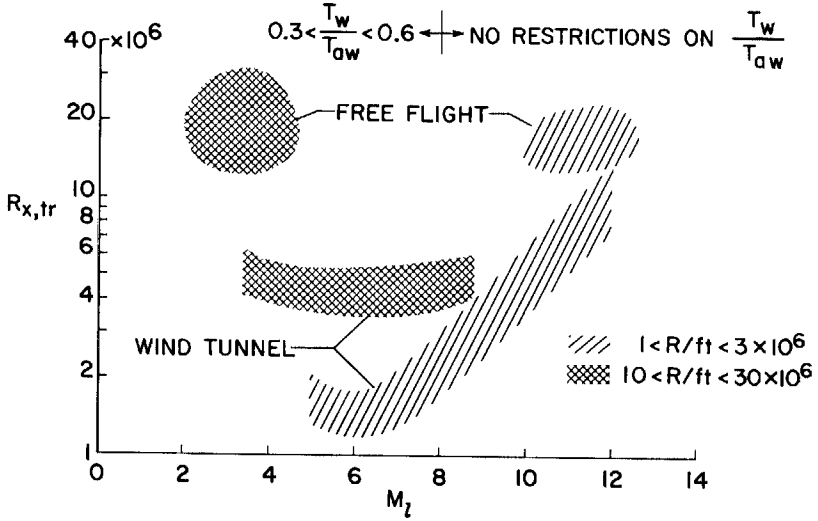

Slide 4. ✓

REASONS TO EXPECT UNIT REYNOLDS NUMBER EFFECT

- NOSE BLUNTING
- HYPERSONIC VISCOUS INTERACTION
- TUNNEL WALL EFFECTS
- ?

Slide 5.

SOME FACTORS AFFECTING TRANSITION

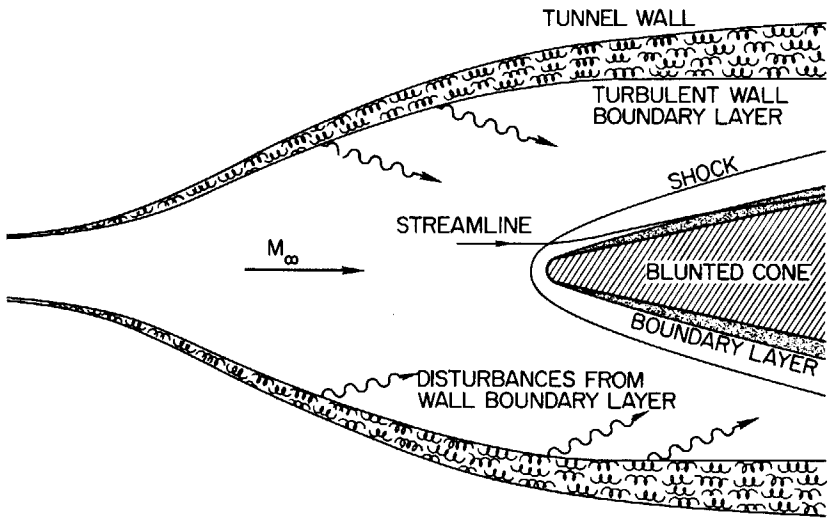

Slide 6.

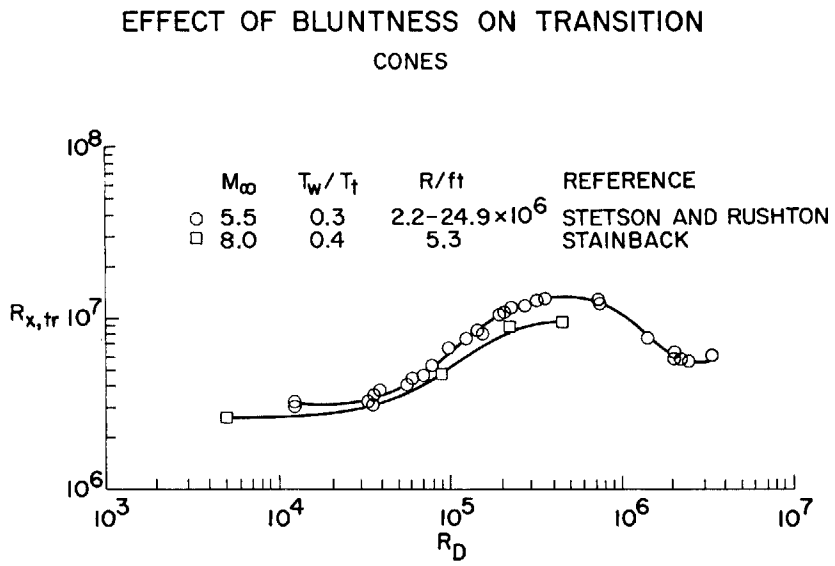

Slide 7.

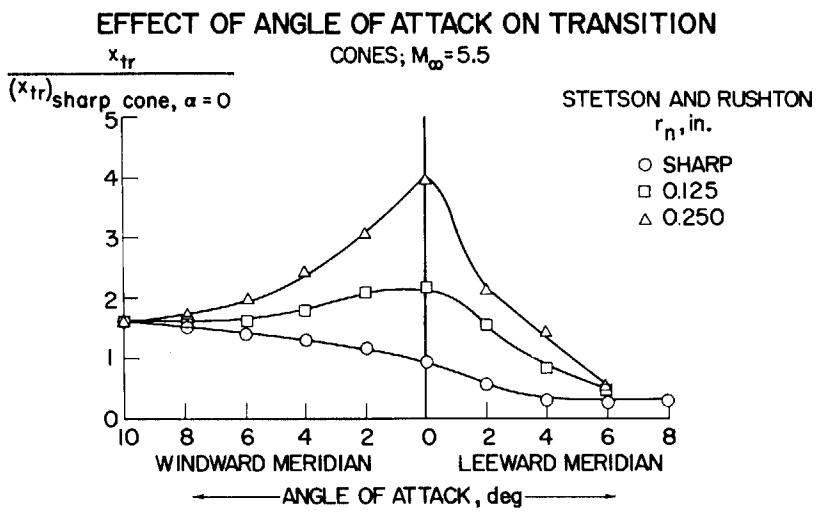

Slide 8.

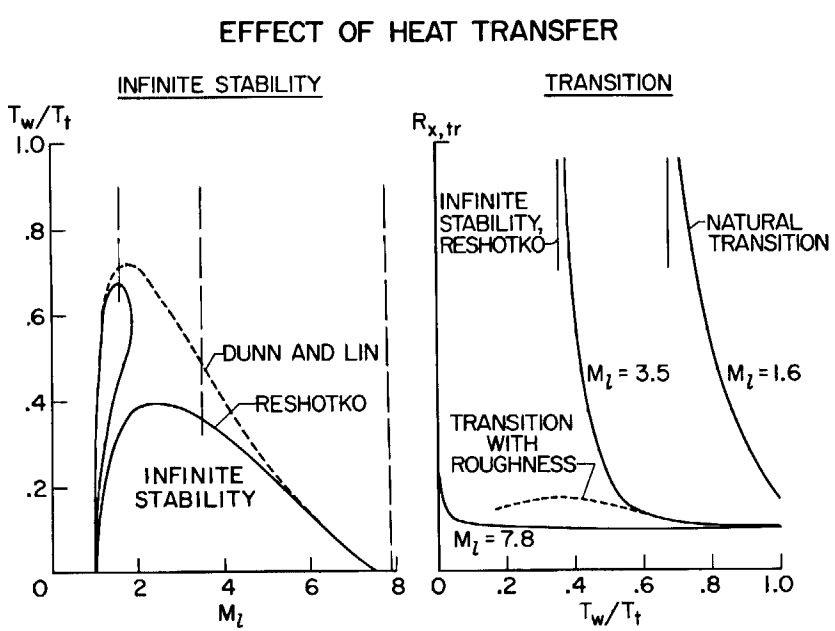

Slide 9.

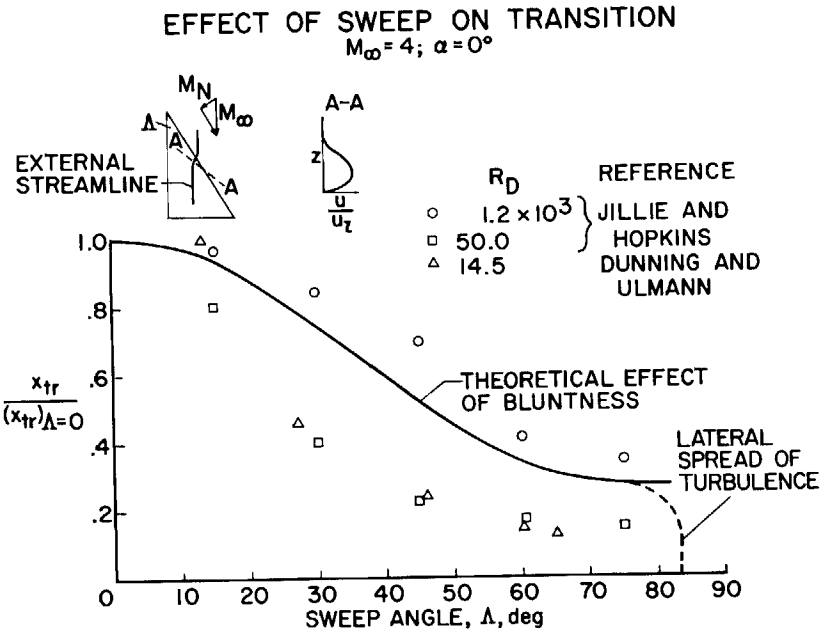

Slide 10.

13. Transition Fixing for Hypersonic Flow - James R. Sterrett, E. Leon Morrisette, Allen H. Whitehead, and Raymond M. Hicks 13

PAINT PATTERN DOWNSTREAM OF ROUGHNESS ELEMENT

5° BLUNTED CONE; $M_\infty \approx 8$; $k/\delta_k \approx 2.4$

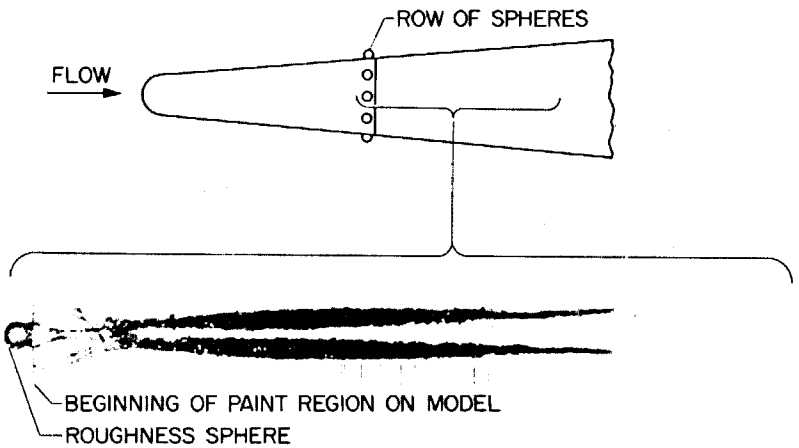

Slide 1.

METHODS FOR DETECTING TRANSITION

$M_\infty = 6$

HEAT TRANSFER

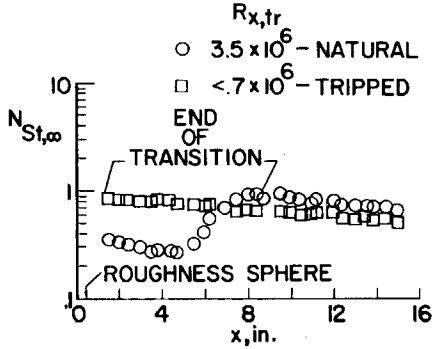

VELOCITY PROFILES

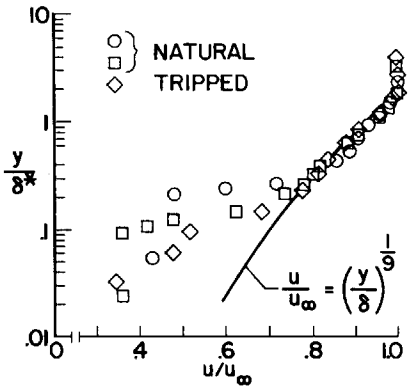

Slide 2.

J. R. Sterrett

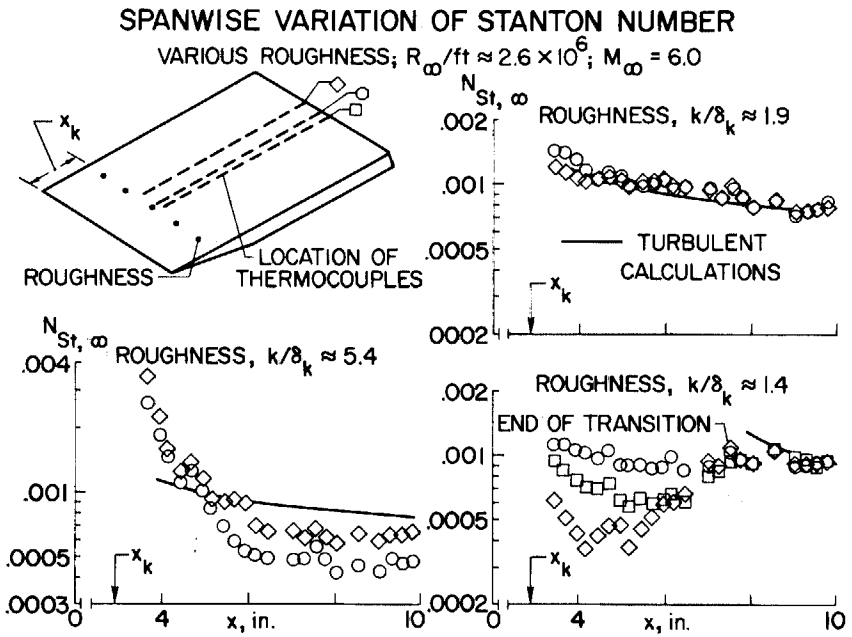

Slide 3.

ROUGHNESS-TRANSITION PARAMETERS

1-PRESSURE GRADIENT
2-WALL TEMPERATURE
3-SPACING
4-LOCAL MACH NUMBER
5-ROUGHNESS POSITION REYNOLDS NUMBER, $R_{x,k}$
6-UNIT REYNOLDS NUMBER
7-TYPE OF ROUGHNESS
8-HEIGHT REYNOLDS NUMBER, R_k
9-MODEL CONFIGURATION

Slide 4.

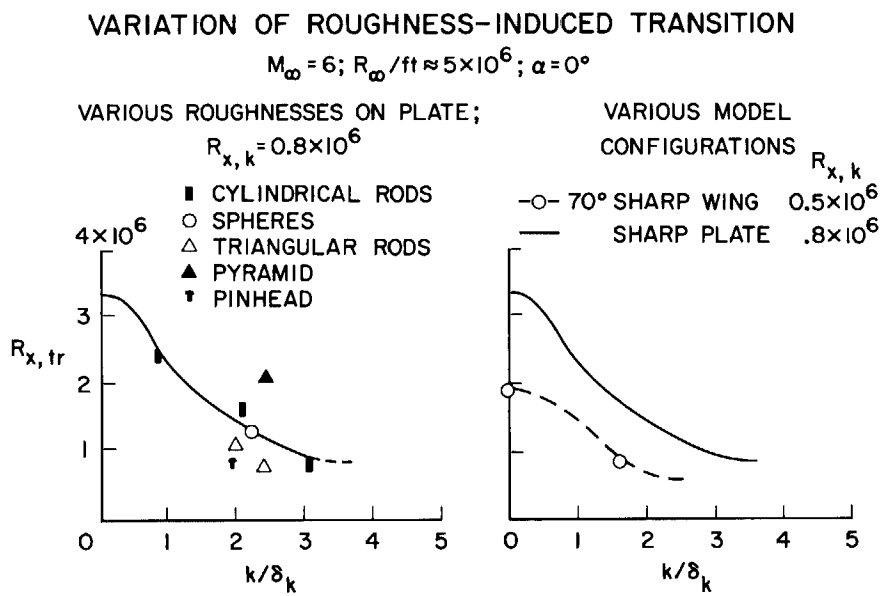

Slide 5.

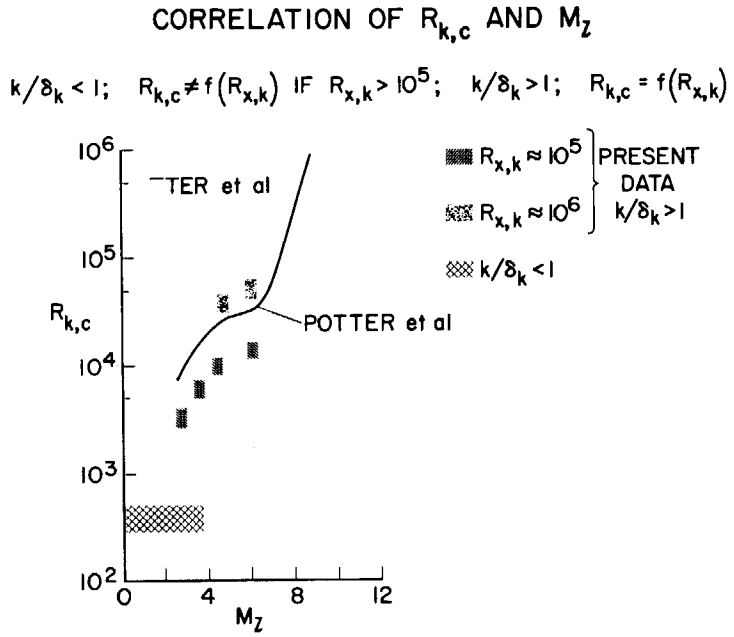

Slide 6.

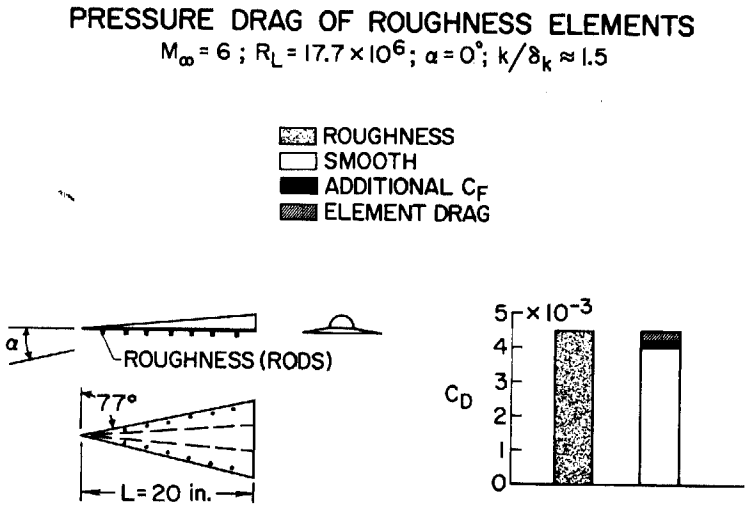

Slide 7.

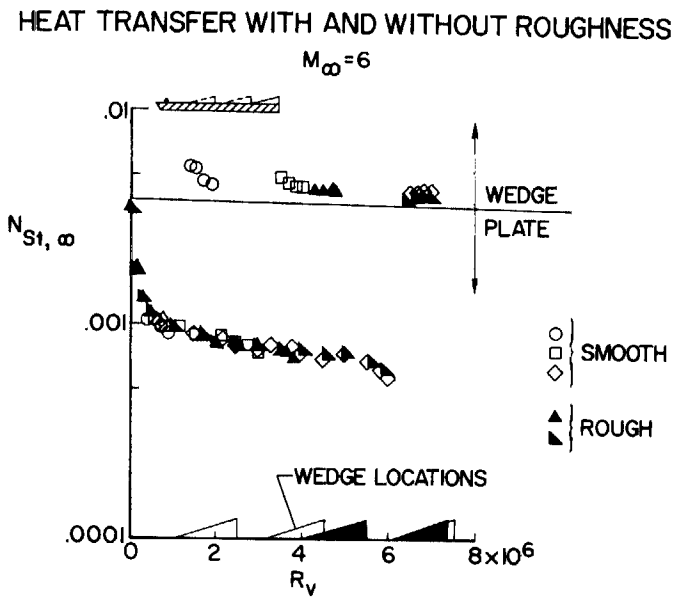

Slide 8.

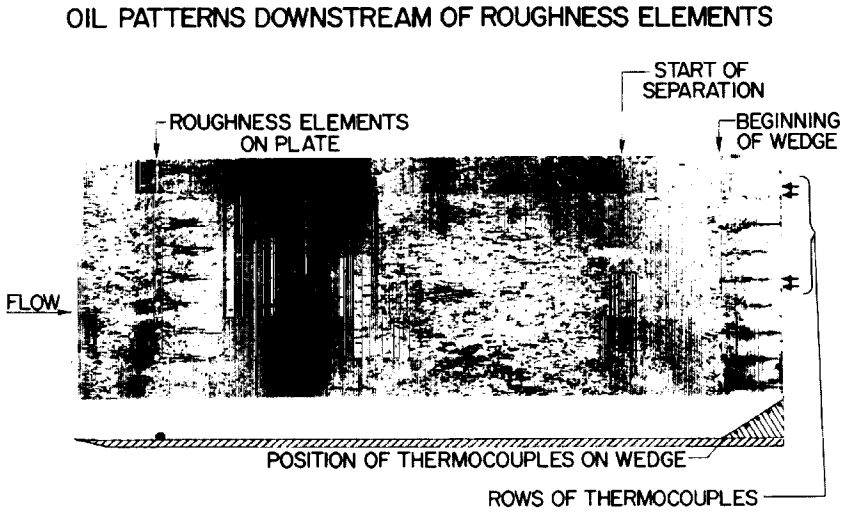

Slide 9.

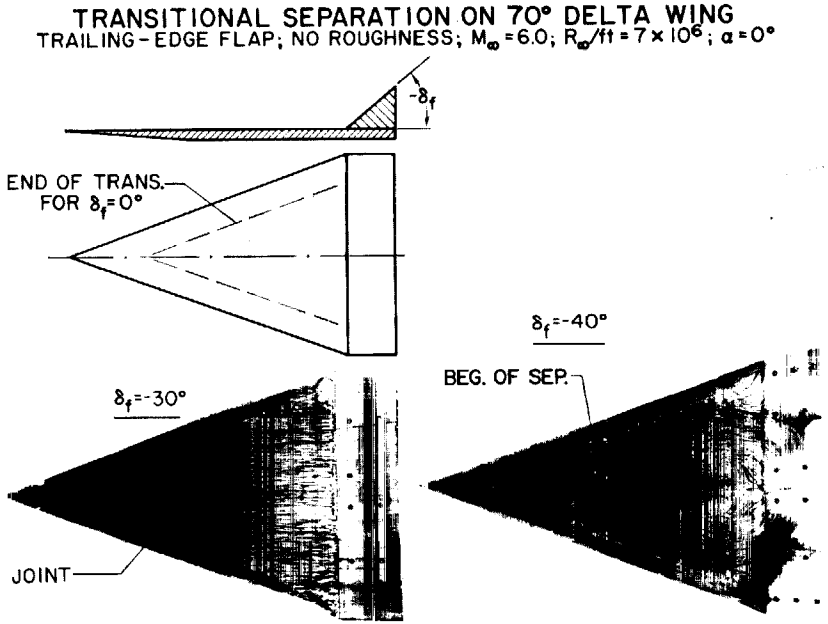
TRANSITIONAL SEPARATION ON 70° DELTA WING
TRAILING-EDGE FLAP; NO ROUGHNESS; $M_\infty = 6.0$; $R_\infty/ft = 7 \times 10^6$; $\alpha = 0°$
$-\delta_f$
END OF TRANS. FOR $\delta_f = 0°$
$\delta_f = -30°$
JOINT
$\delta_f = -40°$
BEG. OF SEP.

Slide 10.

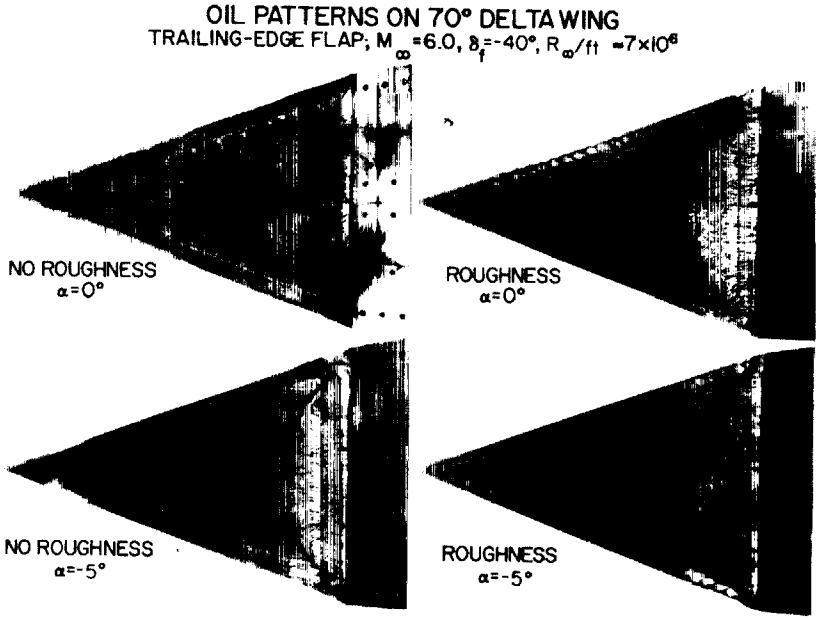

Slide 11.

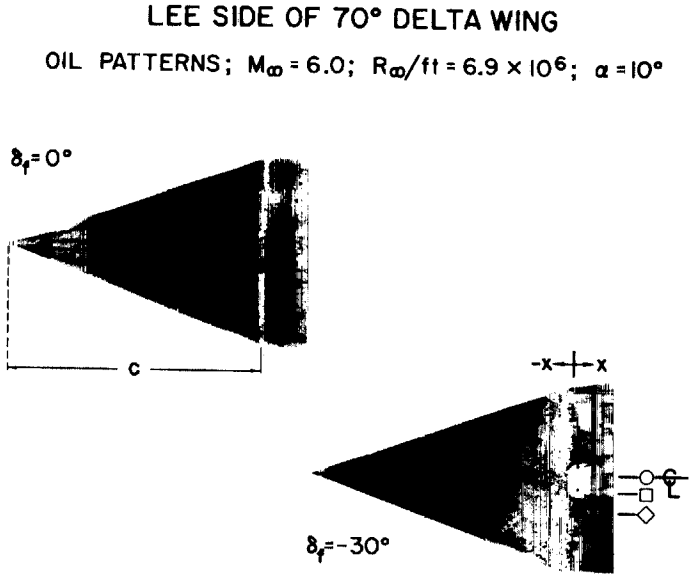

Slide 12.

LEE SIDE OF 70° DELTA WING

$M_\infty = 6.0$; $R_\infty/ft = 6.9 \times 10^6$; $\alpha = 10°$

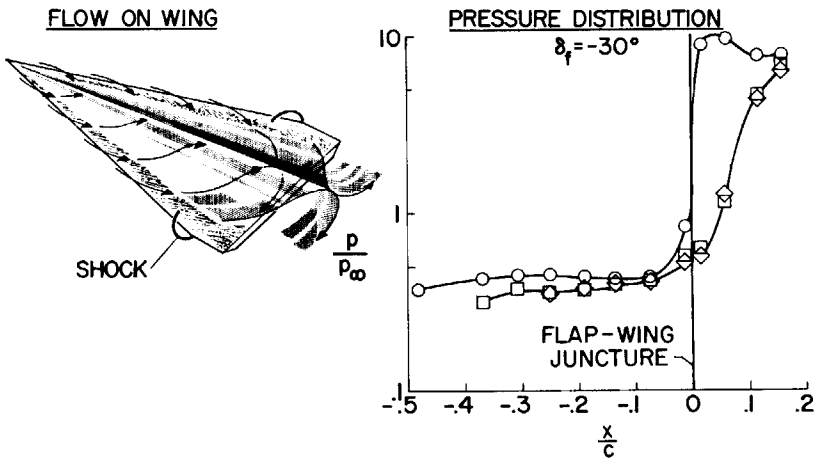

Slide 13.

TRANSITION CLOSE TO ROUGHNESS

TYPICAL TUNNEL CONDITIONS FOR A PLATE

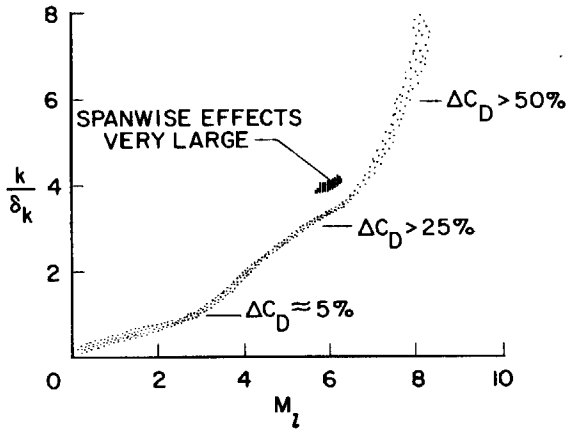

Slide 14.

14. Some Topics in Hypersonic Turbulent Boundary Layer, Heat Transfer, and Skin Friction - Mitchel H. Bertram and Aubrey M. Cary, Jr. 14

TOPICS IN TURBULENT BOUNDARY LAYER

- EFFECT OF WALL TEMPERATURE
- TRANSFORMED VELOCITY PROFILES
- HEAT TRANSFER TO DELTA WINGS

Slide 1.

X-15 HEAT-TRANSFER RESULTS

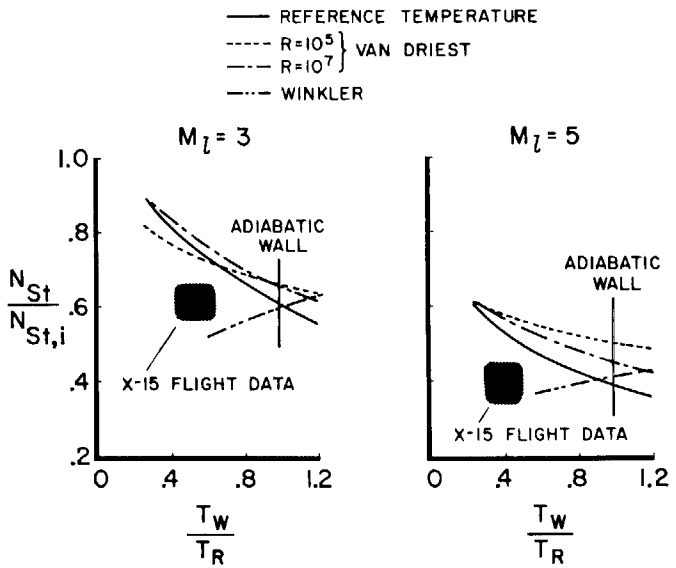

Slide 2.

EFFECT OF WALL TEMPERATURE ON TURBULENT HEAT TRANSFER

FLAT PLATE ; $M_\infty = 6$; NATURAL TRANSITION

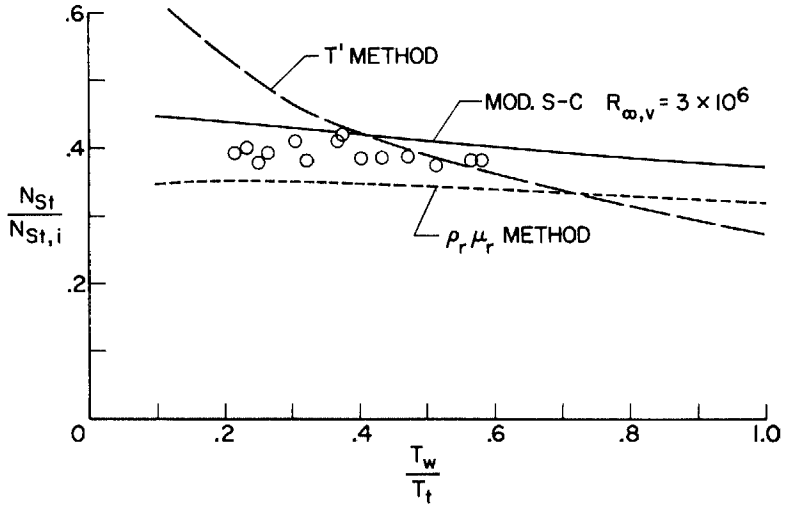

Slide 3.

COMPARISON OF TURBULENT PREDICTION METHODS WITH C.A.L. DATA

FLAT PLATE; NATURAL TRANSITION

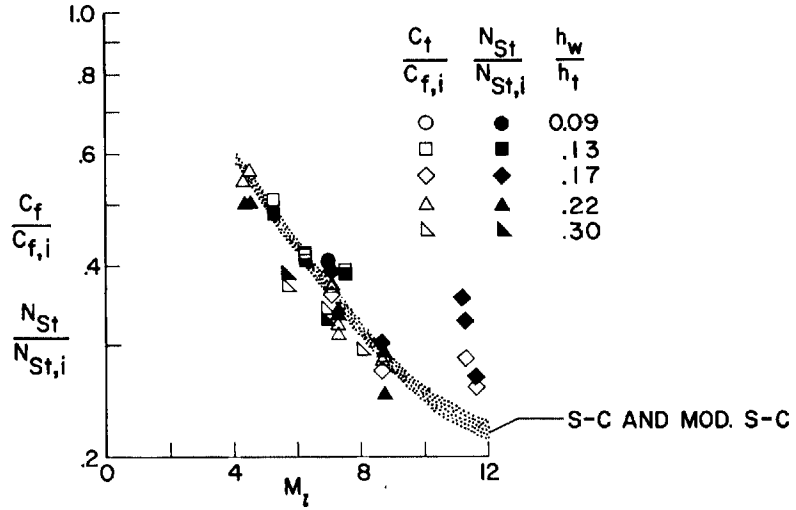

Slide 4.

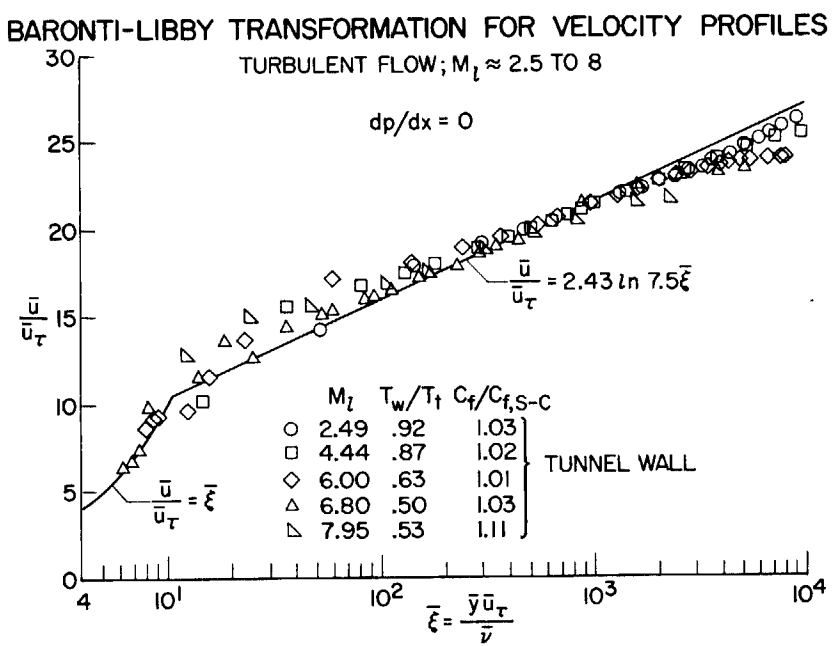

Slide 5.

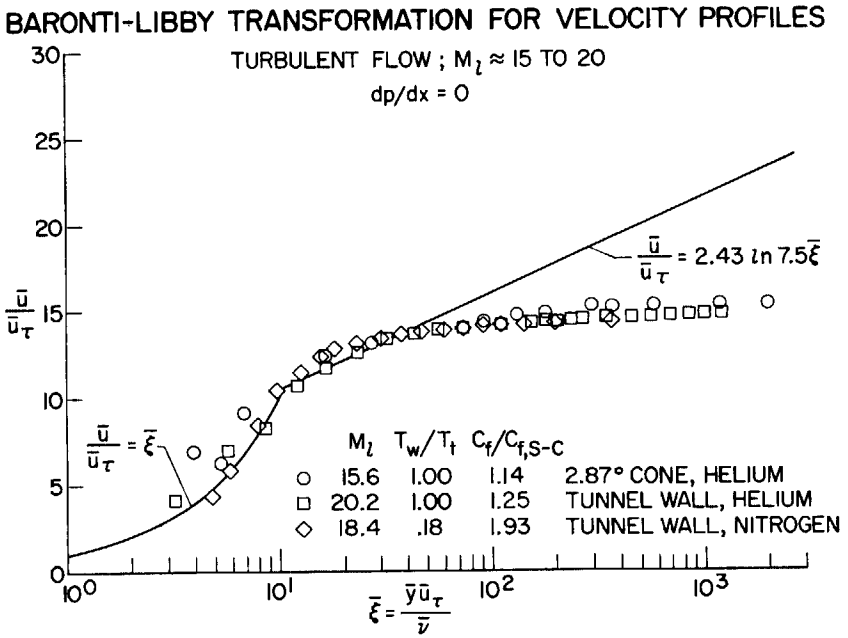
BARONTI-LIBBY TRANSFORMATION FOR VELOCITY PROFILES
TURBULENT FLOW ; $M_l \approx 15$ TO 20
dp/dx = 0
$\frac{\bar{u}}{\bar{u}_\tau} = 2.43 \ln 7.5\bar{\xi}$
$\frac{\bar{u}}{\bar{u}_\tau} = \bar{\xi}$
M_l T_w/T_t $C_f/C_{f,S-C}$
15.6 1.00 1.14 2.87° CONE, HELIUM
20.2 1.00 1.25 TUNNEL WALL, HELIUM
18.4 .18 1.93 TUNNEL WALL, NITROGEN
$\frac{\bar{u}}{\bar{u}_\tau}$
$\bar{\xi} = \frac{\bar{y}\bar{u}_\tau}{\bar{\nu}}$

Slide 6.

SKIN-FRICTION RESULTS FROM BARONTI-LIBBY TRANSFORMATION

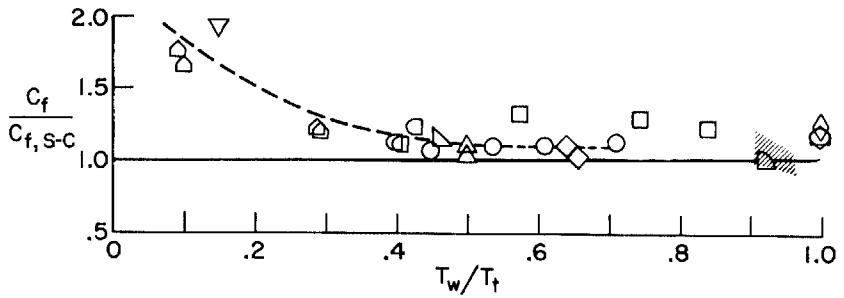

Slide 7.

	M_l	R_θ	SOURCE
▒	2-4.2	$2.2-702\times10^3$	BARONTI, LIBBY
○	5-6.8	6.5-8.6	LOBB et al., NOZ. TEST SECT., AIR
□	5.2	2.0-5.9	WINKLER, CHA, FLAT PLATE, AIR
◇	6.0	19-49	BERTRAM, NEAL, NOZ. TEST SECT., AIR
△	6.8	13-30	BERTRAM, NEAL, NOZ. TEST SECT., AIR
◺	6.0	12.9	SAMUELS et al., CYLINDER, AIR
◺	6.0	7.1	STERRETT, BARBER, FLAT PLATE, AIR
⌂	7.5	2.0	MADDALON et al., 10° CONE, HELIUM
◇	15.6	2.6	HENDERSON et al., 2.87° CONE, HELIUM
◊	20.2	5.2	BERTRAM, NEAL, NOZ. TEST SECT., HELIUM
⌂	7.2-7.9	3.5-58	C.A.L. SHOCK TUN., NOZ. TEST SECT., AIR
▽	18.4	1.25	HARVEY, CLARK, NOZ. TEST SECT., NITROGEN
◻	7.9	11-24	FELLER, NOZ. TEST SECT., AIR

Slide 8.

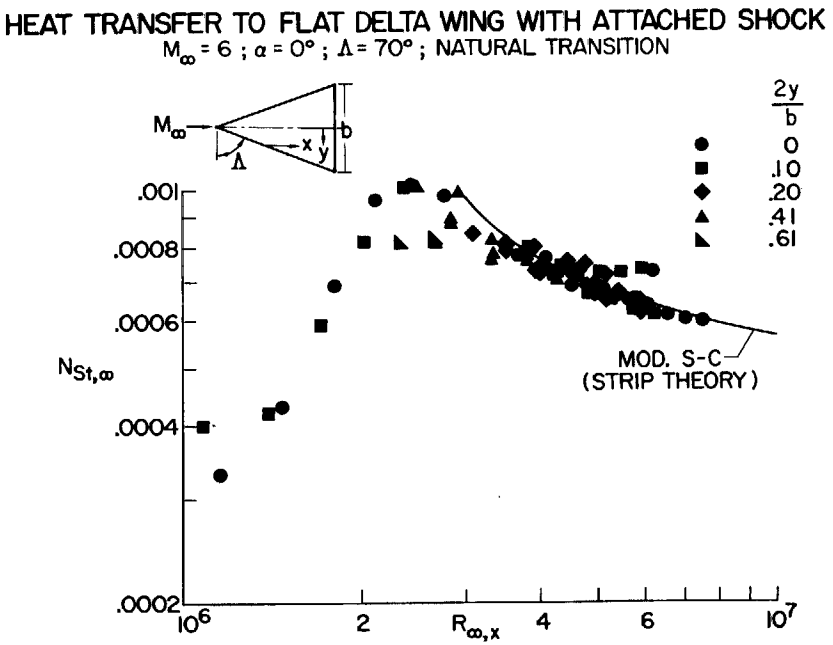

Slide 9.

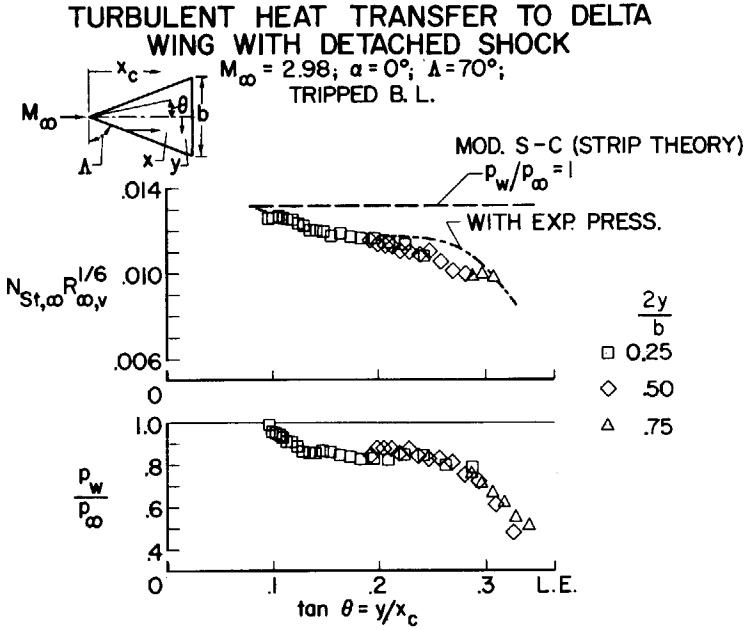

Slide 10.

PRESSURES ON FLAT DELTA WING, ATTACHED SHOCK (?)

$M_\infty=6;\ \alpha=-5°;\ \Lambda=70°$

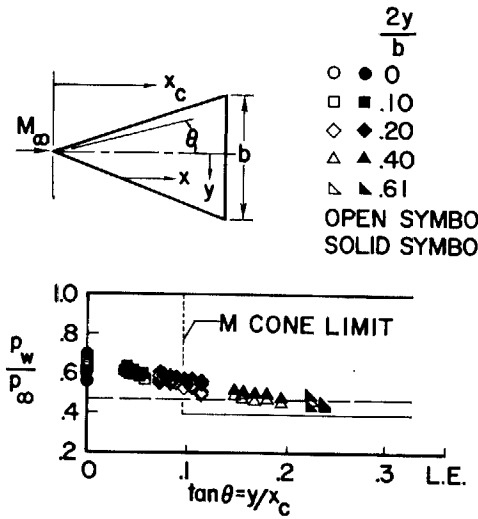

Slide 11.

HEAT TRANSFER TO FLAT DELTA WING, ATTACHED SHOCK (?)

$M_\infty=6;\ \alpha=-5°;\ \Lambda=70°$

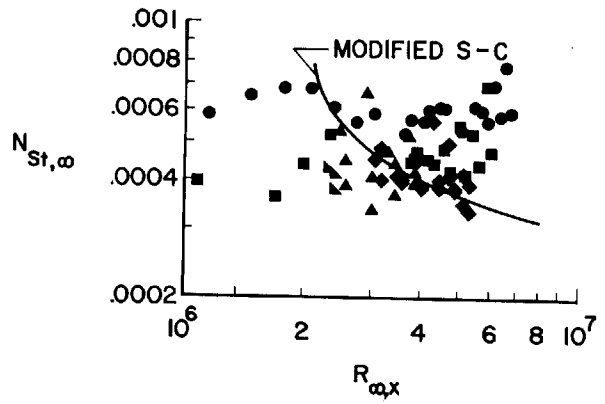

Slide 12.

15. Corner Flow at Hypersonic Speeds - P. Calvin Stainback and Leonard M. Weinstein

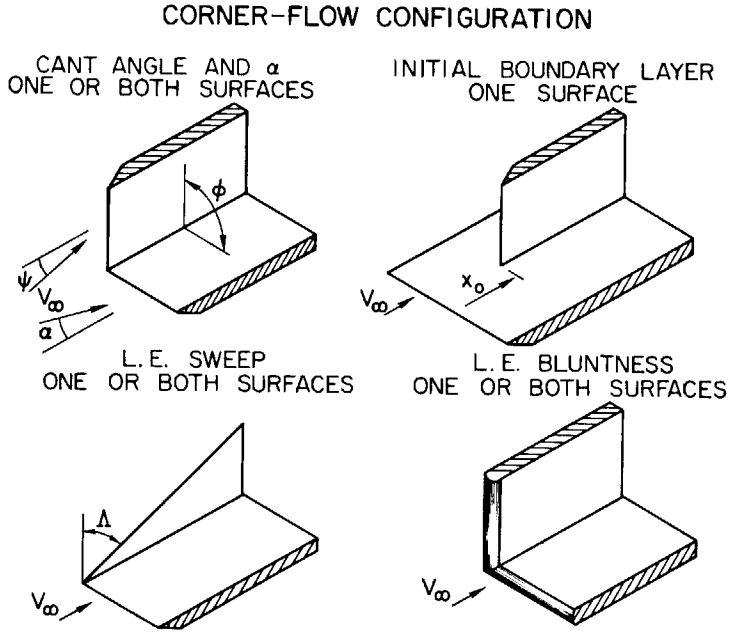

Slide 1.

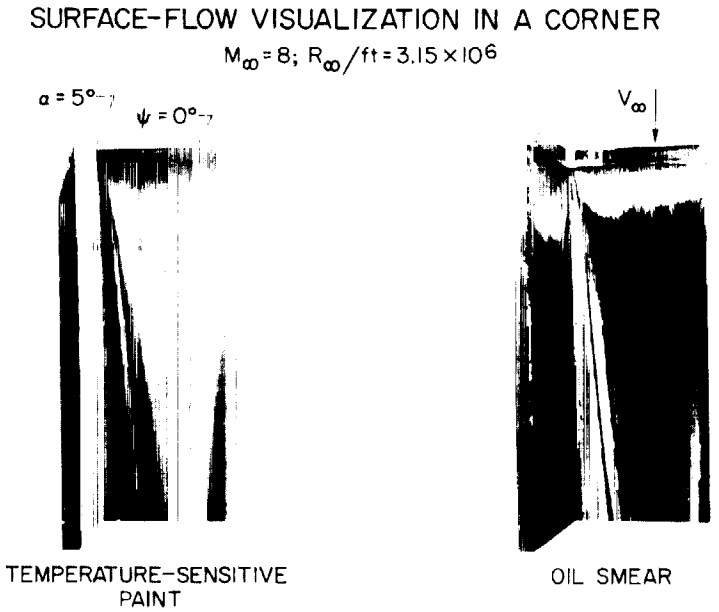

Slide 2.

FACTORS WHICH INFLUENCE LAMINAR PEAK HEATING IN CORNER REGION

INCREASES PEAK HEATING	DECREASES PEAK HEATING
INCREASING:	INCREASING:
• MACH NUMBER	• LEADING-EDGE SWEEP
• ANGLE OF ATTACK	• CANT OR ROLL-OUT ANGLE
• NOSE RADIUS	• FILLETS

Slide 3.

ELECTRON-BEAM CORNER-FLOW VISUALIZATION

$M_\infty = 20$ IN HELIUM; R/in. $= 0.38 \times 10^6$; $\alpha = 10°$; $\psi = 10°$; $\phi = 90°$

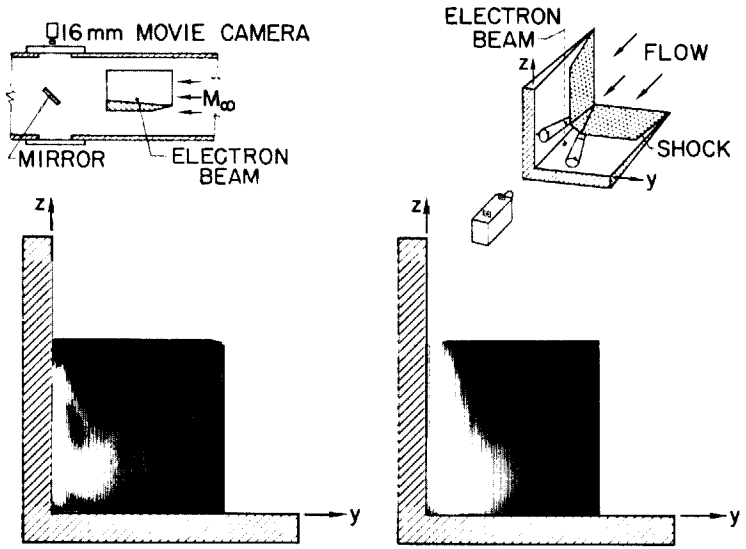

Slide 4.

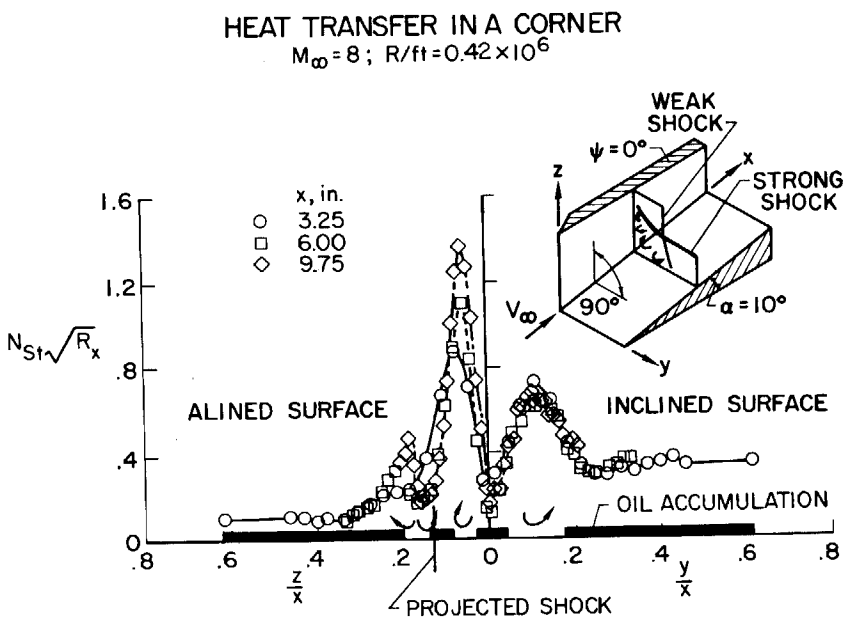

Slide 5.

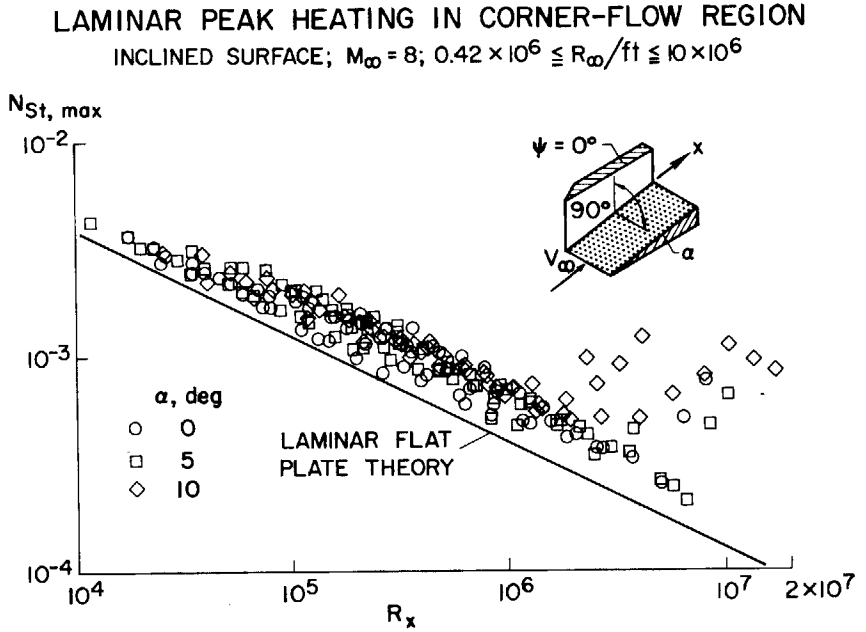

Slide 6.

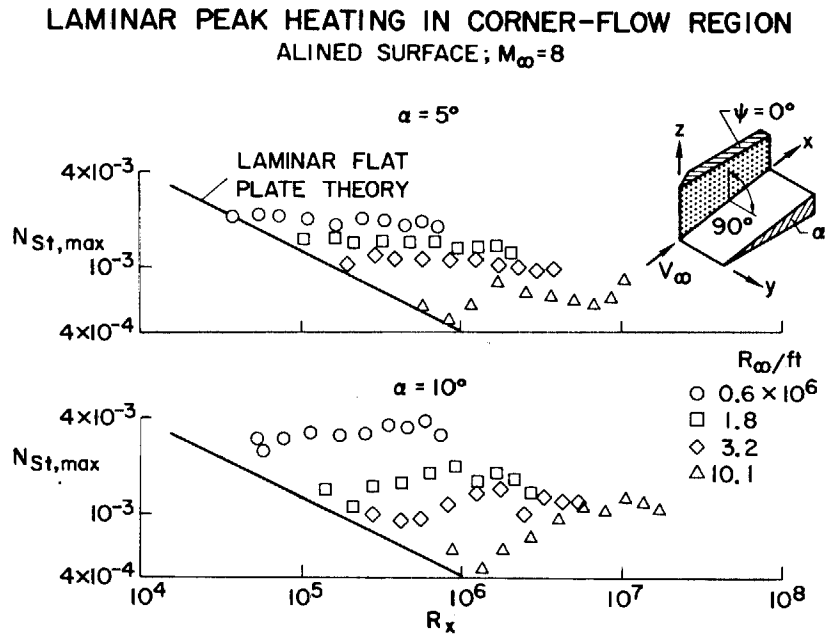

Slide 7.

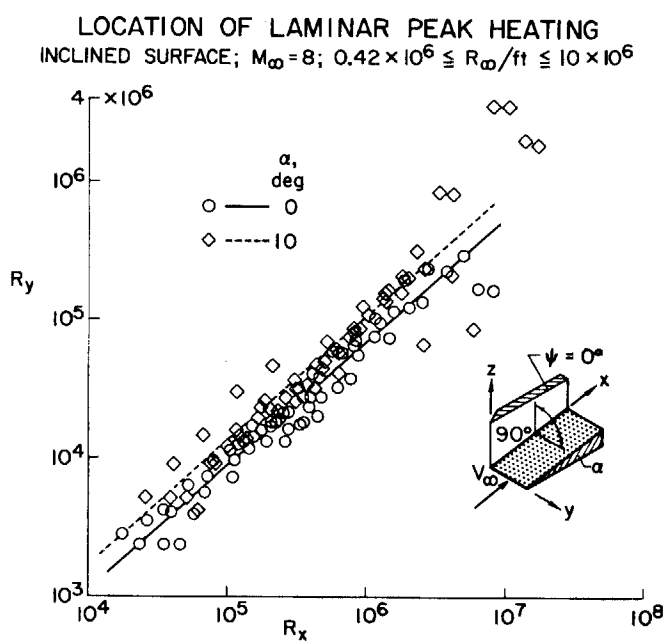

Slide 8.

EFFECT OF CANT ANGLE ON LAMINAR PEAK HEATING

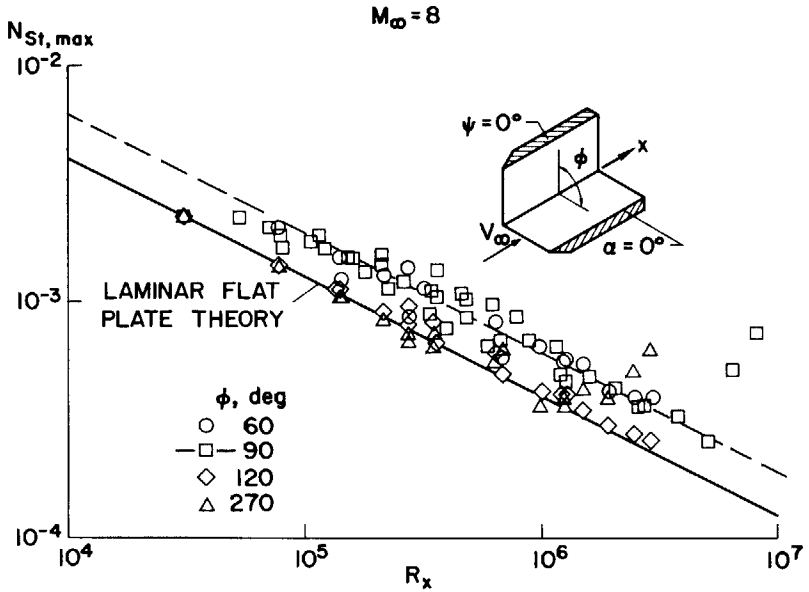

Slide 9.

TURBULENT HEATING IN A CORNER

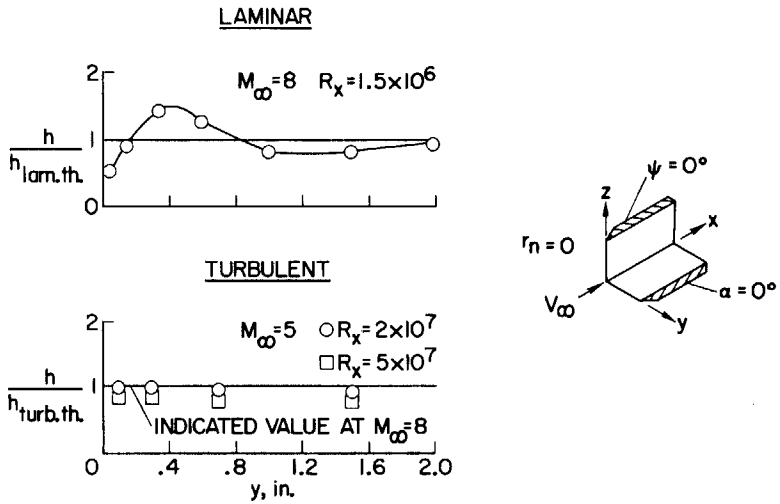

Slide 10.

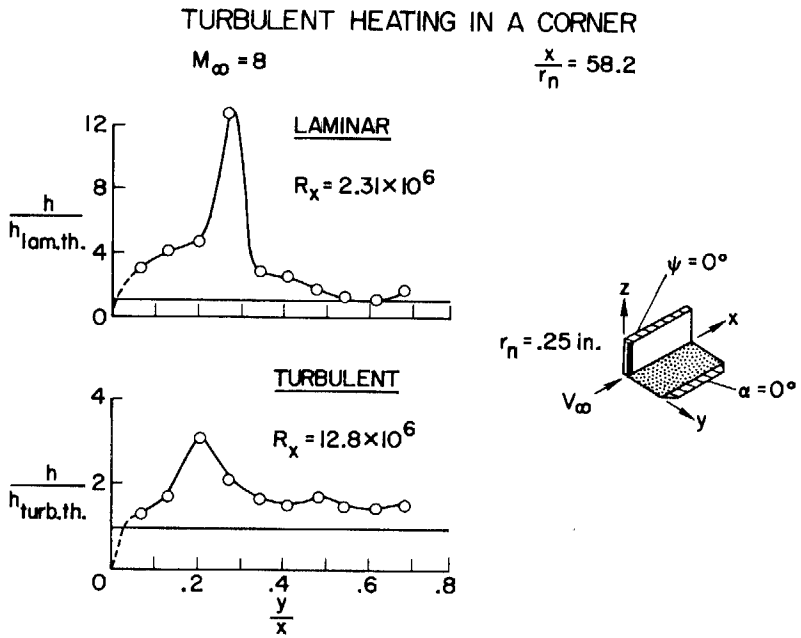
TURBULENT HEATING IN A CORNER
$M_\infty = 8$
$\frac{x}{r_n} = 58.2$
LAMINAR
$R_x = 2.31 \times 10^6$
$\frac{h}{h_{lam.th.}}$
12
8
4
0
TURBULENT
$R_x = 12.8 \times 10^6$
$\frac{h}{h_{turb.th.}}$
4
2
0
.2
.4
.6
.8
$\frac{y}{x}$
$\psi = 0°$
z
x
$r_n = .25$ in.
V_∞
$\alpha = 0°$
y

Slide 11.

16. Effects of Shock Impingement and Other Factors on Leading-Edge Heat Transfer - Dennis M. Bushnell

INTERFERING FLOW FIELDS

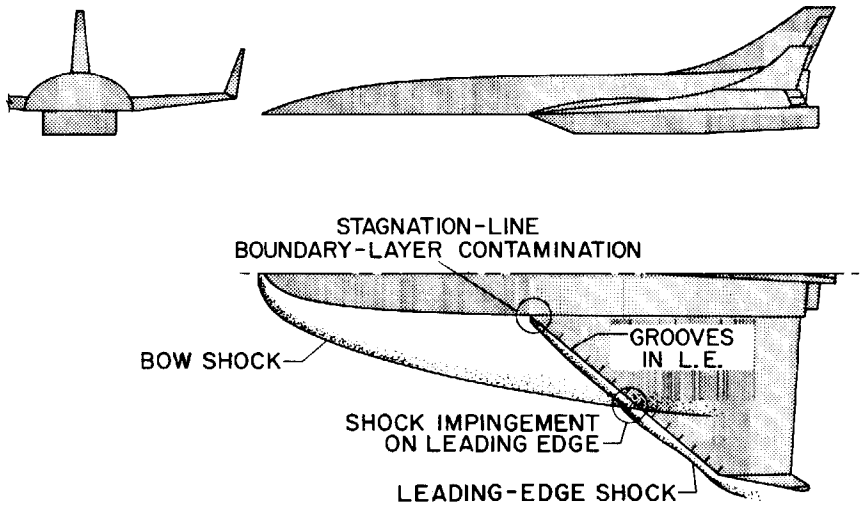

Slide 1.

FLOW FIELD
ASSOCIATED WITH LEADING-EDGE SHOCK IMPINGEMENT

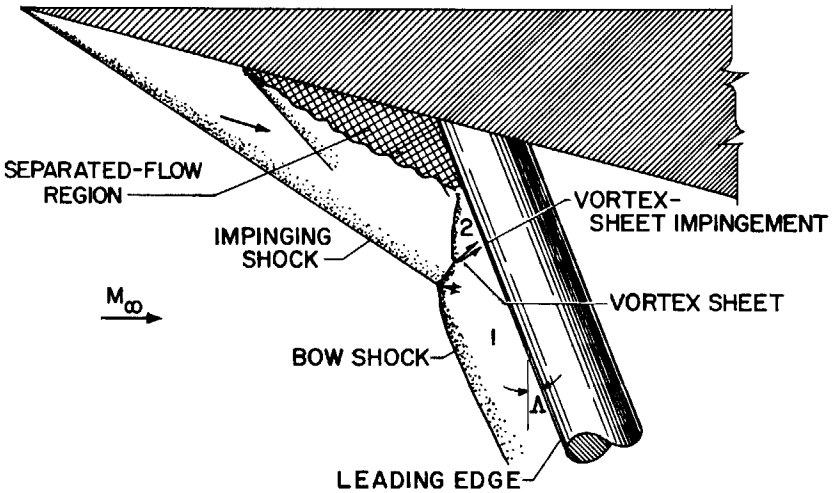

Slide 2

LEADING-EDGE SHOCK IMPINGEMENT

$\Lambda = 0°$; $M_\infty = 8$

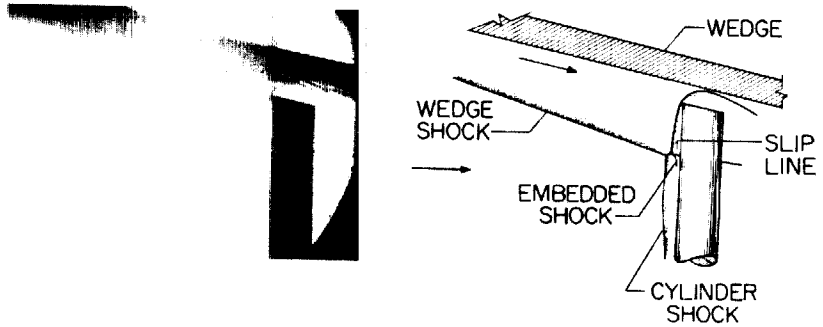

Slide 3.

EFFECT OF SHOCK IMPINGEMENT ON MAXIMUM HEATING

CYLINDRICAL LEADING EDGE ; $\Lambda = 0°$

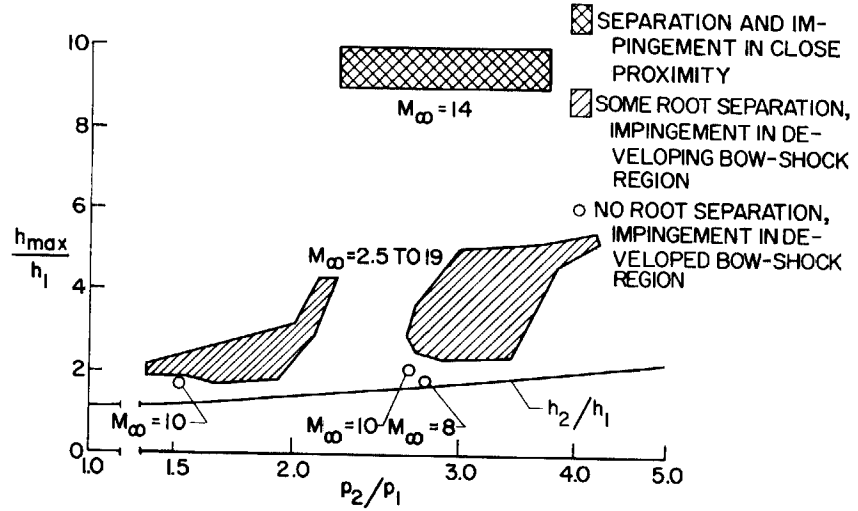

Slide 4.

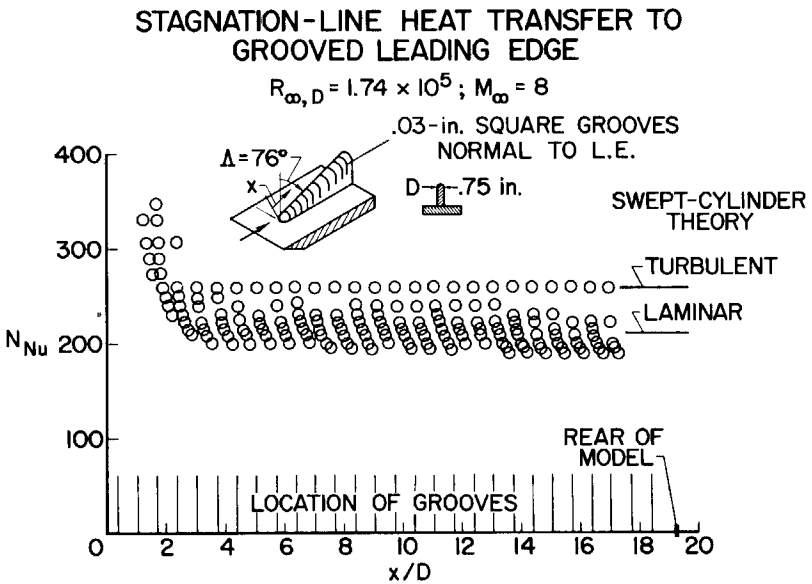

Slide 5.

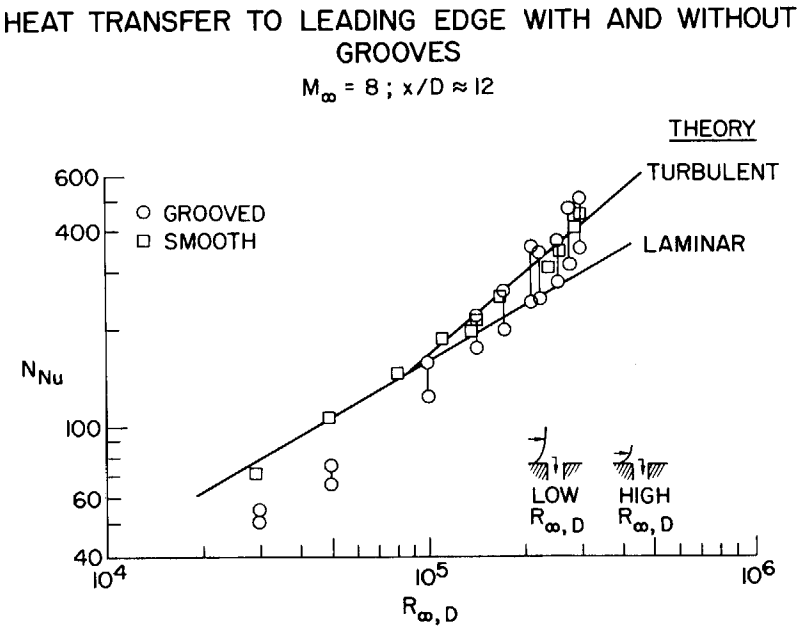

Slide 6.

RESULTS OF SURVEY OF TRANSITION DATA ON SWEPT LEADING EDGES

$2.5 < M_\infty < 8$; $\Lambda > 40°$

"DELTA WING" CONFIGURATIONS	CONFIGURATIONS HAVING END CONTAMINATION
$(R_{\infty, D})_{transition} > 8 \times 10^5$	$(R_{\infty, D})_{transition} \approx 2 \times 10^5$

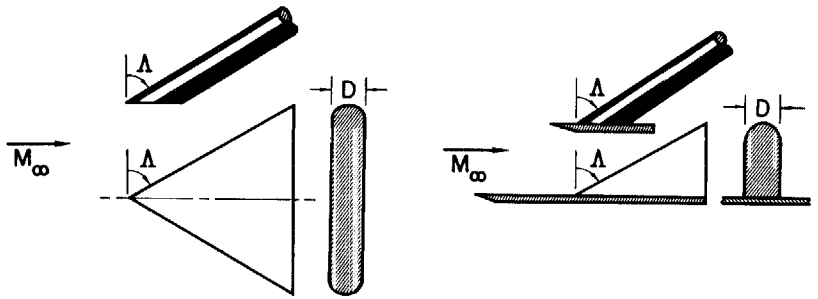

Slide 7.

17. A Study of Hypersonic Inlet Technology - Norman E. Sorensen, Shelby J. Morris, Jr., and Frank A. Pfyl

N. E. Sorensen

STUDY OF HYPERSONIC INLET TECHNOLOGY
OBJECTIVES

- SUMMARIZE PRESENT STATE OF THE ART
- DESCRIBE AND EVALUATE COMPUTER PROGRAM
- EXTEND PROGRAM USAGE TO INLET DESIGN

Slide 1.

INLET TYPES
SUBSONIC BURNING

ADVANTAGES	TYPES	DISADVANTAGES
1. HIGH P.R. POTENTIAL 2. LOW COWL DRAG 3. LOW C_{D_0} 4. HIGH MASS FLOW	INTERNAL COMPRESSION 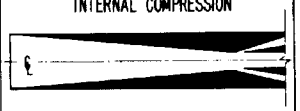	1. LONGEST INLET 2. DIFFICULT TO START 3. HIGH B.L. BLEED
1. SHORT INLET 2. NO STARTING REQUIREMENT	EXTERNAL COMPRESSION	1. HIGH COWL DRAG 2. HIGH C_{D_0} 3. MARGINAL P.R. 4. INADEQUATE TRANSONIC MASS FLOW
1. HIGH P.R. POTENTIAL 2. LOW COWL DRAG 3. LOW C_{D_0}	MIXED COMPRESSION 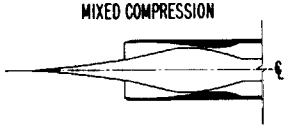	1. POTENTIAL UNREALIZED 2. MARGINAL TRANSONIC MASS FLOW 3. LONGER THAN EXTERNAL COMPRESSION INLET

Slide 2.

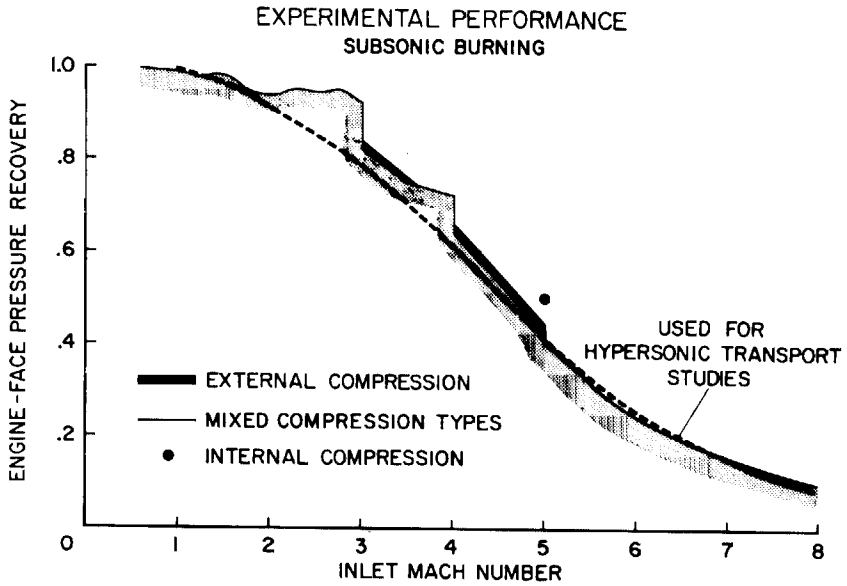

Slide 3.

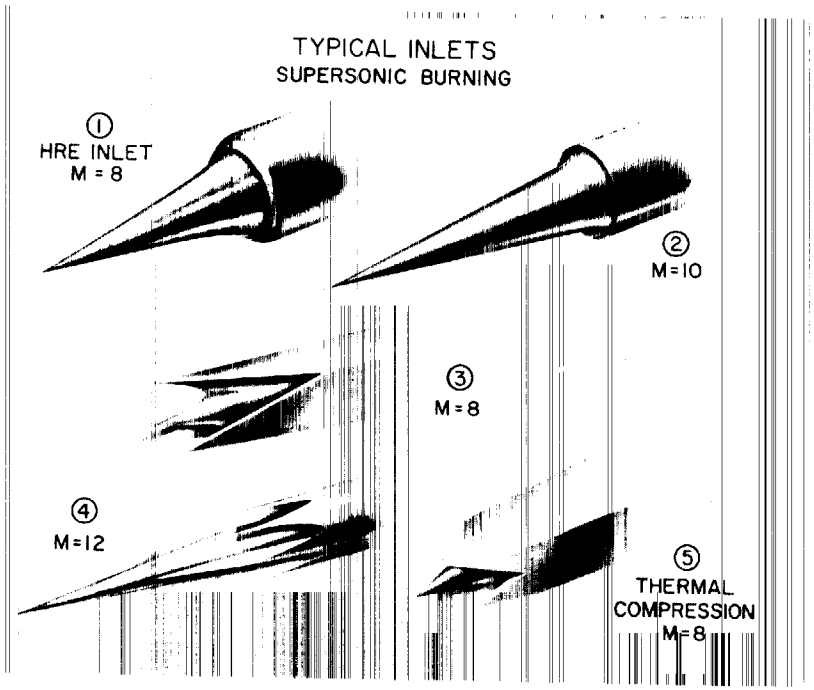

Slide 4.

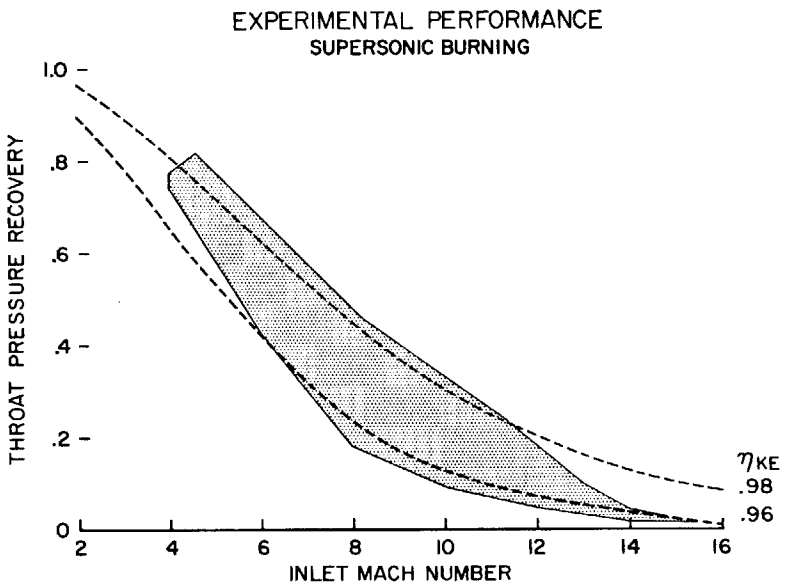

Slide 5.

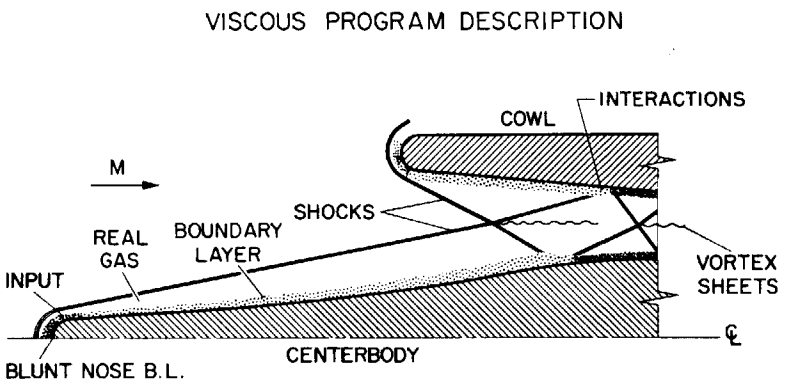

Slide 6.

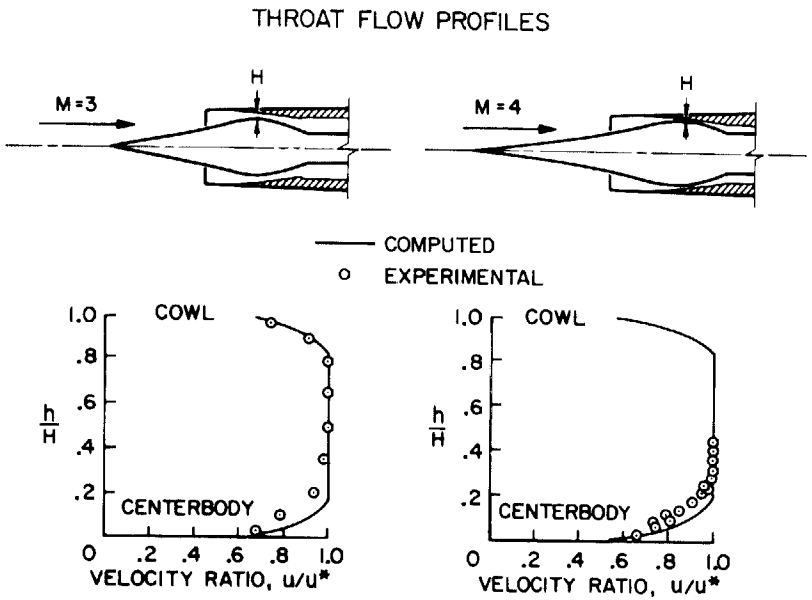

Slide 7.

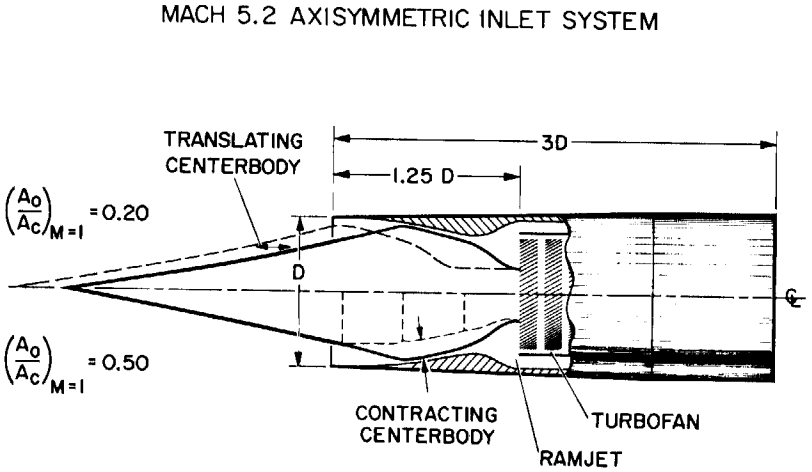

Slide 8.

FLOW FIELD MODEL
COMPUTER PROGRAMS

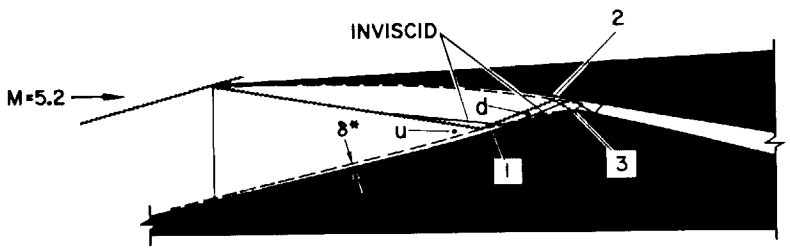

$\frac{p_d}{p_u}$	1	2	3
INVISCID	2.37	1.59	1.62
VISCOUS	4.80	3.74	1.88

Slide 9.

BOUNDARY-LAYER SEPARATION CRITERIA
M = 5.2

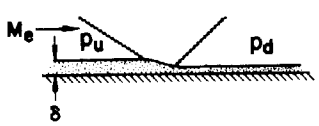

	INVISCID	VISCOUS	IMPINGMENT
● ○	●	○	1st
■ □	■	□	2nd
▲ △	▲	△	3rd

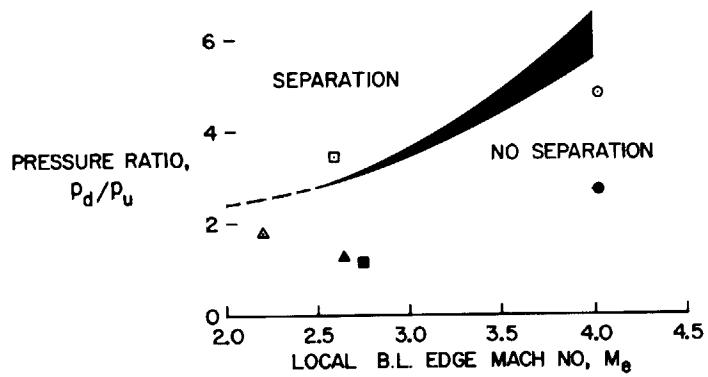

Slide 10.

18. Two-Dimensional Boundary Layer and Flow Fields of Hypersonic Inlets - A. Vernon Gnos, William F. Gallo, and Eldon A. Latham

TYPICAL HYPERSONIC INLET

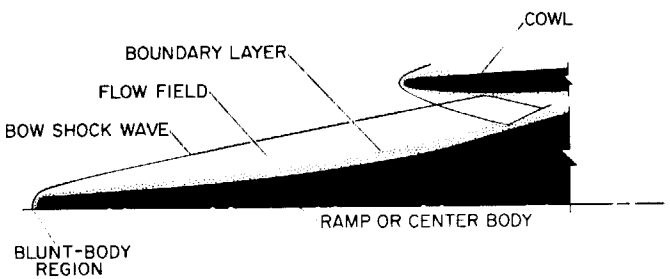

Slide 1.

SCHEMATIC OF TEST MODEL

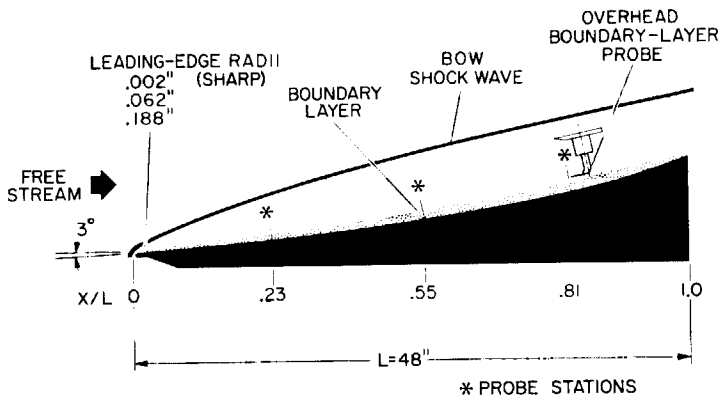

Slide 2.

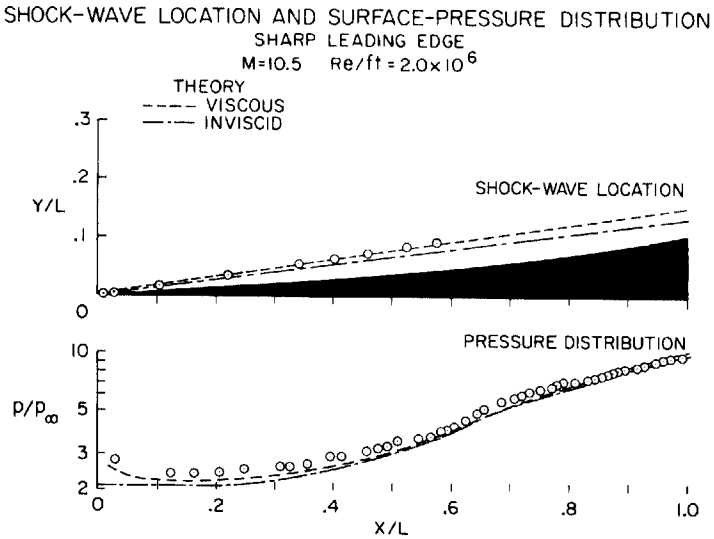

Slide 3.

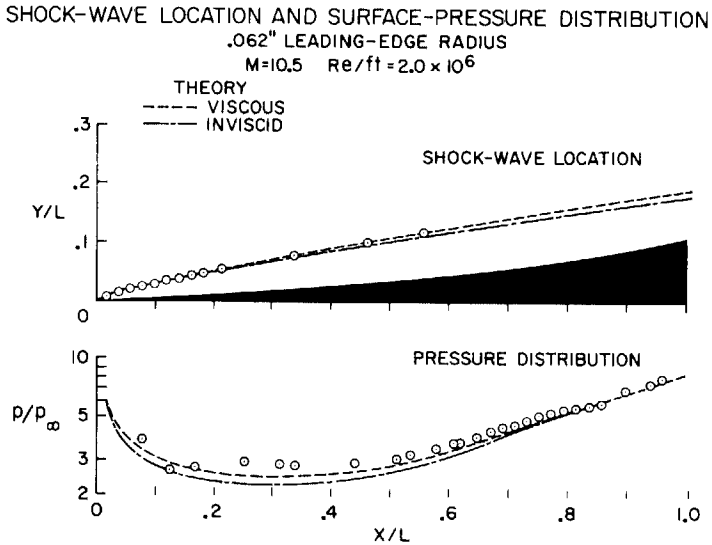

Slide 4.

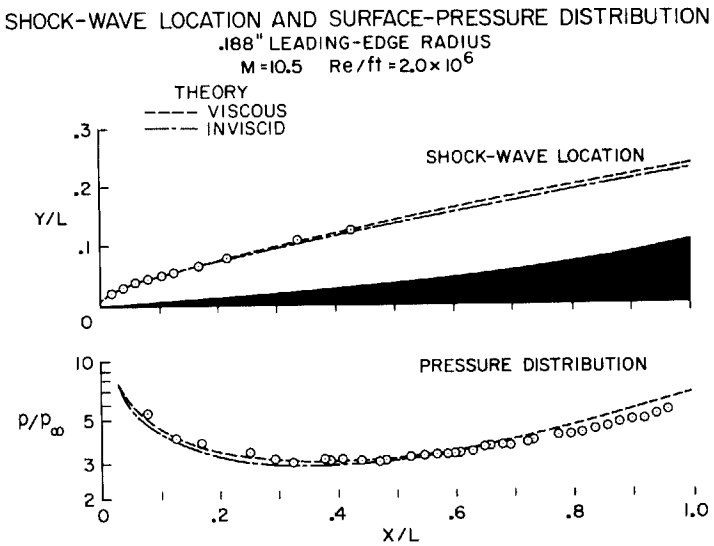

Slide 5.

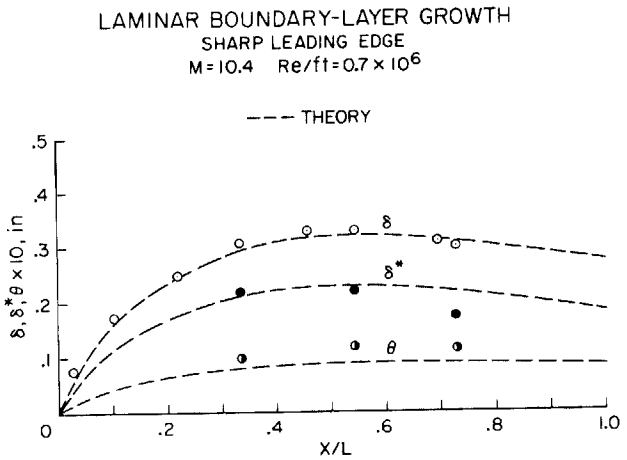

Slide 6.

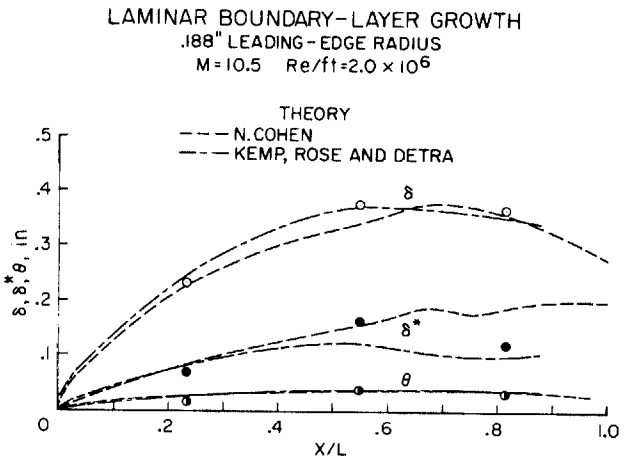

Slide 7.

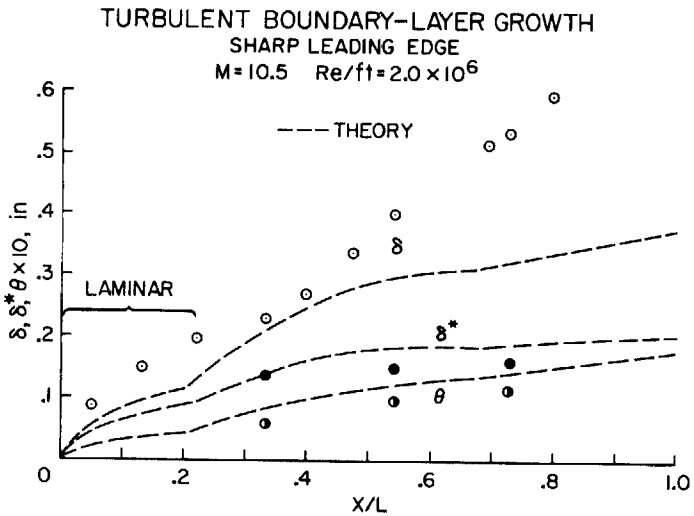

Slide 8.

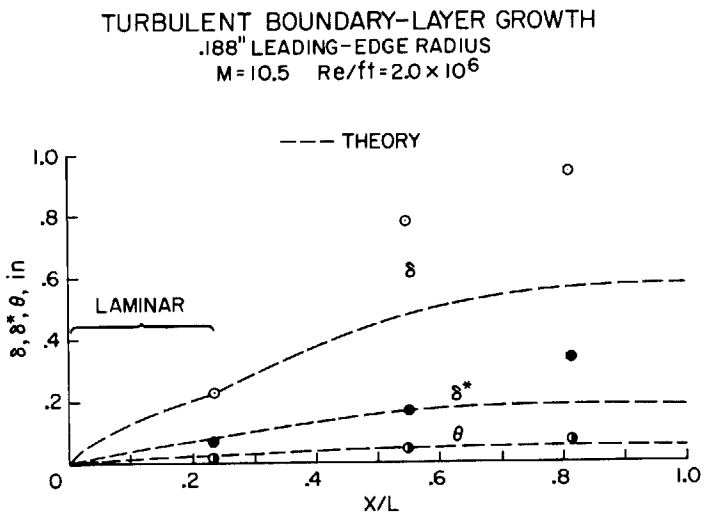

Slide 9.

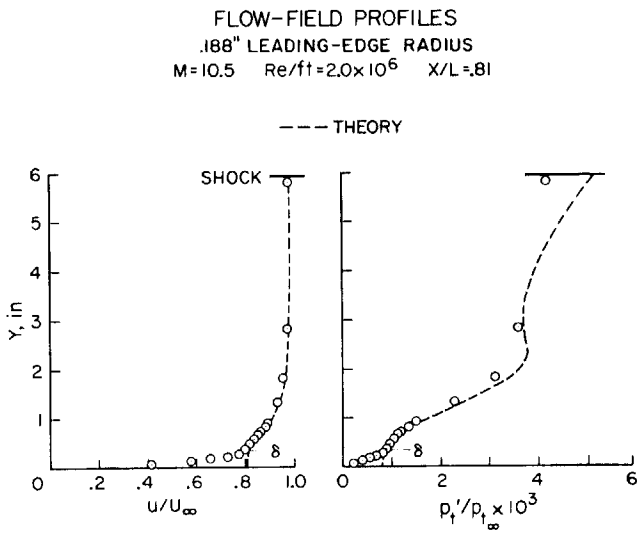

Slide 10.

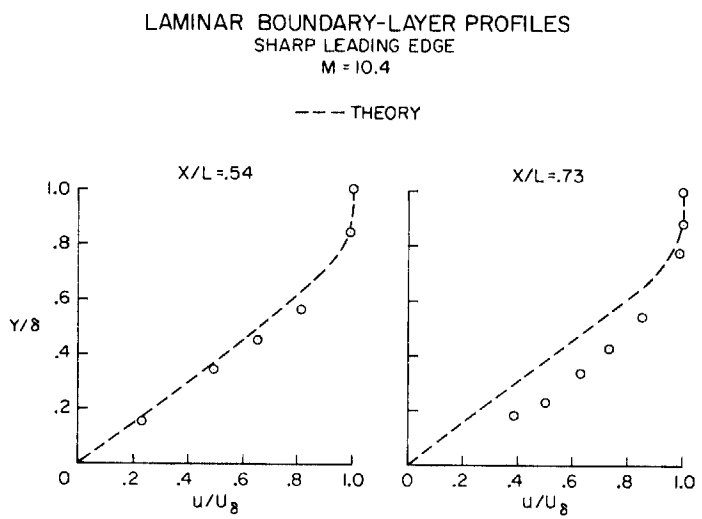

Slide 11.

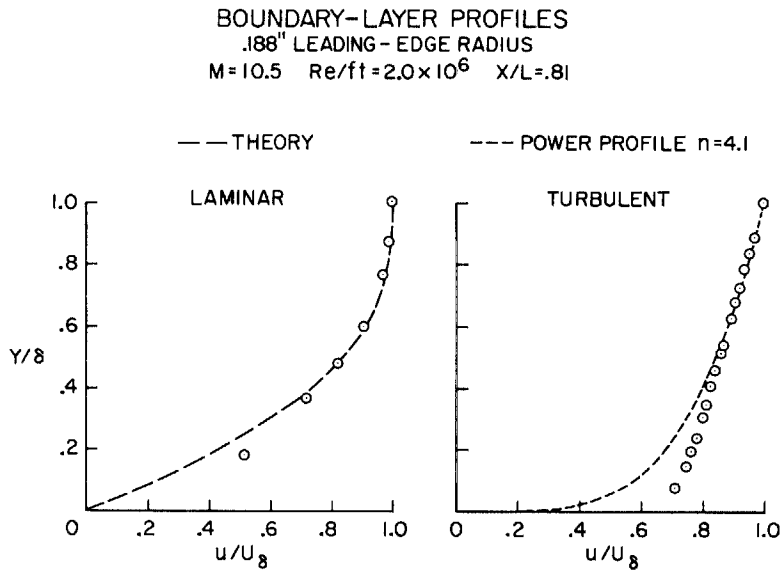

Slide 12.

CONFIDENTIAL

19. Shock-Wave Boundary-Layer Interactions in Hypersonic Inlets - Earl C. Watson, John D. Murphy, and William C. Rose

CONFIDENTIAL

E. C. Watson

INTERACTIONS OF BOUNDARY LAYERS AND SHOCK WAVES
AT HYPERSONIC SPEEDS

EXTERNAL FLOW STUDIES

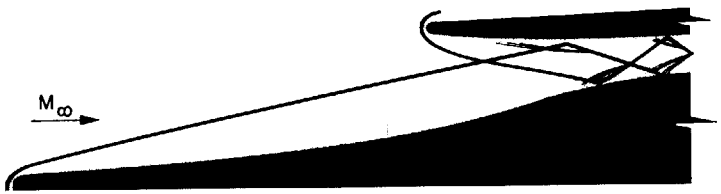

INTERNAL FLOW STUDIES

Slide 1.

INTERACTION OF SHOCK WAVE WITH LAMINAR BOUNDRY LAYER
SCHEMATIC

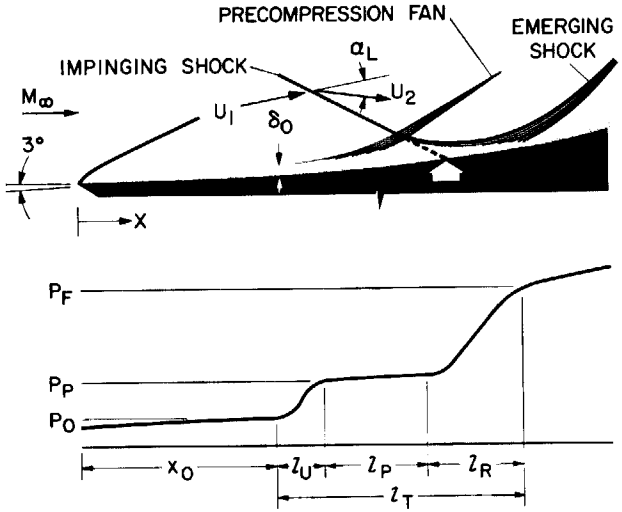

Slide 2.

INTERACTION OF SHOCK WAVE WITH LAMINAR BOUNDARY LAYER
FLAT PLATE

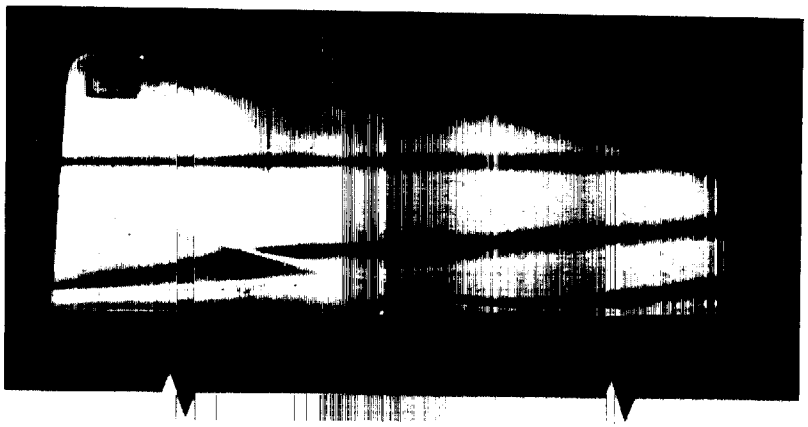

Slide 3a

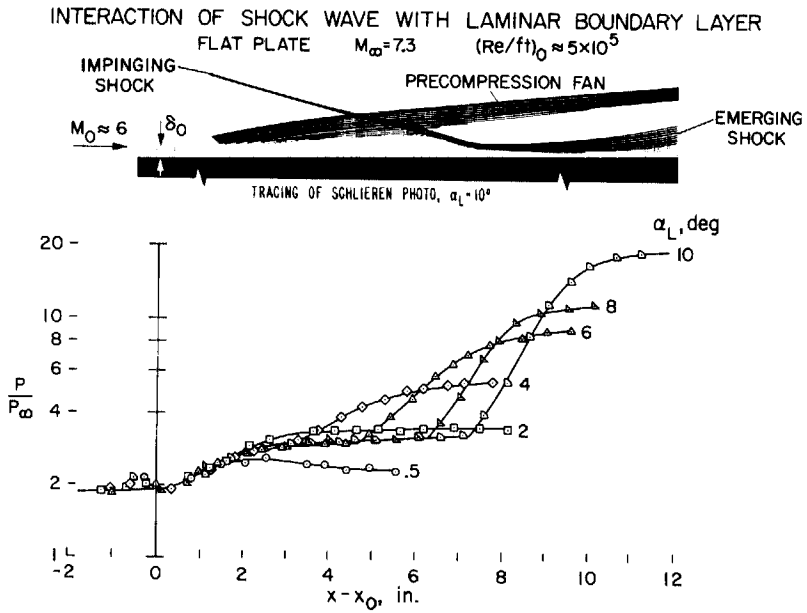

Slide 3b

INTERACTION OF SHOCK WAVE WITH LAMINAR BOUNDARY LAYER
COMPRESSION SURFACE

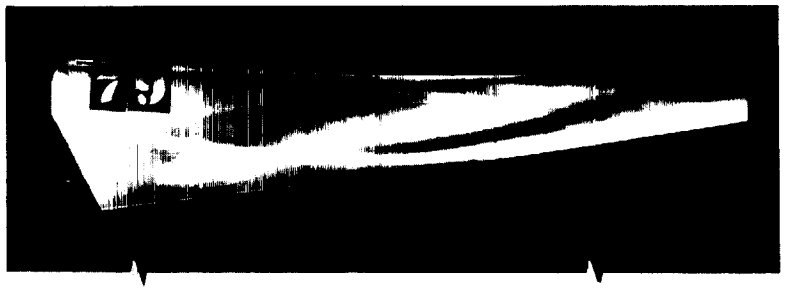

Slide 4a

INTERACTION OF SHOCK WAVE WITH LAMINAR BOUNDARY LAYER
COMPRESSION SURFACE $M_\infty = 7.3$ $(Re/ft)_0 \approx 2.8 \times 10^5$

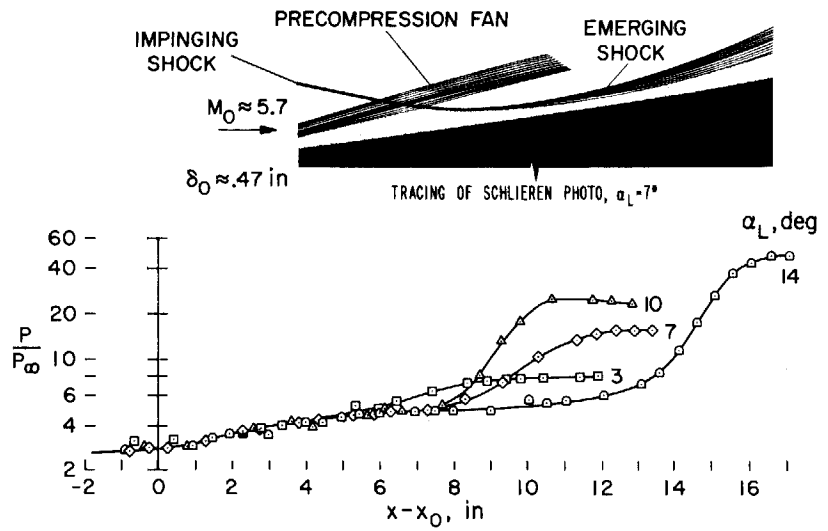

Slide 4b

[redacted]

INTERACTION OF SHOCK WAVE WITH TURBULENT BOUNDARY LAYER
FLAT PLATE

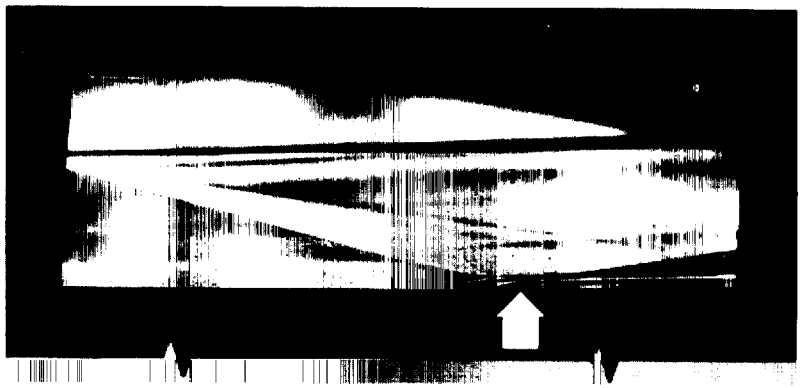

Slide 5a

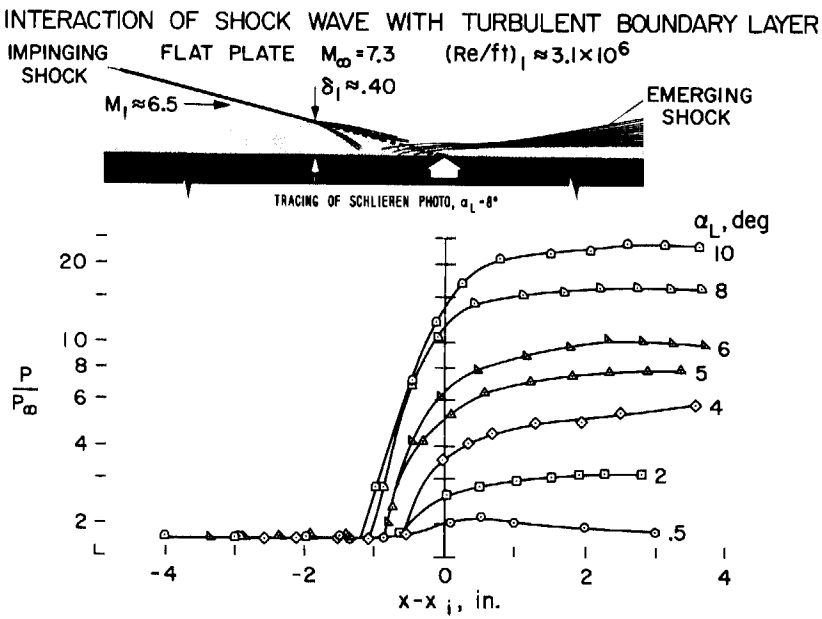

Slide 5b

[redacted]

INTERACTION OF SHOCK WAVE WITH TURBULENT BOUNDARY LAYER
COMPRESSION SURFACE

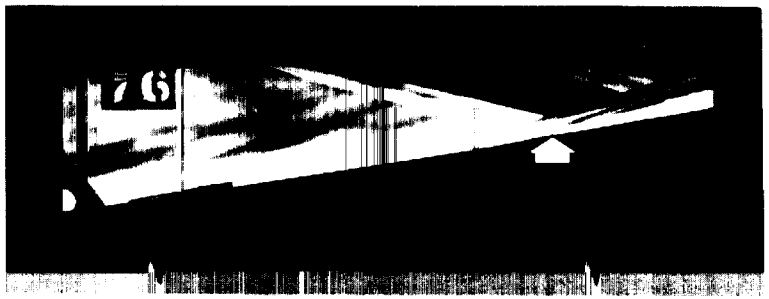

Slide 6a

INTERACTION OF SHOCK WAVE WITH TURBULENT BOUNDARY LAYER
COMPRESSION SURFACE $M_\infty = 7.3$ $(Re/ft)_1 \approx 3.2 \times 10^6$

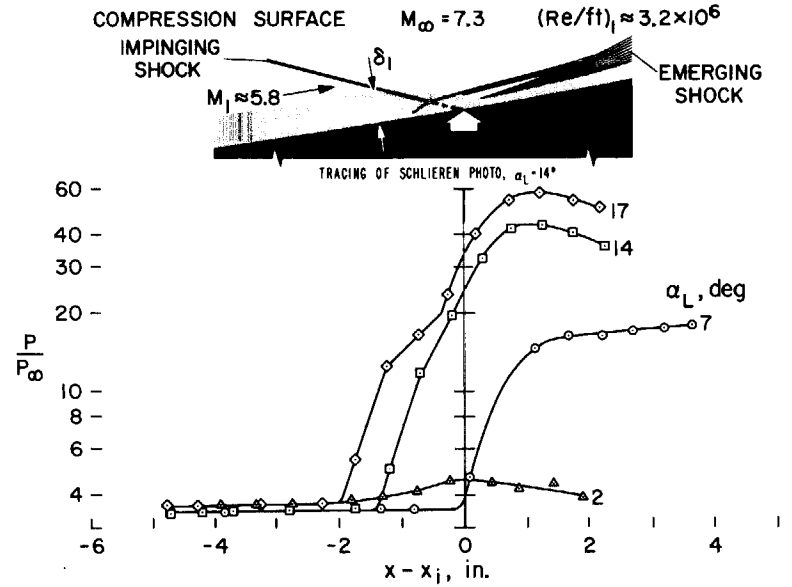

Slide 6b

CONFIDENTIAL

PRESSURE CORRELATION SUMMARY

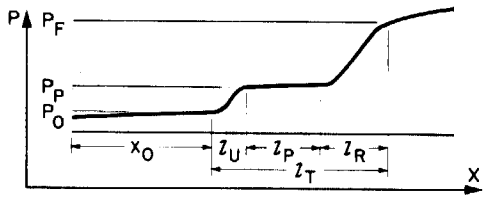

ITEM	LAMINAR	TURBULENT
1. C_P INCIPIENT	PRESENT STUDY	POPINSKI (1966)
2. C_P PLATEAU	NEEDHAM	POPINSKI (1966)
3. FREE INTERACTION	NO UNIVERSAL PROFILE	NONE FROM PRESENT TEST
4. REATTACHMENT	NO UNIVERSAL PROFILE	NONE FROM PRESENT TEST
5. UNSEPARATED	NO UNIVERSAL PROFILE	NO UNIVERSAL PROFILE

Slide 7

LENGTH CORRELATION SUMMARY

ITEM	LAMINAR	TURBULENT
1. FREE INTERACTION LENGTH, ℓ_U	PRESENT STUDY	POPINSKI (1965)
2. PLATEAU LENGTH, ℓ_P	IMPROVEMENT NEEDED	NONE
3. REATTACHMENT LENGTH, ℓ_R	NONE	NONE
4. SHOCK INTERCEPT 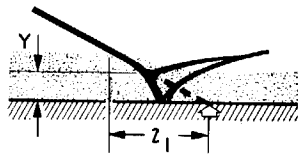	(NOT APPLICABLE)	PRESENT TEST RESULTS DIFFER FROM THOSE OF PINCKNEY
5. TOTAL LENGTH, ℓ_T	IMPROVEMENT NEEDED	

Slide 8

CONFIDENTIAL

INTERACTION MODEL
LAMINAR BOUNDARY LAYER

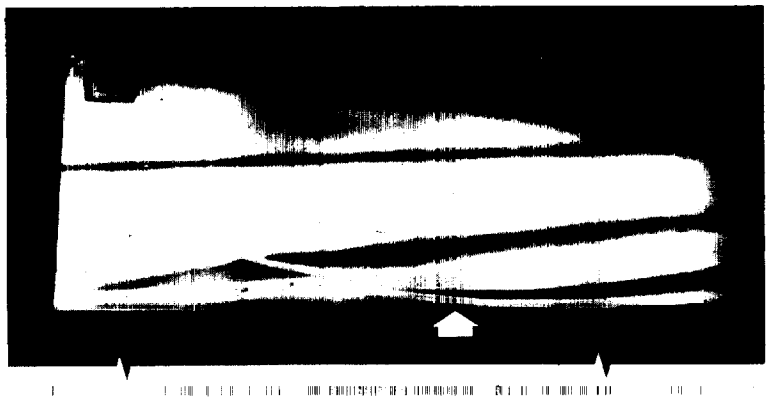

Slide 9a

INTERACTION MODEL
LAMINAR BOUNDARY LAYER
$M_0 = 6.1$ $(Re/ft)_0 = 5.3 \times 10^5$ $\alpha_L = 8°$

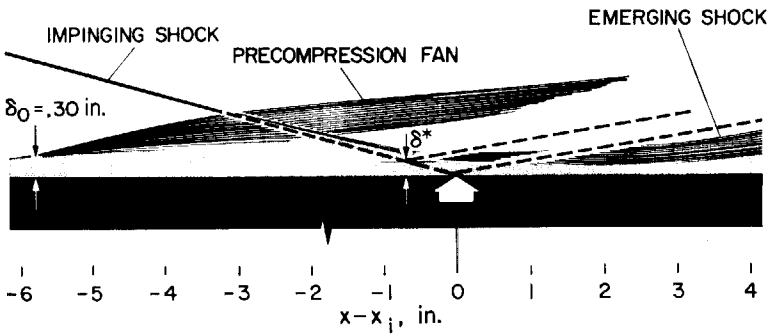

Slide 9b

INTERACTION MODEL
TURBULENT BOUNDARY LAYER

Slide 10a

INTERACTION MODEL
TURBULENT BOUNDARY LAYER
$M_1 = 6.5$ $(Re/ft)_1 = 3.1 \times 10^6$ $\alpha_L = 5°$

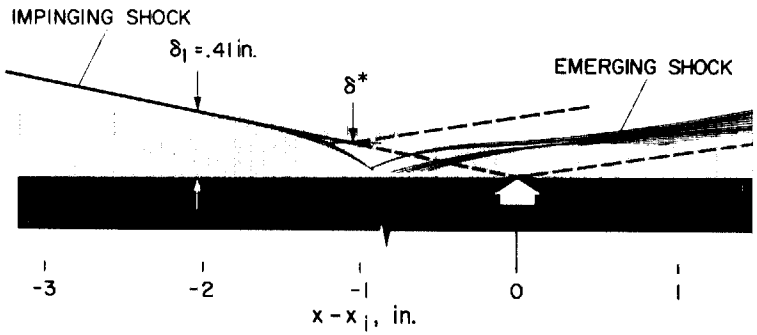

Slide 10b

PREDICTION OF SHOCK STRUCTURE BY METHOD OF CHARACTERISTICS

TURBULENT BOUNDARY LAYER

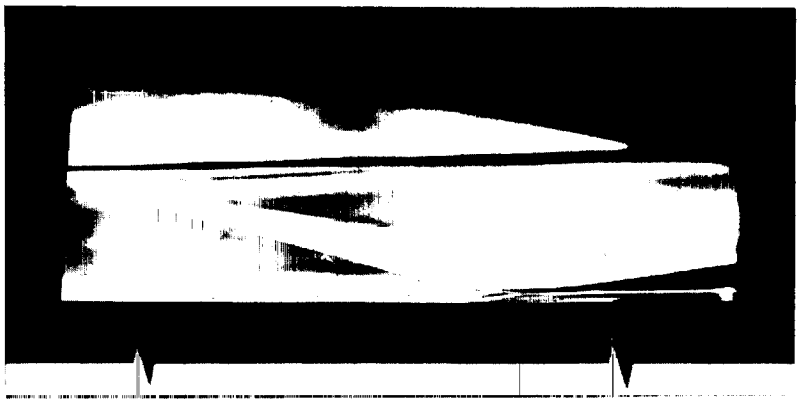

Slide 11a

PREDICTION OF SHOCK STRUCTURE BY METHOD OF CHARACTERISTICS

TURBULENT BOUNDARY LAYER

$M_1 = 6.5$ $(Re/ft)_1 = 3.1 \times 10^6$ $\alpha_L = 8°$

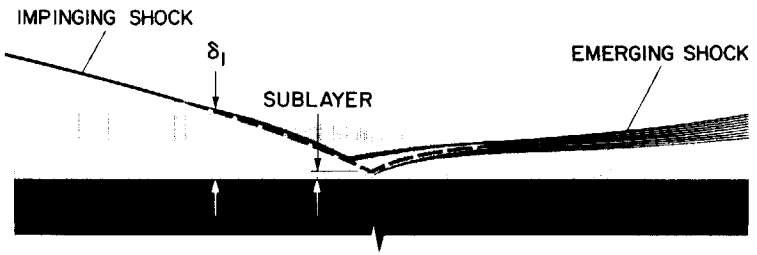

Slide 11b

20. Fuel Injection and Mixing in Scramjet Combustors - John R. Henry

J. R. Henry

SCRAMJET FUEL INJECTION
FEATURES AND PARAMETERS

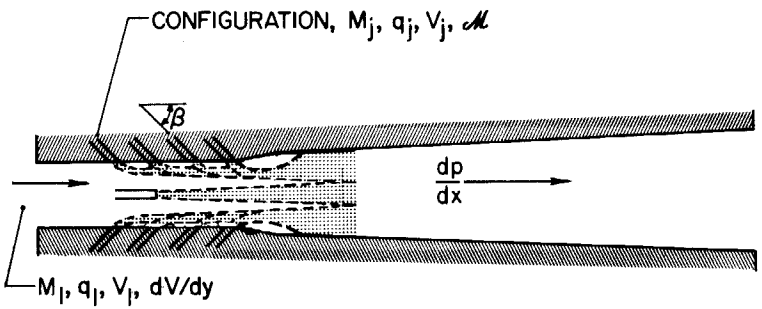

STATUS

WALL INJECTION.....DATA CORRELATION
STREAM INJECTION.....SEMIEMPIRICAL THEORIES

Slide 1.

SCHEMATIC OF FLOW FIELD WITH WALL INJECTION

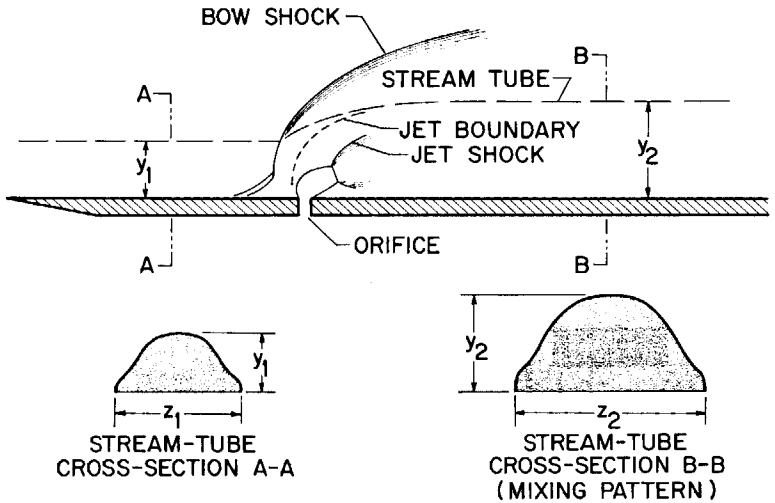

Slide 2.

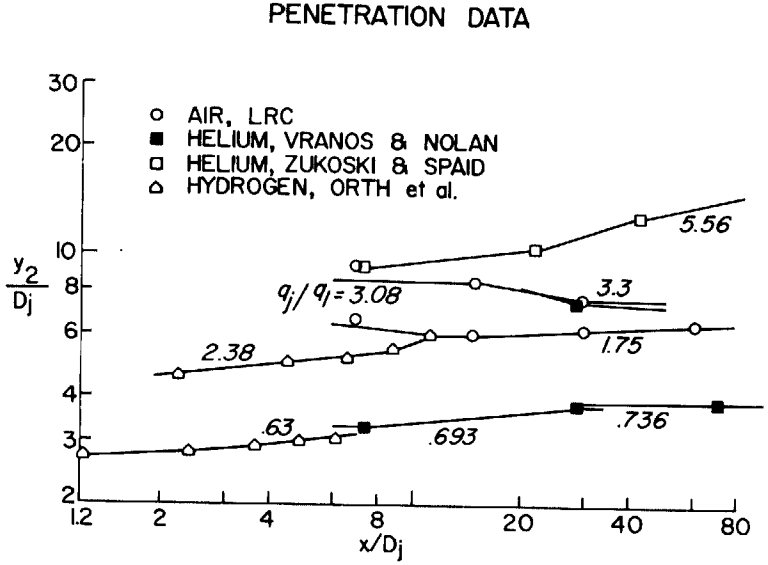

Slide 3.

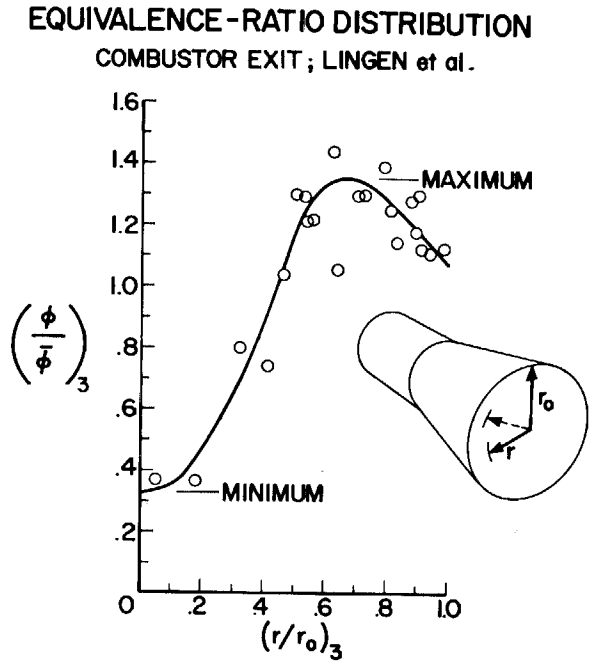

Slide 4.

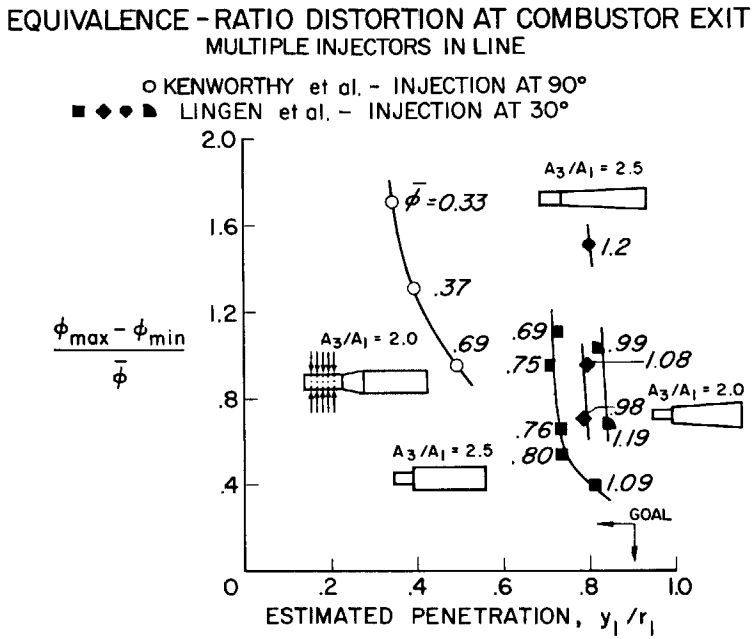

Slide 5.

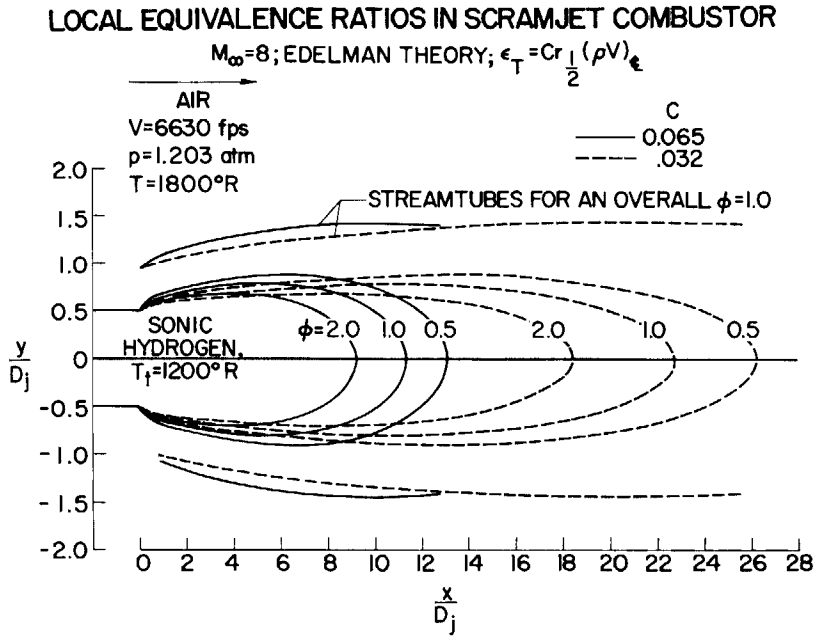

Slide 6.

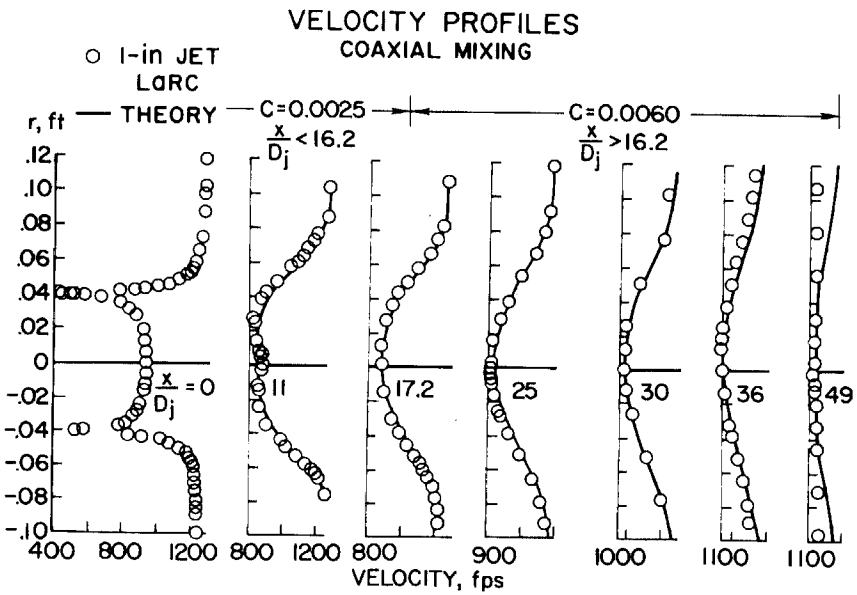

Slide 7.

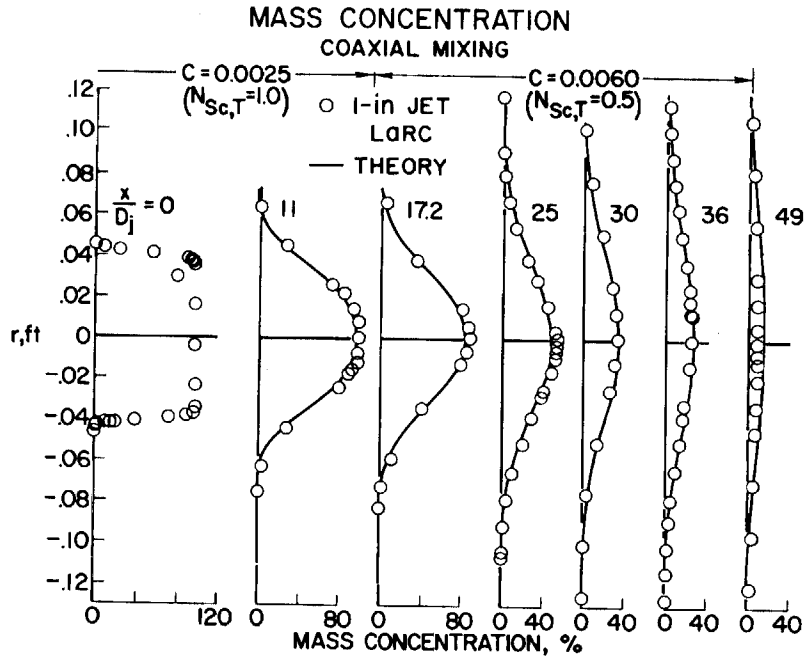

Slide 8.

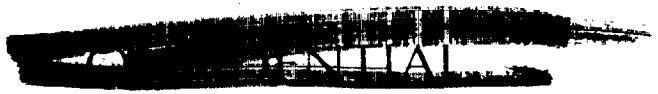

21. Ignition and Chemical Kinetics in Hypersonic Ramjets - Erwin A. Lezberg

E. Lezberg

IGNITION AND CHEMICAL KINETICS

- REACTION TIME
  - IGNITION DELAY
  - CONSUMPTION OF REACTANTS
  - RECOMBINATION
- REACTION RATES AND CHEMISTRY
- ANALYTICAL CALCULATION OF IGNITION
- AERODYNAMIC AND CHEMICAL EFFECTS ON IGNITION
- REACTION RATE LIMITING COMBUSTION

Slide 1.

HYDROGEN-AIR REACTIONS

INITIATION (SMALL PART OF DELAY)

1. $H_2 + O_2 = OH + OH$

CHAIN PROPAGATION AND BRANCHING

2. $H_2 + OH = H_2O + H$
3. $H + O_2 = OH + O$
4. $O + H_2 = OH + H$
5. $O + H_2O = OH + OH$

GAS PHASE QUENCHING (LOW TEMP - HIGH PRESSURE)

6. $H + O_2 + M = HO_2 + M$
7. $HO_2 + H_2 = H_2O_2 + H$ (SLOW)

RECOMBINATION - DISSOCIATION (BULK OF ENERGY RELEASE)

8. $H_2 + M = H + H + M$
9. $O_2 + M = O + O + M$
10. $H + OH + M = H_2O + M$
11. $O + H + M = OH + M$

Slide 2.

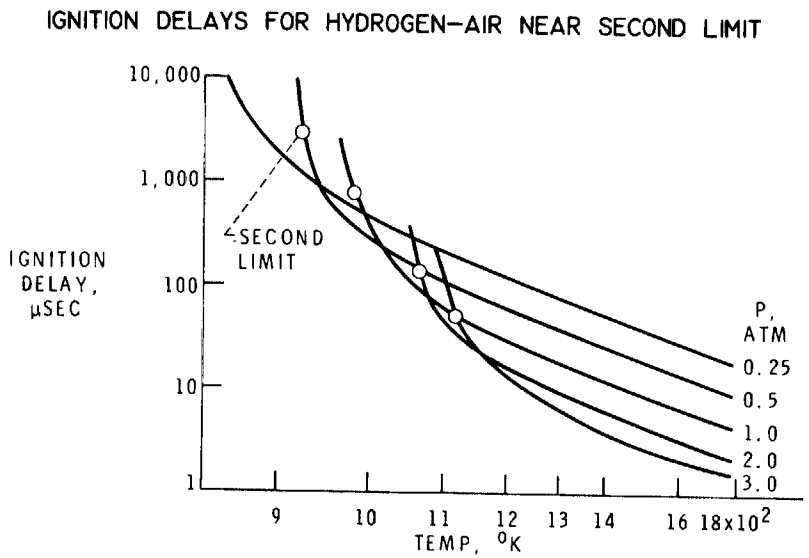

Slide 3.

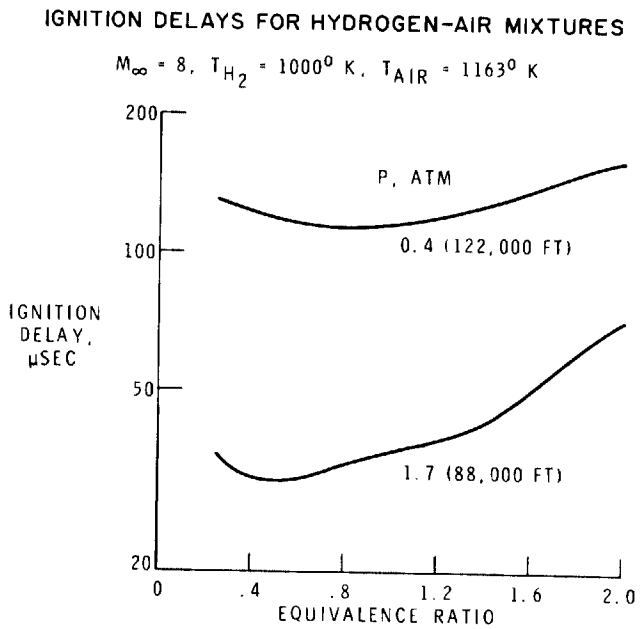

Slide 4.

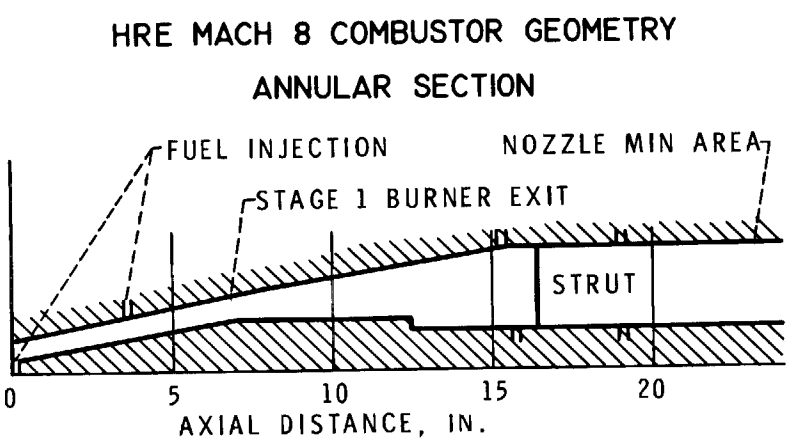

Slide 5.

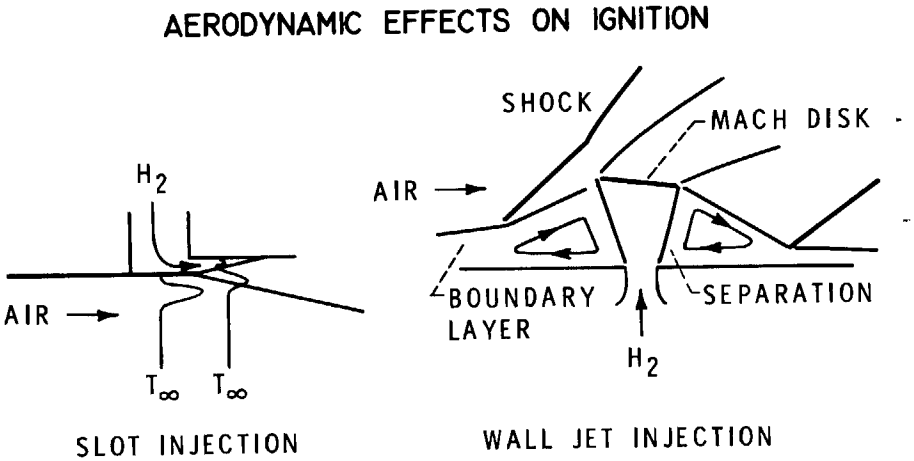

Slide 6.

E. Lezberg

EFFECTS OF BOUNDARY LAYER HEATING ON IGNITION

$T_{MAX} = T_W + 1/4(T_0 - T_W)^2 \; T_0 - T_\infty$

$\delta/\tau_{(T\ MAX)} u_{(T\ MAX)} > 1$ FOR IGNITION

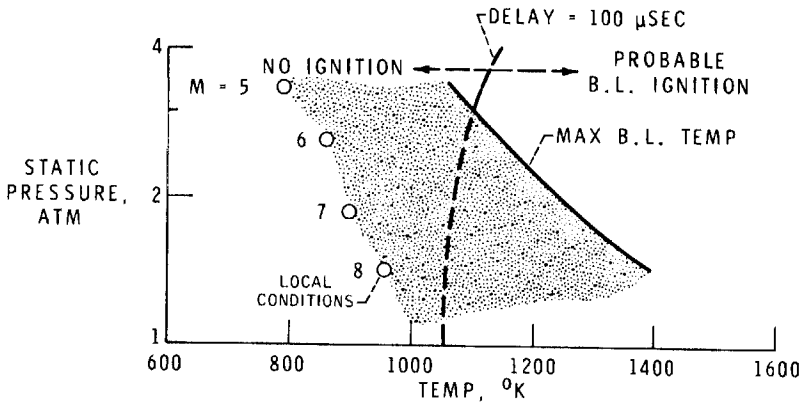

Slide 7.

EFFECT OF WATER ON SECOND EXPLOSION LIMIT

STOICHIOMETRIC H_2-AIR, P = 2 ATM

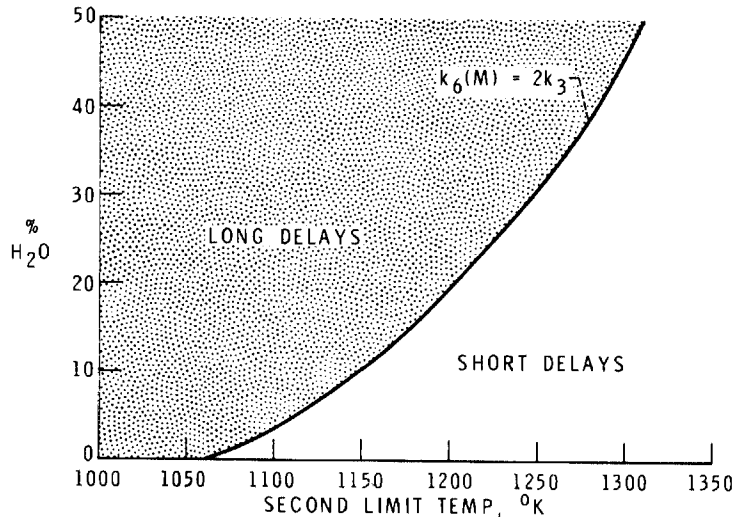

Slide 8.

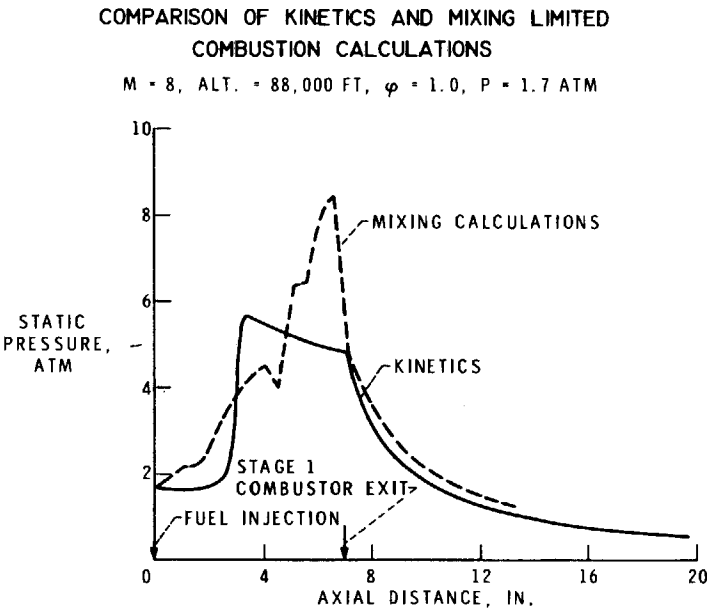

Slide 9.

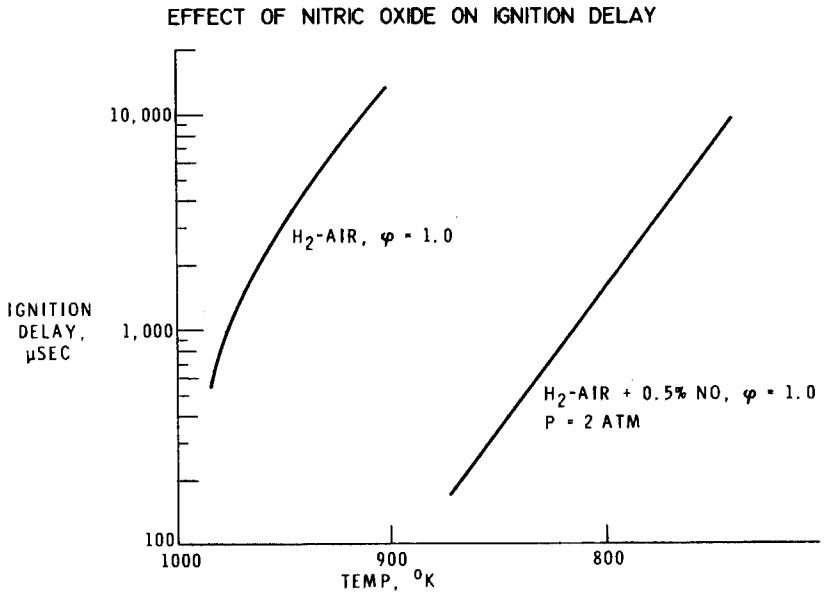

Slide 10.

E. Lezberg

[redacted]

KINETIC CALCULATIONS OF BURNER HEAT RELEASE

M_∞ = 8, ALTITUDE = 122,000 FT, COMB. INLET TEMP = 1121° K,
P = 0.4 ATM, STOICHIOMETRIC H_2-AIR

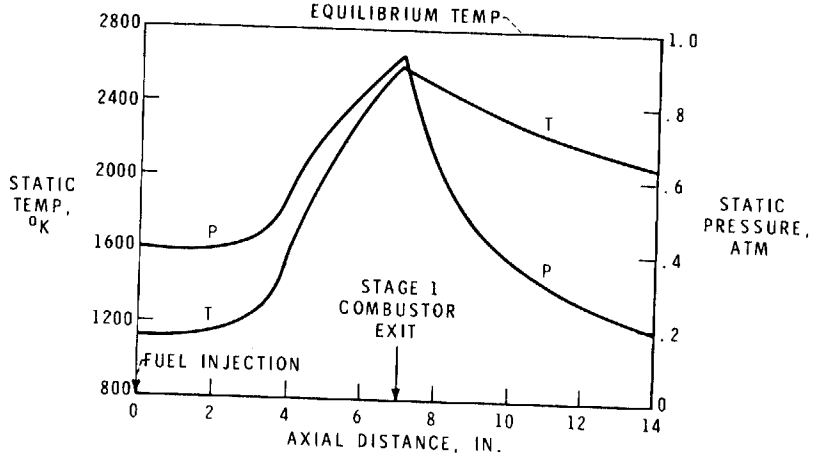

Slide 11.

KINETIC CALCULATIONS OF HYDROGEN MASS FRACTION

M_∞ = 8, ALTITUDE = 122,000 FT, COMB. INLET TEMP = 1121° K,
P = 0.4 ATM, STOICHIOMETRIC H_2-AIR

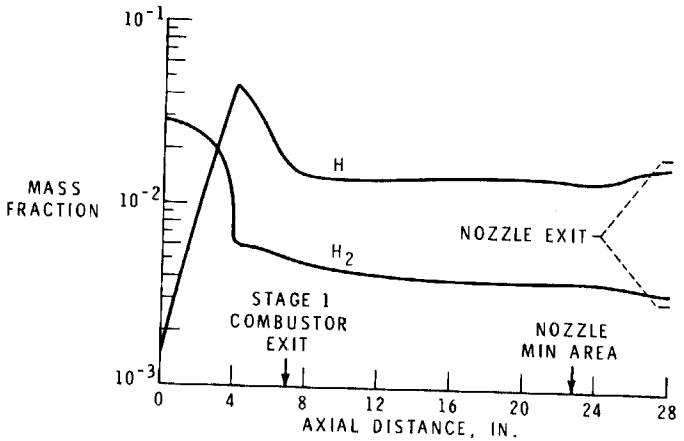

Slide 12.

[redacted]

PERFORMANCE PARAMETERS

COMPARISON OF LOW AND HIGH ALTITUDE CHEMICAL LOSSES

$$\eta_{CH} = \frac{X_{H_2}(1) - (X_{H_2} + 1/2\, X_{OH} + 1/2\, X_H)_2}{X_{H_2}(1) - (X_{H_2} + 1/2\, X_{OH} + 1/2\, X_H)_{2,\,EQ.}}$$

$$\eta_C = \frac{IVAC\ (3) - IVAC\ (1)}{IVAC\ (3') - IVAC\ (1)}$$

ALTITUDE, FT	CHEMICAL EFFICIENCY, η_{CH}			COMBUSTOR EFFICIENCY, η_C
	COMBUSTOR EXIT	NOZZLE ENTRANCE	NOZZLE EXIT	
	A · R = 1.1	A · R = 4.0	A · R = 23.6	A · R = 1.1
88,000	0.920	0.905	0.905	
122,000	0.853	0.798	0.795	0.648

Slide 13.

[redacted]

22. Variable Pitch Supersonic Inflow Compressor and Its Application in a Hypersonic Engine - Emanuel Boxer

[redacted]

SCHEMATIC DIAGRAMS OF VARIABLE-PITCH ENGINE

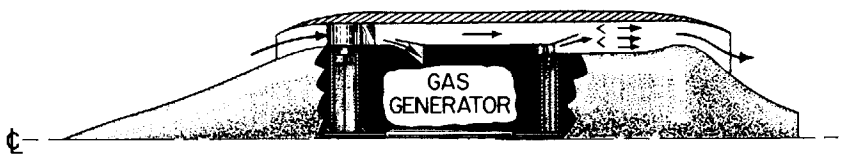

TURBOFAN OPERATION

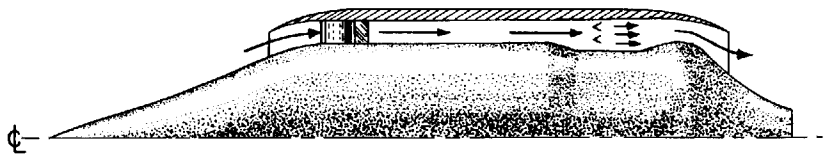

RAMJET OPERATION

Slide 1.

EFFECT OF FAN PERFORMANCE ON ENGINE CYCLE

LH_2 FUEL; $\phi = 1.0$

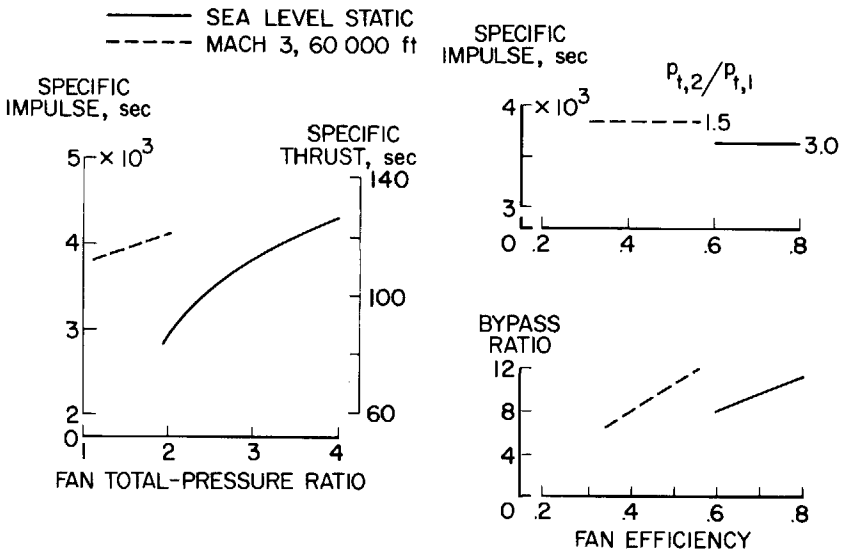

Slide 2.

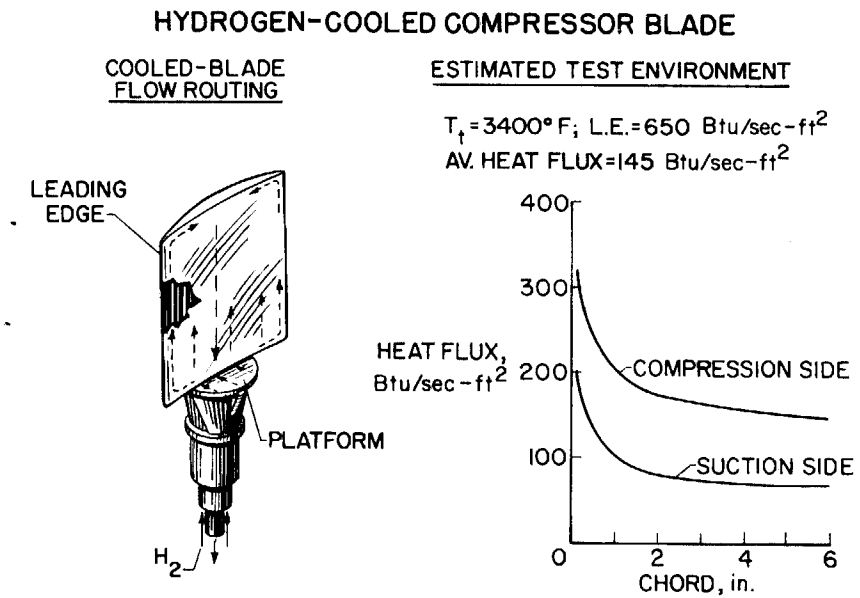

Slide 3.

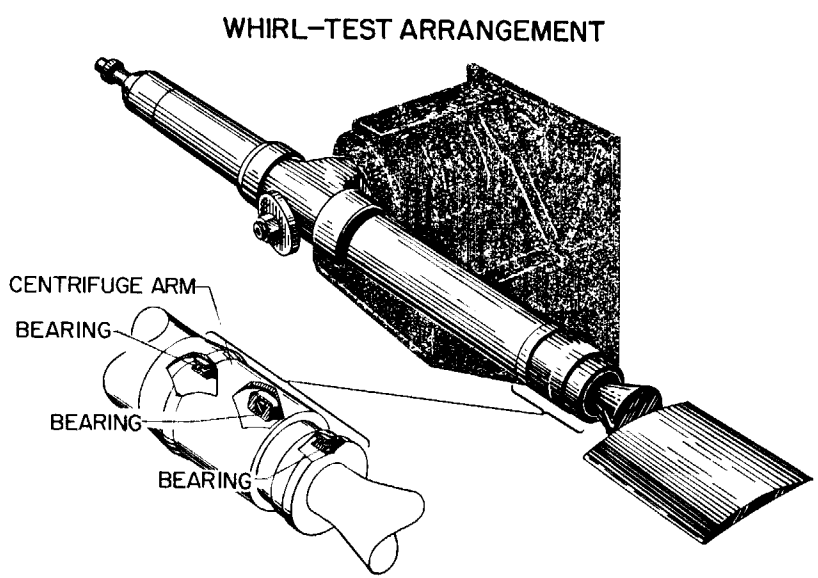

Slide 4.

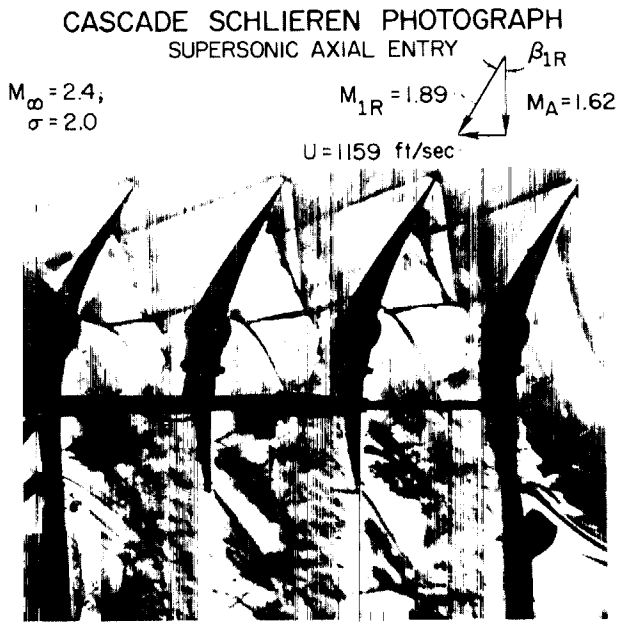

Slide 5.

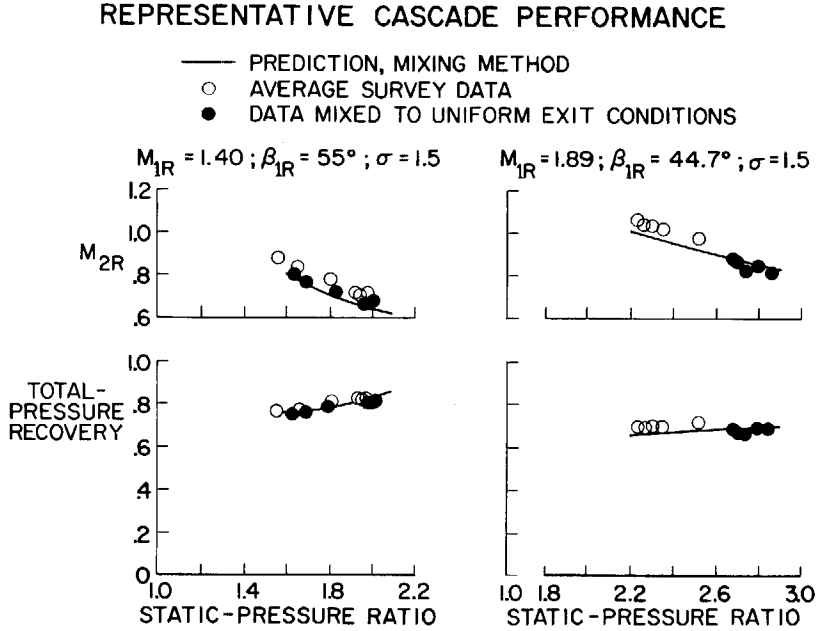

Slide 6.

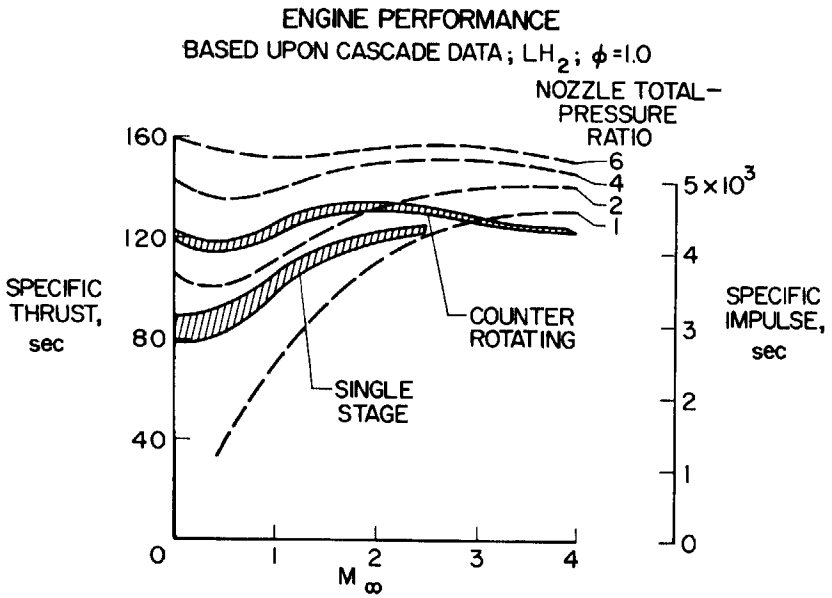
ENGINE PERFORMANCE
BASED UPON CASCADE DATA; LH_2; ϕ=1.0
NOZZLE TOTAL-PRESSURE RATIO
6
4
2
1
160
120
80
40
0
SPECIFIC THRUST, sec
5×10^3
4
3
2
1
0
SPECIFIC IMPULSE, sec
COUNTER ROTATING
SINGLE STAGE
1
2
3
4
M_∞

Slide 7.

23. Measurement Techniques for Hypersonic Propulsion Research - Lloyd N. Krause, Donald R. Buchele, and Isidore Warshawsky

PERFORMANCE PARAMETERS

COMPONENT TESTING

INLET: EFFICIENCY, PRESSURE RATIO, SKIN FRICTION, HEAT TRANSFER RATES, INLET UNSTART

COMBUSTOR-NOZZLE: EFFICIENCY, INITIAL FUEL DISTRIBUTION, LOCAL FUEL-AIR RATIO, HEAT TRANSFER RATES, SKIN FRICTION, FROZEN OR EQUILIBRIUM CONDITION, DETECTION OF IGNITION POINT

ENGINE: GROUND AND FLIGHT TESTING

INTERNAL THRUST, SPECIFIC IMPULSE, THRUST COEFFICIENT, HEAT TRANSFER RATES

Slide 1.

MAIN PERFORMANCE PARAMETERS

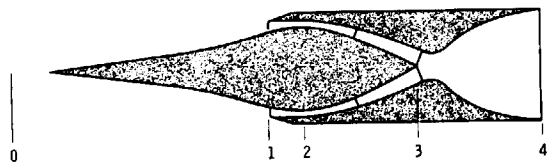

INTERNAL THRUST: $T_i = F_{NET} + D_{EXT} = \dot{M}_{AIR}(V_4 - V_0) + \dot{M}_{H_2}V_4 + P_{S4}A_4 - P_{S0}A$

SPECIFIC IMPULSE: $I = \frac{T_i}{\dot{M}_{H_2}}$

THRUST COEFFICIENT: $C_T = \frac{T_i}{q_0 A}$

PROCESS EFFICIENCY: $K_D = 1 - \frac{\left(\frac{P_{t0}}{P_{t2}}\right)^{\frac{\gamma - 1}{\gamma}} - 1}{\frac{h_{S2}}{h_{S0}} - 1}$

COMBINED COMBUSTOR-NOZZLE CHEMICAL EFFICIENCY: $\eta_{CH_{2-4}} = \frac{(h_{t4} - h_{t2})}{(h_{t4} - h_{t2})_{IDEAL}}$

Slide 2.

[redacted]

MEASURED QUANTITIES

THRUST

TOTAL PRESSURE

STATIC PRESSURE

AIR FLOW RATE

GAS COMPOSITION

FUEL FLOW RATE

TOTAL ENTHALPY

STATIC ENTHALPY

GAS VELOCITY

Slide 3.

FLOW VALUES FOR M8, 120,000 FT-ALTITUDE RAMJET TEST

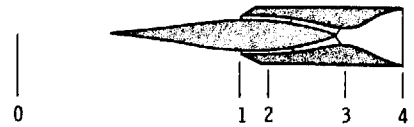

STATION	0	2	3	4
MACH NUMBER	8	3	1.5	4
STATIC PRESSURE, PSIA	0.05	10	30	0.7
TOTAL PRESSURE, PSIA	500	350	100	100
STATIC TEMPERATURE	420° R 230° K	2000° R 1100° K	4900° R 2700° K	1700° R 950° K
TOTAL TEMPERATURE	5700° R 3200° K	5700° R 3200° K	7000° R 3900° K	7000° R 3900° K

Slide 4.

[redacted]

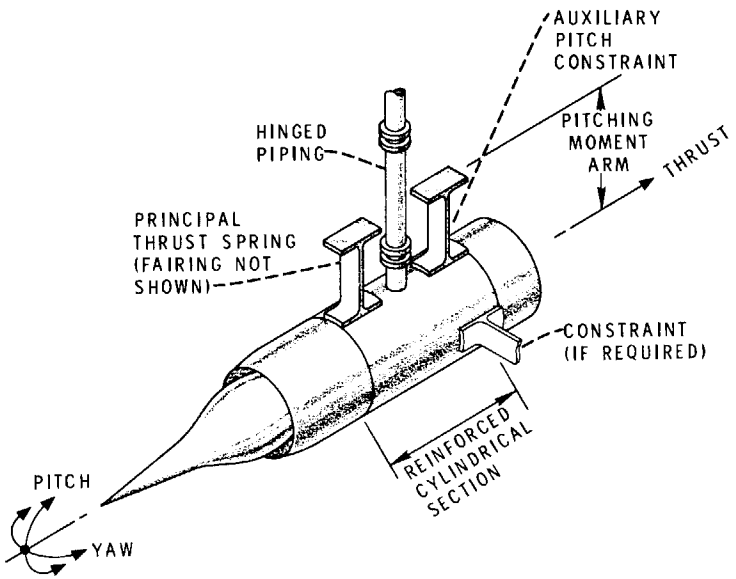

Slide 5.

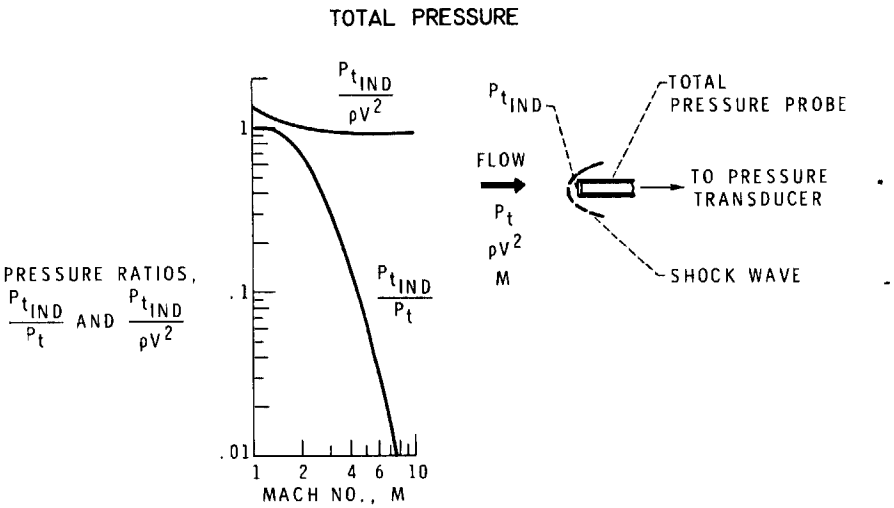

Slide 6.

L. N. Krause

[redacted]

TOTAL PRESSURE RELATED TO THRUST

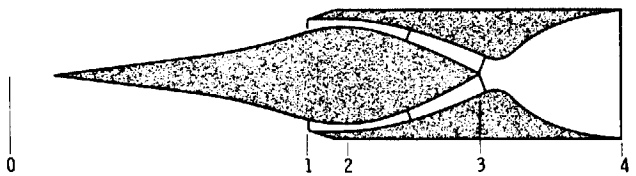

INTERNAL THRUST, $T_i = F_{NET} + D_{EXT} = \dot{M}_{AIR}(V_4 - V_0) + \dot{M}_{H_2}V_4 + P_{S4}A_4 - P_{S0}A$

$$\frac{T_i}{A} = \frac{A_4}{A}\underbrace{(\rho_4 V_4^2 + P_{S4})}_{P_{t4_{IND}}} - \underbrace{(\rho_0 V_0^2 + P_{S0})}_{P_{t0_{IND}}}$$

Slide 7.

STATIC PRESSURE

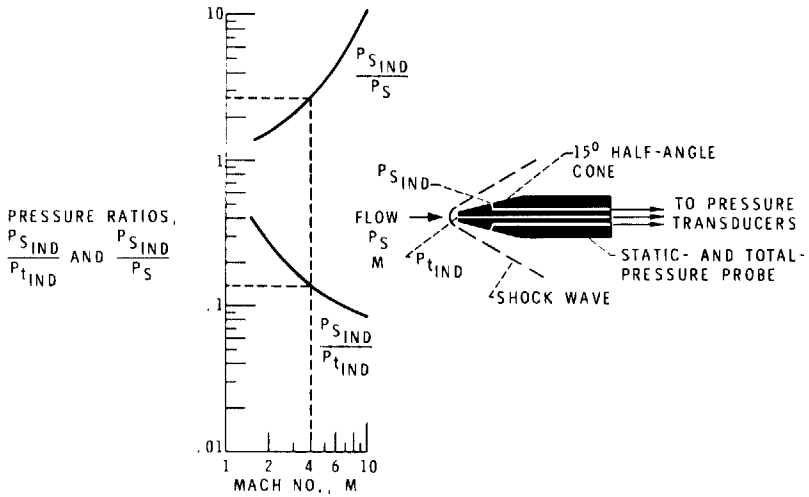

Slide 8.

[redacted]

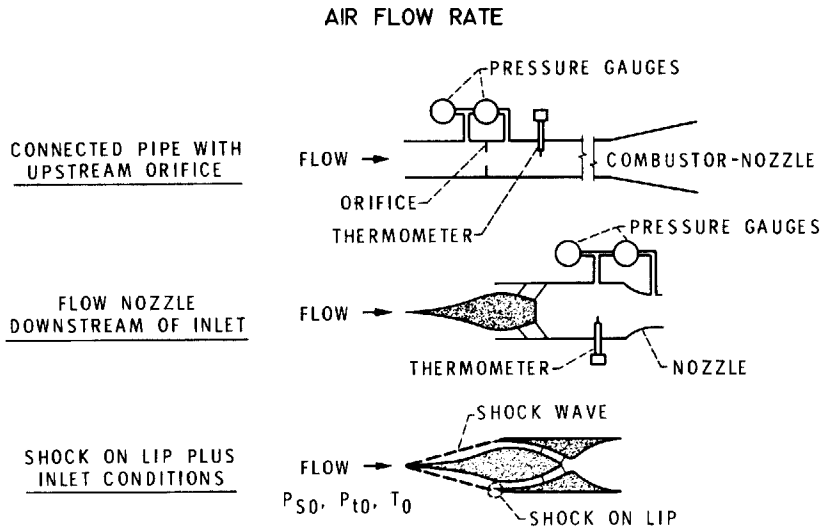

Slide 9.

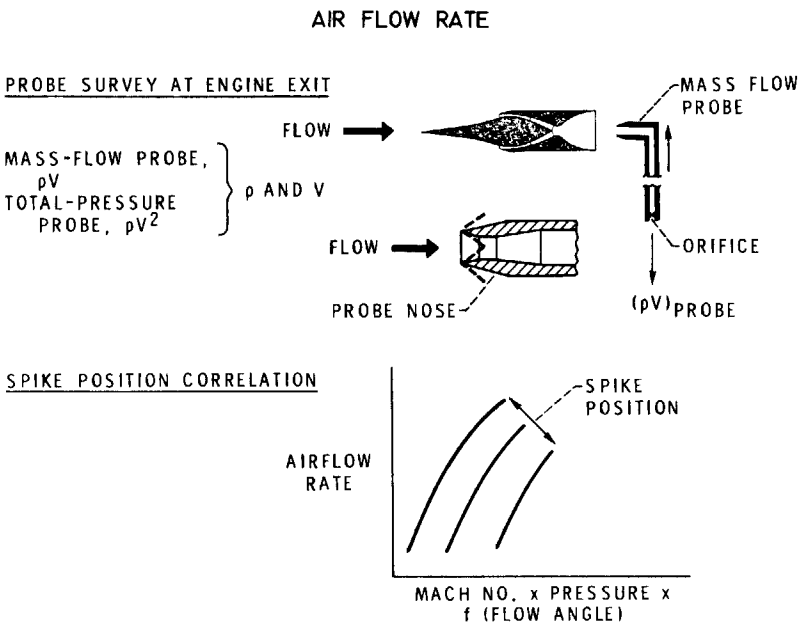

Slide 10.

[redacted]

GAS COMPOSITION

MAIN COMBUSTION PRODUCTS - N_2, H_2O, H_2, O_2, OH, H, O

FUEL-AIR RATIO PROFILE

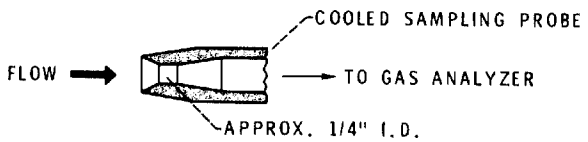

INTERMEDIATE COMPOSITION BY QUENCHING

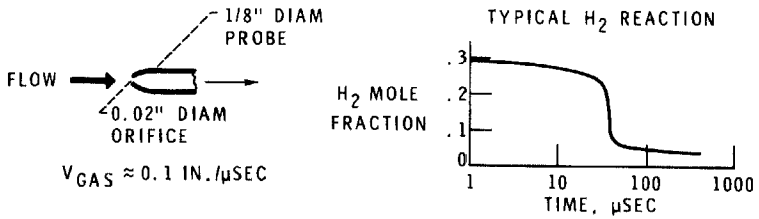

COMPOSITION BY OPTICAL MEANS

Slide 11.

LIQUID-HYDROGEN FLOW METERING

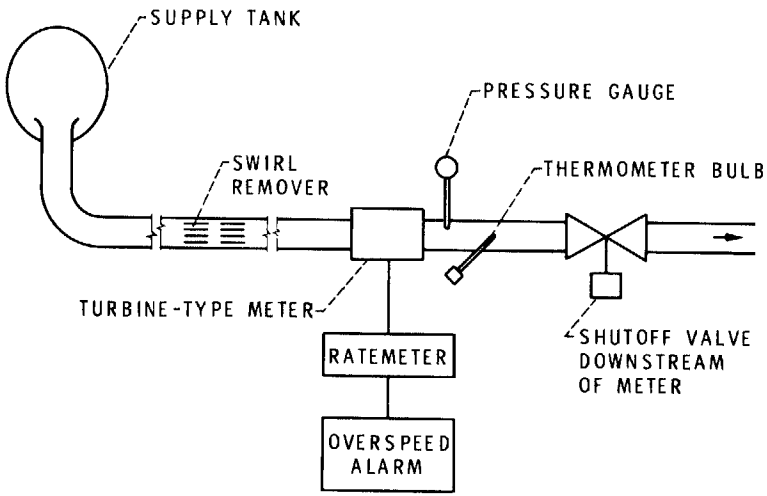

Slide 12.

[redacted]

LOCAL TOTAL ENTHALPY AND RELATED QUANTITIES

ENTHALPY
- CALORIMETRIC PROBE

TEMPERATURE
- THERMOCOUPLES
  - *RADIATION-SHIELDED, HIGH RECOVERY
    - Ir60Rh-Ir — TO 4300° R (2400° K)
  - CONDUCTION- AND RADIATION-COOLED
    - Ir60Rh-Ir — TO 4900° R (2700° K)
  - *RADIATION-COOLED BARE WEDGE
    - Ir60Rh-Ir — TO 4600° R (2500° K)
    - W5Re-W26Re — TO 5000° R (2800° K)
- OPTICAL PYROMETRY OF A SURFACE

HEAT TRANSFER RATE
- *COOLED-GAS PROBE
- *COOLED-TUBE PROBE
- STAGNATION-POINT PROBE

DENSITY
- *PNEUMATIC PROBE

SOUND VELOCITY
- SOUND VELOCITY PROBE

Slide 13.

NONLINEAR SPATIAL AVERAGING

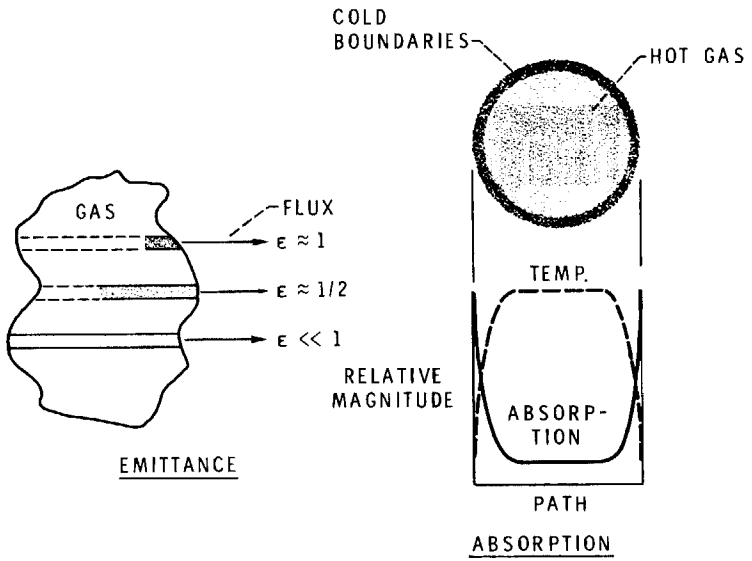

Slide 14.

L. N. Krause

[redacted]

INTEGRATED STATIC TEMPERATURE (RADIATION METHODS)

NULL METHODS	
LINE REVERSAL (Li, Na, Cs, OH, H_2O)	TO 6500^0 R (3600^0 K)
ABSORPTION-EMISSION (KURLBAUM)	TO 6500^0 R (3600^0 K)
NON-NULL METHODS	
ABSORPTION-EMISSION	
EMISSION, TWO PATH-LENGTH	
EMISSION, TWO 'COLOR'	
SPECTRAL INTENSITY DISTRIBUTION	
MICROWAVE ABSORPTION (FOR FLUCTUATIONS)	3500^0 - 5500^0 R (2000^0 - 3000^0 K)

QUANTITIES RELATED TO INTEGRATED STATIC TEMPERATURE

DENSITY
- ABSORPTION OF X-RAYS, β-RAYS, γ-RAYS

SOUND VELOCITY
- $(R_0\gamma T/M_w = \gamma p/\rho)$

CONCENTRATION, BY ABSORPTION MEASUREMENTS
- OH, FROM 306.4 nm BAND
- H_2O, FROM 2.7 μm BAND

Slide 15.

LOCAL STATIC TEMPERATURE (OPTICAL METHODS)

LOCAL INJECTION OF Li Na, Cs

MOVING OPTICAL PROBE

SPECTRAL EXCITATION BY CROSSED BEAM
- ALSO APPLICABLE TO LOCAL-VELOCITY MEAS., SUBJECT TO SPREADING BY
  - (A) VELOCITY PROFILE
  - (B) EDDY DIFFUSION

SPATIAL SCANNING

SPECTRAL SCANNING

Slide 16.

[redacted]

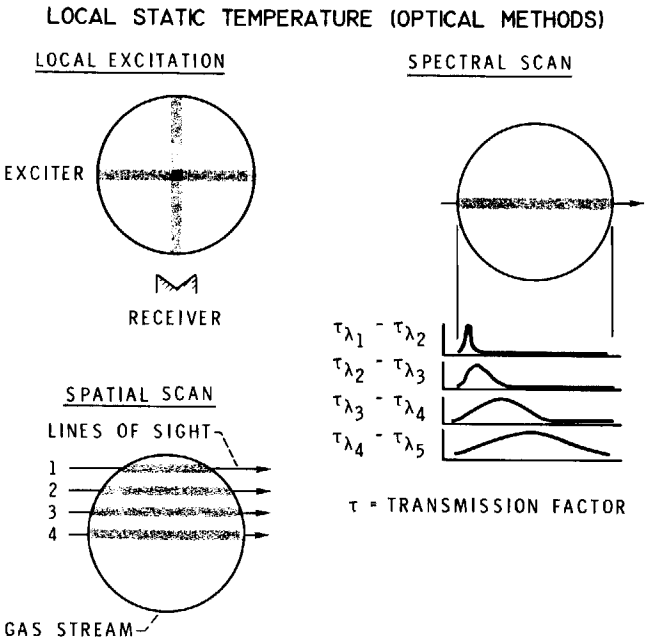
LOCAL STATIC TEMPERATURE (OPTICAL METHODS)
LOCAL EXCITATION
EXCITER
RECEIVER
SPATIAL SCAN
LINES OF SIGHT
1
2
3
4
GAS STREAM
SPECTRAL SCAN
$\tau_{\lambda_1} - \tau_{\lambda_2}$
$\tau_{\lambda_2} - \tau_{\lambda_3}$
$\tau_{\lambda_3} - \tau_{\lambda_4}$
$\tau_{\lambda_4} - \tau_{\lambda_5}$
τ = TRANSMISSION FACTOR

Slide 17.

24. Introductory Remarks - Richard R. Heldenfels

LANGLEY 8-FOOT HIGH TEMPERATURE
STRUCTURES TUNNEL

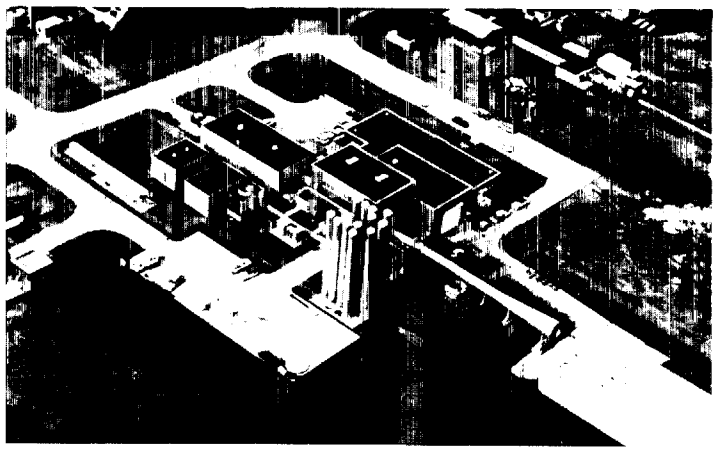

Slide 7.

LANGLEY 8-FOOT HIGH-TEMPERATURE STRUCTURES TUNNEL

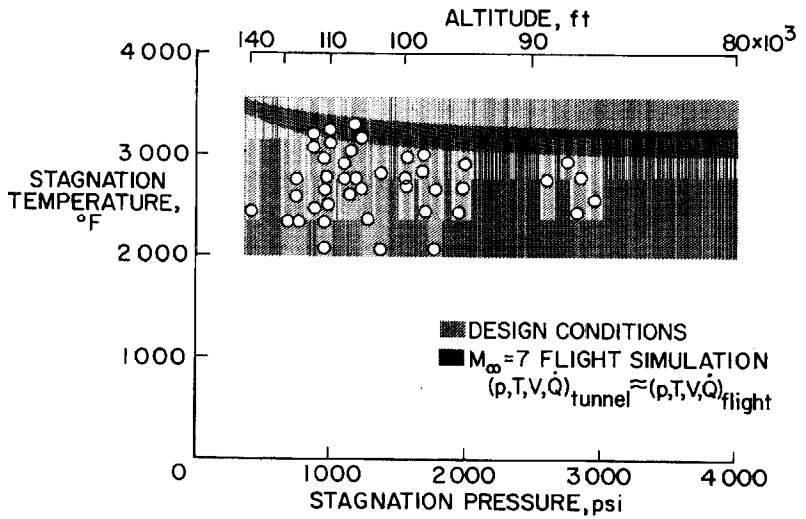

Slide 8.

STRUCTURAL PROBLEM AREAS
HYPERSONIC CRUISE VEHICLES

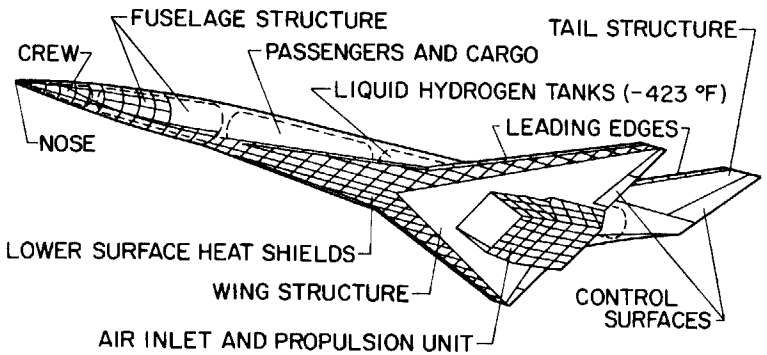

Slide 5.

WING STRUCTURES RESEARCH

CONCEPT ANALYSIS AND EVALUATION

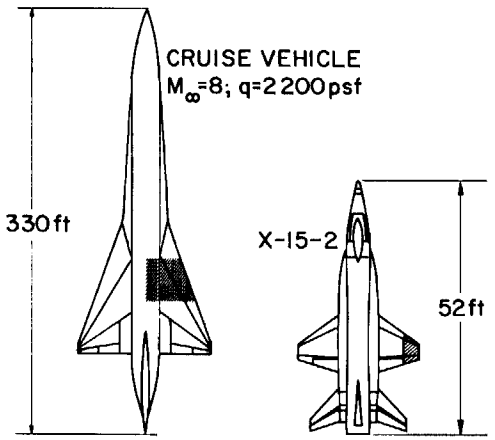

DELTA WING X-15 RESEARCH AIRPLANE

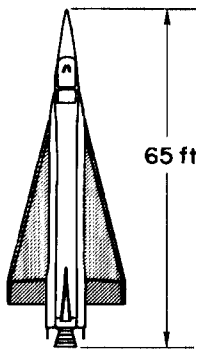

Slide 6.

[redacted]

25. Structural Comparison of All-Body and Wing-Body Liquid Hydrogen Fueled Hypersonic Aircraft - Mark D. Ardema and Thomas J. Gregory

[redacted]

[redacted]

WING - BODY CONFIGURATION

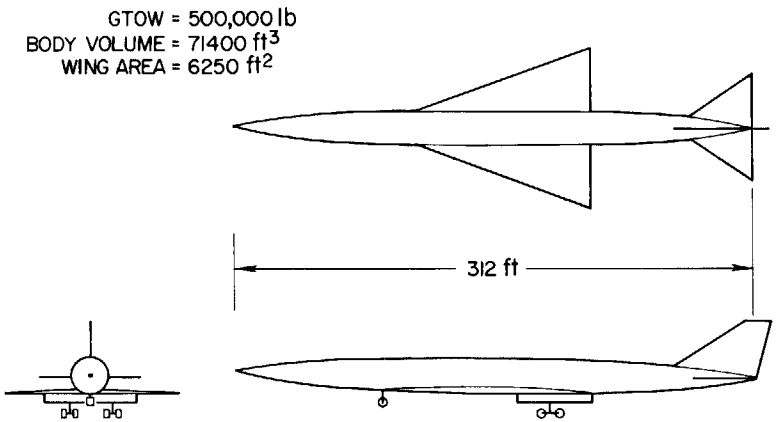

Slide 3.

LOADING MODEL
ALL BODY

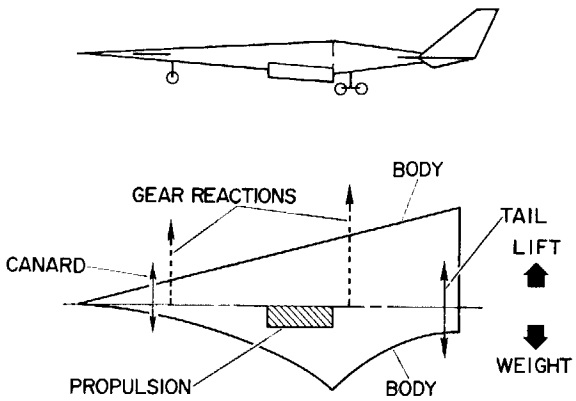

Slide 4.

[redacted]

HYPERSONIC AIRCRAFT CONFIGURATION

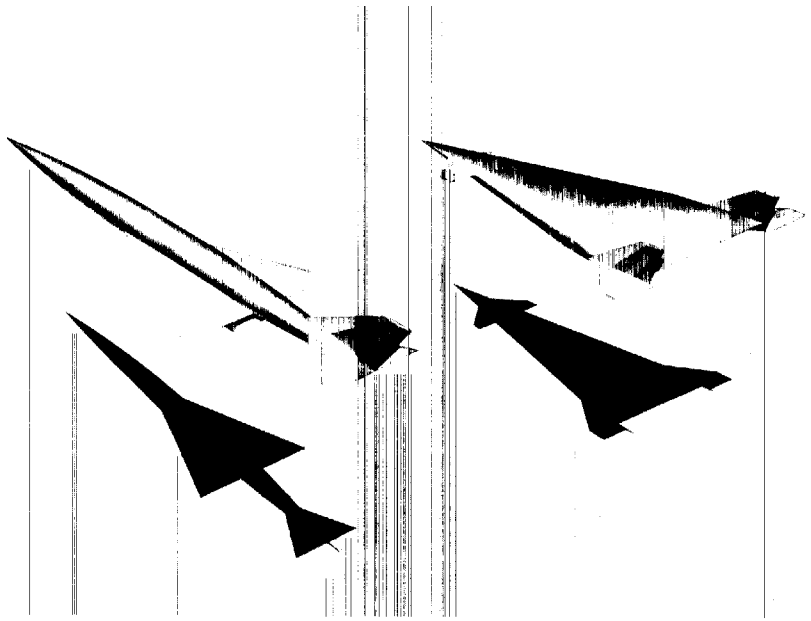

Slide 1.

ALL BODY CONFIGURATION

GTOW = 500,000 lb
BODY VOLUME = 71400 ft^3
PLAN AREA = 9660 ft^2

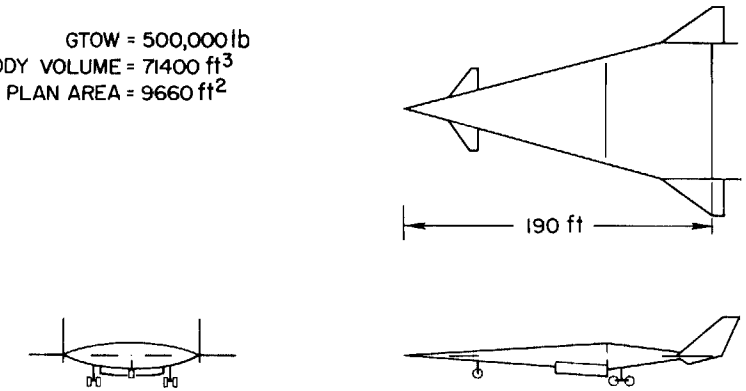

Slide 2.

LOADING MODEL
WING - BODY

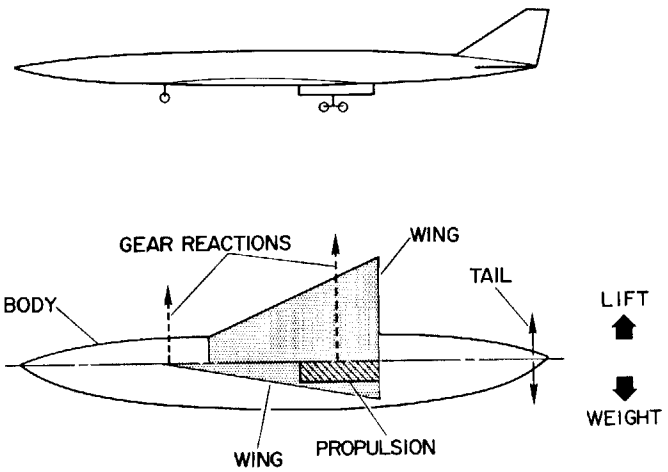

Slide 5.

ANALYSIS CONSIDERATIONS AND ASSUMPTIONS

- LOADING CONDITIONS
  - LONGITUDINAL BENDING
  - 2 psi MAXIMUM INTERNAL PRESSURE
- FAILURE MODES
  - TENSION AND COMPRESSION YIELD STRENGTH
  - PANEL BUCKLING (WIDE COLUMN)
  - GENERAL BUCKLING (FRAME SPACING BY SHANLEY'S METHOD)
- NOMINAL STRUCTURE
  - TRUSS CORE SANDWICH
  - 0.01 in. MINIMUM GAGE
  - REN'E 41 AT 1200° F

Slide 6.

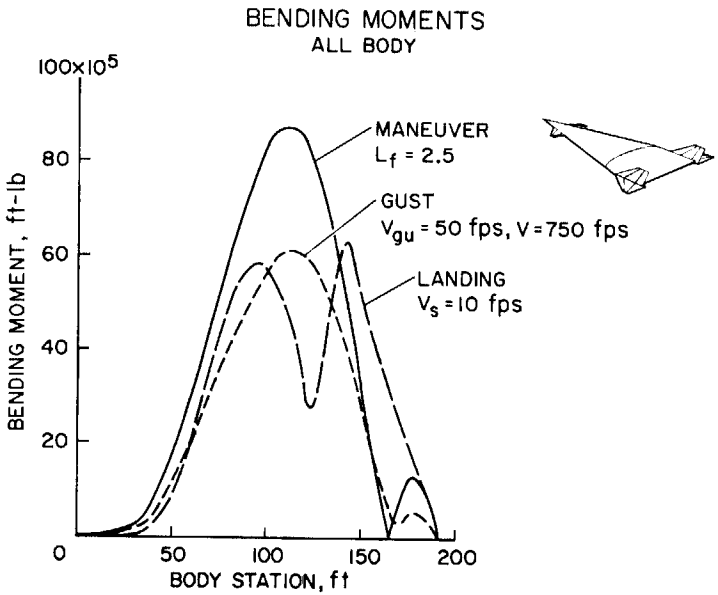

Slide 7.

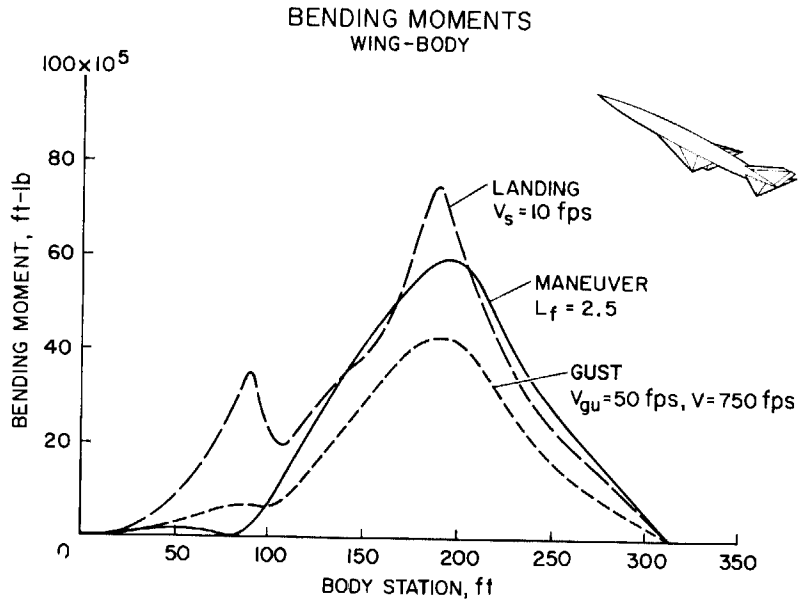

Slide 8.

26. Structural Materials for Hypersonic Aircraft - Bland A. Stein, Walter Illg, and John D. Buckley

EQUILIBRIUM SKIN TEMPERATURES

$M_\infty = 8$; $q = 2200$ psf

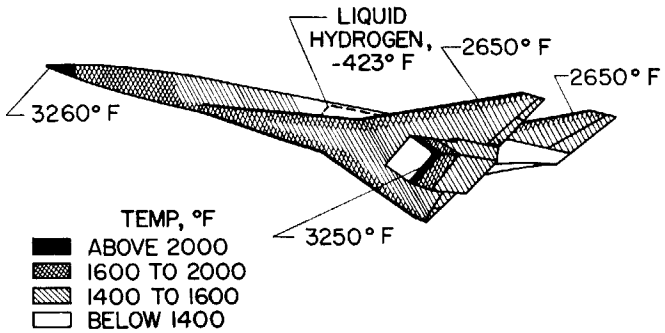

Slide 1.

TEMPERATURE-TIME MINIMUM OBJECTIVES

APPLICATION	TEMPERATURES, °F	EXPOSURE TIMES, hr
• PRIMARY STRUCTURE	BELOW 1600	>5000
• HEAT SHIELDS	1600 TO 2000	>5000
• LEADING EDGES	2000 TO 3100	>50
• NOSE CAP	3100 TO 4000	>5
• HYDROGEN TANKAGE	-423 TO 600	>5000

Slide 2.

PROBLEM AREAS FOR MATERIALS APPLICATIONS

MAJOR PROBLEM AREA

POSSIBLE PROBLEM AREA

NO APPARENT PROBLEMS

PROPERTY	APPLICATION				
	PRIMARY STRUCTURE	HEAT SHIELD	LEADING EDGE	NOSE CAP	HYDROGEN TANKAGE
OXIDATION OR CORROSION					
CREEP					
DUCTILITY					
FATIGUE					
STIFFNESS					
NOTCH SENSITIVITY					
STRENGTH					

Slide 3.

MATERIALS FOR PRIMARY STRUCTURE

OXIDATION AND CREEP

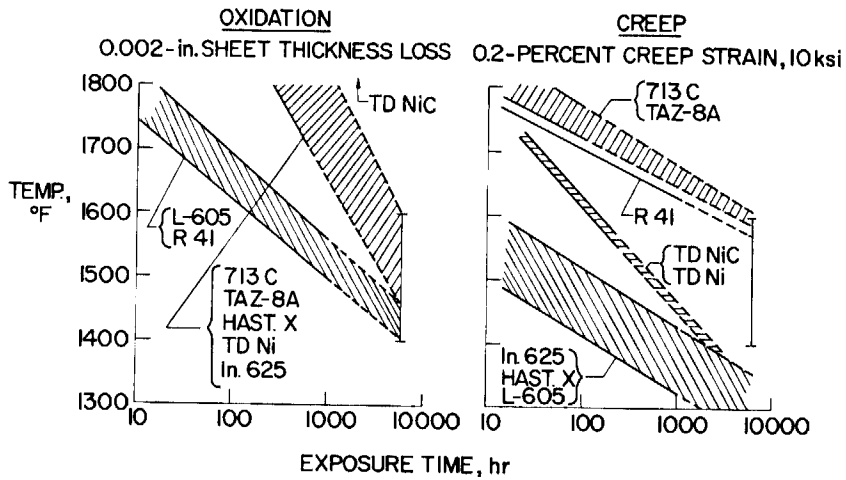

Slide 4.

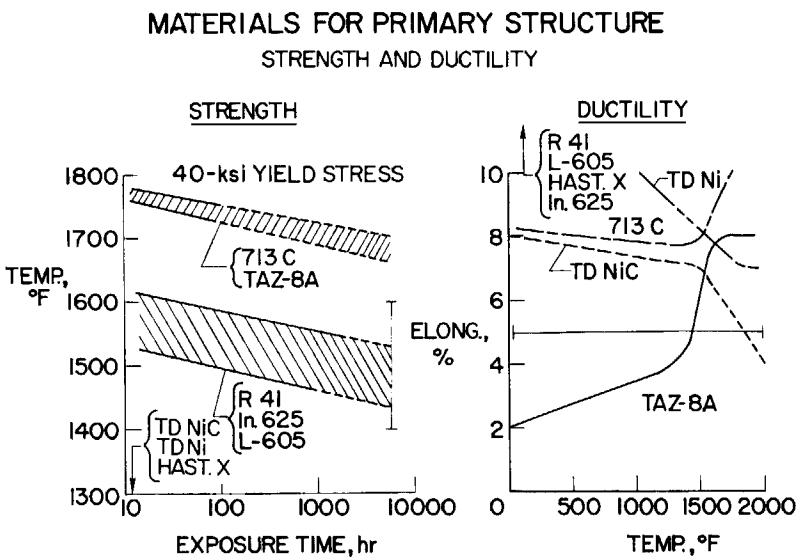

Slide 5.

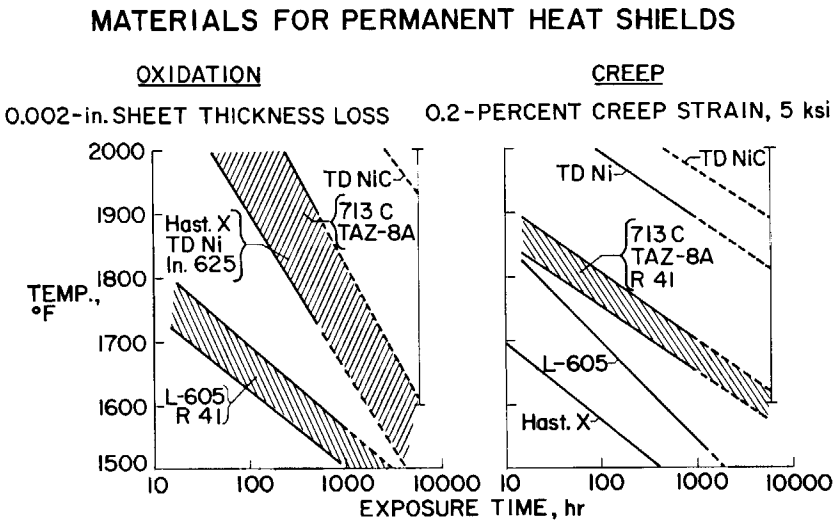

Slide 6.

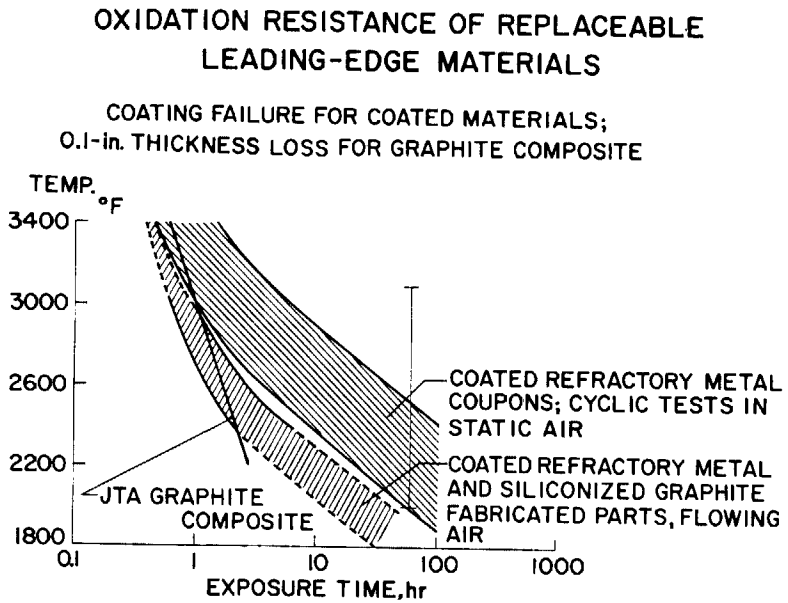

Slide 7.

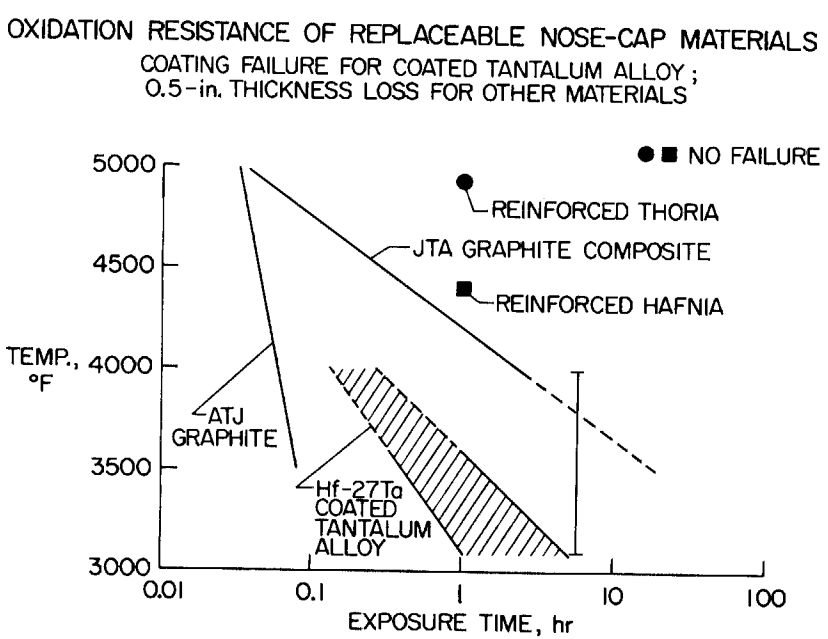

Slide 8.

NOTCH TENSILE STRENGTH FOR HYDROGEN-TANKAGE MATERIALS

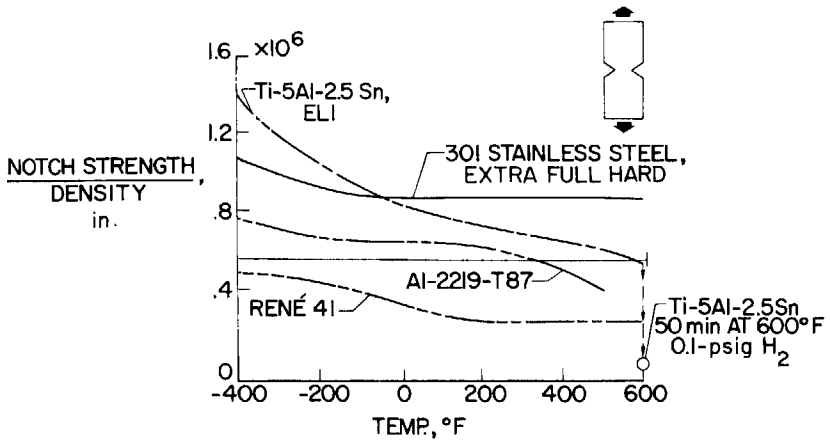

Slide 9.

SUMMARY

- PRIMARY STRUCTURE : AVAILABLE SHEET MATERIALS APPEAR ADEQUATE TO 1400° F ; INADEQUATE AT 1600° F
- HEAT SHIELDS : DISPERSION STABILIZED NICKEL-20 PERCENT CHROMIUM APPEARS PROMISING FROM 1600° F TO 2000° F
- LEADING EDGES : CURRENT MATERIALS REQUIRE REPLACEMENT AFTER 1 OR 2 FLIGHT CYCLES AT 3100° F
- NOSE CAPS : JTA GRAPHITE COMPOSITE APPEARS PROMISING FOR 2 OR 3 CYCLES AT 4000° F

HYDROGEN TANKAGE : STAINLESS STEELS APPEAR MOST PROMISING BECAUSE OF BOTH CRYOGENIC AND ELEVATED TEMPERATURE OPERATION REQUIREMENTS

Slide 10.

27. A Carbon Dioxide Purge and Thermal Protection System for Liquid Hydrogen Tanks - L. Robert Jackson and Ellsworth L. Sharpe

L. R. Jackson

LIQUID HYDROGEN TANKS

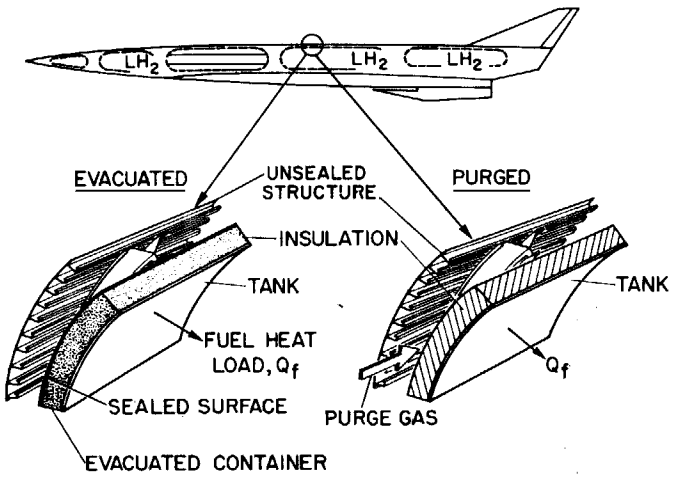

Slide 1.

CO_2 PURGE AND FROST SYSTEM

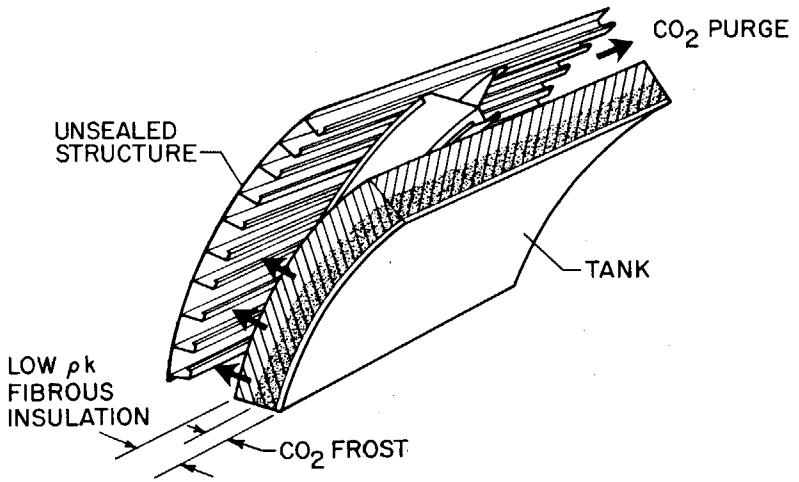

Slide 2.

L. R. Jackson

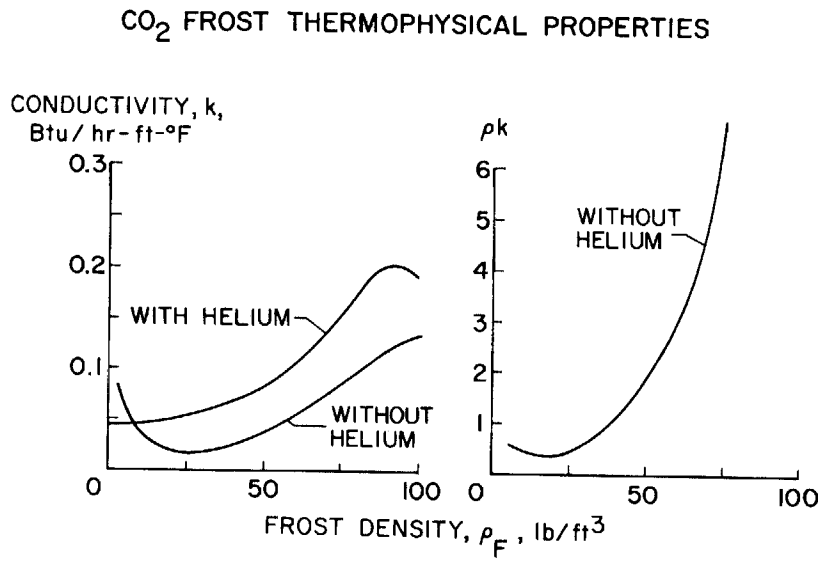

Slide 3.

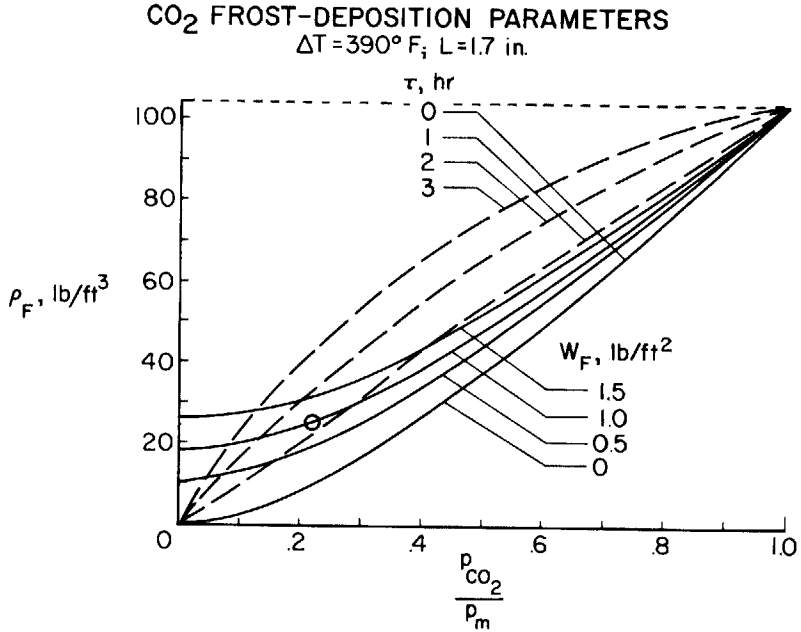

Slide 4.

EFFECT OF DEPOSITION TIME ON CO_2 SYSTEM WEIGHT

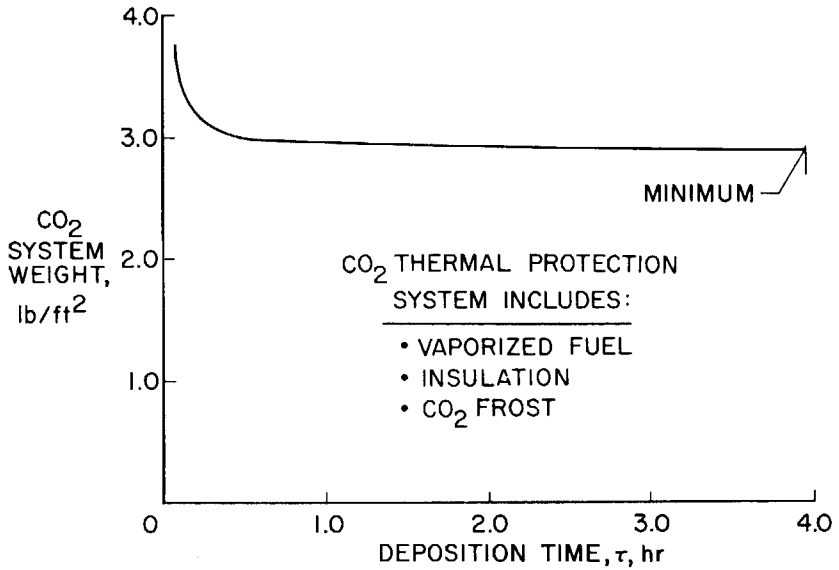

Slide 5.

CO_2 PURGE CONDITIONS DURING AN ABORTED FLIGHT

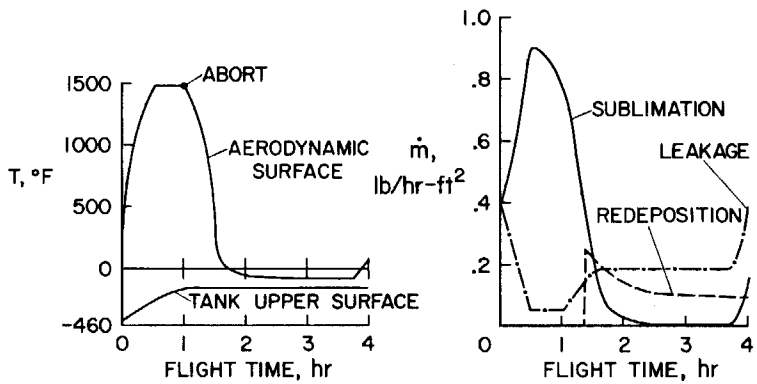

Slide 6.

[redacted]

CO_2 SYSTEM STRUCTURAL MODEL

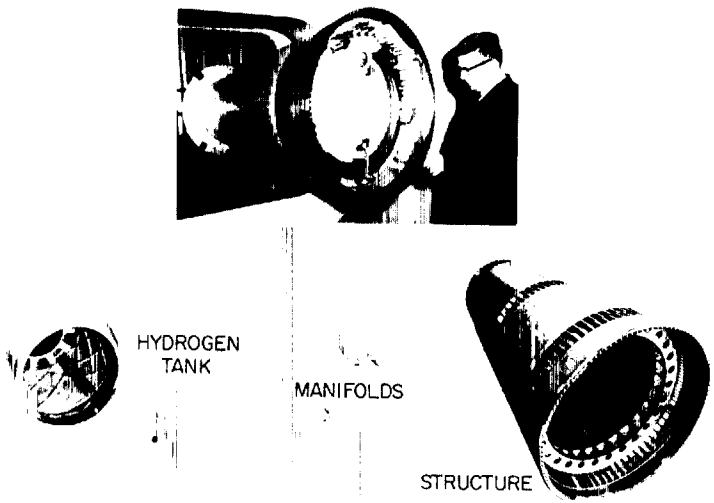

Slide 7.

HYPERSONIC-STRUCTURES TEST APPARATUS

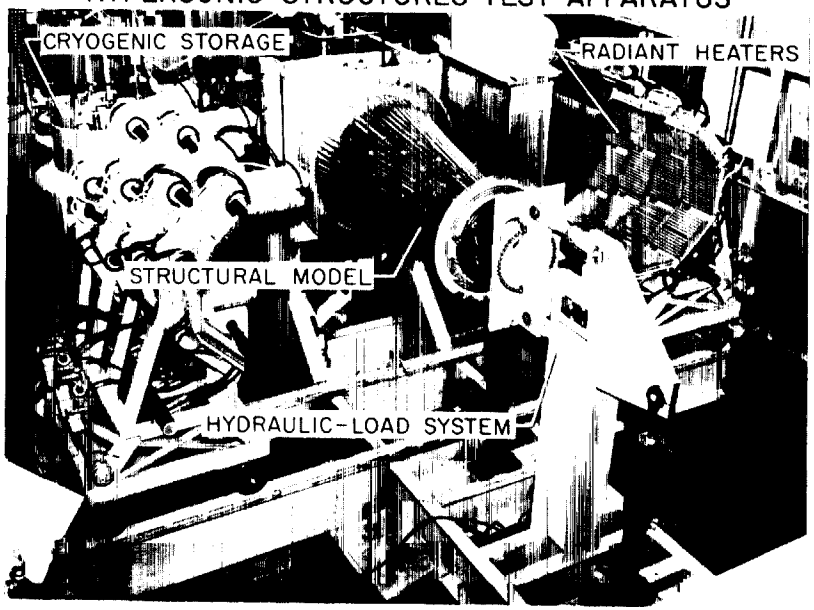

Slide 8.

[redacted]

CO_2 SYSTEM TEST RESULTS

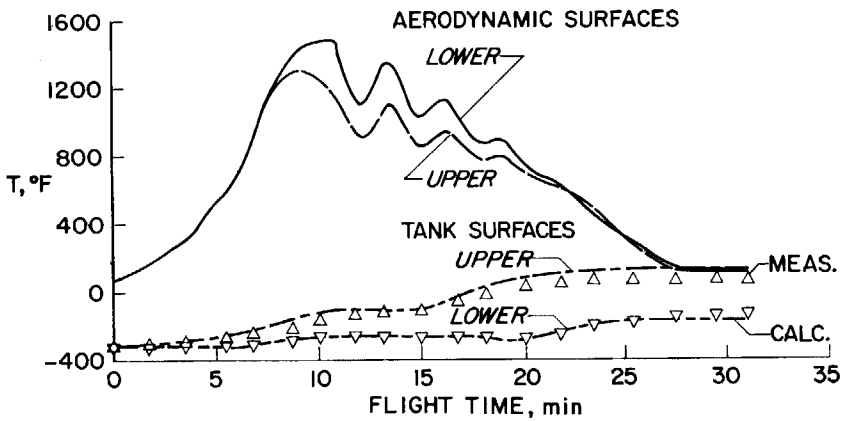

Slide 9.

28. Fuselage and Tank Structures for Hypersonic Aircraft - John L. Shideler and L. Robert Jackson

J. L. Shideler

LH_2 TANK WALL CONFIGURATIONS

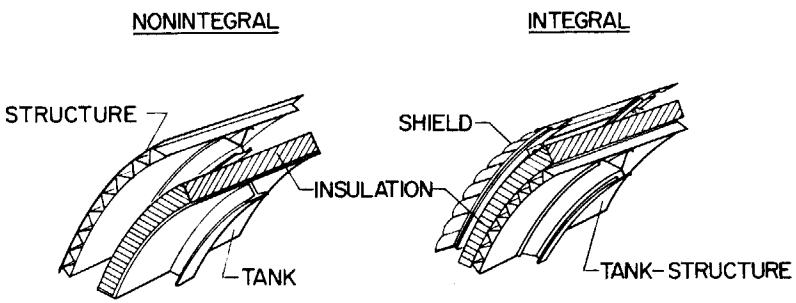

Slide 1.

WEIGHT-STRENGTH ANALYSES OF CYLINDERS SUBJECTED TO AXIAL COMPRESSION

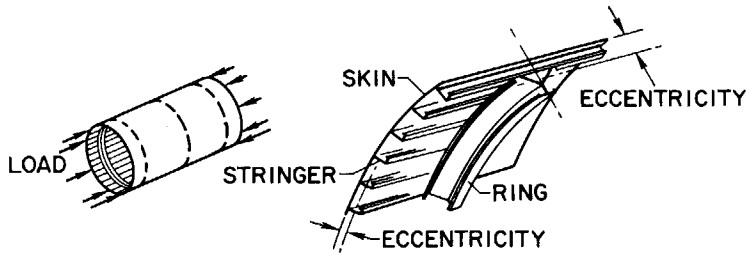

CONSIDERATIONS:

1-INTERNAL OR EXTERNAL RINGS

2-INTERNAL OR EXTERNAL STRINGERS

3-ARBITRARY SKIN, STRINGER, AND RING GEOMETRIES

4-LOCAL INSTABILITY, PANEL INSTABILITY, AND GENERAL INSTABILITY

Slide 2.

ADVANCED FUSELAGE STRUCTURES

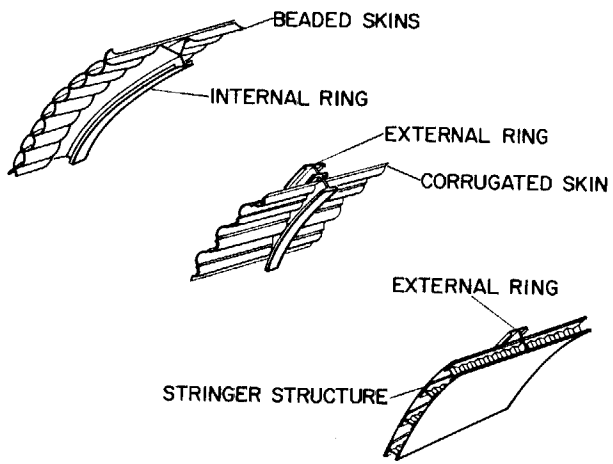

Slide 3.

CYLINDER STRUCTURAL EFFICIENCY

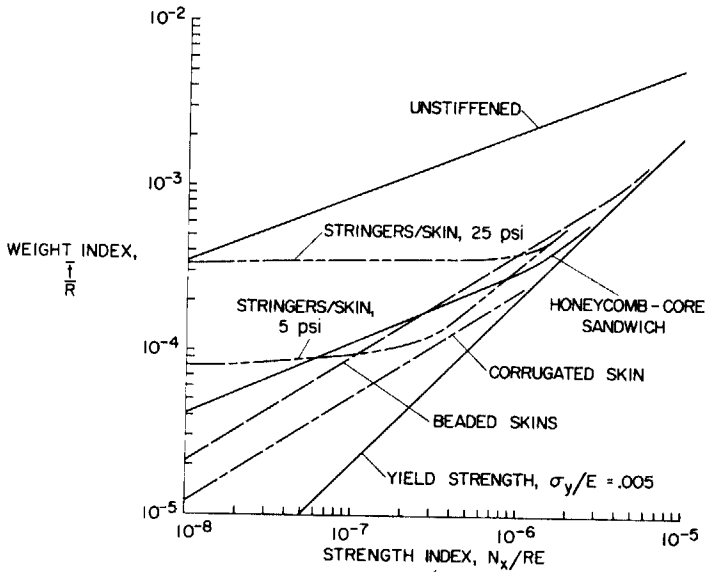

Slide 4.

J. L. Shideler

THERMAL PROTECTION SYSTEMS

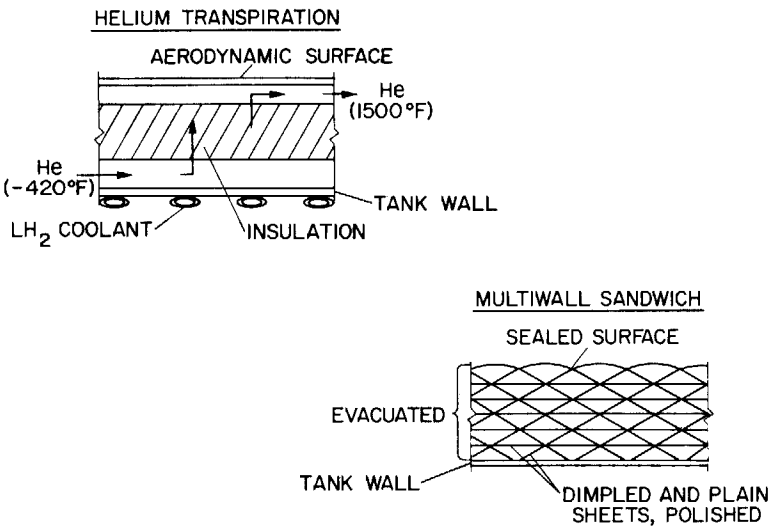

Slide 5.

THERMAL PROTECTION SYSTEMS

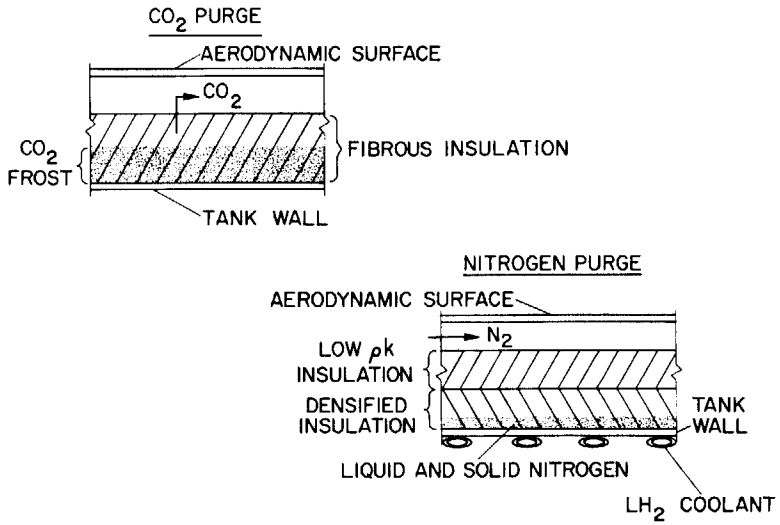

Slide 6.

[redacted]

INTEGRAL LH_2 TANK STRUCTURES

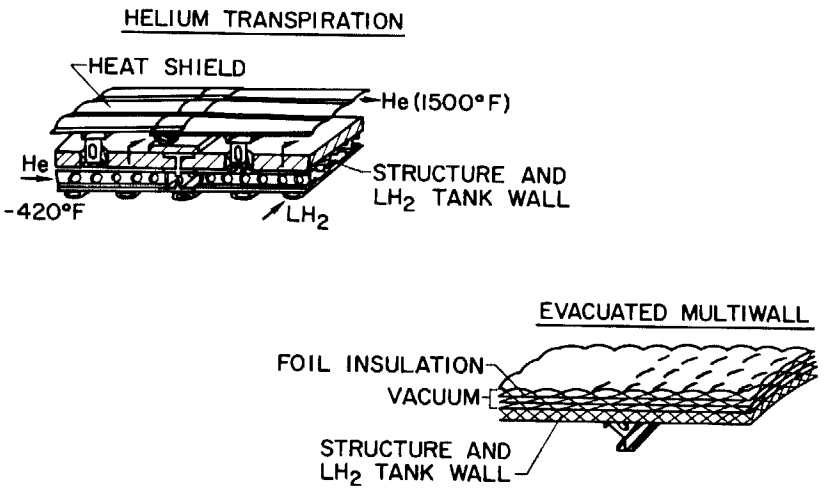

Slide 7.

NONINTEGRAL LH_2 TANK STRUCTURES

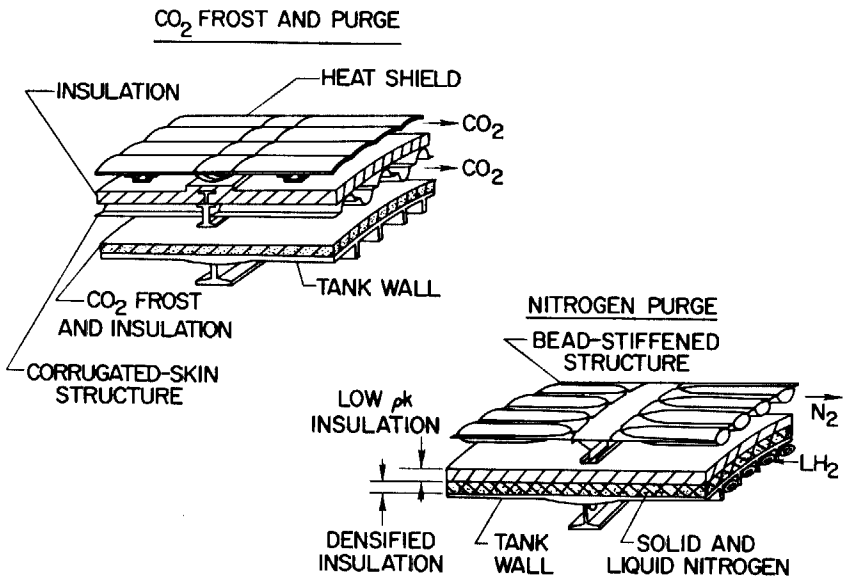

Slide 8.

[redacted]

BASIS OF FUSELAGE-TANK WALL WEIGHTS

HYPERSONIC CRUISE AIRPLANE, MACH 8

(1) PRIMARY STRUCTURE
- (a) BENDING LOAD = 1500 lb/in.
- (b) ALLOWANCE OF 0.75 lb/ft^2 FOR BULKHEADS, REINFORCEMENTS, ETC.

(2) THERMAL PROTECTION
- (a) FLIGHT TIME = 1.5 hr
- (b) AVERAGE AERODYNAMIC SURFACE TEMP. = 1500° F

(3) TANK
- (a) BENDING LOAD = 350 lb/in.
- (b) INTERNAL PRESSURE = 15 psi

(4) HEAT SHIELDS
- (a) PRESSURE LOAD = 0.75 psi
- (b) ALLOWANCE OF 0.25 lb/ft^2 FOR OMEGA SEALS

Slide 9.

STRUCTURAL WEIGHT COMPARISONS

BASED ON CRUISE AIRPLANE MISSION

TYPE OF THERMAL PROTECTION	WEIGHT, lb/ft^2				
	SHIELD	T.P.S.	TANK	STRUCTURE	TOTAL
INTEGRAL CONFIGURATION					
HELIUM TRANSPIRATION	1.0	3.9	—	2.0	6.9
EVACUATED MULTIWALL	0.3	2.0	—	2.0	4.3
NONINTEGRAL CONFIGURATION					
CO_2 FROST	1.0	2.5	1.2	1.5	6.2
N_2 PURGE	—	2.9	1.5	2.4	6.8

Slide 10.

29. Analysis of Wing Structures for Hypersonic Aircraft - Melvin S. Anderson, James C. Robinson, and George F. Klich

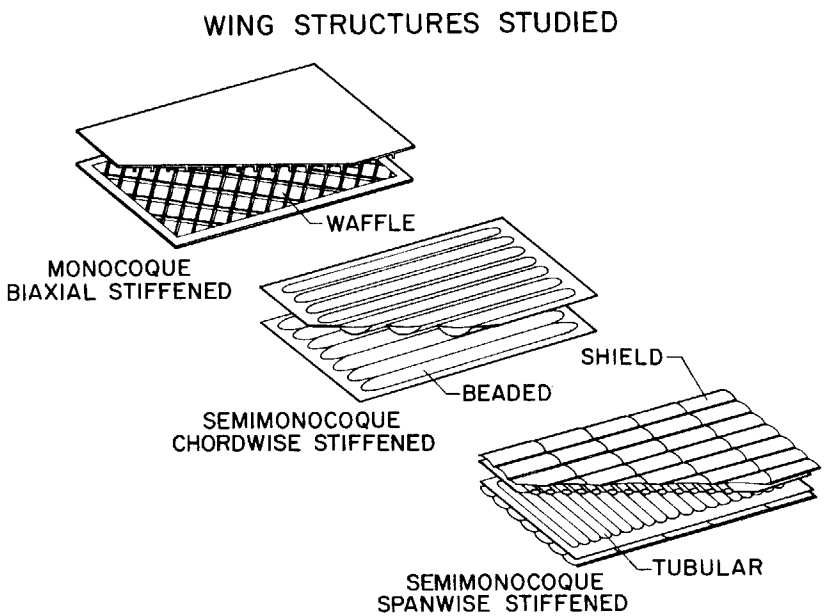

Slide 5.

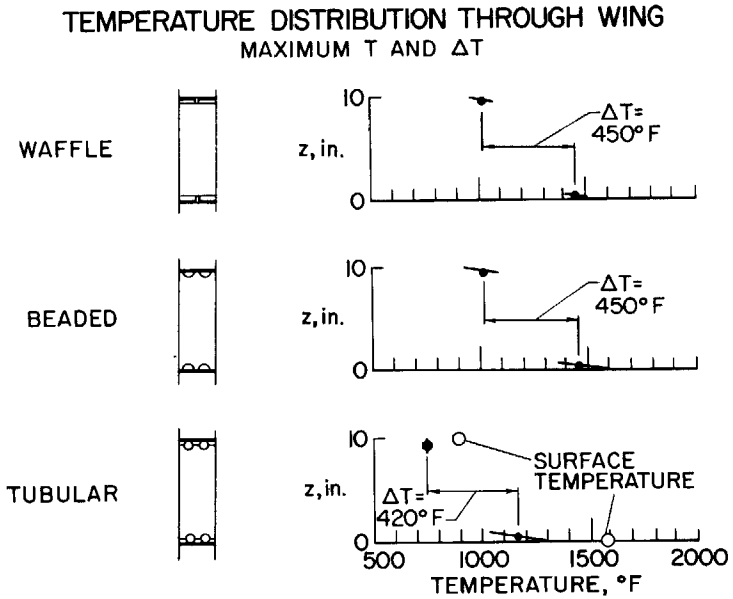

Slide 6.

[redacted]

STRUCTURAL-PANEL TEMPERATURES

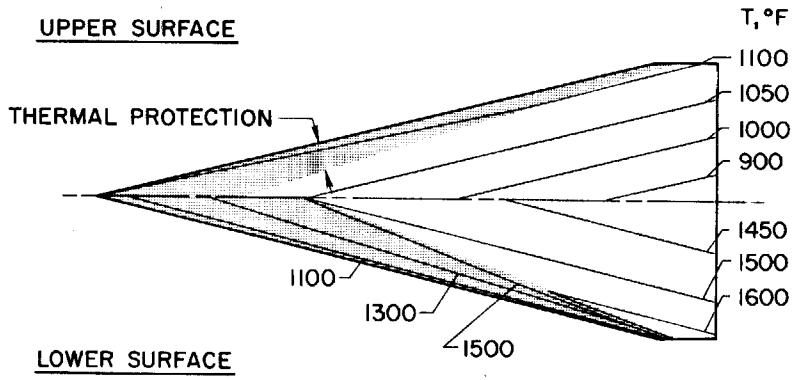

Slide 7.

WING DEFLECTION
FULL SUPPORT; WAFFLE PANEL

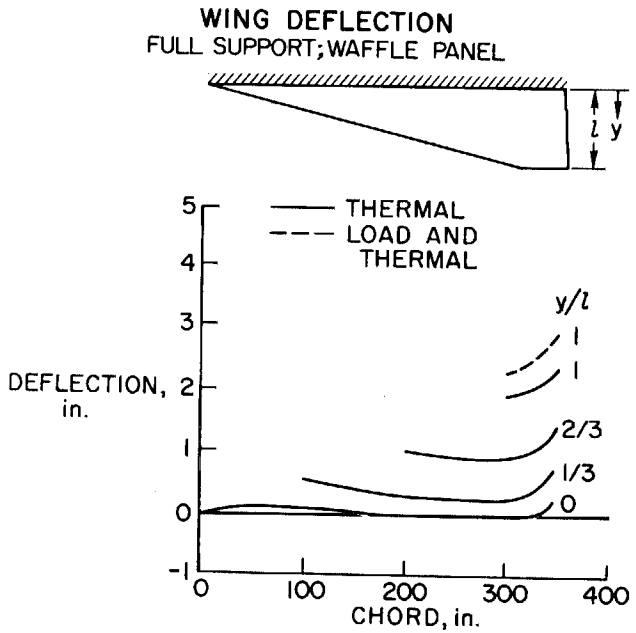

Slide 8.

[redacted]

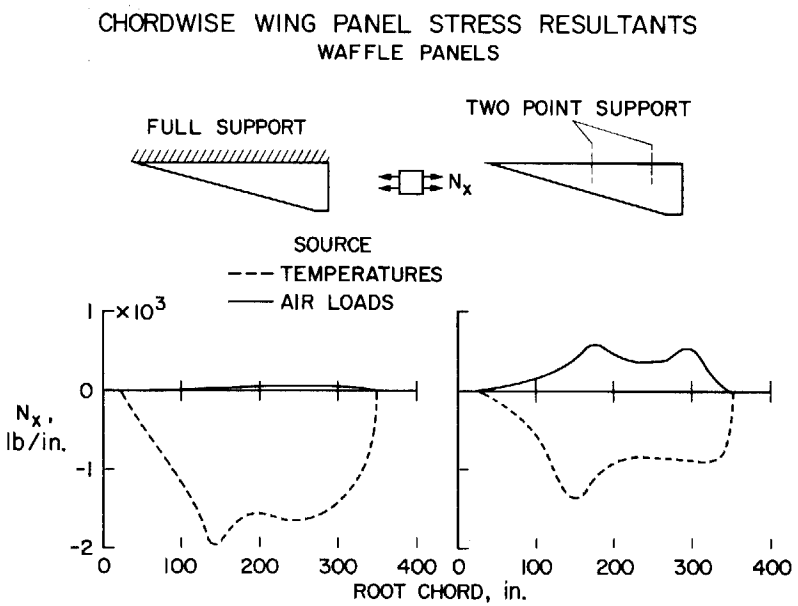

Slide 11.

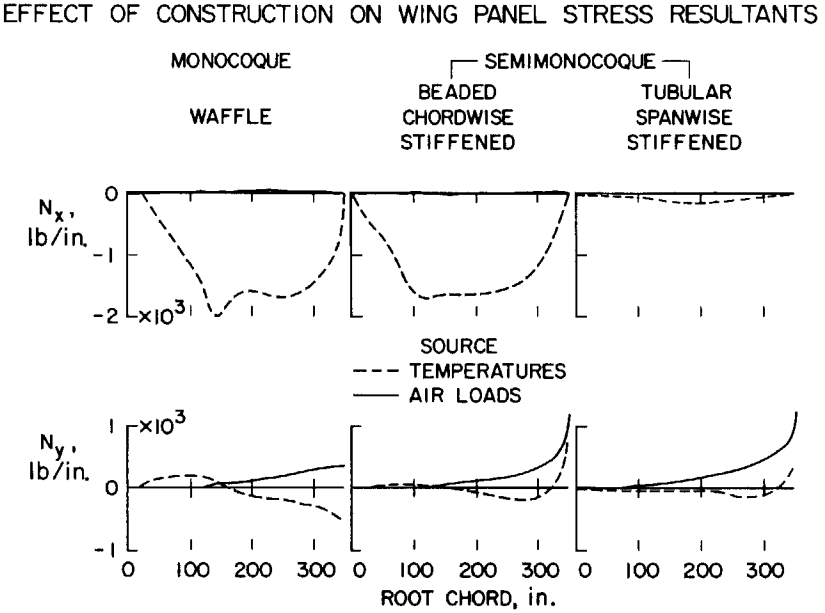

Slide 12.

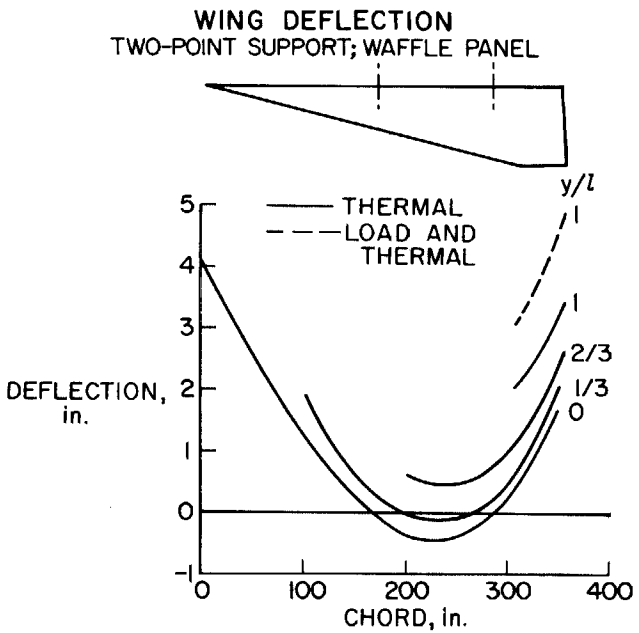

Slide 9.

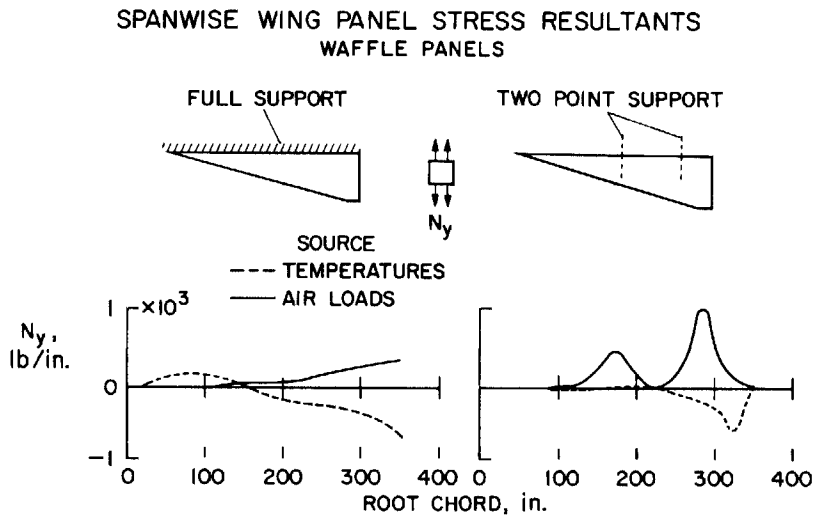

Slide 10.

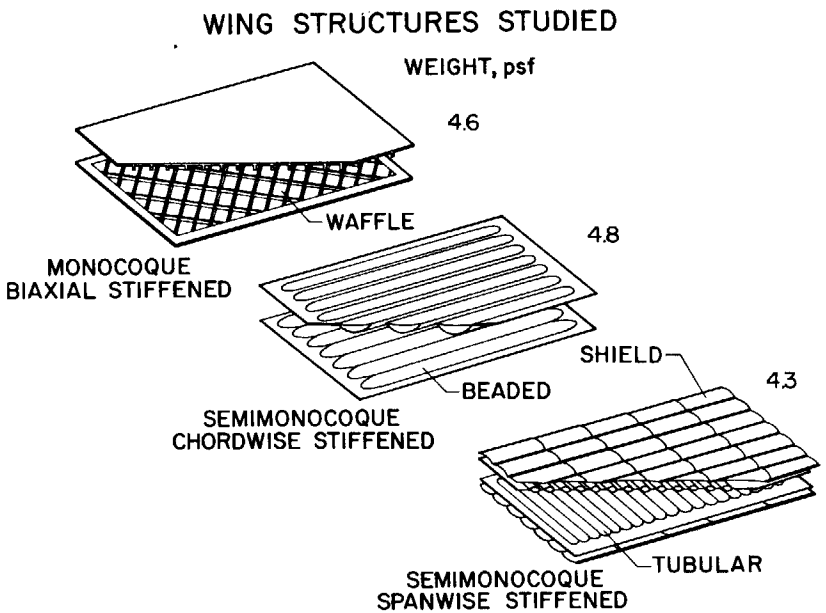
WING STRUCTURES STUDIED
WEIGHT, psf
4.6
WAFFLE
MONOCOQUE
BIAXIAL STIFFENED
4.8
BEADED
SEMIMONOCOQUE
CHORDWISE STIFFENED
SHIELD
4.3
TUBULAR
SEMIMONOCOQUE
SPANWISE STIFFENED

Slide 13.

30. Regeneratively Cooled Structures for Hypersonic Aircraft - H. Neale Kelly and John L. Shideler

PROPULSION SYSTEM STRUCTURE

TWO-DIMENSIONAL AIR INLET

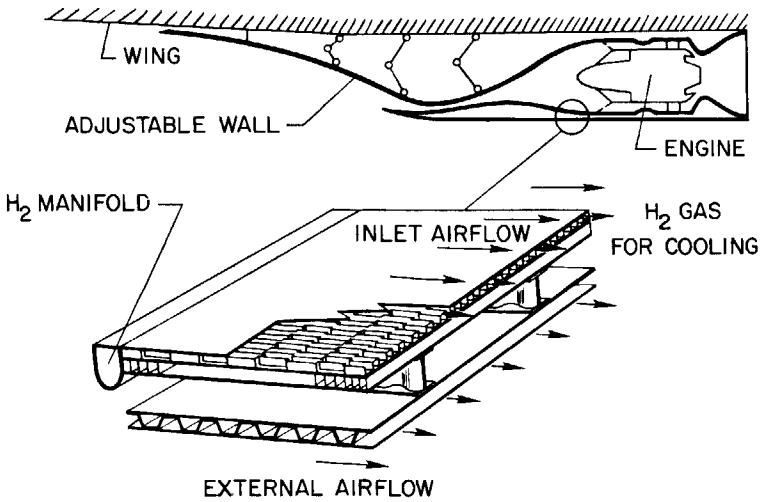

Slide 1.

HYDROGEN PASSAGE GEOMETRY

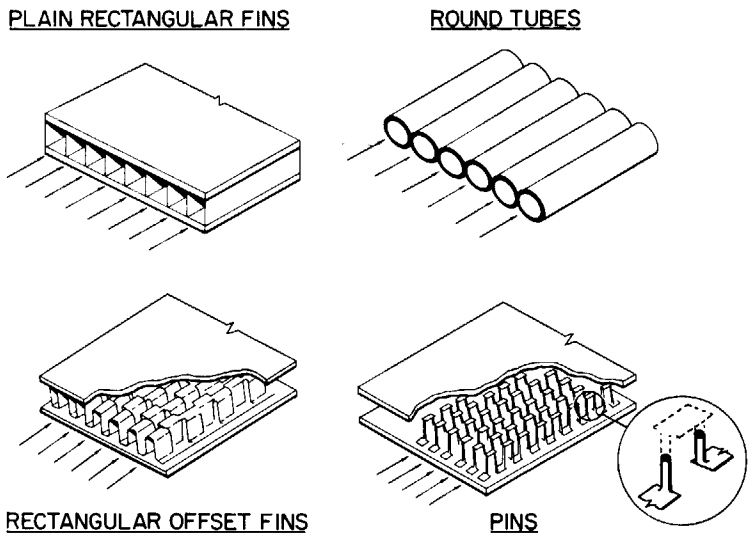

Slide 2.

H. N. Kelly

[redacted]

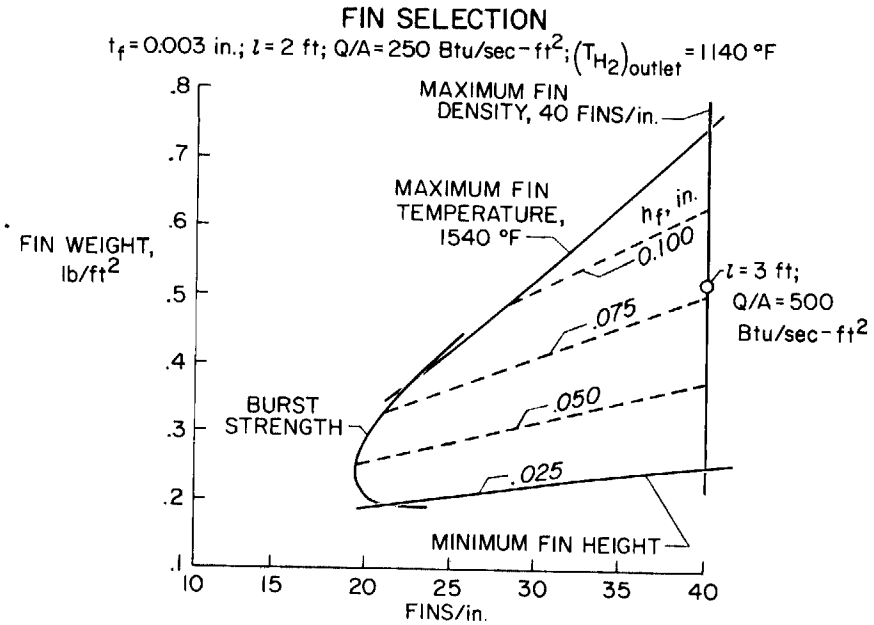

Slide 3.

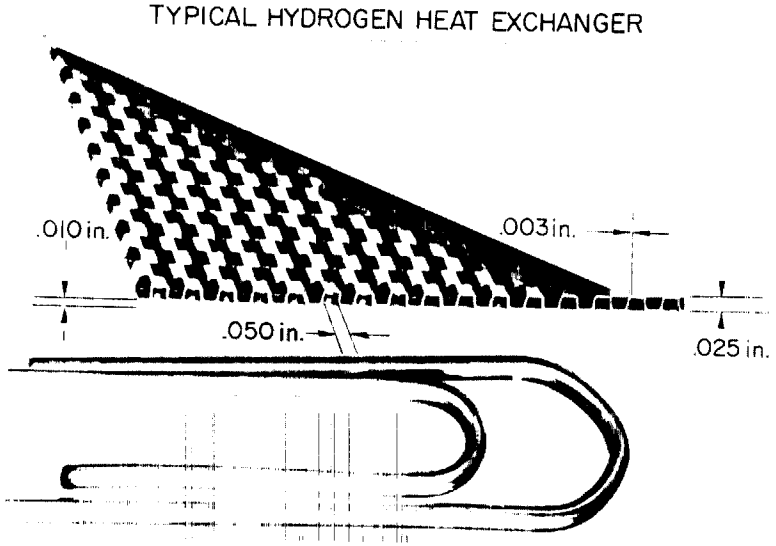

Slide 4.

[redacted]

HYDROGEN-COOLED COMPOSITE-STRUCTURE CONCEPTS

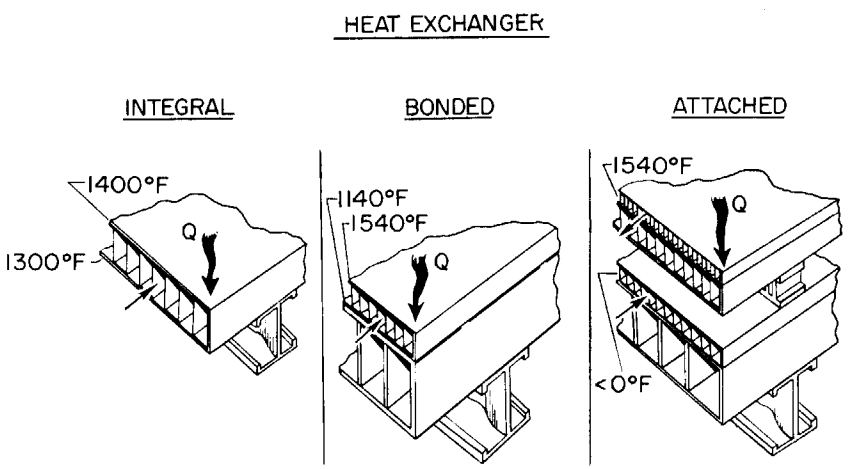

Slide 5.

HYDROGEN-COOLED COMPOSITE-STRUCTURE WEIGHTS

2- BY 2-ft PANEL; $Q/A = 50$ Btu/sec-ft^2; $\left(T_{H_2}\right)_{outlet} = 1140°F$

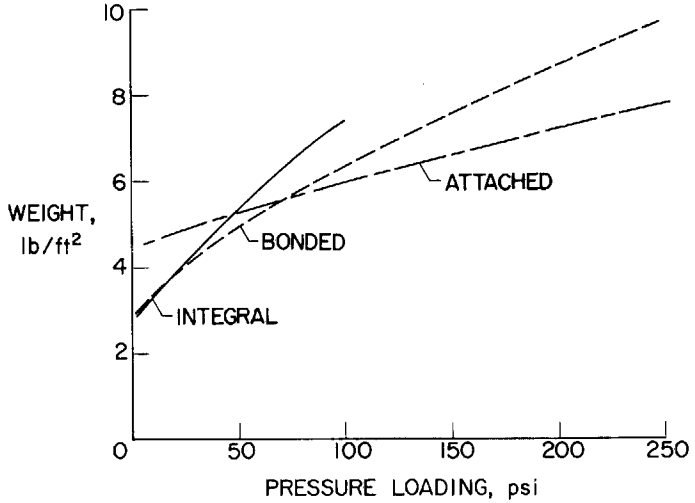

Slide 6.

[redacted]

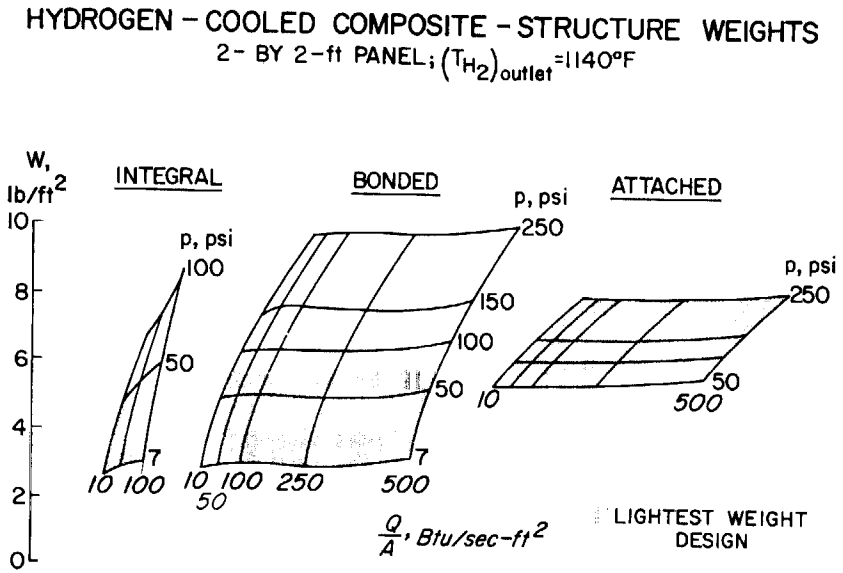

Slide 7.

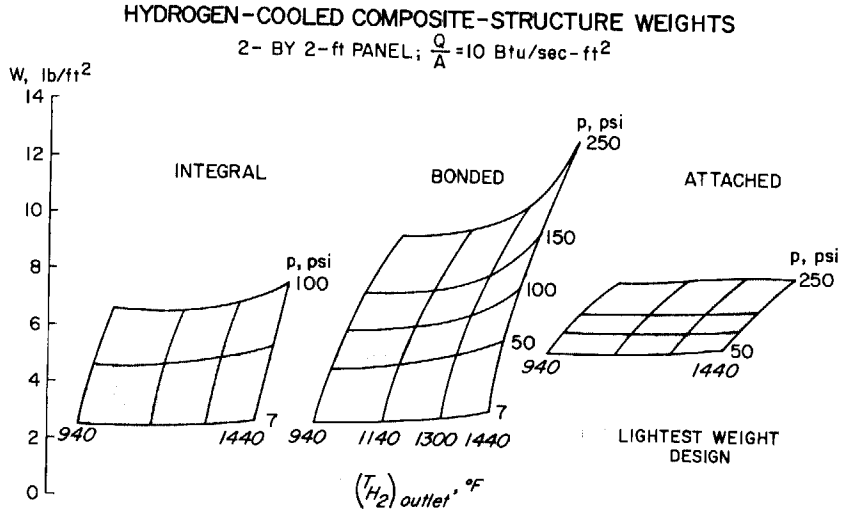

Slide 8.

[redacted]

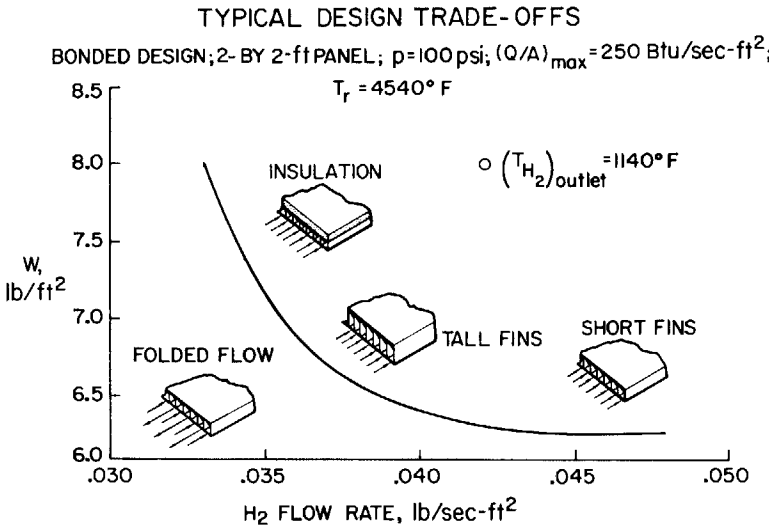

Slide 9.

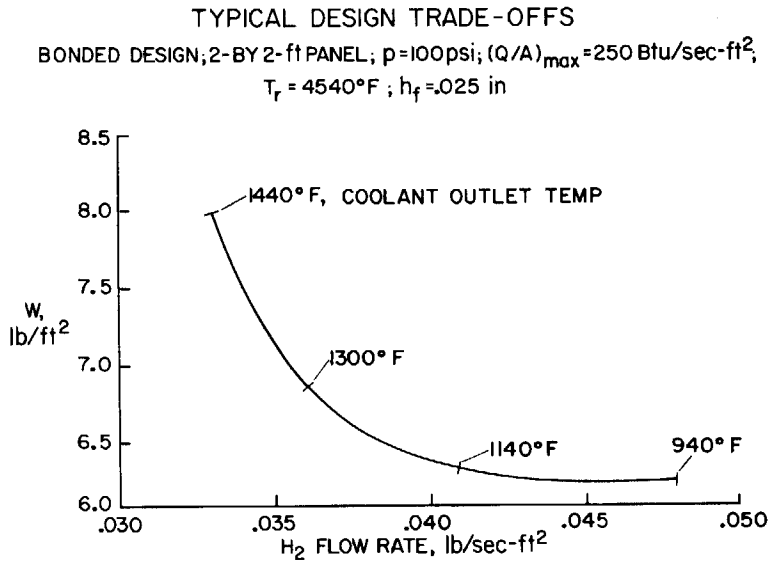

Slide 10.

31. Dynamic and Aeroelastic Consideration of Hypersonic Aircraft - A. Gerald Rainey and Dennis J. Martin

DYNAMIC AND AEROELASTIC CONSIDERATIONS

- ENGINE NOISE
- BOUNDARY-LAYER NOISE
- FUEL SLOSHING
- FLUTTER
- GUST RESPONSE

Slide 1.

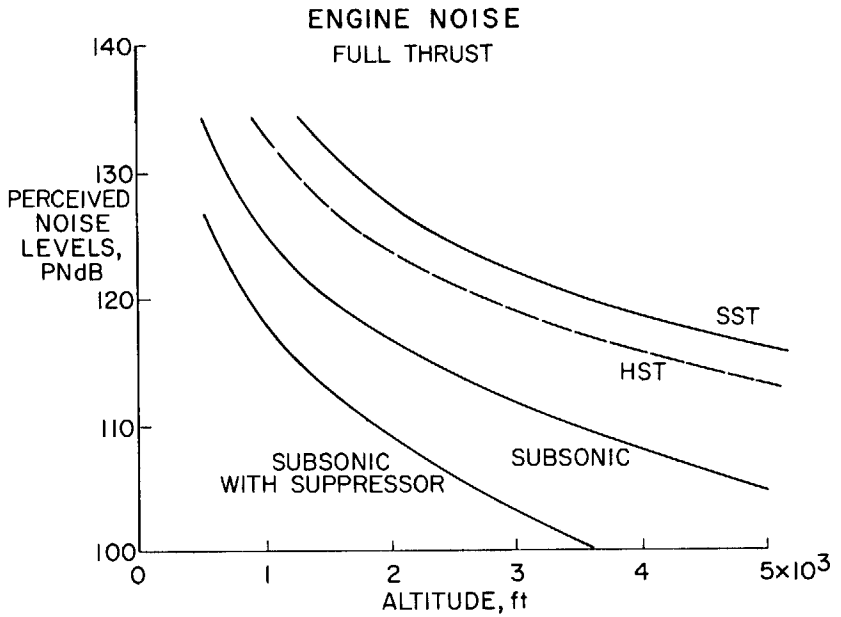

Slide 2.

[redacted]

SPECTRA OF ENGINE NOISE
DISTANCE = 200 ft; FULL THRUST

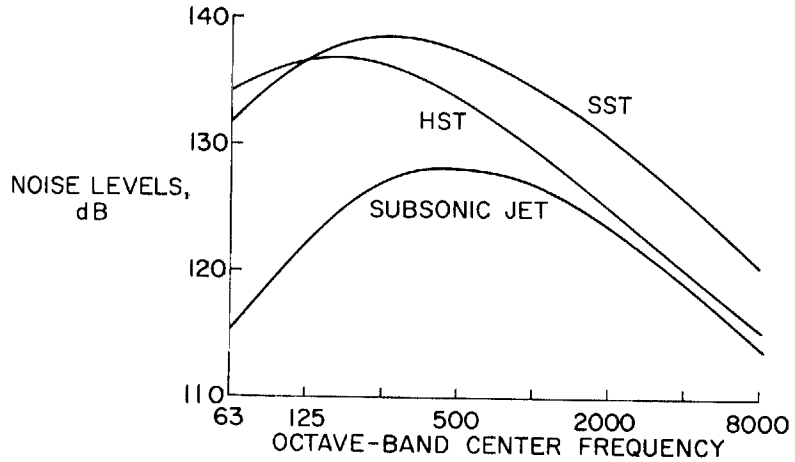

Slide 3.

EXTERNAL BOUNDARY-LAYER NOISE

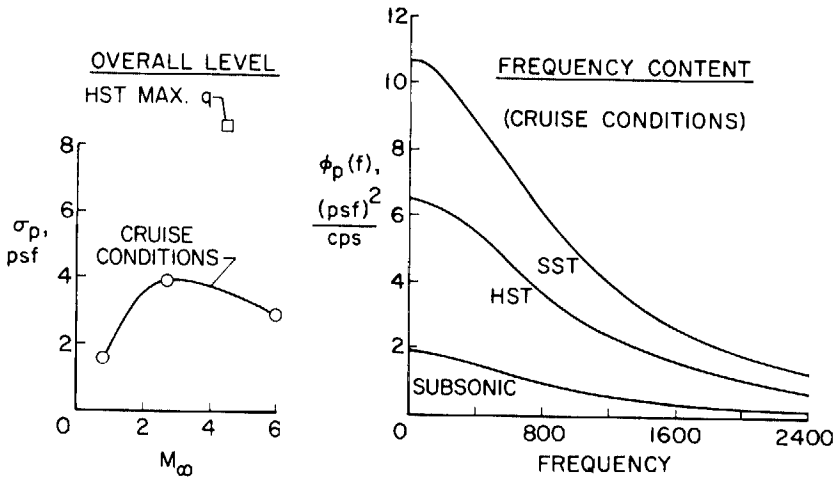

Slide 4.

[redacted]

EFFECTS OF FLEXIBILITY
ON SLOSH DAMPING OF RING BAFFLES

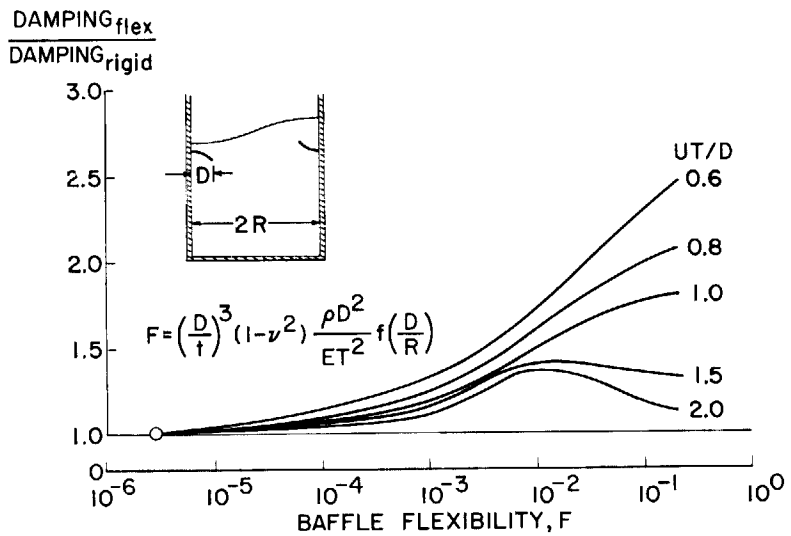

Slide 5.

SUBSONIC FLUTTER RESULTS FOR FLEXIBLE WING-BODIES
$M_\infty \approx 0.2$; HODSON (N.A.A.)

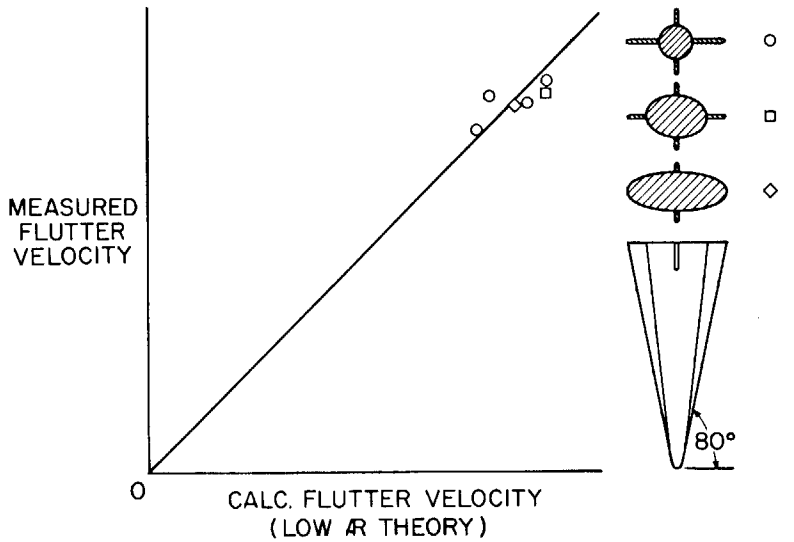

Slide 6.

FLUTTER OF SLENDER DELTA WINGS

M_∞=7; 5-PERCENT-THICK DOUBLE WEDGE

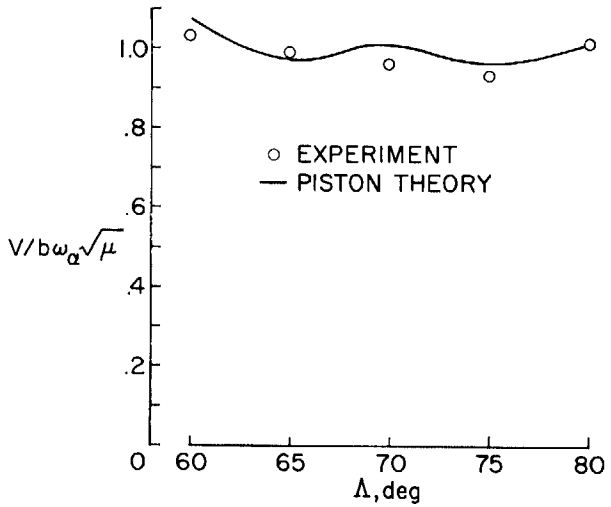

Slide 7.

FLUTTER TRENDS WITH MACH NUMBER

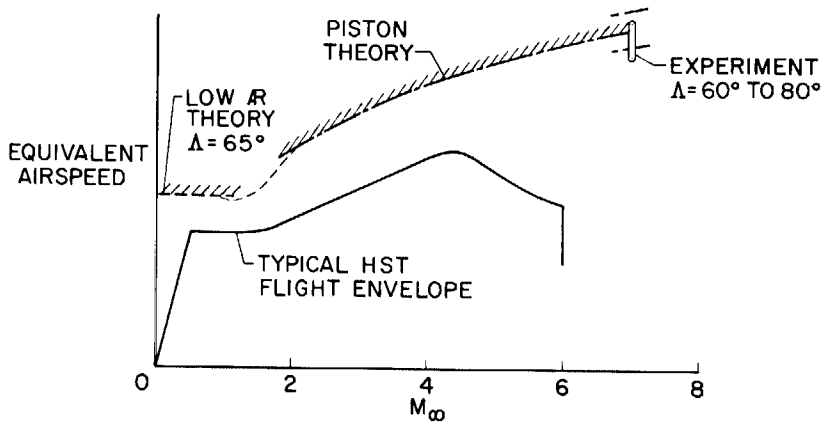

Slide 8.

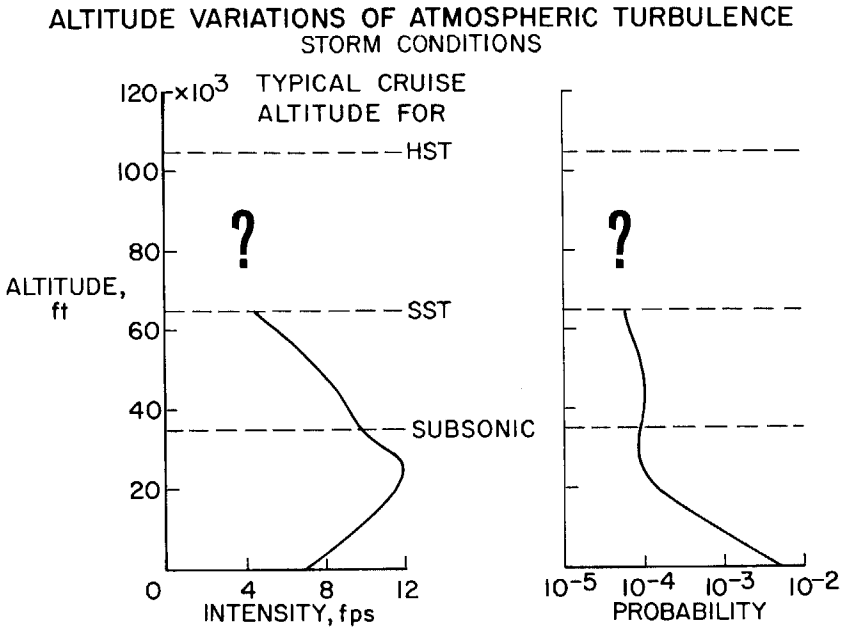

Slide 9.

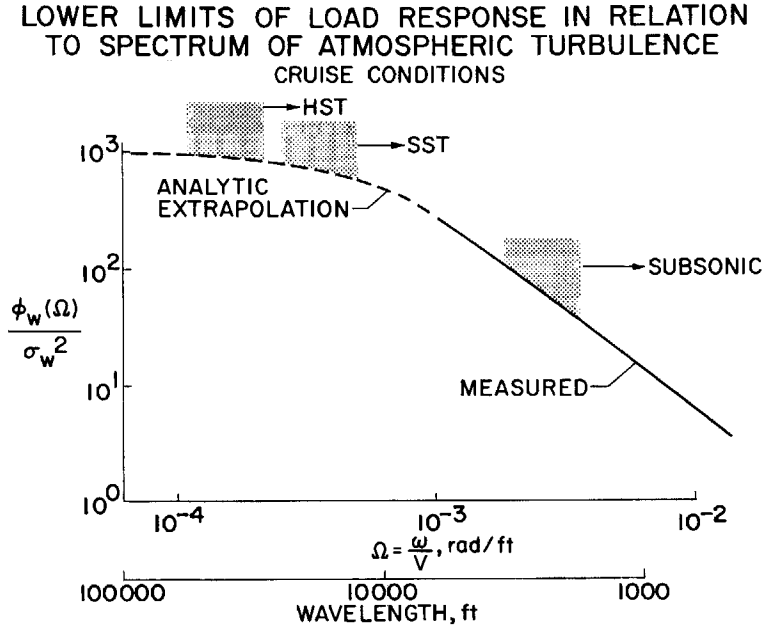

Slide 10.

[redacted]

PILOT-STATION VERTICAL-ACCELERATION SPECTRA SHAPES
TYPICAL SUBSONIC JET TRANSPORT AND XB-70

$$\int_0^6 \frac{\phi_a(f)}{\sigma_a^2}\,df = 1.0$$

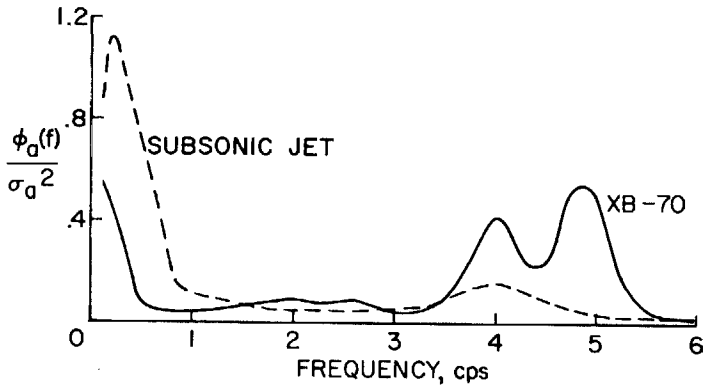

Slide 11.

[redacted]

32. Flutter Design of Stiffened Skin Panels for Hypersonic Aircraft - Herman L. Bohon, Melvin S. Anderson, and Walter L. Heard

H. L. Bohon

EFFECT OF MACH NUMBER ON FLUTTER BOUNDARY

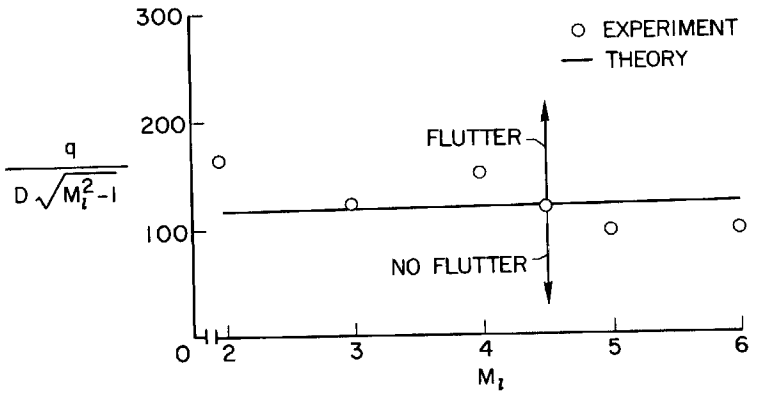

Slide 1.

FLUTTER PARAMETER ON ASCENT TRAJECTORY
MACH 8 CRUISE VEHICLE

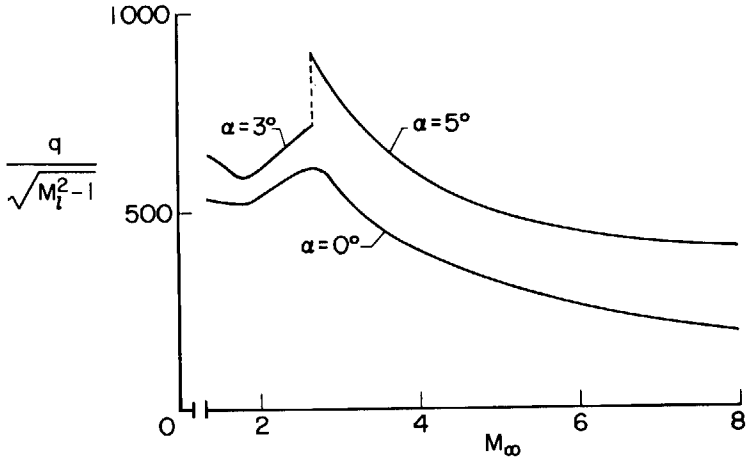

Slide 2.

H. L. Bohon

[redacted]

EDGE - SUPPORT EFFECTS ON PANEL FLUTTER

$M_t = 3$

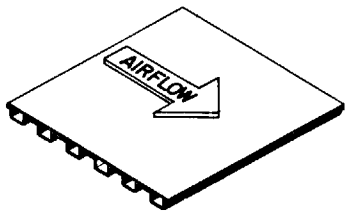

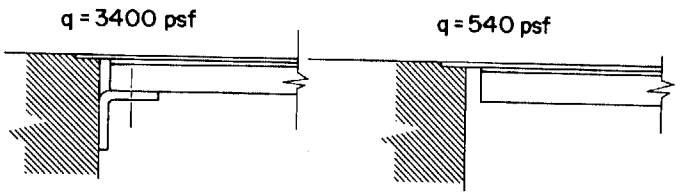

Slide 3.

ORTHOTROPIC PANEL AND COORDINATE SYSTEM

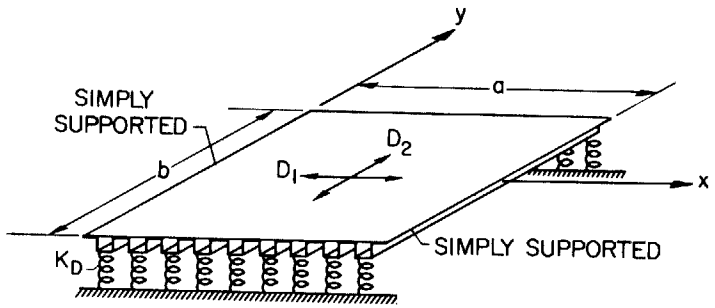

D_1 = BENDING STIFFNESS IN x - DIRECTION
D_2 = BENDING STIFFNESS IN y - DIRECTION
D_{12} = TWISTING STIFFNESS
$D_1 << D_{12} < D_2$

Slide 4.

[redacted]

FLUTTER BOUNDARY FOR FLEXIBLE SUPPORTS

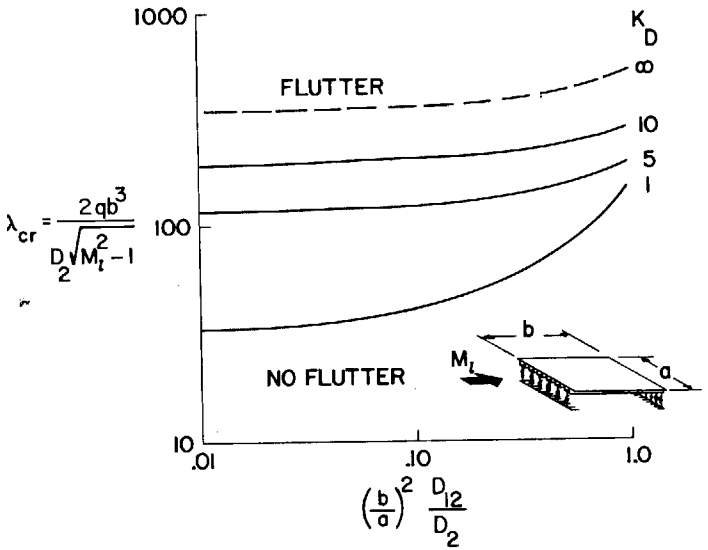

Slide 5.

FLUTTER OF HIGHLY ORTHOTROPIC PANELS
FLOW IN STRONG DIRECTION

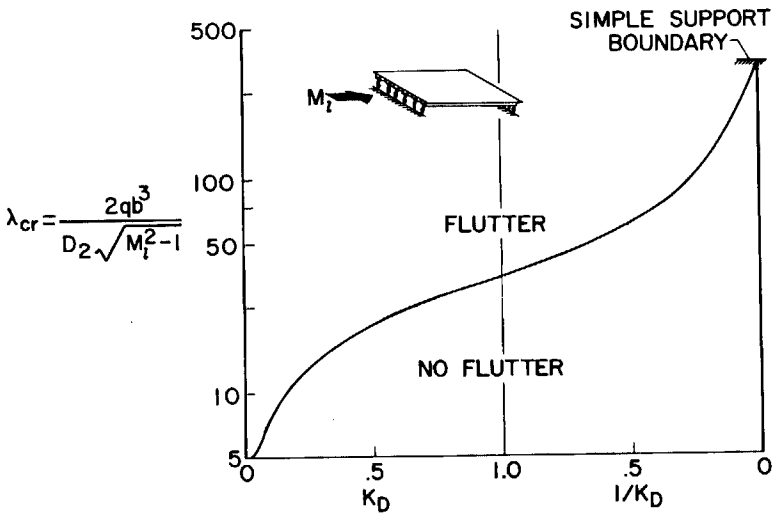

Slide 6.

[redacted]

FLUTTER OF HIGHLY ORTHOTROPIC PANELS

FLOW IN WEAK DIRECTION

$$\lambda^*_{cr} = \frac{2qb^3}{D_1\sqrt{M_i^2-1}}\left(\frac{D_1}{D_{12}}\right)^{3/2}$$

$$C = \frac{D_{12}}{\sqrt{D_1 D_2}}$$

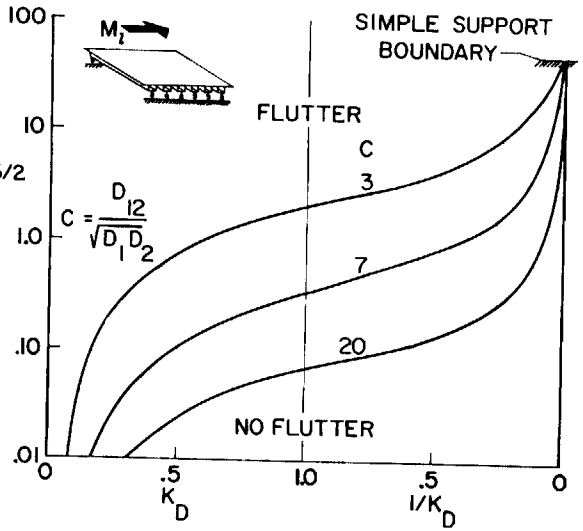

Slide 7.

COMPARISON OF THEORY AND EXPERIMENT

$$\lambda^*_{cr} = \frac{2qb^3}{D_1\sqrt{M_i^2-1}}\left(\frac{D_1}{D_{12}}\right)^{3/2}$$

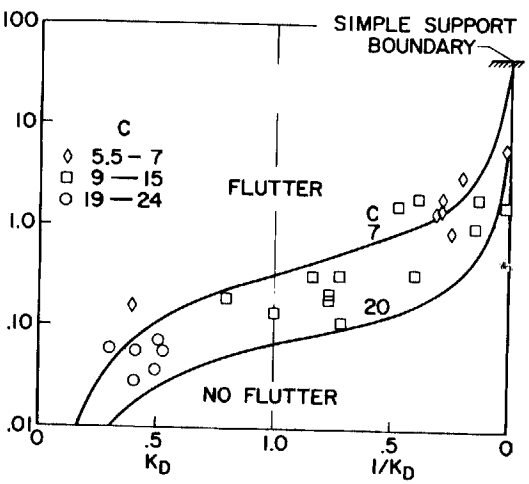

Slide 8.

[redacted]

EFFECT OF EDGE TORSIONAL STIFFNESS

$$\lambda^*_{cr} = \frac{2qb^3}{D_1\sqrt{M_1^2-1}}\left(\frac{D_1}{D_{12}}\right)^{3/2}$$

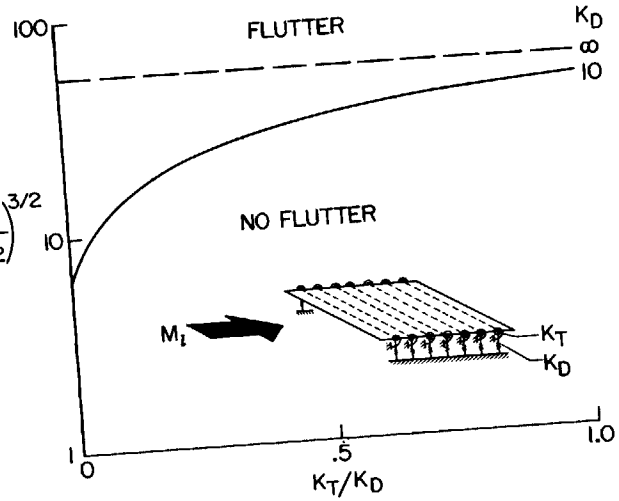

Slide 9.

COMPARISON OF THEORY AND EXPERIMENT

$$\lambda^*_{cr} = \frac{2qb^3}{D_1\sqrt{M_1^2-1}}\left(\frac{D_1}{D_{12}}\right)^{3/2}$$

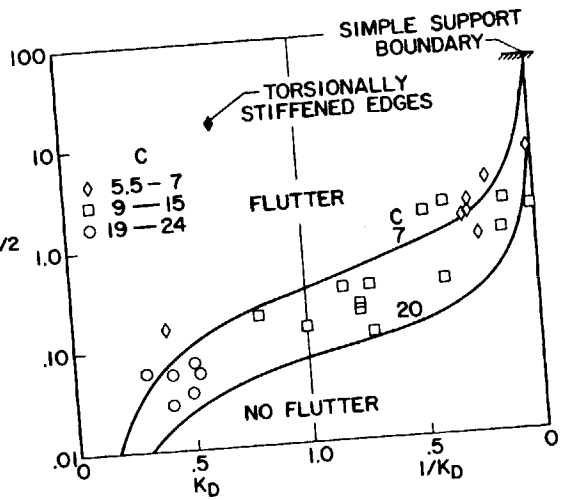

Slide 10.

Ponted in 20" HST @ CRC shows 13 x 10⁶ RN with 18" model
ARC 3½' sets 3½ x 10⁶/ft with 18" model — can we test same model
in both tunnels ?